



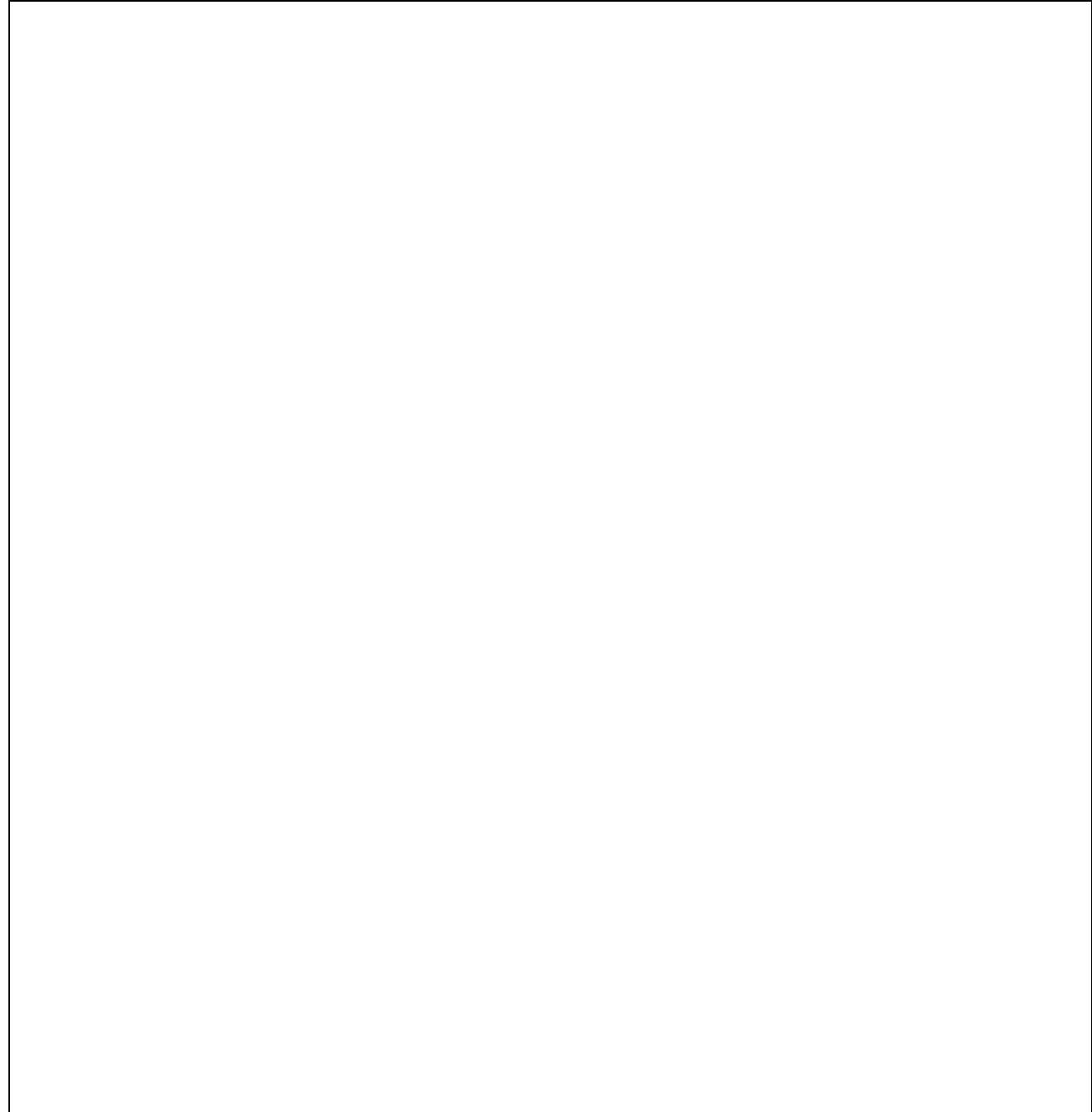
U.S. Department
of Transportation

Federal Highway
Administration

FHWA-PD-96-010
DOT-VNTSC-FHWA-98-2

FHWA TRAFFIC NOISE MODEL (FHWA TNM®) TECHNICAL MANUAL

Final Report
February 1998



Prepared for

U.S. Department of Transportation
Federal Highway Administration
Office of Environment and Planning
Washington, D.C. 20590

Prepared by

U.S. Department of Transportation
Research and Special Programs Administration
John A. Volpe National Transportation Systems Center
Acoustics Facility

FHWA-PD-96-010
DOT-VNTSC-FHWA-98-2

FHWA Traffic Noise Model (FHWA TNM®) Technical Manual



U.S. Department
of Transportation

Federal Highway
Administration

Foster-Miller, Inc.
350 Second Avenue
Waltham, MA 02154

and

Harris Miller Miller & Hanson Inc.
15 New England Executive Park
Burlington, MA 01803

in conjunction with:

Foliage Software Systems, Inc.
Vanderbilt University
University of Central Florida

Final Report
February 1998

Prepared for

U.S. Department of Transportation
Federal Highway Administration
Office of Environment and Planning
Washington, D.C. 20590

Prepared by

U.S. Department of Transportation
Research and Special Programs Administration
John A. Volpe National Transportation Systems Center
Acoustics Facility
Cambridge, MA 02142-1093

NOTICE

This document is disseminated under the sponsorship of the Department of Transportation in the interest of information exchange. The United States Government assumes no liability for its contents or use thereof. This report does not constitute a standard, specification, or regulation.

The United States Government does not endorse products or manufacturers. Trade or manufacturers' names appear herein solely because they are considered essential to the object of this document.

REPORT DOCUMENTATION PAGE

Form Approved
OMB No. 0704-0188

Public reporting burden for this collection of information is estimated to average 1 hour per response, including the time for reviewing instructions, searching existing data sources, gathering and maintaining the data needed, and completing and reviewing the collection of information. Send comments regarding this burden estimate or any other aspect of this collection of information, including suggestions for reducing this burden, to Washington Headquarters Services, Directorate for Information Operations and Reports, 1215 Jefferson Highway, Suite 1204, Arlington, VA 22202-4302, and to the Office of Management and Budget, Paperwork Reduction Project (0704-0188), Washington, DC 20503.

1. AGENCY USE ONLY (leave blank)	2. REPORT DATE February 1998	3. REPORT TYPE AND DATES COVERED Final Report June 1993 - February 1998
4. TITLE AND SUBTITLE FHWA Traffic Noise Model®, Version 1.0 Technical Manual		5. FUNDING NUMBERS HW866/H8008
6. AUTHOR(S) Christopher W. Menge ⁽¹⁾ , Christopher F. Rossano ⁽¹⁾ , Grant S. Anderson ⁽¹⁾ , Christopher J. Bajdek ⁽¹⁾		
7. PERFORMING ORGANIZATION NAME(S) AND ADDRESS(ES) Foster-Miller, Inc.* 350 Second Avenue Waltham, MA 02154		8. PERFORMING ORGANIZATION REPORT NUMBER DOT-VNTSC-FHWA-98-2
9. SPONSORING/MONITORING AGENCY NAME(S) AND ADDRESS(ES) U.S. Department of Transportation * Under Contract to: Federal Highway Administration U.S. Department of Transportation Office of Environment and Planning Research and Special Programs Administration Washington, D.C. 20590 John A. Volpe National Transportation Systems Center Acoustics Facility Cambridge, MA 02142-1093		10. SPONSORING/MONITORING AGENCY REPORT NUMBER FHWA-PD-96-010
11. SUPPLEMENTARY NOTES ⁽¹⁾ Harris Miller Miller & Hanson Inc. 15 New England Executive Park Burlington, MA 01803		
12a. DISTRIBUTION/AVAILABILITY STATEMENT	12b. DISTRIBUTION CODE	
13. ABSTRACT (Maximum 200 words) This Technical Manual is for the Federal Highway Administration's Traffic Noise Model (FHWA TNM®), Version 1.0 -- the FHWA's computer program for highway traffic noise prediction and analysis. Two companion reports, a User's Guide and a data report, respectively, describe the use of TNM and its vehicle noise-emissions data base. The Technical Manual documents the fundamental equations, the acoustical algorithms, and the interactive logic for all computations within TNM. Section 1 overviews the basic elements of TNM's prediction model. It describes the basic concepts of the model, from vehicle noise emissions to predicted sound levels. Section 2 describes TNM's prediction model in more detail, with references to the manual appendixes for detail on algorithms and mathematics. In particular, this section describes the following: (1) vehicle noise emissions for TNM's built-in vehicle types, (2) computation of vehicle speeds, when they are affected by upgrades and traffic-control devices, (3) geometrical complexity in the XY plane, plus computation of free-field sound levels from a roadway segment, (4) geometrical complexity in the vertical plane, along any line between roadway and receiver, plus the computation of attenuation relative to free field along any such line, (5) computation of parallel-barrier degradation for barriers or retaining walls that flank the roadway, and (6) computation of sound-level contours, insertion-loss contours, and level-difference contours. In addition, this manual contains detailed appendixes for each of these subjects.		
14. SUBJECT TERMS Highway traffic-noise prediction, FHWA TNM, digitizer, registration, roadways, traffic, receivers, barriers, building rows, terrain lines, ground zones, tree zones, noise barriers, FHWA policy	15. NUMBER OF PAGES 180	16. PRICE CODE

17. SECURITY CLASSIFICATION OF REPORT Unclassified	18. SECURITY CLASSIFICATION OF THIS PAGE Unclassified	19. SECURITY CLASSIFICATION OF ABSTRACT Unclassified	20. LIMITATION OF ABSTRACT
--	---	--	----------------------------

NSN 7540-01-280-5500

Standard Form 298 (Rev. 2-89)
Prescribed by ANSI Std. Z39-18
298-102

METRIC CONVERSION CHART WILL BE HERE.

PREFACE

This Technical Manual is for the Federal Highway Administration's Traffic Noise Model (FHWA TNM[®]), Version 1.0 -- the Federal Highway Administration's computer program for highway traffic noise prediction and analysis. A companion User's Guide describes how to use TNM [Anderson 1998]. In addition, a companion technical report documents the vehicle noise-emissions data base [Fleming 1995].

Overview of TNM: TNM computes highway traffic noise at nearby receivers and aids in the design of highway noise barriers. As sources of noise, it includes 1994-1995 noise emission levels for the following cruise-throttle vehicle types:

- # Automobiles: all vehicles with two axles and four tires -- primarily designed to carry nine or fewer people (passenger cars, vans) or cargo (vans, light trucks) -- generally with gross vehicle weight less than 4,500 kg (9,900 lb);
- # Medium trucks: all cargo vehicles with two axles and six tires -- generally with gross vehicle weight between 4,500 kg (9,900 lb) and 12,000 kg (26,400 lb);
- # Heavy trucks: all cargo vehicles with three or more axles -- generally with gross vehicle weight more than 12,000 kg (26,400 lb);
- # Buses: all vehicles designed to carry more than nine passengers; and
- # Motorcycles: all vehicles with two or three tires and an open-air driver/passenger compartment.

Noise emission levels consist of A-weighted sound levels, one-third octave-band spectra, and subsource-height strengths for the following pavement types:

- # Dense-graded asphaltic concrete (DGAC);
- # Portland cement concrete (PCC);
- # Open-graded asphaltic concrete (OGAC); and
- # A composite pavement type consisting of data for DGAC and PCC combined.

In addition, TNM includes full-throttle noise emission levels for vehicles on upgrades and vehicles accelerating away from the following traffic-control devices:

- # Stop signs;
- # Toll booths;
- # Traffic signals; and
- # On-ramp start points.

TNM combines these full-throttle noise emission levels with its internal speed computations to account for the full effect (noise emissions plus speed) of roadway grades and traffic-control devices.

TNM propagates sound energy, in one-third-octave bands, between highway systems and nearby receivers. Sound propagation takes the following factors into account:

- # Atmospheric absorption;
- # Divergence;
- # Intervening ground: its acoustical characteristics and its topography;

- # Intervening barriers: walls, berms and their combination;
- # Intervening rows of buildings; and
- # Intervening areas of heavy vegetation.

TNM computes the effect of intervening ground (defined by its type, or optionally by its flow resistivity) with theory-based acoustics that have been calibrated against field measurements. In addition, TNM allows sound to propagate underneath selected intervening roadways and barriers, rather than being shielded by them.

During calculation, TNM perturbs (increases/decreases) intervening barrier heights up and down from their input height, to calculate for multiple heights. Then during acoustical design of selected barriers, combined with selected receivers, TNM displays sound-level results for any combination of height perturbations, where a perturbation is defined as the height increment that a noise barrier's input height is increased (perturbed up) or decreased (perturbed down) during barrier design. It also contains an input-height check, to determine if noise barriers break the lines-of-sight between sources and receivers. In addition, it provides summary cost and benefit information for each barrier design, from user-supplied unit barrier costs and land-use information.

For selected cross sections, TNM also computes the effect of multiple reflections between parallel barriers or retaining walls that flank a roadway. The TNM user can then enter the computed parallel-barrier degradations as adjustment factors for individual receivers in TNM's calculation of receiver sound levels.

TNM computes three measures of highway traffic noise:

- # L_{Aeq1h} : hourly A-weighted equivalent sound level (1HEQ);
- # L_{dn} : day-night average sound level (DNL); and
- # L_{den} : Community Noise Equivalent Level (CNEL), where "den" stands for day/evening/night.

TNM computes these three noise measures at user-defined receiver locations, where it also computes several diagnostics to aid in noise-barrier design. In addition, it computes three types of contours:

- # Sound-level contours;
- # Noise Reduction, i.e., insertion-loss, contours for noise barriers; and
- # Level-difference contours between any two noise-barrier designs.

TNM runs under Microsoft® Windows Version 3.1 (or later). Within Windows, it allows digitized input using a generic Windows digitizer driver, plus the import of DXF files from CAD programs and input files from STAMINA 2.0/OPTIMA. Note: TNM will run under Microsoft® Windows 95 or Windows NT, however, TNM is a 16-bit program and will not take full advantage of the 32-bit architecture associated with Windows 95 or NT.

To aid during input and to document the resulting input and barrier designs, TNM shows the following graphical views:

- # Plan views;
- # Skew sections;
- # Perspective views, including a specialized perspective view for noise-barrier design; and
- # Roadway profiles.

TNM Version 1.0 replaces FHWA's prior pair of computer programs, STAMINA 2.0/OPTIMA. In addition, this Technical Manual replaces FHWA's prior prediction model: *FHWA Highway Traffic Noise Prediction Model*, FHWA-RD-77-108 [Barry 1978].

This manual documents the fundamental equations, the acoustical algorithms, and the interactive logic for all computations within the TNM. The manual is organized as follows:

- Section 1. Overview of TNM:** This section overviews the basic elements of the TNM's prediction model. It describes the basic concepts of the model, from vehicle noise emissions to predicted sound levels.
- Section 2. Model Description:** This section describes the TNM's prediction model in more detail, with references to the manual's appendixes for detail on algorithms and mathematics. In particular, this section describes:
- # Vehicle noise emissions for the TNM's built-in vehicle types.
 - # Computation of vehicle speeds, where they are affected by upgrades and traffic-control devices.
 - # Geometrical complexity in the horizontal plane, plus computation of free-field sound levels from a roadway segment.
 - # Geometrical complexity in the vertical plane, along any line between roadway and receiver, plus the computation of attenuation due to shielding and ground effects along any such line.
 - # Computation of degradation of barrier insertion loss due to multiple reflections between barriers that flank the roadway.
 - # Computation of sound-level contours.

In addition, this manual contains the following detailed appendixes:

- Appendix A. Vehicle noise emissions;**
- Appendix B. Vehicle speeds;**
- Appendix C. Horizontal geometry and acoustics;**
- Appendix D. Vertical geometry and acoustics;**
- Appendix E. Parallel barriers;**
- Appendix F. Contours;**
- Appendix G. Model verification;**
- References;**

Index;

FHWA TNM Announcement and Order Form; and

FHWA TNM Registration Card.

ACKNOWLEDGMENTS

FHWA TNM® was developed in part by:

U.S. Department of Transportation Federal Highway Administration

Robert Armstrong, Steven Ronning, Howard Jongedyk.

U.S. Department of Transportation

John A. Volpe National Transportation Systems Center, Acoustics Facility

Overall management, emission-data design/measurement/analysis, propagation-path development, program testing, User's Guide, Technical Manual, TNM Trainer CD-ROM:

Gregg Fleming, Amanda Rapoza, Cynthia Lee, David Read, Paul Gerbi, Christopher Roof, Antonio Godfrey, Shamir Patel.

Harris Miller Miller & Hanson Inc.

Technical management, emission-analysis design, functional requirements, conceptual program design, acoustical algorithms, design/development/testing of acoustical code and vertical geometry, User's Guide, Technical Manual:

Grant Anderson, Christopher Menge, Christopher Rossano, Christopher Bajdek, Thomas Breen, Douglas Barrett, William Robert.

Foliage Software Systems, Inc.

Program design/specification/development/testing, development of horizontal geometry and interfaces, program documentation:

Ronald Rubbico, George Plourde, Paul Huffman, Christopher Bowe, Nathan Legvold.

Special contributors:

Vanderbilt University: William Bowlby -- emission-data design/measurement/analysis, vehicle speeds [Bowlby 1997].
Bowlby & Associates, Inc.: William Bowlby -- TNM Trainer CD-ROM
Serac Technology Group, Inc.: Theodore Patrick -- TNM Trainer CD-ROM
University of Central Florida: Roger Wayson -- emission-data design/measurement/analysis.
Florida Department of Transportation: Win Lindeman -- Funding and management of subsurface-height study.
Florida Atlantic University: Stewart Glegg, Robert Coulson -- subsurface height measurements [Coulson 1996].
Maryland State Highway Administration: Kenneth Polcak -- emission data.
Ohio University: Lloyd Herman -- emission data.
Emission-data state agencies: California, Connecticut, Florida, Kentucky, Maryland, Massachusetts, Michigan, New Jersey, Tennessee.

Design and Review Panel:

Domenick Billera, James Byers, Rudy Hendriks, Harvey Knauer, Win Lindeman, William McColl, Kenneth Polcak.

National Pooled-Fund Contributing States:

Arizona, California, Florida, Georgia, Hawaii, Illinois, Indiana, Iowa, Kentucky, Maryland, Massachusetts, Michigan, Minnesota, New Jersey, New York, North Carolina, Ohio, Oregon, Pennsylvania, Tennessee, Texas, Utah, Virginia, Washington and Wisconsin.

The development work of Harris Miller Miller & Hanson, Foliage Software Systems, Vanderbilt University and the University of Central Florida was conducted in part under contract to Foster-Miller, Inc. Vanderbilt University and the University of Central Florida were also under contract to the Volpe Center.

TABLE OF CONTENTS

<u>Section</u>	<u>Page</u>
1. OVERVIEW	1
1.1 Vehicle Emission Levels	1
1.2 Free Field Levels	2
1.3 Shielding and Ground Effects	2
1.4 High-level Flow Chart	3
1.5 Parallel Barrier Analysis	3
2. MODEL DESCRIPTION	7
2.1 Vehicle Noise Emission Levels	7
2.2 Vehicle Speed Computation	9
2.3 Free Field Levels and Horizontal Geometry	10
2.3.1 Elemental triangles	10
2.3.2 Traffic flow adjustment	11
2.3.3 Distance and roadway length adjustment	12
2.4 Vertical Geometry Acoustics	12
2.4.1 Basis of the acoustical model	12
2.4.2 Elemental triangles	13
2.4.3 Elements in the propagation path	13
2.4.4 Logic flow and geometry modeling	18
2.5 Parallel Barrier Analysis	20
2.6 Contours	21
2.7 Model Verification	21
Appendix A Vehicle Noise Emissions	23
A.1 Overview	23
A.2 Definition of Variables	24
A.3 A-weighted Noise-Level Emissions and 1/3rd-Octave-Band Spectra, as Measured	24
A.3.1 Built-in vehicle types	25
A.3.2 User-defined vehicle types	25
A.4 Vertical Subsources, as Measured	26
A.4.1 Built-in vehicle types	26
A.4.2 User-defined vehicles	29
A.5 Vertical Subsources, Free Field	29
A.6 Plots of All Noise Emissions	30
Appendix B Vehicle Speeds	49
B.1 Overview	49
B.2 Entrance and Exit Speeds: Overview	50
B.3 Entrance Speeds	51
B.4 Exit Speeds	52
B.5 Regression Equations	52
B.5.1 Regression equation for accelerating vehicles	53
B.5.2 Regression equation for decelerating heavy trucks	54

B.6	Graphs of Acceleration and Deceleration	55
B.6.1	Some additional points	61
Appendix C	Horizontal Geometry and Acoustics	63
C.1	Elemental Triangles	63
C.2	Equations for Traffic Sound Energy and Sound Level	64
C.2.1	Definitions	64
C.2.2	Traffic sound energy: "Reference" conditions	66
C.2.3	Traffic sound energy at true receiver: Free field	68
C.2.4	Traffic sound energy at true receiver: Attenuated	68
C.2.5	Traffic sound levels (L_{Aeq1h} , L_{dn} and L_{ten}) at the true receiver: Attenuated	69
C.3	Outline of Free-field Sorting Computations	70
Appendix D	Vertical Geometry and Acoustics	73
D.1	Overview	73
D.2	Vertical Geometry Elements and Approximation	73
D.2.1	Elements of Vertical Geometry.	74
D.2.2	Approximations.	77
D.3	Propagation Paths	78
D.3.1	Free field.	79
D.3.2	Diffractions.	79
D.3.3	Reflections.	82
D.3.4	Propagation path generation algorithm.	83
D.4	Propagation Path Calculations and Mathematical Description	85
D.4.1	Definitions	85
D.4.2	Free field.	88
D.4.3	Fresnel integral.	88
D.4.4	Diffraction function.	89
D.4.5	Reflection coefficients.	92
D.4.6	Ground-impedance averaging.	97
D.4.7	Tree zones.	98
D.4.8	Rows of buildings.	99
D.4.9	Atmospheric absorption.	100
D.4.10	Foss selection algorithm.	102
D.4.11	Total sound pressure.	104
D.4.12	Attenuation.	104
Appendix E	Parallel Barrier Analysis	105
E.1	Overview	105
E.2	Overview of Parallel-barrier Computations	107
E.3	Required Input	108
E.3.1	Roadway input.	108
E.3.2	Cross-section input.	109
E.3.3	Receiver input.	109
E.4	Ray Tracing	109
E.5	Ray Acoustic Energies	110
E.5.1	Initial ray energy.	110
E.5.2	Reduction in ray energy as the ray propagates outward.	111

E.6	Computation of Parallel-barrier Degradation	114
E.7	Generalization to TNM Sound-level Receivers	114
E.8	Calibration of Results with Field Measurements	115
E.8.1	Initial comparisons of measured and predicted degradations	115
E.8.2	Sensitivity to assumed source height	116
E.8.3	Calibration method	116
E.8.4	Calibration results.	118
Appendix F	Contours	119
F.1	Contour computations	119
F.2	Details about Barrier Perturbations	120
F.3	Details about Grid Spacing	121
F.4	Details about Computation Heights	122
Appendix G	Model Verification	123
G.1	Ground Reflection Model	123
G.2	Measurements Over Grassland	123
G.3	Measurements of Barrier Insertion Loss	124
G.4	Measurements of In-Situ Barrier Performance	124
G.4.1	Rt. 99 in Sacramento, California.	124
G.4.2	I-495 in Montgomery County, Maryland	126
REFERENCES	145
INDEX	149
FHWA TNM ANNOUNCEMENT AND ORDER FORM	155
FHWA TNM REGISTRATION CARD	161

LIST OF FIGURES

<u>Figure</u>	<u>Page</u>
Figure 1. High-level flow chart of TNM calculations.	5
Figure 2. A-Weighted Vehicle Noise Emission Levels under Cruise Conditions	8
Figure 3. First-level elemental triangle.	11
Figure 4. Maximum elemental triangle set to 10 degrees.	11
Figure 5. Absorption coefficient as a function of frequency for selected values of NRC	16
Figure 6. A-weighted sound-level emissions: Average pavement, cruise throttle.	31
Figure 7. A-weighted sound-level emissions: Automobiles, cruise throttle.	32
Figure 8. A-weighted sound-level emissions: Automobiles, full throttle.	32
Figure 9. A-weighted sound-level emissions: Medium trucks, cruise throttle.	33
Figure 10. A-weighted sound-level emissions: Medium trucks, full throttle.	33
Figure 11. A-weighted sound-level emissions: Heavy trucks, cruise throttle.	34
Figure 12. A-weighted sound-level emissions: Heavy trucks, full throttle.	34
Figure 13. A-weighted sound-level emissions: Buses, cruise throttle.	35
Figure 14. A-weighted sound-level emissions: Buses, full throttle.	35
Figure 15. A-weighted sound-level emissions: Motorcycles, cruise throttle.	36
Figure 16. A-weighted sound-level emissions: Motorcycles, full throttle.	36
Figure 17. Emission spectra: Automobiles, average pavement.	37
Figure 18. Emission spectra: Automobiles, DGAC pavement.	37
Figure 19. Emission spectra: Automobiles, OGAC pavement.	38
Figure 20. Emission spectra: Automobiles, PCC pavement.	38
Figure 21. Emission spectra: Medium trucks, full throttle.	39
Figure 22. Emission spectra: Medium trucks, cruise throttle, average pavement.	39
Figure 23. Emission spectra: Medium trucks, cruise throttle, DGAC pavement.	40
Figure 24. Emission spectra: Medium trucks, cruise throttle, OGAC pavement.	40
Figure 25. Emission spectra: Medium trucks, cruise throttle, PCC pavement.	41
Figure 26. Emission spectra: Heavy trucks, full throttle.	41
Figure 27. Emission spectra: Heavy trucks, cruise throttle, average pavement.	42
Figure 28. Emission spectra: Heavy trucks, cruise throttle, DGAC pavement.	42
Figure 29. Emission spectra: Heavy trucks, cruise throttle, OGAC pavement.	43
Figure 30. Emission spectra: Heavy trucks, cruise throttle, PCC pavement.	43
Figure 31. Emission spectra: Buses.	44
Figure 32. Emission spectra: Motorcycles.	44
Figure 33. Sound emissions, high/low energy split: Automobiles.	45
Figure 34. Sound emissions, high/low energy split: Medium trucks, cruise throttle.	45
Figure 35. Sound emissions, high/low energy split: Medium trucks, full throttle.	46
Figure 36. Sound emissions, high/low energy split: Heavy trucks, cruise throttle.	46
Figure 37. Sound emissions, high/low energy split: Heavy trucks, full throttle.	47
Figure 38. Sound emissions, high/low energy split: Buses, cruise throttle.	47
Figure 39. Sound emissions, high/low energy split: Buses, full throttle.	48
Figure 40. Sound emissions, high/low energy split: Motorcycles.	48
Figure 41. Geometrics for speed effects of upgrades and traffic-control devices.	50
Figure 42. Entrance and exit speeds.	51
Figure 43. Acceleration away from traffic-control devices: Automobiles and motorcycles.	56
Figure 44. Acceleration away from traffic-control devices: Medium trucks and buses.	56
Figure 45. Acceleration away from traffic-control devices: Heavy trucks.	57

Figure 46. Deceleration caused by upgrades 1.5 percent or more: Heavy trucks. 57

Figure 47. Speeds for Roadway 16: Upgrades. 59

Figure 48. Speeds for Roadway 22: Traffic-control devices and subsequent grades. 60

Figure 49. Initial elemental triangle. 64

Figure 50. Maximum elemental triangle set to 10 degrees. 64

Figure 51. Definition of relevant distances and angles. 66

Figure 52. Vertical geometry definitions. 74

Figure 53. Barrier face definitions. 75

Figure 54. Example berm, shown at four perturbation heights. 76

Figure 55. Propagation path through tree zone. 76

Figure 56. Single diffraction geometry. 80

Figure 57. Example of multiple diffraction. 81

Figure 58. Example of an effective single diffraction from a multiple diffraction path. 81

Figure 59. Example of a geometry with reflections. 82

Figure 60. Example directions of propagation paths. 83

Figure 61. Diffraction geometry. 89

Figure 62. Example geometry showing reflection. 95

Figure 63. Example geometry showing an impedance discontinuity. 96

Figure 64. Example geometry for corner diffraction. 97

Figure 65. Ground impedance evaluation at two frequencies. 98

Figure 66. Foss double-barrier geometry. 103

Figure 67. Typical depressed section in a highly urbanized area. 106

Figure 68. Detailed input and representative rays. 108

Figure 69. Partial reflection near tops of parallel barriers. 113

Figure 70. Subdivision of grid cells during contouring. 121

Figure 71. Ground-effect model comparison, EFR = 10 cgs Rayls. 128

Figure 72. Ground-effect model comparison, EFR = 100 cgs Rayls. 129

Figure 73. Ground-effect model comparison, EFR = 1000 cgs Rayls. 130

Figure 74. Ground-effect model comparison, EFR = 10,000 cgs Rayls. 131

Figure 75. Comparison with measurements over grassland,
distance = 35 meters (114 feet). 132

Figure 76. Comparison with measurements over grassland,
distance = 62 meters (202 feet). 133

Figure 77. Comparison with measurements over grassland,
distance = 110 meters (360 feet). 134

Figure 78. Comparison with measurements over grassland,
distance = 195 meters (640 feet). 135

Figure 79. Comparison with measurements over grassland,
distance = 348 meters (1140 feet). 136

Figure 80. Comparison of barrier insertion loss in octave bands,
receiver ht. = 1.5 m (5 ft), barrier ht. = 1.8 m (6 ft). 137

Figure 81. Comparison of barrier insertion loss in octave bands,
receiver ht. = 1.5 m (5 ft), barrier ht. = 4.9 m (16 ft). 138

Figure 82. Comparison of barrier insertion loss in octave bands,
receiver ht. = 3 m (10 ft), barrier ht. = 1.8 m (6 ft). 139

Figure 83. Comparison of barrier insertion loss in octave bands,
receiver ht. = 3 m (10 ft), barrier ht. = 4.9 m (16 ft). 140

Figure 84. Comparison of barrier insertion loss in octave bands, receiver ht. = 6 m (20 ft), barrier ht. = 1.8 m (6 ft).	141
Figure 85. Comparison of barrier insertion loss in octave bands, receiver ht. = 6 m (20 ft), barrier ht. = 4.9 m (16 ft).	142
Figure 86. Comparison of barrier insertion loss in octave bands, receiver ht. = 12 m (40 ft), barrier ht. = 1.8 m (6 ft).	143
Figure 87. Comparison of barrier insertion loss in octave bands, receiver ht. = 12 m (40 ft), barrier ht. = 4.9 m (16 ft).	144

LIST OF TABLES

<u>Table</u>	<u>Page</u>
Table 1. Sound Energy Distribution Between Sub-source Heights	9
Table 2. Ground Type and Effective Flow Resistivity	14
Table 3. Effective Flow Resistivity used for values of Noise Reduction Coefficient (NRC).	15
Table 4. Attenuation through Dense Foliage	17
Table 5. Constants for A-weighted sound-level emissions and 1/3rd-octave-band spectra.	27
Table 6. Constants for subsource-height split.	29
Table 7. Multiplier, m , for each built-in subsource height.	30
Table 8. Regression coefficients for accelerating vehicles.	54
Table 9. Regression coefficients for decelerating heavy trucks.	54
Table 10. Effective Flow Resistivity used for values of Noise Reduction Coefficient (NRC).	93
Table 11. Absorption coefficients as a function of frequency, for selected values of Noise Reduction Coefficient (NRC).	94
Table 12. Attenuation through dense foliage.	99
Table 13. Maximum attenuation for rows of buildings by frequency.	100
Table 14. Atmospheric absorption by frequency for default atmospheric conditions.	102
Table 15. Parallel-barrier degradations: Initial comparison of measured and computed values.	115
Table 16. Sensitivity of computed degradations to assumed source height.	116
Table 17. Rt. 99 CA: BEFORE (no barrier) levels.	125
Table 18. Rt. 99 CA: AFTER (barrier) levels.	125
Table 19. Rt. 99 CA: Barrier insertion loss.	126
Table 20. I-495 MD: AFTER (barrier) levels.	127

1. OVERVIEW

The Federal Highway Administration Traffic Noise Model (FHWA TNM[®]), like many other noise prediction models, computes a predicted noise level through a series of adjustments to a reference sound level. In the TNM, the reference level is the Vehicle Noise Emission Level, which refers to the maximum sound level emitted by a vehicle pass-by at a reference distance of 15 meters (50 feet). Adjustments are then made to the emission level to account for traffic flow, distance, and shielding. These factors are related by the following equation:

$$L_{Aeq1h} = EL_i + A_{\text{traff}(i)} + A_d + A_s , \quad (1)$$

where EL_i represents the vehicle noise emission level for the i^{th} vehicle type (Sections 1.1 & 2.1),

$A_{\text{traff}(i)}$ represents the adjustment for traffic flow, the vehicle volume and speed for the i^{th} vehicle type (Sections 1.2 & 2.3.2),

A_d represents the adjustment for distance between the roadway and receiver and for the length of the roadway (Sections 1.2 & 2.3.3), and

A_s represents the adjustment for all shielding and ground effects between the roadway and the receiver (Sections 1.3 & 2.4).

The TNM is based on a three-dimensional coordinate system and is designed to run on a personal computer (PC).¹ This manual documents the equations and algorithms that form the TNM.

1.1 Vehicle Emission Levels

The TNM incorporates an entirely new data base of vehicle noise emission levels, based on measurements conducted throughout the U.S. in 1994 and 1995 [Fleming 1995]. Components of those data include:

- # Slow-speed and accelerating vehicles
- # Bus and motorcycle data
- # Vehicles on grade
- # Vehicles on different pavement types, including dense-graded asphaltic concrete (DGAC), open-graded asphaltic concrete (OGAC), and Portland cement concrete (PCC).

Other aspects of the noise emission data are:

- # Energy apportioned to two source heights: one at the pavement level and one at 1.5 meters (5 feet) above the pavement, except for heavy trucks, where the upper height is 3.66 meters (12 feet) above the pavement.
- # Data stored in $\frac{1}{3}$ -octave bands.

¹ See the User's Guide for details on the recommended PC platform.

Further details on vehicle noise emission levels are given in Section 2.1 and Appendix A of this manual.

1.2 Free Field Levels

Characteristics of the free-field noise level computations include:

- # TNM computes three different sound-level descriptors, depending on user selection: the energy-equivalent sound level over a one-hour time period (IHEQ, represented by the symbol, L_{Aeq1h}), the average day-night sound level (DNL, represented by the symbol, L_{dn}), or the average day-evening-night sound level, designated as the Community Noise Equivalent Level (CNEL, represented by the symbol, L_{den}).²
- # Traffic control devices can be inserted, and the TNM computes vehicle speeds and emission levels accordingly. Such devices include traffic signals, stop signs, toll booths, and on-ramp start points.
- # Computations are performed in $\frac{1}{3}$ -octave bands for increased accuracy; this aspect is not visible to users.
- # The TNM computes noise contours if specified; the NMLOT Version 3.05 contouring program is used for compatibility with the Federal Aviation Administration's Integrated Noise Model (INM) Version 5.0 and higher [Olmstead 1996], and the U.S. Air Force's NOISEMAP program [Moulton 1990].

More details on the computation of vehicle speeds are given in Section 2.2 and Appendix B of this manual; details on the computation of free field levels are given in Section 2.3 and Appendix C.

1.3 Shielding and Ground Effects

The TNM incorporates state-of-the-art sound propagation and shielding algorithms. These algorithms are based on fairly recent research on sound propagation over ground of different types, atmospheric absorption, and the shielding effects of barriers, berms, ground, buildings, and trees. The TNM does not account for atmospheric effects such as varying wind speed or direction or temperature gradients. The TNM propagation algorithms assume neutral atmospheric conditions. Characteristics of the propagation algorithms include:

- # Ground location and type is incorporated in the TNM. Users input terrain lines to define ground location. Users input default ground type or define ground zones to specify ground type, which varies in acoustic "hardness" (effective flow resistivity).
- # Berms can be defined, with user-selectable heights, top widths and side slopes; they are computed as if they were terrain lines.
- # Rows-of-buildings attenuation is included, with user-definable height and percentage of area blocked relative to the source roadway(s).
- # Tree zones can be defined; the ISO standard for attenuation by dense foliage is used [ISO 1996].

² All noise descriptors in the TNM are consistent with the definitions in American National Standard, ANSI S1.1-1994, Acoustical Terminology [ANSI 1994].

- # Multiple reflections between parallel barriers that flank a roadway are computed in two dimensions, unlike other TNM acoustics, which are computed in three dimensions. This is discussed further in Section 1.5 and Appendix E.
- # Double-barrier diffraction is included. The net effect of diffraction from the most effective *pair* of barriers, berms or ground points that interrupt the source-receiver line-of-sight is computed. The other objects that interrupt the path are ignored.

More details on the computation of shielding and ground effects are given in Sections 2.4, 2.5, 2.6, and Appendix D of this manual.

1.4 High-level Flow Chart

This section presents a flow chart to outline the overall flow of the TNM during sound level calculation. It is presented as Figure 1.

1.5 Parallel Barrier Analysis

A two-dimensional multiple-reflections module has been included within the TNM for computing the degradation of barrier performance due to the presence of a reflective barrier on the opposite side of the roadway. The results from this module are generalized by the user to modify the TNM's results where multiple reflections exist. The module is most effective in computing the effects of sound-absorbing material on the surfaces of barriers or retaining walls. More details on the parallel barrier module are given in Appendix E of this manual.

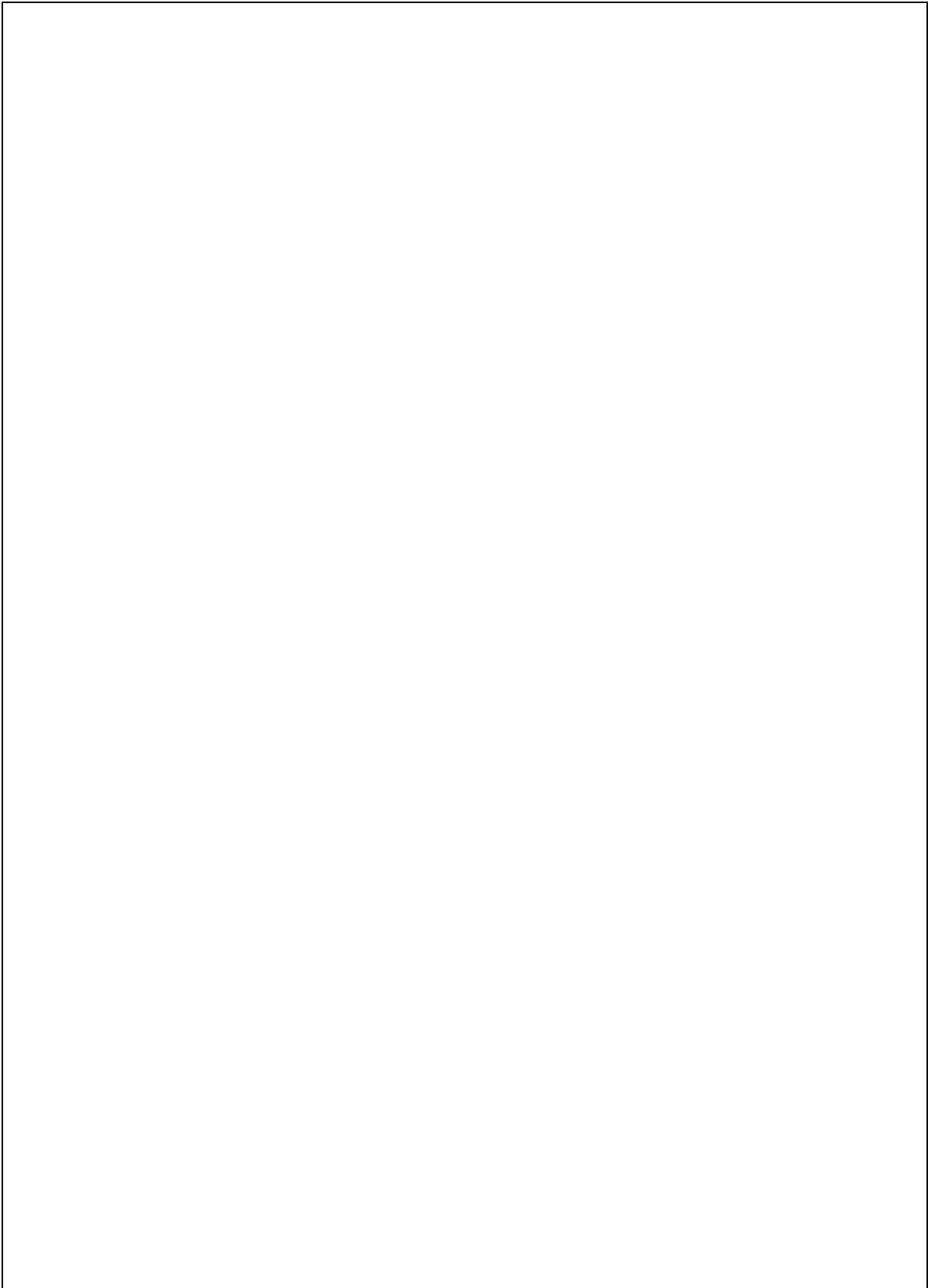


Figure 1. High-level flow chart of TNM calculations.

2. MODEL DESCRIPTION

The following section of the manual describes the basic formulation, capabilities and logic flow of the FHWA TNM[®]. As appropriate, references are given to the literature and the detailed appendices. This section limits mathematical description to a minimum; some equations are used where necessary for clarity. The detailed mathematical description is given in the appendixes.

The organization of this section roughly parallels that of the preceding Section 1. First, vehicle noise emission levels are discussed (Section 2.1), followed by discussions of vehicle speed computation (Section 2.2), and free-field noise levels (Section 2.3). A large section is then devoted to the “vertical geometry” and acoustics (Section 2.4), including the basis of the acoustical model, the combining of two cross sections to represent an “elemental triangle,” elements in the propagation path, and the logic flow and the geometry modeling of path elements. A section is devoted to the two-dimensional parallel-barrier calculation module (Section 2.5), and lastly, a section on noise contours is included (Section 2.6).

2.1 Vehicle Noise Emission Levels

In 1994 and 1995, the Volpe National Transportation Systems Center Acoustics Facility organized and collected vehicle pass-by noise emission data as the basis for a new emissions data base for the TNM [Fleming 1995]. Approximately 6000 vehicles were measured in 9 states. As described in Section 1, data were collected for many vehicles under various operating conditions. The data base includes automobiles (2 axles and 4 tires), medium trucks (2 axles and 6 tires), heavy trucks (3 or more axles and 6 or more tires), buses (2 or 3 axles and 6 or more tires) and motorcycles (2 or 3 tires). Data were collected for vehicles cruising, accelerating, idling, and for vehicles on grades. In addition, data were obtained for vehicles traveling different pavement types, including DGAC, OGAC, and PCC. Both **a**-octave band data and A-weighted sound level data were collected.

Figure 2 shows the A-weighted noise emission levels as a function of speed for autos, medium trucks, heavy trucks and buses under cruise conditions and traveling over average pavement (DGAC and PCC combined). The complete set of emission level curves for all vehicle types under all conditions is given in Appendix A. The appendix also shows the generalized vehicle spectra at various speeds. The **a**-octave band emission level spectra are used by the TNM for all sound level calculations.

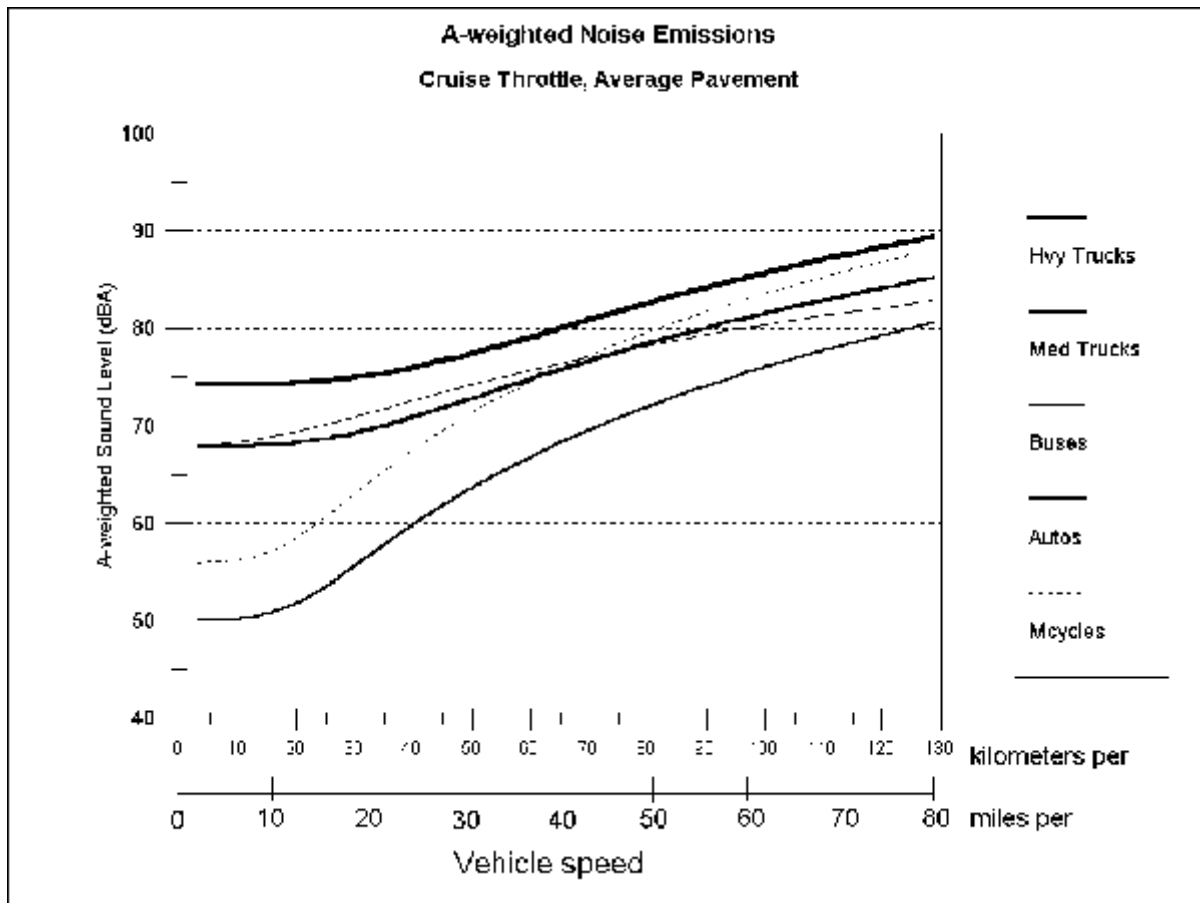


Figure 2. A-Weighted Vehicle Noise Emission Levels under Cruise Conditions

Noise data acquisition methods, data analysis procedures, and the complete set of emission levels for vehicles under all conditions are documented in *Development of National Reference Energy Mean Emission Levels for the FHWA Traffic Noise Model* [Fleming 1995]. Additional detail pertaining to accelerating vehicles are documented by Bowlby [Bowlby 1997].

TNM uses the full-throttle emission levels where there is an upgrade roadway (heavy trucks only on grades equal to 1.5 percent or more) or where user-entered traffic control devices indicate an acceleration condition. (The next section discusses speed computations associated with these conditions.)

An additional field study was undertaken to determine the effective source heights of various vehicles [Coulson 1996]. This study assigned two “sub-source” heights to each vehicle type. They are 0 meters (0 feet) and 1.5 meters (5 feet) above the pavement for all vehicles except heavy trucks, where the upper source is 3.66 meters (12 feet) above the pavement. The study also determined the ratio of sound energy distributed at the lower and upper heights as a function of frequency, vehicle type, and throttle condition (cruising or full throttle). Table 1 shows the percentage of total emission sound energy distributed to the upper source height at the low frequencies and at the high frequencies. In the middle

frequency range, between 500 and 2000 Hz, the sound energy distribution transitions gradually between the two values. Further detail about the energy distribution is presented in Appendix A, including curves showing the sound energy split by frequency for each vehicle type.

Table 1. Sound Energy Distribution Between Sub-source Heights

Vehicle Type	Operating Condition	Percentage of Total Sound Energy at Upper Sub-source Height: 1.5m (5 ft), except 3.66m (12 ft) for HT	
		At Low Frequencies (500 Hz and below)	At High Frequencies (2000 Hz and above)
Autos	Cruise or Full Throttle	37%	2%
Medium Trucks & Buses	Cruise	57	7
Medium Trucks & Buses	Full Throttle	58	13
Heavy Trucks	Cruise	37	26
Heavy Trucks	Full Throttle	37	28
Motorcycles	Cruise or Full Throttle	58	13

Further detail about the energy distribution is presented in Appendix A, Section A.4.

2.2 Vehicle Speed Computation

The TNM computes adjusted speeds based on the user input speeds, roadway grade, and traffic control devices. For level or down-grade roadways, TNM uses the speeds assigned to the roadway by the user (the “input speed”). For heavy trucks (only) on upgrades equal to 1.5 percent or more, TNM reduces the input speeds. The speeds are reduced depending on the steepness and length of the upgrade in accordance with speed-distance curves similar to those published for geometric design by the American Association of State Highway and Transportation Officials [AASHTO 1990 and TRB 1985]. The TNM speed-distance curves were calibrated to the speeds measured during the emission level noise measurement program. Appendix B describes the details of these computations and gives examples.

The TNM allows the user to enter the following traffic-control devices: traffic signals, stop signs, toll booths, and on-ramp start points. The reason for these devices is to allow a more precise modeling of vehicle speeds and emission levels under these interrupted-flow conditions. TNM will compute speeds all along any roadways with traffic control devices. These devices abruptly reduce speeds to the device's “speed constraint,” for the device's “percentage of vehicles affected.” Stop signs, toll booths, and on-ramp start points affect 100 percent of the vehicles. However, traffic signals affect only the portion of the traffic stopped at the red signal phase, so the TNM allows the user to define the percentage of vehicles affected by traffic signals. Speed computations are stopped at whichever comes first: the vehicles accelerate back up to the user's input speed, or the end of the current roadway. TNM never tracks vehicles from one roadway to the next when computing speeds. Appendix B provides more

detailed descriptions of the way speeds are computed and the conditions under which they are computed.

2.3 Free Field Levels and Horizontal Geometry

The following section describes the way the TNM computes free-field sound levels. In this section, we define two of the three adjustment terms in the equation for L_{Aeq1h} presented in Section 1, $A_{\text{traff}(i)}$ for traffic flow and A_d for distance and roadway length. First, the way in which TNM divides up the “horizontal geometry” into “elemental triangles” is described.

2.3.1 Elemental triangles.

The term “horizontal geometry” represents the x - y plane (the geometry in plan view). Before any details in the vertical plane (z direction) are evaluated, TNM must break down the overall geometry into small “elemental triangles,” each defined by a receiver and two points on a roadway segment. An elemental triangle is the smallest unit of a roadway line segment that TNM evaluates; there can be no points inside an elemental triangle, only at its edge. Various input objects may cross inside the triangle, such as barriers, terrain lines, buildings, and tree zone lines. The acoustical effects of these elements are considered separately, and are discussed below in Section 2.4.2. Figure 3 shows how first-level roadway-to-receiver elemental triangles are defined by the closest spacing of the object endpoints in the x - y plane.

To ensure sufficient precision where object endpoints are not closely spaced (as in Figure 3), TNM divides elemental triangles so that the maximum subtended angle is no larger than a fixed size. For example, Figure 4 shows Figure 3 after TNM imposes upon it a maximum angle of 10 degrees. Further subdivision of elemental triangles is not performed.

The primary factors of concern in the horizontal geometry are roadway geometry relative to the receiver, and traffic flow. These combine with the vehicle noise emission levels to produce an overall free-field sound level at the receiver associated with each elemental triangle.

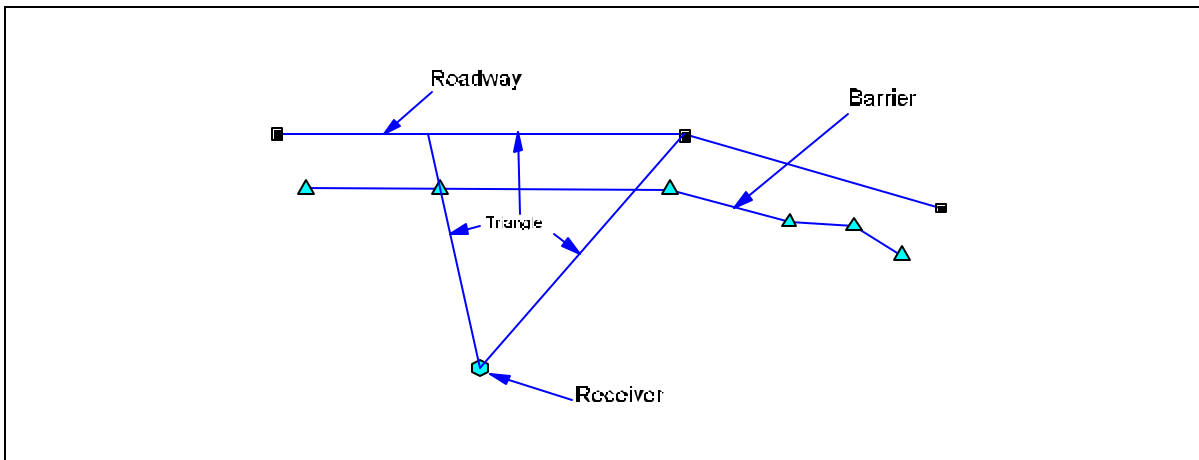


Figure 3. First-level elemental triangle.

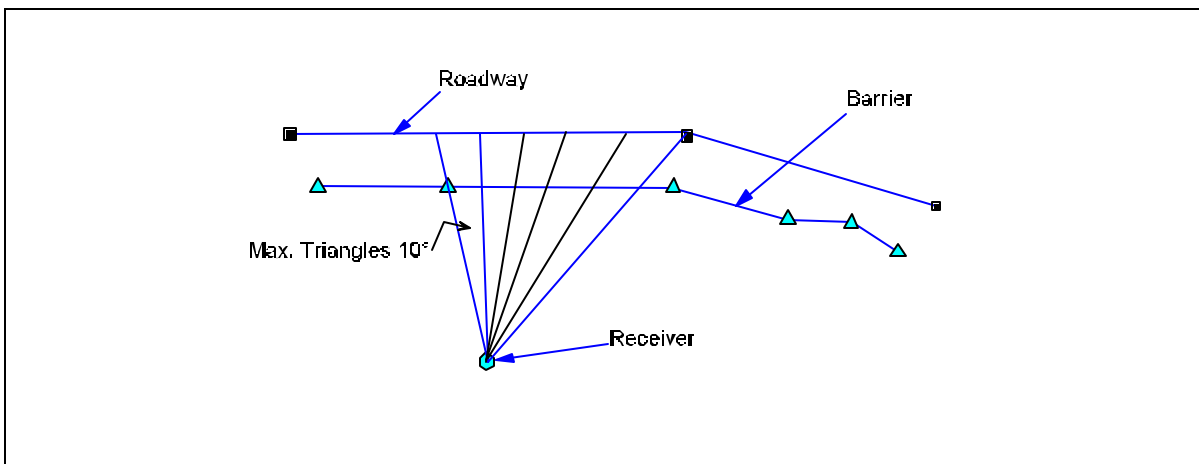


Figure 4. Maximum elemental triangle set to 10 degrees.

2.3.2 Traffic flow adjustment.

The adjustment for traffic flow is simply a function of vehicle volume (number of vehicles per hour) and speed. Of course, the adjustment is computed separately for each vehicle type:

$$A_{\text{traff}(i)} = 10 \times \text{Log}_{10} \left(\frac{V_i}{S_i} \right) - 13.2 \text{ dB}, \quad (2)$$

where V_i is the vehicle volume in vehicles per hour,
and S_i is the vehicle speed in kilometers per hour.

Although not shown here, the computation of $A_{\text{traff}(i)}$ is performed in a -octave bands for each sub-source height. Those details are shown in Appendix C.

Computation of L_{dn} and L_{den} : TNM will compute L_{dn} or L_{den} instead of L_{Aeq1h} , if specified by the user. The only differences for computation are the time-of-day weightings and the traffic volumes. For L_{dn} for example, users specify the percentages of total daily traffic volume that occur during the daytime and nighttime periods. TNM multiplies the nighttime traffic volume by 10 to account for the 10-dB nighttime weighting, before combining with the daytime traffic. Details on calculation of the equivalent volume are given in Appendix C.

2.3.3 Distance and roadway length adjustment.

The adjustment for distance from the elemental roadway segment to the receiver and for the length of the segment is given by the following:

$$A_d = 10 \times \text{Log}_{10} \left[\left(\frac{15}{d} \right) \left(\frac{a}{180} \right) \right] \text{ dB} , \tag{3}$$

where d is the perpendicular distance to the line representing the roadway segment in meters, and θ is the angle subtended by the elemental roadway segment in degrees.

This adjustment is the same for all vehicle types, source heights and frequencies. TNM uses a different equation for cases where the three points of the elemental triangle are collinear ($d = 0$ and $\theta = 0$) or nearly collinear. The equation is based on the distances from the receiver to the two endpoints of the elemental roadway segment (d_1 and d_2):

$$A_d = 10 \times \text{Log}_{10} \left[\frac{|d_2 - d_1|}{d_2 d_1} \right] + 12 \text{ dB} . \tag{4}$$

Appendix C illustrates these adjustments in more detail.

2.4 Vertical Geometry Acoustics

This section of the manual describes the “vertical geometry acoustics,” the acoustical propagation algorithms that are used to compute A_s , the adjustment for ground effects and shielding. The description of the vertical geometry acoustics has been divided into four subsections. The first describes the basis of the acoustical model, the second deals with the results for an entire elemental triangle, the third discusses how various elements in the propagation path are handled, and the fourth presents the logic flow and geometry modeling. In this section, all references are to the two-dimensional vertical plane (except for brief references to elemental triangles), and all of the computations are based on point-source mathematics. Appendix D provides a more complete description of the implementation of the vertical geometry algorithms and the mathematics behind them.

2.4.1 Basis of the acoustical model.

The TNM’s acoustical algorithms for determining the effects of ground and shielding are based on fairly recent sound propagation research. Reflection from ground of finite impedance is based on the work

of many researchers over the past 20 years. Chessell [Chessell 1977] described the approach used within TNM to compute the reflection coefficient. His formulation incorporated and expanded on the work of many others, including Delany and Bazley [Delany 1970], who derived a way to define the normal acoustic impedance of the ground by means of a single parameter, the effective flow resistivity (EFR). Embleton, Piercy, and Daigle [Embleton 1983] later determined appropriate values of EFR for ground of various types (acoustic hardness) by comparing computed values of the interference between direct and reflected paths to those measured over selected ground types. The TNM incorporates selected ground types with values of EFR based on these measurements.

The diffraction model is based on Fresnel diffraction theory, as described by De Jong, Moerkerken, and Van der Toorn [De Jong 1983]. In their formulation, the authors incorporated diffraction from wedges, berms, barriers and impedance discontinuities on the ground (such as where pavement meets grass). The TNM incorporates all of the components of De Jong's formulation for diffraction. De Jong's approach works well for a limited number of reflections and diffractions in series, but it cannot correctly compute the large number of components that could make up a typical highway cross-section geometry. For these more complex geometries, the TNM creates a straight-line regression fit to the (two-dimensional) ground and averages the ground impedance in the vicinity of the reflection point using the approach recently described by Boulanger, Waters-Fuller, Attenborough and Li [Boulanger 1997]. This method has been validated through scale-model measurements, and agrees well with the De Jong model for simpler cases, where the De Jong model performs properly.

2.4.2 Elemental triangles.

As described in Section 2.3.1, elemental triangles represent the smallest unit of roadway segment evaluated by TNM; they represent the "building blocks" for the entire roadway line source. The attenuation due to shielding and ground effects (A_s) is computed by the vertical geometry acoustical algorithms in the two-dimensional vertical plane using point-source mathematics. The attenuation is computed separately for each side (leg) of the triangle, and the attenuation for the triangle as a whole is the energy average of the attenuations along the two legs of the triangle.

2.4.3 Elements in the propagation path.

This section describes the individual elements that may be present in the propagation path. A more detailed discussion of how the elements are implemented in the TNM is presented in Appendix D.

Ground points and segments: A ground point defines the location of the ground. Ground points are always placed below the source and receiver, and at the edge of roadways. Terrain lines define the ground explicitly and become ground points in the vertical geometry. Other elements in the geometry define ground points, including barriers, berms, rows of buildings, and ground zone boundaries. In the calculations, berms are converted to either three or four ground points; the base of the berm is defined by two points, and the top is defined by either one (if the top width is less than 0.1 m, i.e., a wedge) or two points.

Ground points define ground segments in which reflections can occur. Sound reflection from ground segments of different types can be very different. The interference between the direct and reflected paths over soft ground (low EFR) often creates substantial destructive interference (cancellation) across a broad range of frequencies, typically between 200 Hz and 1000 Hz. This is the "ground-effect" interference that causes excess attenuation over soft ground. The softer the ground is, the greater the

ground-effect attenuation is for sources and receivers relatively near the ground. The TNM allows users to enter various ground types, which are based on the effective flow resistivity measured by Embleton [Embleton 1983]. The ground types and associated EFR are given in Table 2.

Table 2. Ground Type and Effective Flow Resistivity

Ground Type Name	Effective Flow Resistivity (cgs Rayls)
Pavement *	20,000
Water	20,000
Hard Soil (& dirt road)	5,000
Loose Soil (& gravel)	500
Lawn	300
Field Grass *	150
Granular Snow	40
Powder Snow	10

* Note: TNM's Pavement and Water ground types represents a generic acoustically hard ground surface. TNM's Field Grass ground type represents a generic acoustically soft ground surface.

Impedance discontinuities: Impedance discontinuities occur where one ground type changes to another. An impedance discontinuity can occur without the user specifying one explicitly, as at the edge of the roadway when the default ground type is “lawn.” They also occur where a user has entered a “ground zone” with a different ground type from the default.

Diffraction components are often computed at impedance discontinuities. Where a reflection occurs near an impedance discontinuity, a diffracted path from the impedance discontinuity must be computed to modify the magnitude and phase of the reflected path. The diffracted component is needed for the sound field to remain continuous across the discontinuity.

Barriers: Barriers stand vertically, have a base (ground) point, a height, and Noise Reduction Coefficient (NRC) associated with their sides. Barriers may be specified with multiple heights (height “perturbations”). The TNM can compute diffraction from the barrier top and its base points on both sides.

The De Jong [De Jong 1983] model requires computation of reflections in the barrier surfaces to compute single-barrier diffraction properly. This is the way the model accounts for the pressure doubling that occurs at the barrier top on the source side. In these reflections, the NRC on the barrier's surface influences the diffracted sound energy. The effect is relatively small: approximately 1 dB to 1½ dB additional barrier insertion loss for NRC's in the range of 0.7 to 0.9 for a 4.6-meter (15-ft) barrier and mixed traffic.

The users specify an NRC for a barrier surface, which is then used to compute a reflection coefficient. The approach taken to determine a reflection coefficient based on barrier surface NRC follows the approach used for ground surfaces, to maintain consistency within the model. As with ground, the barrier's surface impedance is computed from a value of effective flow resistivity (EFR). The approach is described in detail in Appendix D; it is described here briefly. The absorption coefficient at a given frequency is related to the "reflection factor," which is a function of the impedance of the surface and the impedance of air. The surface impedance was derived from the EFR from Delany's empirical fit for fibrous materials [Delany1970]. Individual values of EFR were found that corresponded to values of NRC (see Table 3). This approach allowed a single parameter to be used for each value of NRC chosen by the user. Figure 5 shows the absorption coefficients as a function of frequency that are used within TNM for selected values of NRC.

Table 3. Effective Flow Resistivity used for values of Noise Reduction Coefficient (NRC).

NRC	EFR(cgs rayls)
0.00	20000.0
0.05	4250.0
0.10	1570.0
0.15	865.0
0.20	555.0
0.25	385.0
0.30	282.0
0.35	214.0
0.40	165.0
0.45	129.0
0.50	102.0
0.55	81.0
0.60	64.0
0.65	50.0
0.70	39.0
0.75	30.0
0.80	22.0
0.85	16.0
0.90	10.4
0.95	5.5
1.00	0.1

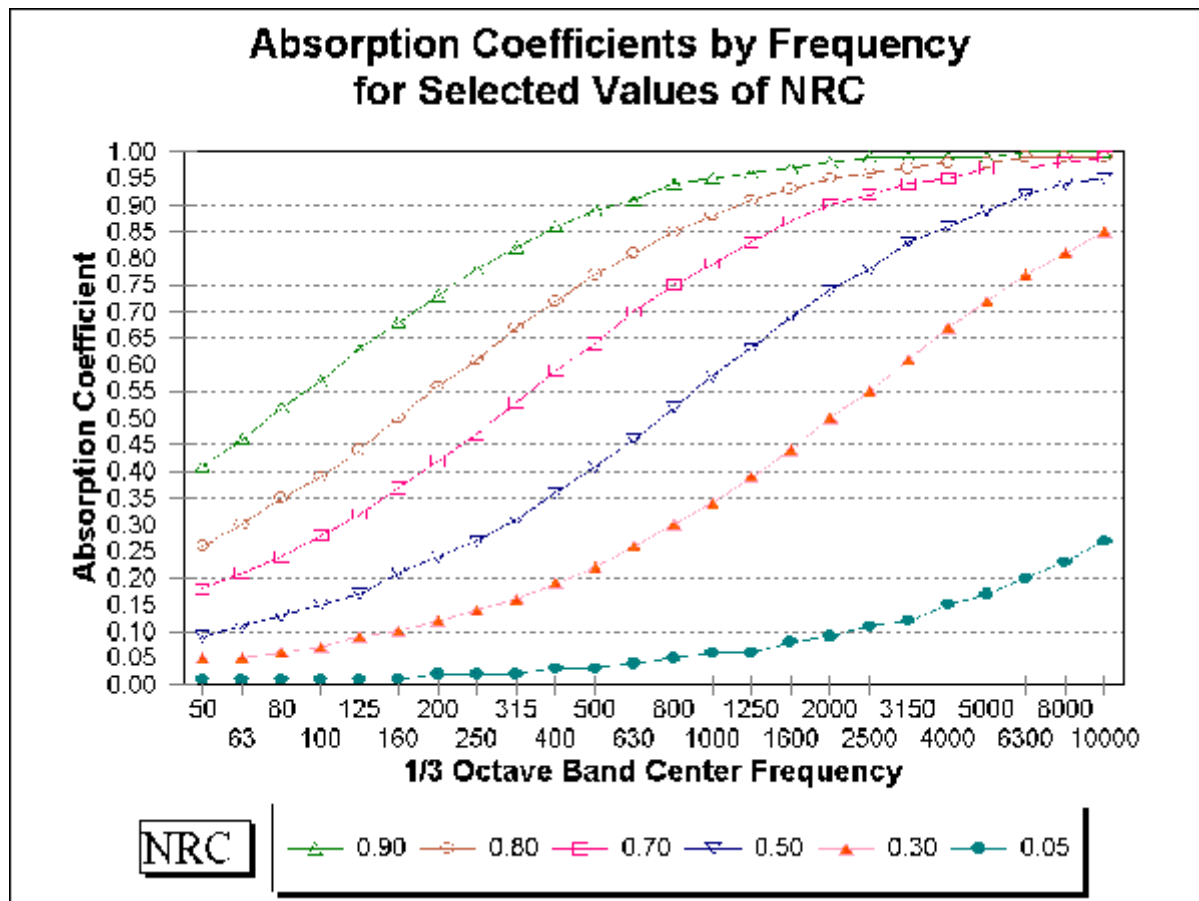


Figure 5. Absorption coefficient as a function of frequency for selected values of NRC

Berms: To the TNM's acoustical calculations, berms are simply a series of ground points. Users have the option of entering berms as a type of barrier, with heights, top widths, and side slopes. In that case, the TNM's vertical geometry routines must compute the location of the intersections between the bases of berms and the ground. Those intersections then become ground points in the vertical geometry. Berms that break the source-to-receiver line of sight and that are defined with a finite top width have two diffracting edges. This will lead to somewhat greater insertion loss than for "wedges" (berms with no top width). Although TNM maintains a default value of 0 for berm top width, the width can be changed. However, TNM has shown some apparent anomalies in the diffraction algorithms for berms with a top width.

Berms assume the default ground type or, if a berm is inside a ground zone, the type of ground defined for that zone. Therefore, if the default ground type is "lawn" or "field grass" berms will be earth berms and diffraction will be computed accordingly. If the default ground type is "pavement," the berm will be acoustically hard.

Tree zones: The TNM incorporates tree zones as an optional element in the propagation path. Tree zones have both ground height and top height, and therefore define ground points at their edges. The vertical geometry algorithms compute the distance the propagation paths travel through tree zones. TNM uses the 1996 ISO standard attenuation for dense foliage [ISO 9613-2], which is defined as “sufficiently dense to completely block the view along the propagation path; i.e., it is impossible to see a short distance through the foliage.” The octave-band attenuation as a function of distance through foliage is given in Table 4. In TNM, the octave-band values shown in Table 4 are applied to each of the $\frac{1}{3}$ -octave bands within the associated octave band.

Table 4. Attenuation through Dense Foliage

Octave-band center frequency (Hz)	63	125	250	500	1K	2K	4K	8K
Attenuation (dB, total) for d_f (distance through foliage) less than 10 meters (33 feet)	0	0	0	0	0	0	0	0
Attenuation (dB, total) for d_f between 10 meters (33 feet) and 20 meters (66 feet)	0	0	1	1	1	1	2	3
Attenuation (dB per meter) for d_f between 20 meters (66 feet) and 200 meters (660 feet)	0.02	0.03	0.04	0.05	0.06	0.08	0.09	0.12
Maximum attenuation (dB) for $d_f \leq 200$ meters (660 feet)	4	6	8	10	12	16	18	24

Building rows: The TNM incorporates rows of buildings as optional elements in the propagation path. Like tree zones, they have both ground height and top height, but building rows have no width. Rows of buildings are also characterized by a “building percentage,” the percentage of area in a single row blocked by buildings. The building percentage and the height are both used in computing the attenuation of the most effective intervening row, according to the equation of the German rail industry standard [Kurze 1988] (see Appendix D for details). The number of rows of buildings also factors into the total attenuation, adding 1½ dB for each additional row after the most effective. A maximum of 10 dB attenuation is allowed (based on a mixed-traffic spectrum; the limits are 8.4 dB at 500 Hz and 10.4 dB at 1000 Hz). Rows of buildings are not treated like barriers within TNM, in that propagation paths are allowed to go through building rows. TNM restricts users from entering building percentages greater than 80 percent or less than 20 percent. Therefore, users must employ barriers to model building rows without significant gaps between the buildings.

Atmospheric absorption: TNM incorporates variable atmospheric absorption depending on temperature and relative humidity as specified by the user. The 1993 ISO standard is used [ISO 9613-1]. Details of the equations employed are given in Appendix D.

2.4.4 Logic flow and geometry modeling.

This section outlines the logic and the modeling approaches incorporated in TNM's vertical geometry algorithms; it describes the process of evaluating a leg of an elemental triangle. Many of the modeling approaches discussed relate to limits placed on TNM's computations to enhance run time or to constrain array sizes. For example, limits have been placed on the number of barriers and the number of ground points that are calculated. All of the topics presented are covered in greater detail in Appendix D, often with illustrations and examples.

Perturbable barriers: The TNM has been designed to handle up to two perturbable barriers in the source-receiver path. If three or more perturbable barriers are encountered, TNM will choose the most effective pair of barriers based on their *input* heights. This test is performed at the beginning of the evaluation of a given vertical geometry, and TNM then discards all other perturbable barriers for the remainder of the elemental triangle's analysis. This conservative approach allows only two barriers in series, limiting total attenuation. The choice of the most effective pair of barriers is made with the "Foss selection algorithm" [Foss 1976]. This is a relatively simple and quick procedure that computes attenuation for two barriers in series from path length differences. The procedure follows directly from Foss' scale model measurements, which show good agreement with the algorithm. The equations and an illustration are given in Appendix D.

Highest path points, including barriers and ground points: The TNM next determines how many points in the geometry cause the shortest path from the source to receiver to diffract downward. These "highest path points" (HPPs) could be barriers or ground points, which could be associated with berms, terrain lines or roadways. If three or more HPPs are encountered, TNM will not compute diffraction from all of them, and only the most effective pair is retained. Again, the choice is made with the Foss selection algorithm. The primary reason for excluding more than two HPPs from calculation was that additional points would cause additional diffraction, reducing sound levels, and no empirical data on such multiple diffraction was available for the purpose of validation.

Initial geometry smoothing: The next step in the process involves the "smoothing" away of multiple ground points that have small effects on the overall shape of the ground. This is performed to reduce computation time, since the effect on the sound level is small. The smoothing algorithm has been designed to make only small changes to the vertical geometry. Only inflection points in terrain of the same ground type are considered for smoothing (including small berms); ground-impedance discontinuities are never smoothed away.

Regression ground and near-highest path points: The TNM next evaluates the complexity of the geometry and if necessary, approximates it as discussed below. To enable TNM to handle complex geometry and to improve run time for those cases, straight-line approximations to the ground has been combined with a method of ground-impedance averaging [Boulanger 1997], which is described below as it occurs in the logic flow. This (combined) approach is used where more diffraction points are encountered than the De Jong model can properly handle, such as would be encountered with one or more intervening roadways or hilly terrain. Potential diffraction points occur at each impedance discontinuity and at each ground inflection point that has not been smoothed away by the initial smoothing algorithm (described above).

Ground regression is performed at this stage in the process. The ground regression is performed differently for two different frequency regions. For the potentially most significant diffraction point in the geometry, a test is performed to determine if the point is in the source-to-receiver Fresnel zone for

$N > -0.3$. If the point is inside that zone, a transition frequency, f_T , at which the point moves outside of the Fresnel zone is computed. Then, for frequencies above f_T , the ground regression algorithm approximates the ground between “source” and “receiver” (either of which can be a highest path point), and the sound propagation paths are generated (see below) based on that representation of the ground. For frequencies below f_T , the point is designated a “near-highest path point” (NHPP) and the ground regression algorithm is used separately to approximate the ground between the source and the NHPP and again between the NHPP and the receiver. A separate set of propagation paths are then generated for the revised geometry, including the NHPP as a diffraction point. By using different representations of the geometry based on the frequency-dependent significance of individual points allows for a more continuous change in the overall sound level as the position of a point in the geometry is gradually changed (such as with a barrier perturbation).

Any impedance discontinuities present in the original geometry are projected onto the regression ground line(s), and the ground-impedance averaging is performed as described below, after the paths are constructed.

Propagation path generation: In the next step, TNM generates all possible direct, reflected and diffracted paths between the true source and receiver. If a near-highest path point is designated in the geometry, the set of sound propagation paths is different for frequencies below and above f_T .

Path significance test: Next, a Fresnel zone test is used for each *propagation path* generated, to determine if the path is significant enough to be included for computation. Segments of the path that include bright-zone diffraction points are evaluated relative to paths that do not include those points. A path is considered significant and is computed if the receiving point falls into the region where the Fresnel number is greater than -0.3. To maintain continuity of results, the test is performed at a low frequency, 250 Hz. Since $N = 2^*/8$, the path length difference, $*$, must be greater than 0.2 meters (0.7 feet) for a path to be excluded. This quick test was incorporated into the TNM to avoid the time-consuming computation of the many possible diffraction paths in the more complex geometries with barriers. For example, the diffraction from the bottom edges of tall barriers will often be eliminated, because the contribution to the total sound level will be insignificant. Note that this test is performed for bright-zone diffractions only, and that all diffraction paths where the receiving point is in the shadow zone are assumed to be significant.

Ground-impedance averaging: The Boulanger approach to ground-impedance averaging is then used for cases where: (1) more than one impedance discontinuity is present in the local geometry between source and receiver or highest path points; or (2) a single discontinuity has not been chosen to be computed explicitly (as it would if designated a *near* highest path point). Instead of computing the multiple diffraction paths explicitly, this approach computes a Fresnel ellipse about the reflection point on the ground and computes the *area* inside the ellipse represented by each type of ground. Then, an average reflection coefficient is computed from the reflection coefficient for each ground type weighted by the ratio of its area to the total area. The average reflection coefficient is used, and no diffraction terms are computed at all. However, the size of the ellipse is a function of frequency, so the average impedance and therefore the reflection coefficient will often change for each \mathbf{a} octave band. Appendix D explains this approach further and includes an illustrative example.

Sum over propagation paths: Finally, for each \mathbf{a} -octave frequency band, TNM computes contributions to the acoustic pressure from each propagation path at the receiver. The complex sum (magnitude and phase) of each these paths represents the combined effect of all of the paths and all of

the elements in each path. This sum is then referenced to the free field pressure to determine the adjustment factor, A_s , for shielding and ground effects.

2.5 Parallel Barrier Analysis

The TNM incorporates a two-dimensional ray-tracing module for computing multiple sound reflections [Menge 1991]. The module is designed to assist users in calculating the acoustical effects of parallel barriers or retaining walls on both sides of a highway.

Two things change acoustically when a roadway is flanked by parallel barriers or retaining walls. First, direct lines-of-sight between vehicles and receivers are interrupted by the intervening barrier or retaining wall. Second, the parallel barriers or retaining walls cause multiple reflections of the noise, from side to side across the roadway. The resulting reverberation tends to increase noise levels at receivers; this increase is called “degradation” of barrier insertion loss.

The TNM’s regular sound-level computations cannot take multiple reflections into account, and therefore cannot predict the degradation of barrier performance due to parallel barriers or retaining walls. However, TNM contains a special module that can be used to compute values of degradation due to multiple reflections in two dimensions.

Users enter the vertical-plane cross-section geometry and assign values of NRC to each surface. (Appropriate values of NRC are 0.05 for hard surfaces like pavement and concrete walls, and 0.30 for grass.) The module can handle very general cross sections, including tilted barriers and walls.

TNM’s multiple-reflections module begins its computation of parallel-barrier degradation by tracing individual acoustic rays outward from each traffic noise sub-source. Some rays come close enough to receivers or diffraction edges to register a “hit” and therefore contribute their portion of sound energy to the total. For these rays, TNM computes the effects of divergence, ground attenuation, absorption upon reflection, and barrier attenuation, to derive two sound levels at each receiver. One level is based on all multiple reflections and the NRCs entered by the user. The second is similar, except that rays that hit one of the flanking barriers or retaining walls are completely absorbed, as if the barrier or wall were not there. Then TNM subtracts the two sound levels at each receiver, to obtain the degradation value.

The TNM’s multiple-reflections module allows complete flexibility in cross-sectional geometry, the location of roadways between the parallel barriers or retaining walls, and the location of adjacent receivers. The resulting parallel-barrier degradation is a function of: (1) traffic on each roadway; (2) the location of the roadways; (3) the detailed location, orientation, and NRC of each reflecting surface; (4) the location of the diffracting edges at each side of the cross section; and (5) the location of each receiver.

Appendix E contains details of TNM’s parallel-barrier computations.

2.6 Contours

The TNM computes sound levels and analyzes barrier designs at receivers that are individually entered by the user. In addition, the TNM allows the user to compute contours within specified contour zones. Three types of contours are available:

- # Sound-level contours for a specified barrier design, in the user's chosen set of sound-level units:
 L_{Aeq1h} , L_{dn} , or L_{den}
- # Insertion-loss contours for a specified barrier design
- # Level-difference contours between two specified barrier designs.

To compute contours, TNM first generates a regular grid of special receivers within the user's contour zone. It then interpolates the ground elevation and computes the sound level at each such receiver, at the receiver height above the ground. If needed, it subdivides each grid cell and adds additional receivers to obtain the user's requested contour tolerance.

Once the TNM obtains computed values at all receivers, it generates a so-called "grid" file with these computed values, the XY coordinates of the receivers, and other miscellaneous data. It then submits this grid file to the computer program NMPLOT Version 3.05, which computes the corresponding contours and returns them to the TNM for display.

Appendix F provides more detail on contours.

2.7 Model Verification

Comparisons of TNM results to measurements and to the model results of others were made. Specifically, five different data sets were used for the comparisons, three of which involved point-source geometry, and the remaining two involved in-situ measurements of barrier performance along actual highways.

Appendix G provides more detail on the data sets used and presents the results of TNM model verification.

APPENDIX A

VEHICLE NOISE EMISSIONS

This appendix contains noise-emission equations and graphs for the five built-in vehicle types within FHWA TNM®:

- # Automobiles: all vehicles having two axles and four tires — designated primarily for transportation of nine or fewer passengers, i.e., automobiles, or for transportation of cargo, i.e., light trucks. Generally, the gross vehicle weight is less than 4500 kg (9900 lb).
- # Medium trucks: all cargo vehicles with two axles and six tires. Generally, the gross vehicle weight is greater than 4,500 kg (9,900 lb), but less than 12,000 kg (26,400 lb).
- # Heavy trucks: all cargo vehicles with three or more axle. Generally, the gross vehicle weight is greater than 12,000 kg (26,400 lb).
- # Buses: all vehicles having two or three axles and designated for transportation of nine or more passengers
- # Motorcycles: all vehicles with two or three tires with an open-air driver and/or passenger compartment.

For each vehicle type, this appendix contains equations for the following components of sound-level emissions:

- # A-weighted sound-level emissions
- # 1/3rd-octave-band spectra, relative to A-weighted sound-level emissions
- # Vertical subsources strengths, relative to 1/3rd-octave-band spectra.

In addition, this appendix describes how user-defined vehicles merge with TNM's built-in noise-emission equations.

A.1 Overview

As a single vehicle passes by a microphone 15 meters (50 feet) to the side, its sound level rises, reaches a maximum, and then falls as the vehicle recedes down the roadway. The maximum A-weighted sound level during the passby is called that vehicle's noise-emission level.

Measurement of vehicle noise-emission levels for TNM are reported separately [Fleming 1995]. These TNM emission-level measurements were confined to relatively flat ground, with the microphone at height 1.5 meters (5 feet) and horizontal distance 15 meters (50 feet). Generally the ground between the roadway edge and the microphone was acoustically absorptive, although not always. At the moment of maximum A-weighted sound level, the vehicle's 1/3rd-octave-band spectrum was also measured at the microphone. This spectrum, relative to the A-weighted sound level, is called the vehicle's noise-emission spectrum.

Measurement of vertical subsources for TNM are also reported separately [Coulson 1996]. These subsource measurements were also confined to relatively flat ground, with an array of microphone heights at horizontal distance 7.5 meters (25 feet). For these measurements, the ground between the roadway edge and the microphone array was acoustically hard, although the data were analyzed to subtract out the effects of ground reflections.

This appendix describes the results of all TNM emission-level measurements and their statistical analysis.

A.2 Definition of Variables

To calculate sound levels for entire traffic streams, TNM must incorporate *energy-average* vehicle noise emissions for each vehicle type. These energy-average emission levels depend upon the following variables:

- f nominal 1/3rd-octave-band center frequency, in Hz
- i index over vehicle types: built-in types and user-defined types
- p index over pavement types:
 - # Average (of DGAC and PCC)
 - # DGAC (dense-graded asphaltic concrete), often called asphalt
 - # PCC (Portland cement concrete), often called concrete
 - # OGAC (open-graded asphaltic concrete).
- s vehicle speed, in kilometers per hour. Speed varies with roadway segment. It may also vary by vehicle type, either because the user enters a different input speed or because TNM internally calculates speed due to upgrades or traffic-control devices (see Appendix B).

A.3 A-weighted Noise-Level Emissions and 1/3rd-Octave-Band Spectra, as Measured

TNM needs three constants to compute A-weighted noise-level emissions: A, B and C. In addition, it needs fourteen additional constants to convert these A-weighted noise-level emissions to 1/3rd-octave-band spectra: D_1 , D_2 , E_1 , E_2 , F_1 , F_2 , G_1 , G_2 , H_1 , H_2 , I_1 , I_2 , J_1 and J_2 .

These seventeen constants depend upon two variables, i and p (vehicle type and pavement type, respectively), plus whether the vehicle is full throttle or not. Vehicles are full throttle when they accelerate away from traffic-control devices, until they reach the user's input speed. In addition, heavy trucks are full throttle on upgrades equal to 1.5 percent or more, until later level grades and downgrades allow them to accelerate back up to the user's input speed.

A.3.1 Built-in vehicle types Table 5 contains the required seventeen constants, for all combinations of vehicle type, pavement type, and throttle condition.

For any roadway/traffic situation, the pavement type and throttle condition will be known. The traffic will include several different vehicle types, i , each with its own speed, s_i . For these emission calculations, TNM substitutes the relevant constants from Table 5 into the following set of equations, to determine each vehicle type's total measured noise emissions:

$$\begin{aligned}
 E_A(s_i) &= (0.6214s_i)^{A/10} 10^{B/10} + 10^{C/10} \\
 L_{\text{emis},i}(s_i, f) &= 10 \times \text{Log}_{10}(E_A) + (D_1 + 0.6214D_2s_i) + (E_1 + 0.6214E_2s_i) [\text{Log}_{10}f] \\
 &\quad + (F_1 + 0.6214F_2s_i) [\text{Log}_{10}f]^2 + (G_1 + 0.6214G_2s_i) [\text{Log}_{10}f]^3 \\
 &\quad + (H_1 + 0.6214H_2s_i) [\text{Log}_{10}f]^4 + (I_1 + 0.6214I_2s_i) [\text{Log}_{10}f]^5 \\
 &\quad + (J_1 + 0.6214J_2s_i) [\text{Log}_{10}f]^6 \\
 E_{\text{emis},i}(s_i, f) &= 10^{(L_{\text{emis},i}/10)},
 \end{aligned} \tag{5}$$

where speed, s , is in kilometers per hour and “Log₁₀” denotes the common logarithm (base 10).

The first of these equations yields the energy form, E_A , of the maximum passby A-weighted sound level for the vehicle type. The second equation converts this E_A to a 1/3rd-octave-band spectrum. This spectrum is also A-weighted, because each of its measured one-third-octave-band levels has been A-weighted. Therefore, when the energies are added for each frequency band, using the equation for $L_{\text{emis},i}(s_i, f)$, the sum, converted to a level, is the A-weighted sound level, without need for further A-weighting. The third equation converts these 1/3rd-octave-band levels to their energy form.

This set of equations determines each built-in vehicle type's energy-mean emission spectrum, as measured during individual vehicle passbys at 15 meters (50 feet) over flat, generally absorptive terrain.

A.3.2 User-defined vehicle types Subject to FHWA policy guidelines, TNM allows user-defined vehicle types to supplement its built-in vehicle types.

FHWA provides specific instructions in [Lee 1997] for the required field measurements and data analysis. In brief, each vehicle type's A-weighted emission levels must be measured in the field, as a function of speed, and then energy-mean emissions must be regressed against vehicle speed. This regression yields the three vehicle-emission constants: A, B and C. Next the resulting constant B must be converted into the vehicle's energy-mean emissions at 80 kilometers per hour (50 miles per hour), which the user enters along with A and C into TNM's traffic dialog box for user-defined vehicles.

Through this process, TNM incorporates customized A-weighted sound-level emissions for user-defined vehicles. For the user-defined vehicle type, TNM substitutes the spectrum constants (D through J) for whichever built-in vehicle the user designates as most similar, again in the traffic dialog box.

A.4 Vertical Subsources, as Measured

TNM needs five additional constants to compute vertical subsource vehicle emissions: L, M, N, P and Q. These constants also depend upon the two variables, i and p , plus throttle condition.

A.4.1 Built-in vehicle types Table 6 contains the measured values of these five constants, for all combinations of vehicle type, pavement type, and throttle condition.

For any roadway/traffic situation, the pavement type and throttle condition will be known. The traffic will include several different vehicle types, i , each with its own speed, s_i . For this calculation, TNM then substitutes the relevant five constants from Table 6 into the following equation, to determine the subsource-split ratio, r_i :

$$r_i(f) = L + (1 - L - M) \left[1 + e^{(N \log_{10} f + P)} \right]^Q . \tag{6}$$

Note that the frequency, f , appears explicitly in this equation and also that the equation is independent of vehicle speed, s_i . In this equation, r is the ratio of upper-height to lower-height energy spectra. Intuitively, one might expect the subsource height split to be a function of vehicle speed, e.g., as speed increases, the split should be more heavily weighted towards the lower height because of the increased effect of tire/road noise. The current subsource height data base contains limited data at low speeds (less than 30 mph). If additional subsource height data is obtained at low speeds, it is expected that the above equation would need to be modified to take into account vehicle speed.

TNM next combines these ratios, r_i , with each vehicle type's total measured emissions from the previous section, to split its total emissions into vertical subsources:

$$\begin{aligned} E_{\text{emis}, i, \text{upper}}(s_i, f) &= \left(\frac{r_i}{r_i + 1} \right) E_{\text{emis}, i} \\ E_{\text{emis}, i, \text{lower}}(s_i, f) &= \left(\frac{1}{r_i + 1} \right) E_{\text{emis}, i} . \end{aligned} \tag{7}$$

Physically, this last equation represents each vehicle type's energy-mean emission spectrum, split into its two vertical subsources, as measured during individual vehicle passbys at 15 meters (50 feet) over flat, generally absorptive terrain. Note that L, M, N, P, and Q were obtained by regression from data at 7.5 meters (25 feet) over flat hard terrain. However, these data were analyzed in a manner that subtracts out the effect of the hard terrain and makes their use here, in this manner, legitimate.

Table 5. Constants for A-weighted sound-level emissions and 1/3rd-octave-band spectra.

Table 6. Constants for subsource-height split.

Vehicle type, <i>i</i>					Pavement type, <i>p</i>					Full throttle		Constants				
												For a user-defined vehicle, use the TNM-equivalent vehicle to choose the relevant table row for these five constants				
Au	MT	HT	Bus	MC	Avg	DG AC	OG AC	PCC	Yes	No	L	M	N	P	Q	
X					X	X	X	X	X	X	0.37323 9	0.97637 8	-13.195596	39.491299	-2.583128	
	X				X	X	X	X	X		0.57926 1	0.87135 4	-177.249214	558.980283	-0.026532	
	X				X	X	X	X		X	0.56693 3	0.93352	-25.497631	80.239979	-0.234435	
		X			X	X	X	X	X		0.57739 4	0.60978 7	-309.046731	890.880597	-8519.429646	
		X			X	X	X	X		X	0.59484 8	0.64331 7	-36.503587	102.627995	-132.679357	
			X		X	X	X	X	X		0.57926 1	0.87135 4	-177.249214	558.980283	-0.026532	
			X		X	X	X	X		X	0.56309 7	0.92808 6	-31.517739	99.099777	-0.263459	
				X	X	X	X	X	X		0.39135 2	0.97840 7	-19.278172	60.404841	-0.614295	
				X	X	X	X	X		X	0.39135 2	0.97840 7	-19.278172	60.404841	-0.614295	

A.4.2 User-defined vehicles For a user-defined vehicle, TNM substitutes the subsource heights for the built-in vehicle that the user designates as most similar. Table 6 mentions this substitution in the appropriate column heading.

A.5 Vertical Subsources, Free Field

Next TNM eliminates the ground effects within these measured vehicle emissions. To do this, it multiplies each measured vertical subsource emission by the values in Table 7.

Mathematically:

$$E_{emis, i, upper, ff}(s_i, f) = m_{upper} E_{emis, i, upper}$$

$$E_{emis, i, lower, ff}(s_i, f) = m_{lower} E_{emis, i, lower} \cdot$$
(8)

The subscripts, ff, stand for free field. Physically, this last equation represents each vehicle type's measured energy-mean emission spectrum, as if the vehicles passed by during measurements at 15 meters (50 feet) without any intervening ground (that is, free field).

Table 7. Multiplier, m , for each built-in subsource height.

Freq (Hz)		50	63	80	100	125	160	200	250	315	400	500	630
Multiplier, m	Height: 3.66 m	0.32	0.35	0.41	0.51	0.76	1.66	6.46	4.79	0.95	0.41	0.41	1.00
	Height: 1.5 m	0.30	0.30	0.32	0.34	0.37	0.44	0.55	0.81	1.55	5.37	4.47	1.02
	Height: zero	0.30	0.31	0.32	0.34	0.35	0.38	0.41	0.44	0.47	0.50	0.54	0.56

Freq (Hz)		800	1000	1250	1600	2000	2500	3150	4000	5000	6300	8000	10000
Multiplier, m	Height: 3.66 m	1.00	1.00	1.00	1.00	1.00	1.00	1.00	1.00	1.00	1.00	1.00	1.00
	Height: 1.5 m	1.00	1.00	1.00	1.00	1.00	1.00	1.00	1.00	1.00	1.00	1.00	1.00
	Height: zero	0.56	0.54	0.49	0.42	0.35	0.30	0.25	0.22	0.21	0.21	0.3	0.36

These values were derived by using the propagation algorithms of TNM to determine the effect of the (absorptive) ground present during the emission-level measurements.

A.6 Plots of All Noise Emissions

Figure 6 shows A-weighted sound-level emissions for TNM's built-in vehicle types, for average pavement and cruise throttle. The following figures plot all noise emissions, separately by vehicle type and throttle condition (cruise or full):

- # Figures 7 through 16: A-weighted sound-level emissions
- # Figures 17 through 32: emission spectra, separately by pavement type
- # Figures 33 through 40: high/low energy split.



Figure 6. A-weighted sound-level emissions: Average pavement, cruise throttle.



Figure 7. A-weighted sound-level emissions: Automobiles, cruise throttle.



Figure 8. A-weighted sound-level emissions: Automobiles, full throttle.

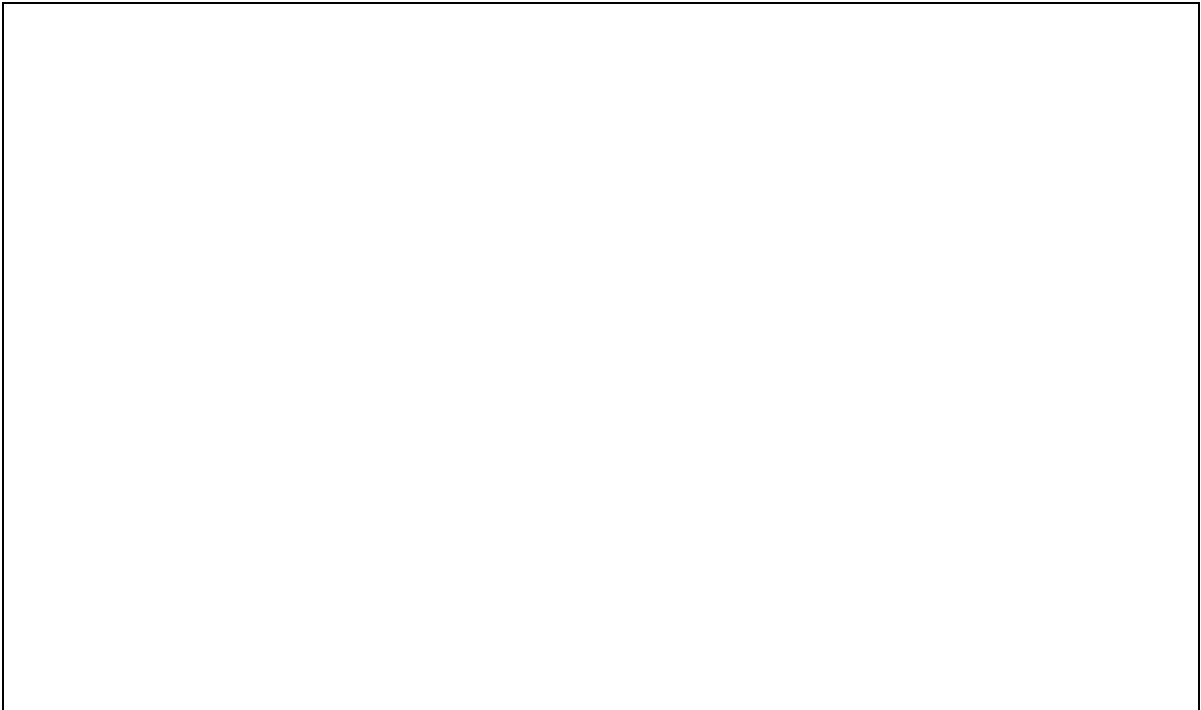


Figure 9. A-weighted sound-level emissions: Medium trucks, cruise throttle.

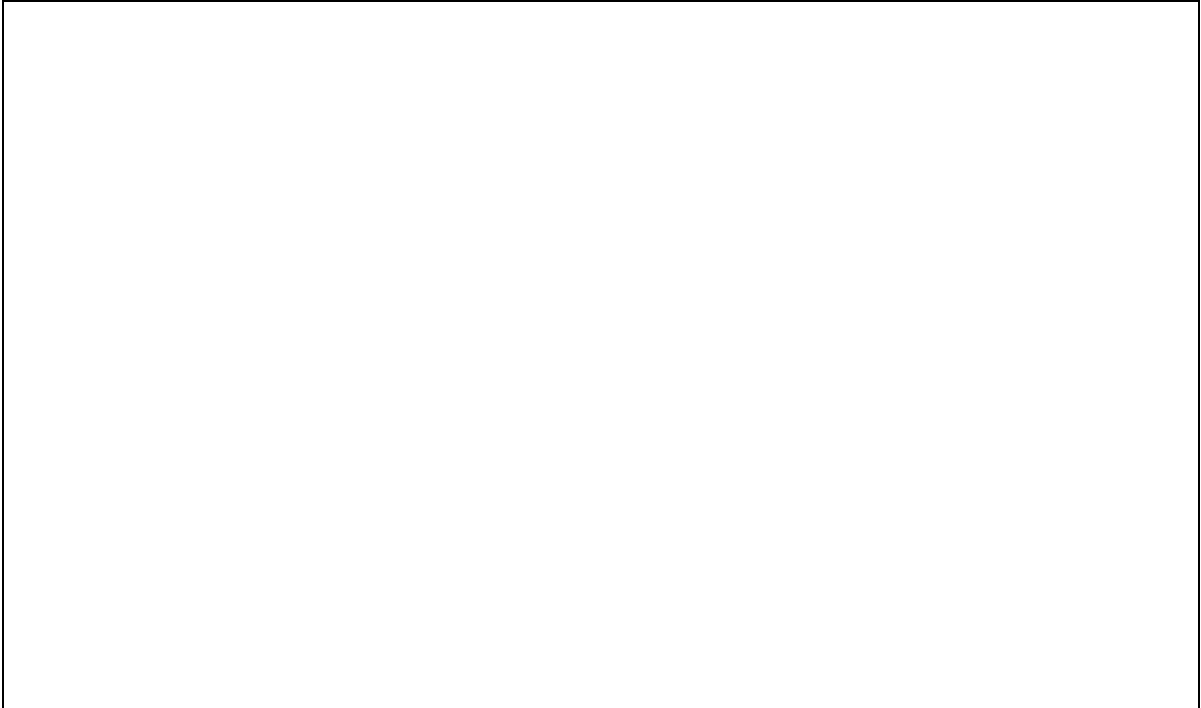


Figure 10. A-weighted sound-level emissions: Medium trucks, full throttle.



Figure 11. A-weighted sound-level emissions: Heavy trucks, cruise throttle.

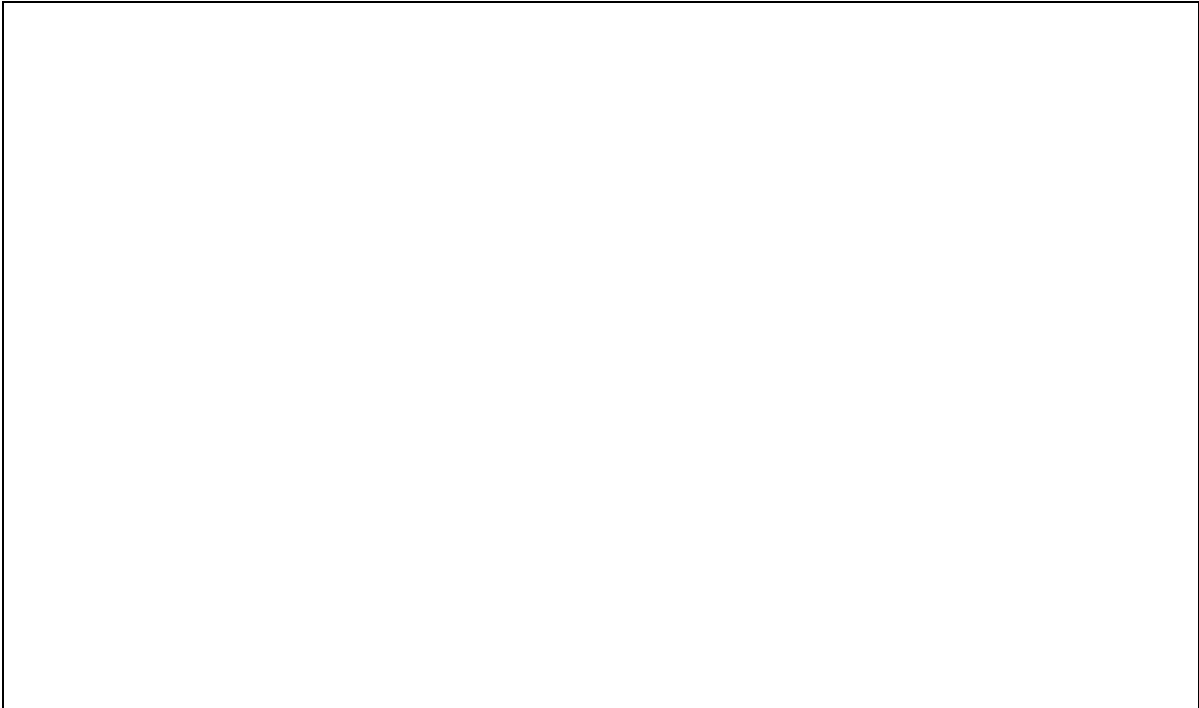


Figure 12. A-weighted sound-level emissions: Heavy trucks, full throttle.

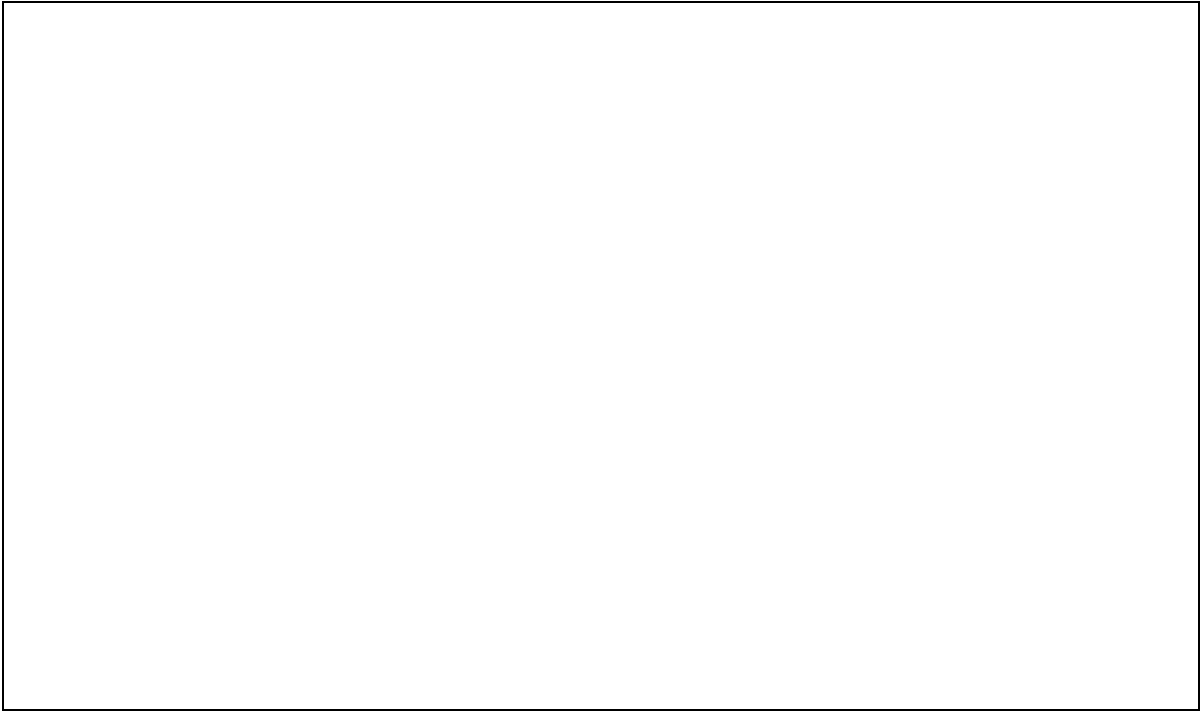


Figure 13. A-weighted sound-level emissions: Buses, cruise throttle.

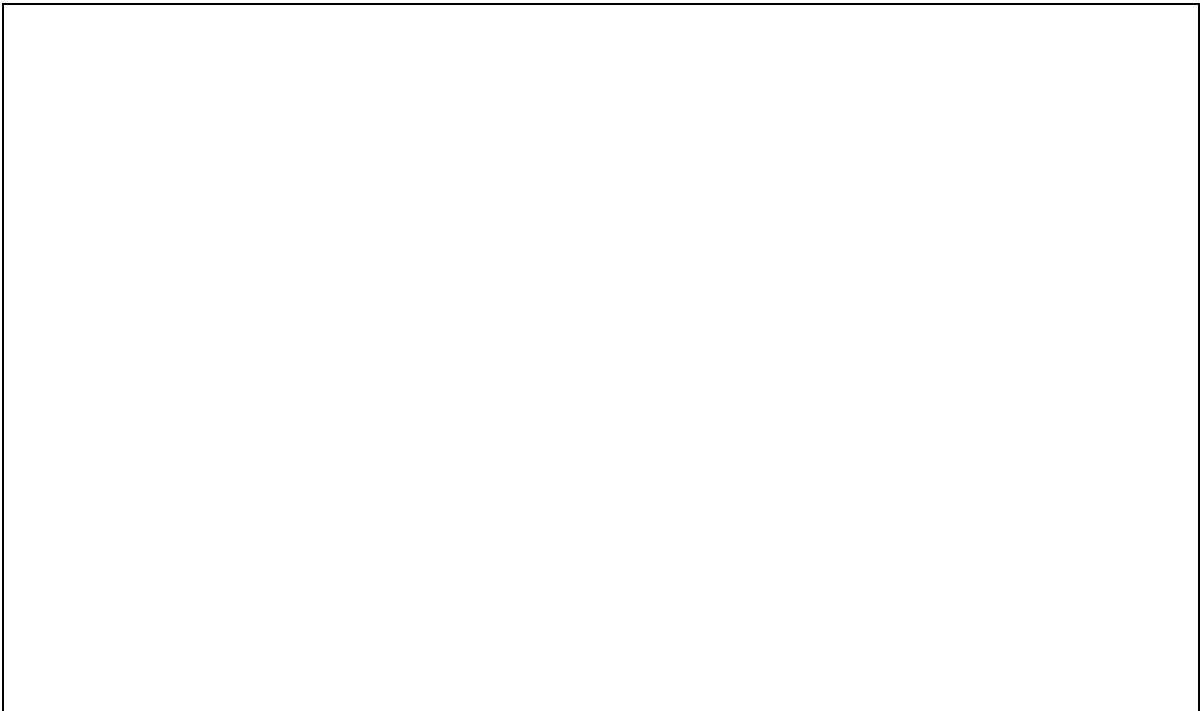


Figure 14. A-weighted sound-level emissions: Buses, full throttle.

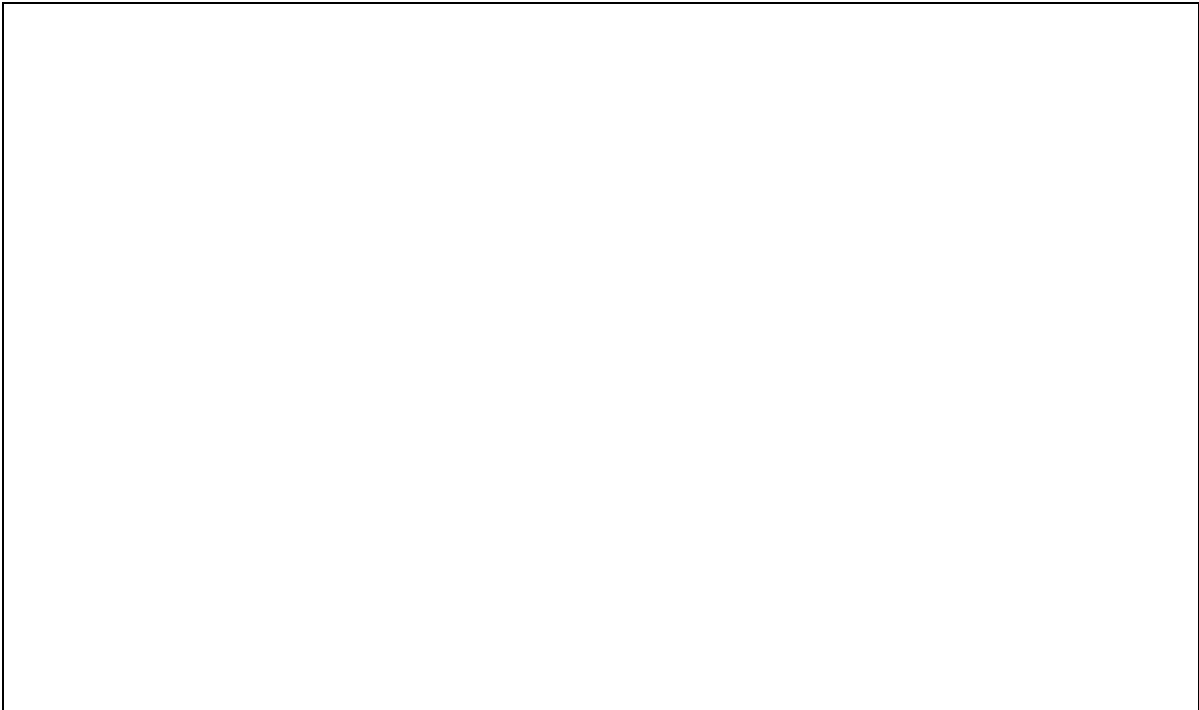


Figure 15. A-weighted sound-level emissions: Motorcycles, cruise throttle.

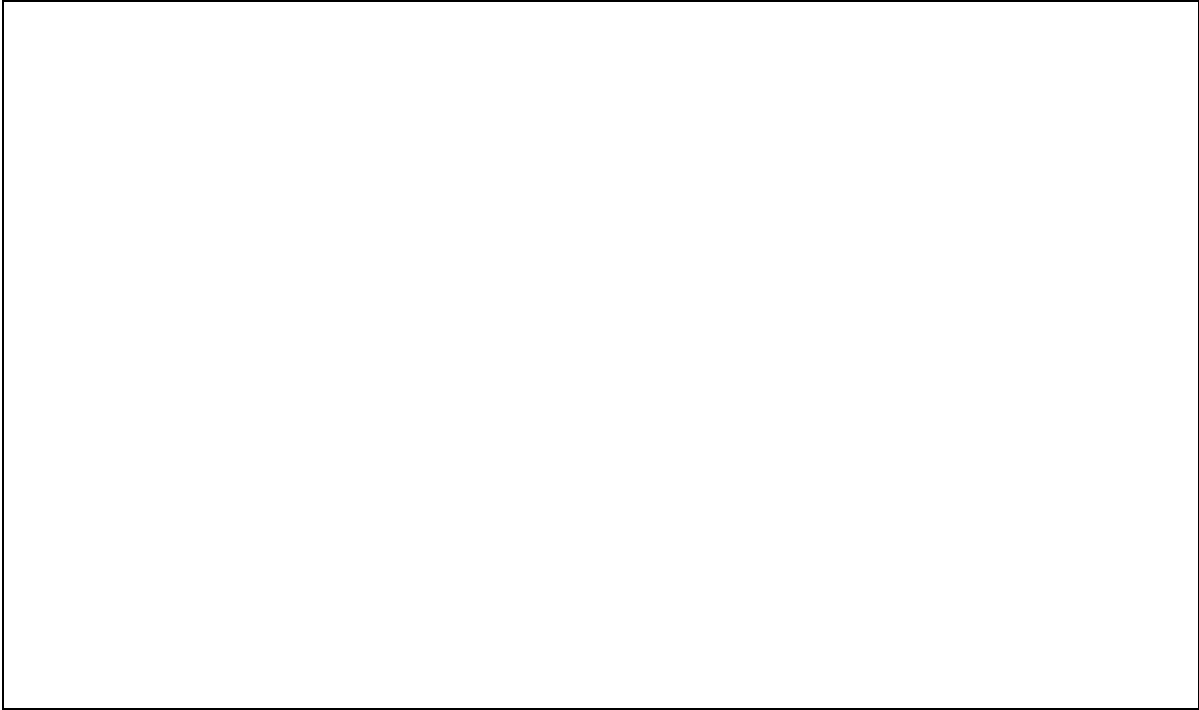


Figure 16. A-weighted sound-level emissions: Motorcycles, full throttle.

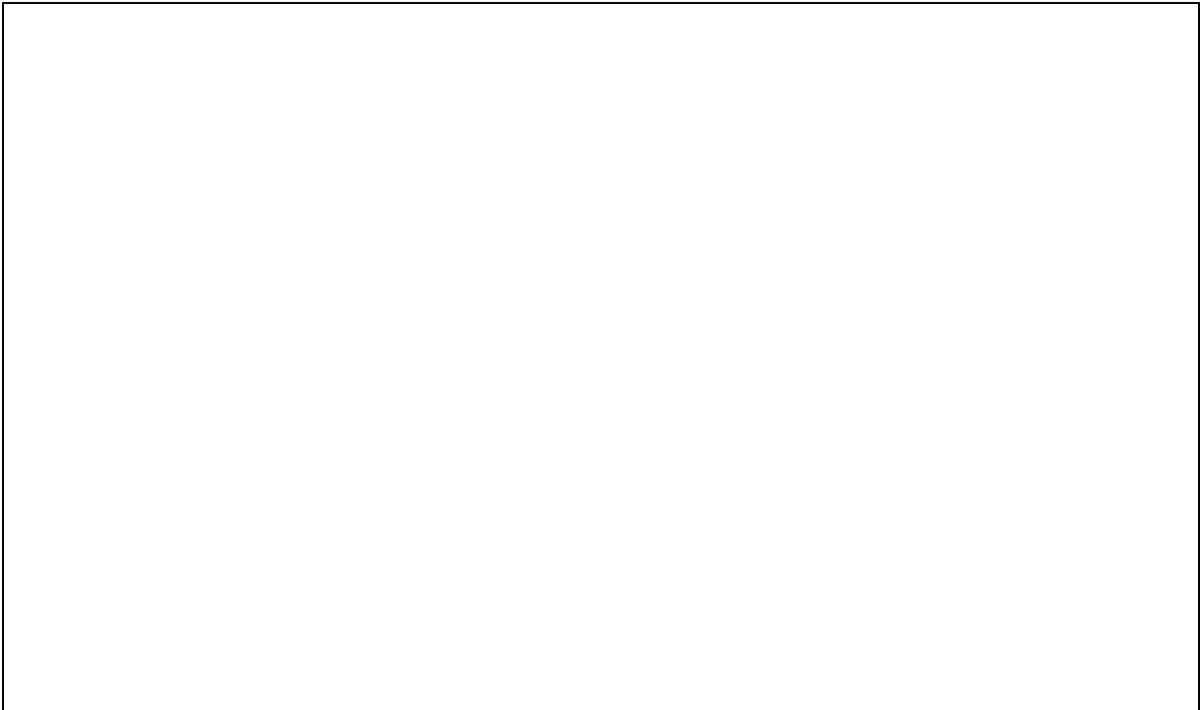


Figure 17. Emission spectra: Automobiles, average pavement.



Figure 18. Emission spectra: Automobiles, DGAC pavement.

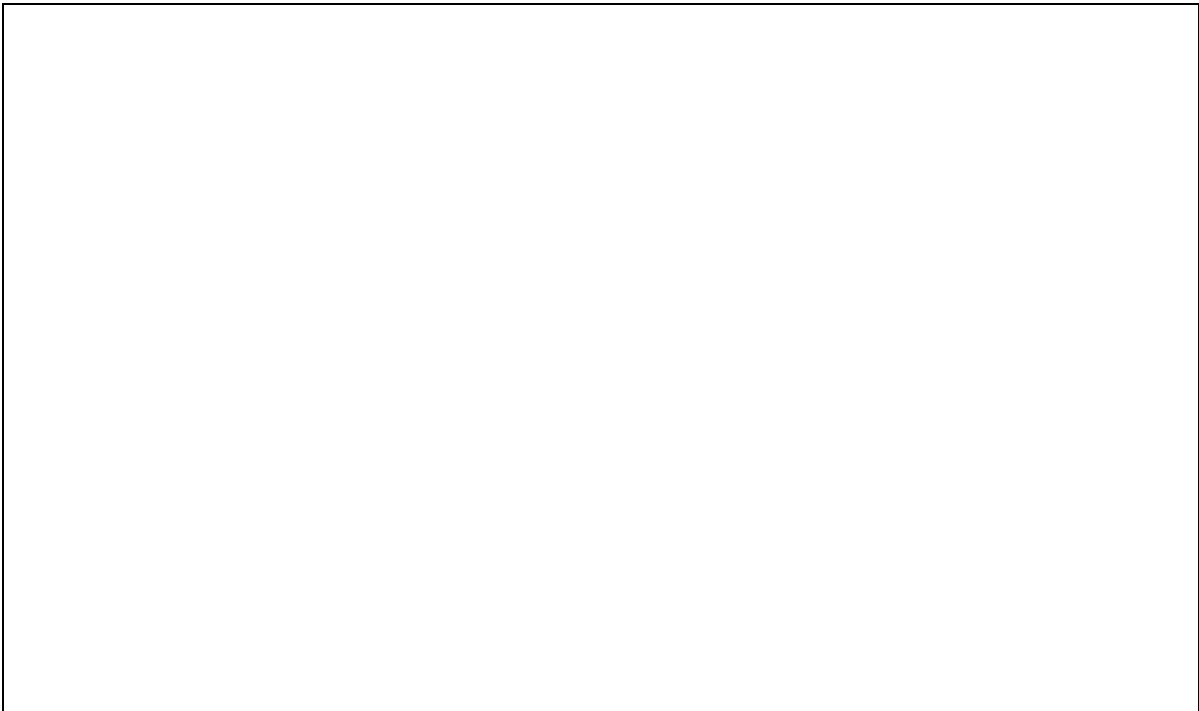


Figure 19. Emission spectra: Automobiles, OGAC pavement.

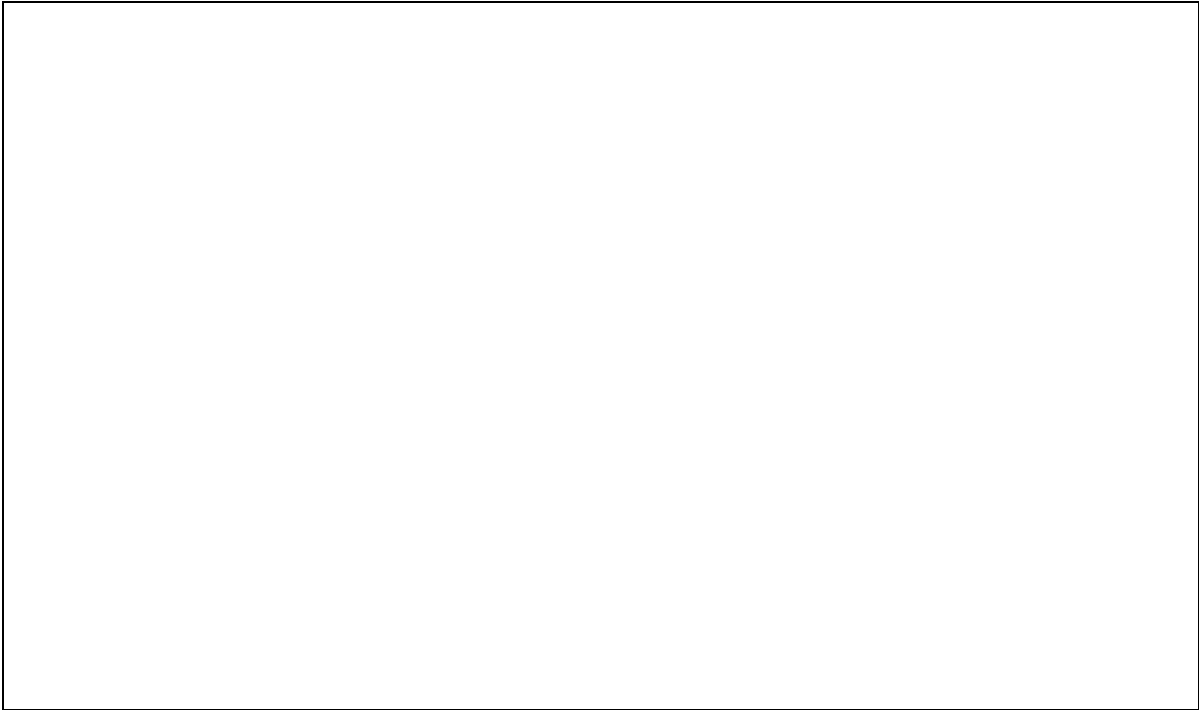


Figure 20. Emission spectra: Automobiles, PCC pavement.



Figure 21. Emission spectra: Medium trucks, full throttle.

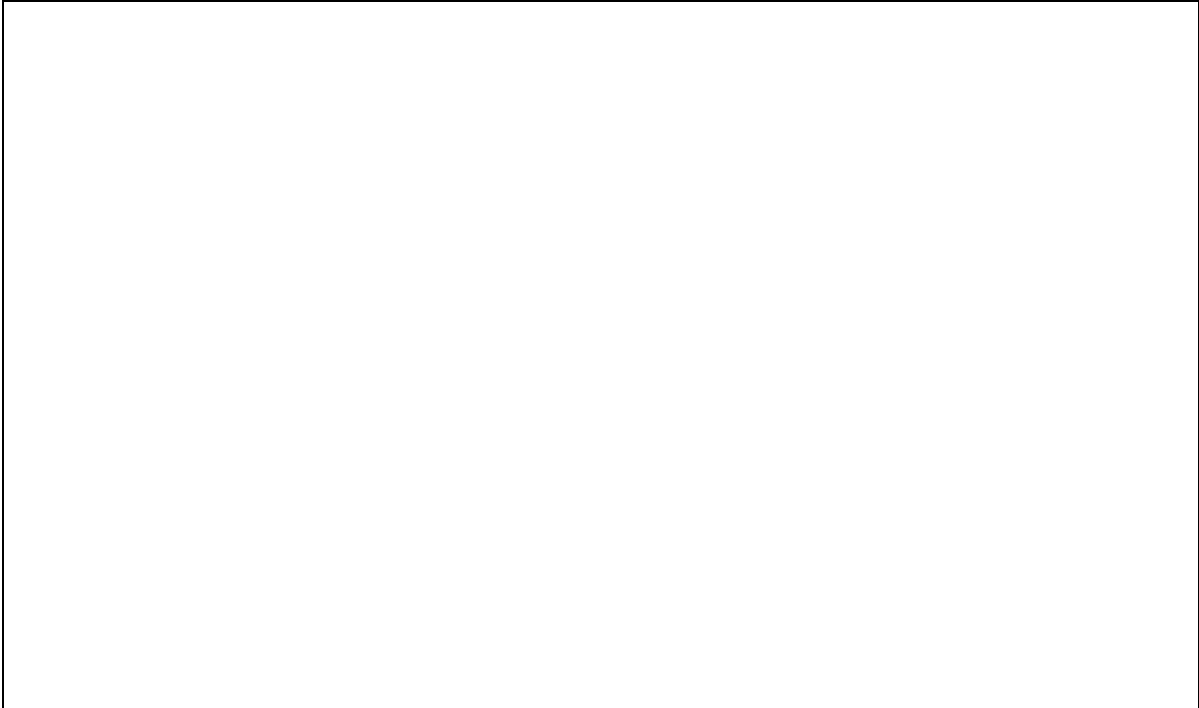


Figure 22. Emission spectra: Medium trucks, cruise throttle, average pavement.



Figure 23. Emission spectra: Medium trucks, cruise throttle, DGAC pavement.



Figure 24. Emission spectra: Medium trucks, cruise throttle, OGAC pavement.

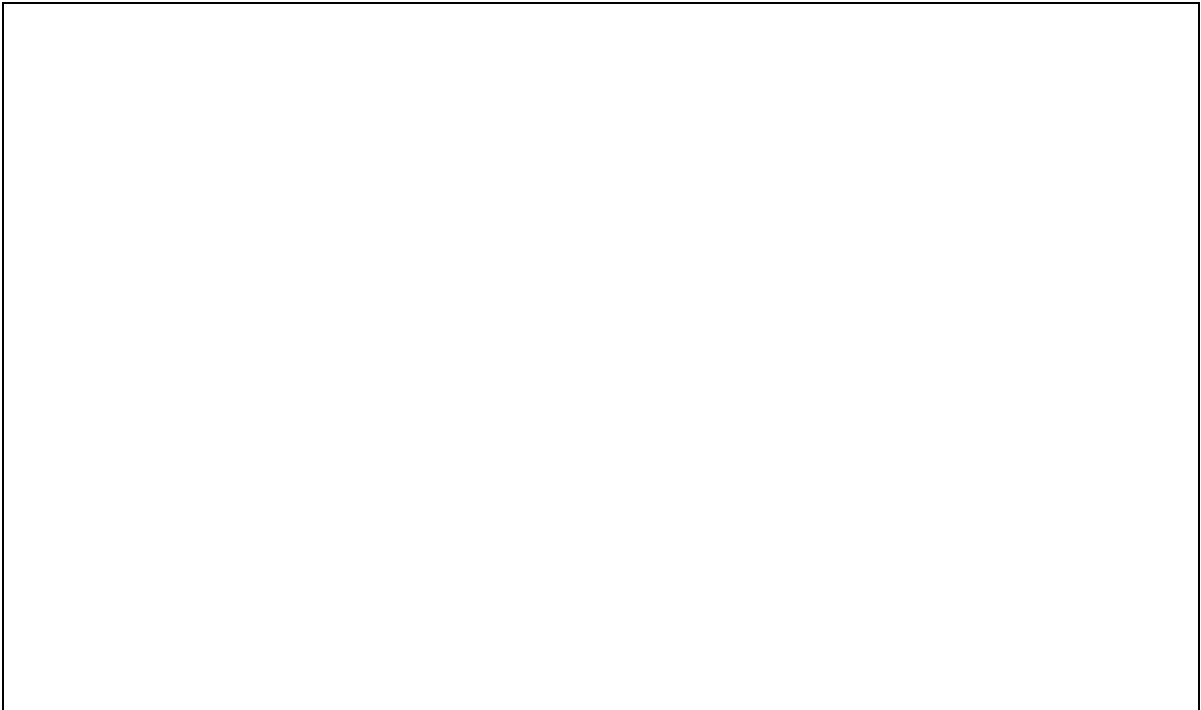


Figure 25. Emission spectra: Medium trucks, cruise throttle, PCC pavement.

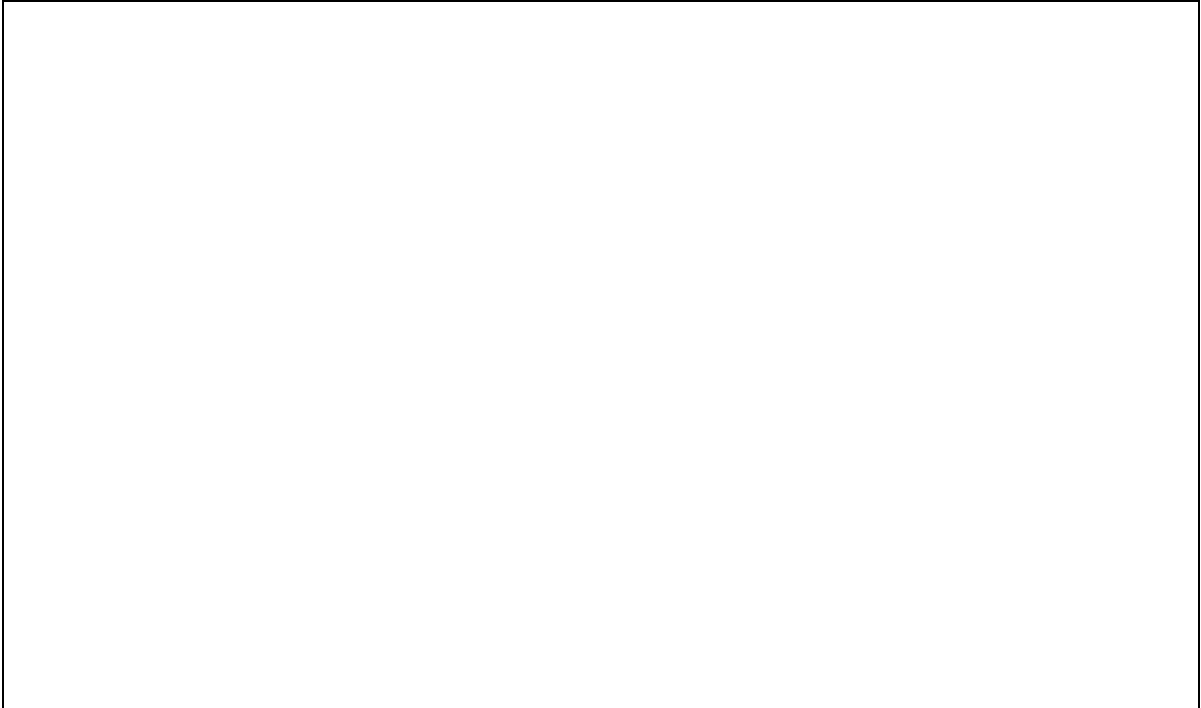


Figure 26. Emission spectra: Heavy trucks, full throttle.

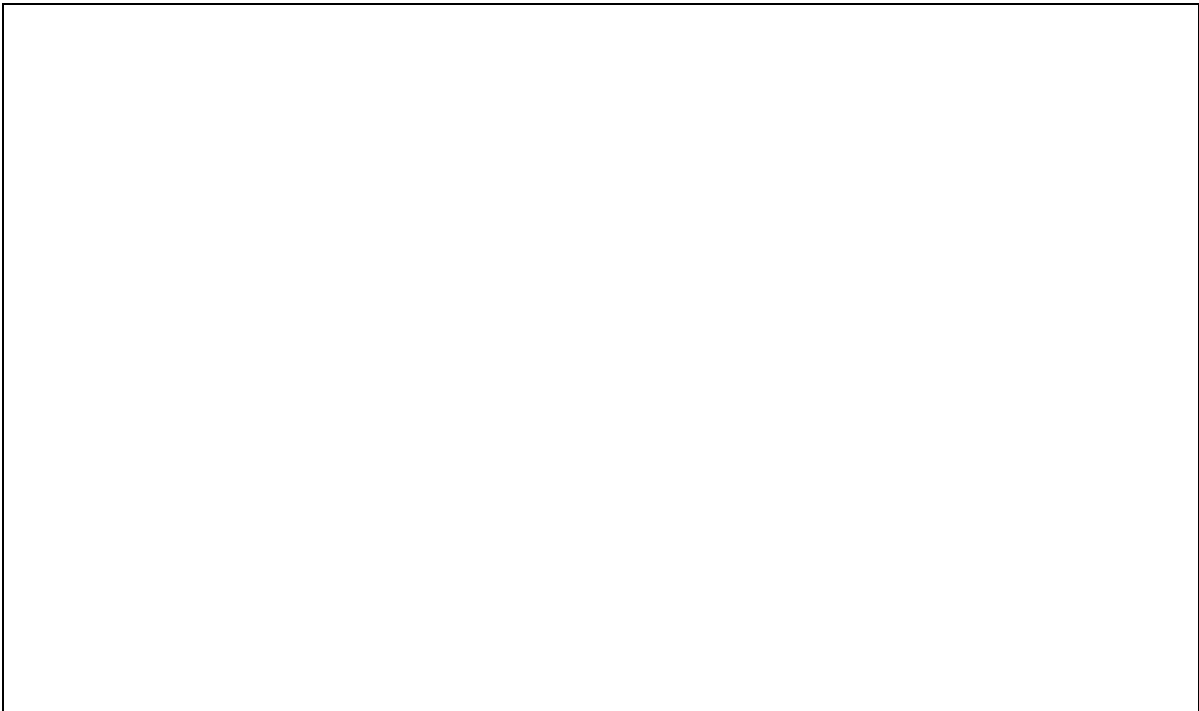


Figure 27. Emission spectra: Heavy trucks, cruise throttle, average pavement.

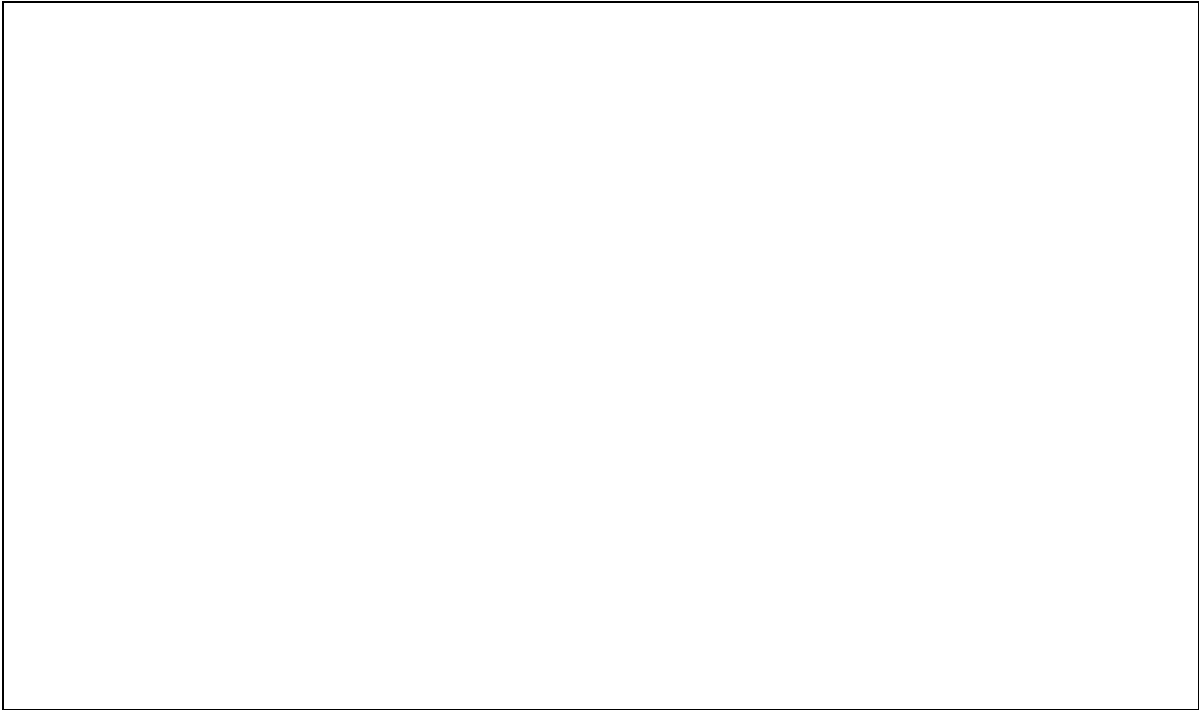


Figure 28. Emission spectra: Heavy trucks, cruise throttle, DGAC pavement.

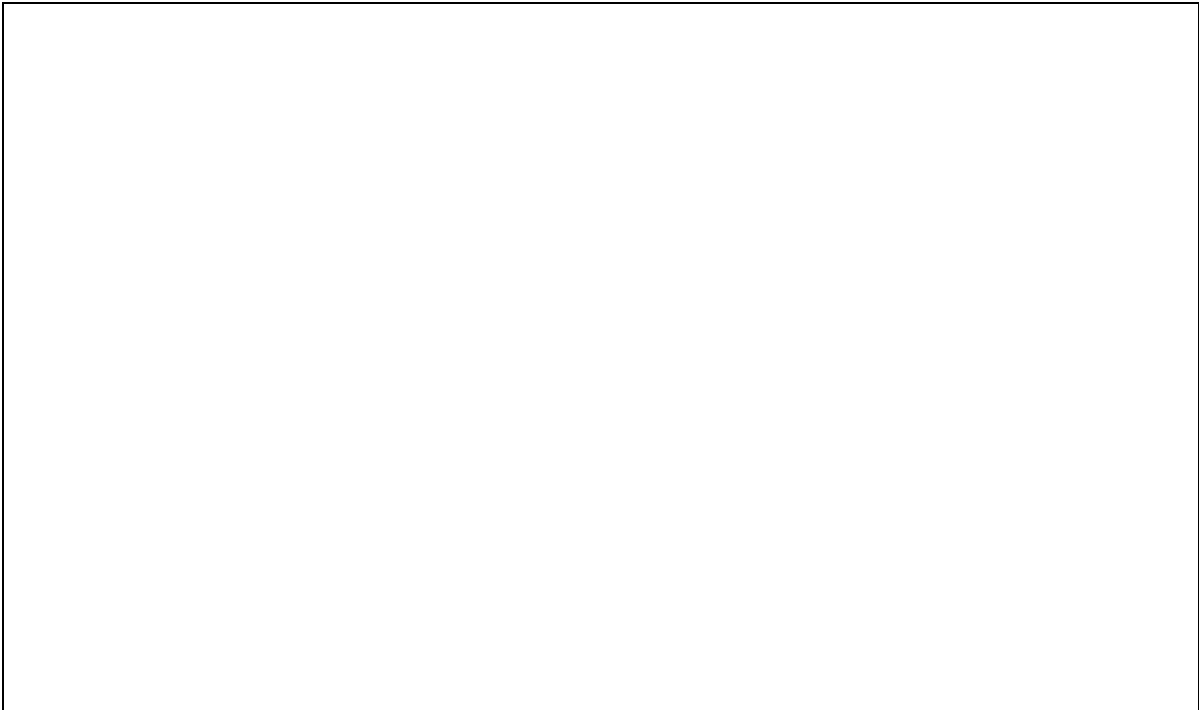


Figure 29. Emission spectra: Heavy trucks, cruise throttle, OGAC pavement.

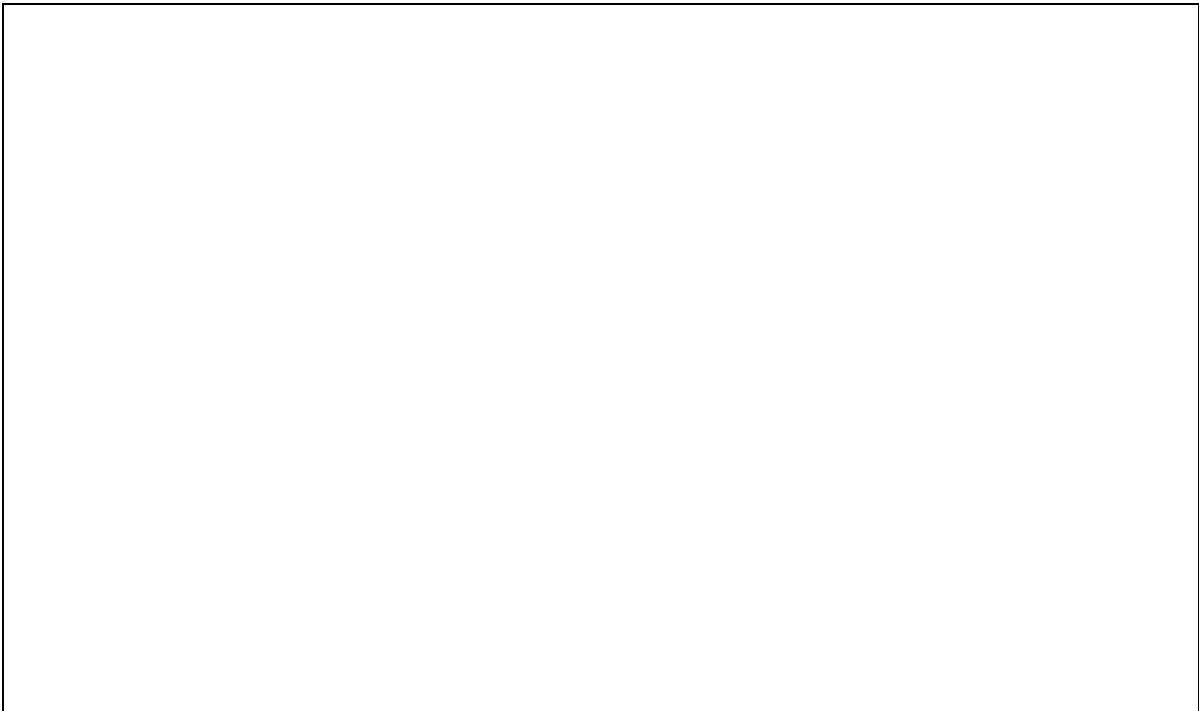


Figure 30. Emission spectra: Heavy trucks, cruise throttle, PCC pavement.



Figure 31. Emission spectra: Buses.



Figure 32. Emission spectra: Motorcycles.

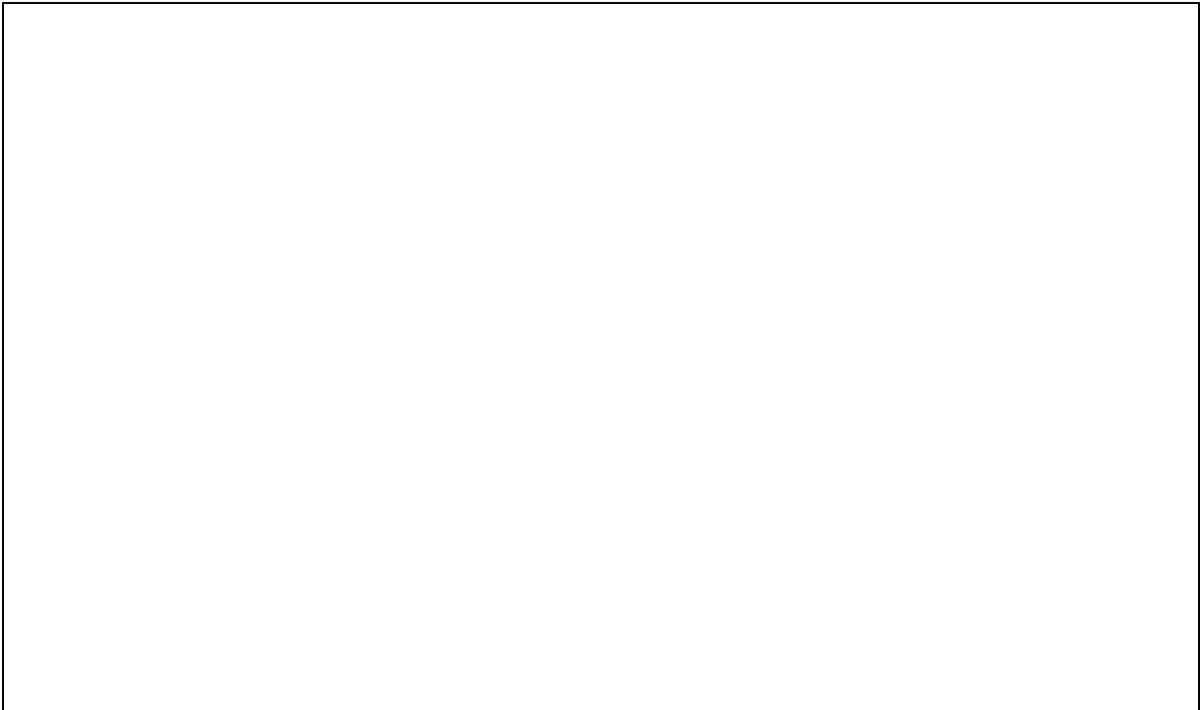


Figure 33. Sound emissions, high/low energy split: Automobiles.



Figure 34. Sound emissions, high/low energy split: Medium trucks, cruise throttle.



Figure 35. Sound emissions, high/low energy split: Medium trucks, full throttle.



Figure 36. Sound emissions, high/low energy split: Heavy trucks, cruise throttle.



Figure 37. Sound emissions, high/low energy split: Heavy trucks, full throttle.



Figure 38. Sound emissions, high/low energy split: Buses, cruise throttle.



Figure 39. Sound emissions, high/low energy split: Buses, full throttle.



Figure 40. Sound emissions, high/low energy split: Motorcycles.

APPENDIX B

VEHICLE SPEEDS

Under most situations, FHWA TNM[®] uses vehicle speeds that are input by the user. However, in two situations TNM computes vehicle speeds on its own, instead: (1) whenever traffic speeds are reduced by upgrades; and (2) whenever they are reduced by traffic-control devices. This appendix details how and when TNM performs its internal speed computations.

B.1 Overview

Figure 41 illustrates the speed effects of upgrades and traffic-control devices. The upper frame in the figure illustrates the influence of upgrades on heavy trucks and on any user-defined vehicles that mimic heavy trucks. The lower frame illustrates the influence, on all vehicles, of traffic-control devices and subsequent roadway grades.

A single roadway is drawn bold in each frame of the figure. Within TNM's roadway "loop," this is the "current" roadway being computed. Other roadways are dashed in the figure. In addition, the figure shows grades for each segment of the current roadway and the location of a traffic-control device in the lower frame.

Also shown in the figure are the locations at which TNM starts and stops computing speeds. For upgrades, TNM starts computing heavy-truck speeds where the upgrade equals 1.5 percent or more. In the upper frame, this occurs at the entrance point of the segment labeled "1.7 percent up." It is at this point that the roadway grade begins to affect heavy-truck speeds. For traffic-control devices, TNM starts computing speeds at the location of the device, itself. Traffic-control devices abruptly reduce speeds to the device's "speed constraint," for the device's "percentage of vehicle affected." Most traffic-control devices affect 100 percent of the vehicles. However, traffic signals affect only a portion of the traffic: that portion stopped at the red signal phase. The remainder of the vehicles progress as if the device was not there.

TNM stops computing speeds at whichever happens first: either (1) the vehicles accelerate back up to the user's input speed; or (2) the vehicles come to the end of the *current* TNM roadway. TNM never "tracks" vehicles from one roadway to the next when computing speeds. For this reason, speed computations on the current roadway are completely independent of speeds on connecting roadways: before, after, or ramp-like connections in the middle.

For example, in the bottom frame of the figure, TNM does not track accelerating onramp vehicles onto the dashed mainline. Instead, all vehicles on the mainline proceed at mainline vehicle speeds. Traffic on the ramp and the mainline are not "linked" in any sense. If the user wishes TNM to continue accelerating vehicles after they merge with mainline traffic, the user must extend the onramp far enough, parallel to the mainline roadway, and only then connect the onramp into the mainline.

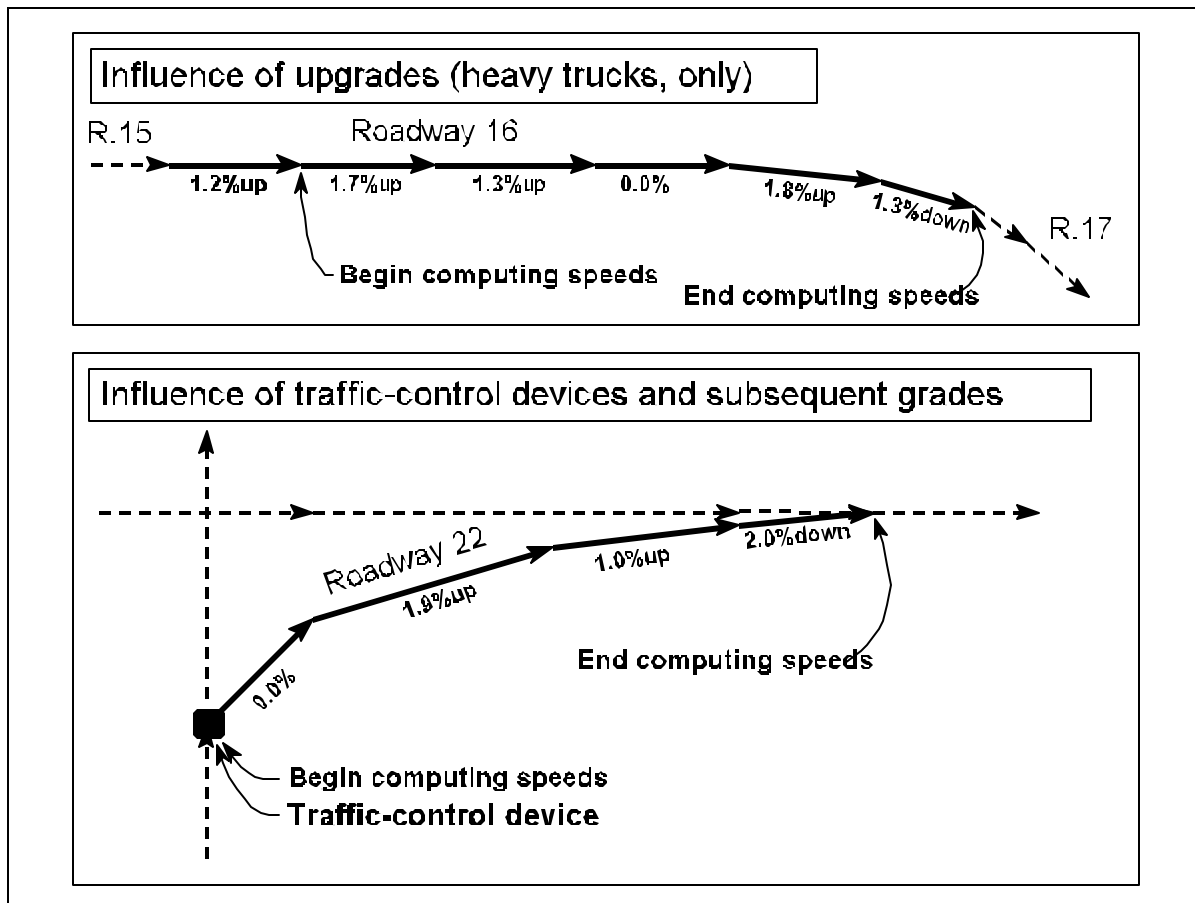


Figure 41. Geometrics for speed effects of upgrades and traffic-control devices.

The following sections of this appendix describe this speed-computation process further, with illustrations.

B.2 Entrance and Exit Speeds: Overview

Figure 42 shows a subdivided elemental triangle, inside the innermost computation “loop” for sound levels. At this point in the acoustical computations, TNM is computing sound levels for a specific receiver from a specific input roadway segment, and has now finished subdividing that roadway segment into the smallest portions (subsegments) needed for computation.

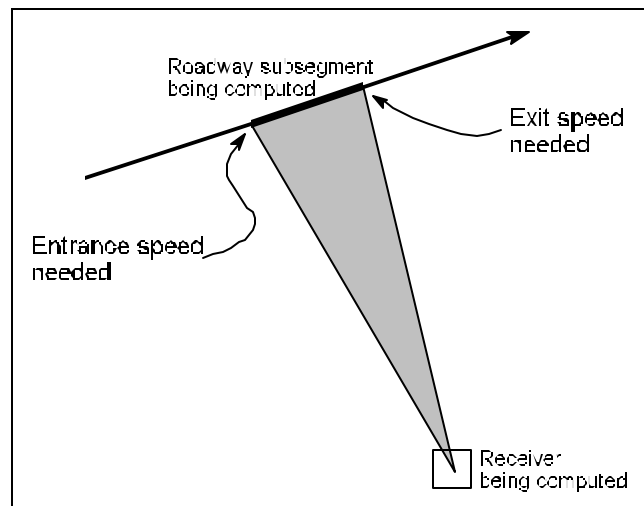


Figure 42. Entrance and exit speeds.

At this point, TNM needs to determine the acoustical energy at the receiver from the traffic on this roadway subsegment. To determine this, TNM must first know the average vehicle speed, s_{average} , for each type of vehicle on the subsegment.

TNM calculates average speeds from the *entrance* and *exit* speeds of each vehicle type, as follows:

$$s_{\text{average}} = \frac{(s_{\text{entrance}} + s_{\text{exit}})}{2} . \quad (9)$$

Because of this averaging equation, TNM only needs to know speeds at entrances and exits, not continuously along the roadway subsegment.

B.3 Entrance Speeds

In general, a vehicle type's entrance speed sometimes equals: (1) the speed entered by the user, sometimes; (2) a control-device's speed constraint; and sometimes (3) the exit speed of the previous subsegment. The distinction among these depends upon whether TNM is "tracking" that vehicle's speed or not.

In particular:

- # **The first entrance speed for upgrades:** When traffic first encounters an upgrade equal to 1.5 percent or more, TNM begins to track heavy-truck speeds, plus the speeds of all user-defined vehicles that mimic heavy trucks. For the first subsegment, TNM sets entrance speed equal to the user's input speed.

- # **The first entrance speed for traffic-control devices:** If a traffic-control device is located on the first point of a segment, then TNM begins tracking speeds for all vehicles along this segment. For the first subsegment, TNM sets the entrance speed of all vehicle types to the device's speed constraint entered by the user. If the device is a traffic signal, TNM also remembers that speed tracking only pertains to the device's "percentage of vehicles affected."
- # **Subsequent entrance speeds:** Then as vehicles progress from subsegment to subsegment, TNM preserves speed continuity. Specifically, it first computes each vehicle type's exit speed for the current subsegment, i , as described in the next section. Then it assigns these speeds as entrance speeds for the next subsegment, $i+1$. Level grades and downgrades allow vehicles to accelerate back upwards towards user's input speeds. Once this happens for a particular vehicle type, then TNM stops tracking speed for that vehicle type.

B.4 Exit Speeds

In general, a vehicle type's exit speed sometimes equals its input speed and sometimes is computed from the entrance speed, the roadway grade and the length of the subsegment.

Whenever TNM is tracking speed for a particular vehicle type, it must compute subsegment exit speeds. For each vehicle type, TNM requires an equation for:

s_{exit} vehicle speed at the end of the segment, in kilometers per hour,

as a function of the following:

$s_{entrance}$ vehicle speed at the beginning of the segment, in kilometers per hour,

x , length of the segment, in meters,

g , roadway grade, in percent,

i , vehicle type,

plus whether the vehicle is accelerating or decelerating.

B.5 Regression Equations

For every possible roadway grade (upgrade, level, and downgrade), heavy trucks have a so-called "crawl speed." As TNM tracks heavy-truck speeds along a roadway segment, whenever the heavy-truck speed at the beginning of the segment, $s_{entrance}$, is less than $s_{HTcrawl}$ for that grade, then the heavy trucks will *accelerate* upwards towards their crawl speed. On the other hand, whenever the speed at the beginning of the segment, $s_{entrance}$, is greater than $s_{HTcrawl}$ for that grade, then heavy trucks will *decelerate* down towards their crawl speed.

In short, heavy trucks:

- # accelerate when $s_{\text{entrance}} < s_{\text{HTcrawl}}$,
- # decelerate when $s_{\text{entrance}} > s_{\text{HTcrawl}}$, and
- # keep speed constant when $s_{\text{entrance}} = s_{\text{HTcrawl}}$.

In the last unlikely situation, note that TNM still continues to track speed on the segment, even though this speed is constant, because the heavy truck is not yet up to the user's input speed.

Other TNM vehicles have no crawl speed. TNM does not slow them down due to upgrades. When TNM tracks vehicles other than heavy trucks, it always *accelerates* them upwards, until they reach the user's input speed.

B.5.1 Regression equation for accelerating vehicles For vehicles accelerating from an entrance speed of zero,

$$s_x = 1.609 A \left\{ 1 - \exp \left[- \left(\frac{0.3048 x}{B} \right)^C \right] \right\}, \tag{10}$$

where s_x is vehicle speed, in kilometers per hour, at distance x along the roadway subsegment, in meters. For this equation, A, B and C appear in Table 8. The function “exp(...)” means the constant “e” raised to the (...) power.

Note that some of these regression coefficients are functions of roadway grade, g . Also note the distinction between G (a regression coefficient) and g (the roadway grade), in percent.

When the entrance speed is not zero, TNM uses the following equation, which is derived from the previous one:

$$s_x = 1.609 A \times \left\{ 1 - \exp \left[- \left(\frac{\left\{ 0.3048 x + B \left[\ln(A) - \ln(A - 0.6214 s_{\text{entrance}}) \right] \right\}^{1/C}}{B} \right)^C \right] \right\}, \tag{11}$$

where s_{entrance} is vehicle speed, in kilometers per hour, at the entrance to the roadway subsegment, and s_x is vehicle speed, in kilometers per hour, at distance x along the subsegment, in meters.

Table 8. Regression coefficients for accelerating vehicles.

Vehicle type	A	B	C
Automobiles and motorcycles	D exp(-E g), where D = 130.300 E = 0.119	F exp(-G g), where F = 3950.000 G = 0.208	0.482
Medium trucks and all buses	D exp(-E g), where D = 85.714 E = 0.119	F exp(-G g), where F = 1838.149 G = 0.197	0.521
Heavy trucks	D exp(-E g), where D = 70.721 E = 0.137	F exp(-G g), where F = 1849.803 G = 0.231	0.510

B.5.2 Regression equation for decelerating heavy trucks For heavy trucks decelerating from an entrance speed of 121 kilometers per hour (75 miles per hour),

$$s_x = 1.609A + (121 - 1.609A) \exp \left[- \left(\frac{0.3048 x}{B} \right)^C \right], \tag{12}$$

where s_x is vehicle speed, in kilometers per hour, at distance x along the roadway subsegment, in meters. For this equation, A, B and C appear in Table 9. Note that some of these coefficients are functions of roadway grade, g , in percent.

Table 9. Regression coefficients for decelerating heavy trucks.

Vehicle type	A	B	C
Heavy trucks	D exp(-E g), where D = 72.803 E = 0.180	F exp(-G g), where F = 3792.117 G = 0.105	1.303

When the entrance speed is not 121 kilometers per hour (75 miles per hour), TNM uses the following equation, which is derived from the previous one:

$$s_x = 1.609 A + (121 - 1.609A) \times \exp \left[- \left(\frac{\left\{ 0.3048 x + B \left[\ln (121 - 1.609A) - \ln (s_{\text{entrance}} - 1.609A) \right]^{1/C} \right\}^C}{B} \right) \right], \quad (13)$$

where s_{entrance} is vehicle speed, in kilometers per hour, at the entrance to the subsegment, and s_x is the speed at distance x along the subsegment, in meters.

B.6 Graphs of Acceleration and Deceleration

Figures 43 through 46 plot Eqs. (10) and (12) from above. They show TNM's functional relationships between vehicle speed and distance along a roadway subsegment, starting at zero speed for acceleration and 121 kilometers per hour (75 miles per hour) for deceleration.

These functional relationships resemble the official performance curves currently in use for highway geometric design [AASHTO 1990] [TRB 1985]. The curves here have been regressed to the same functional form as the official performance curves, but from vehicle acceleration and deceleration data during measurement of TNM's emission levels for full-throttle vehicles (heavy trucks on upgrades and all vehicles as affected by traffic-control devices). Because of this regression based on field-measured speed data, the TNM curves are fully consistent with TNM's full-throttle emission levels. Moreover, the heavy-truck curves for both acceleration and deceleration are consistent with performance curves for a truck with a weight-to-horsepower ratio of 97 kg/kW (160 lb/hp) and a weight-to-frontal area ratio of 1,760 kg/m² (360 lb/ft²).

The curves in each of these figures show vehicle dynamics for an average vehicle, as a function of grade. In Figure 45, for example, a heavy truck starting from speed zero on a 4-percent upgrade would reach 43 kilometers per hour (27 miles per hour) after traveling 305 meters (1,000 feet), and 53 kilometers per hour (33 miles per hour) after traveling another 305 meters (1,000 feet), for a total of 610 meters (2,000 feet). Then after traveling another 3,050 meters (10,000 feet) — for a total of 3,660 meters (12,000 feet) — this truck would reach its maximum sustainable speed for this grade: 66 kilometers per hour (41 miles per hour). This speed is called the truck's "crawl speed." If the truck started out at 43 kilometers per hour (27 miles per hour), instead, the distance/speed relationships would be the same: 53 kilometers per hour (33 miles per hour) after 305 meters (1,000 feet), 66 kilometers per hour (41 miles per hour) after another 3,050 meters (10,000 feet), for a total of 3,355 meters (11,000 feet). The starting speed, combined with distance, determine the ending speed.

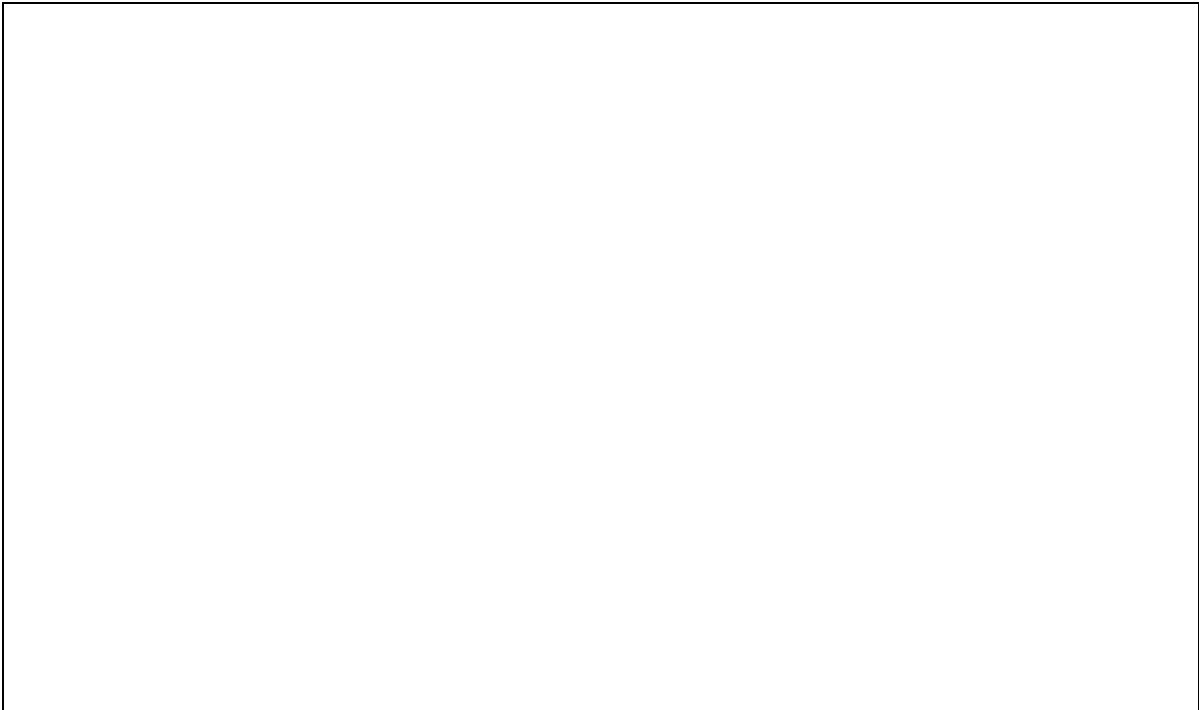


Figure 43. Acceleration away from traffic-control devices: Automobiles and motorcycles.

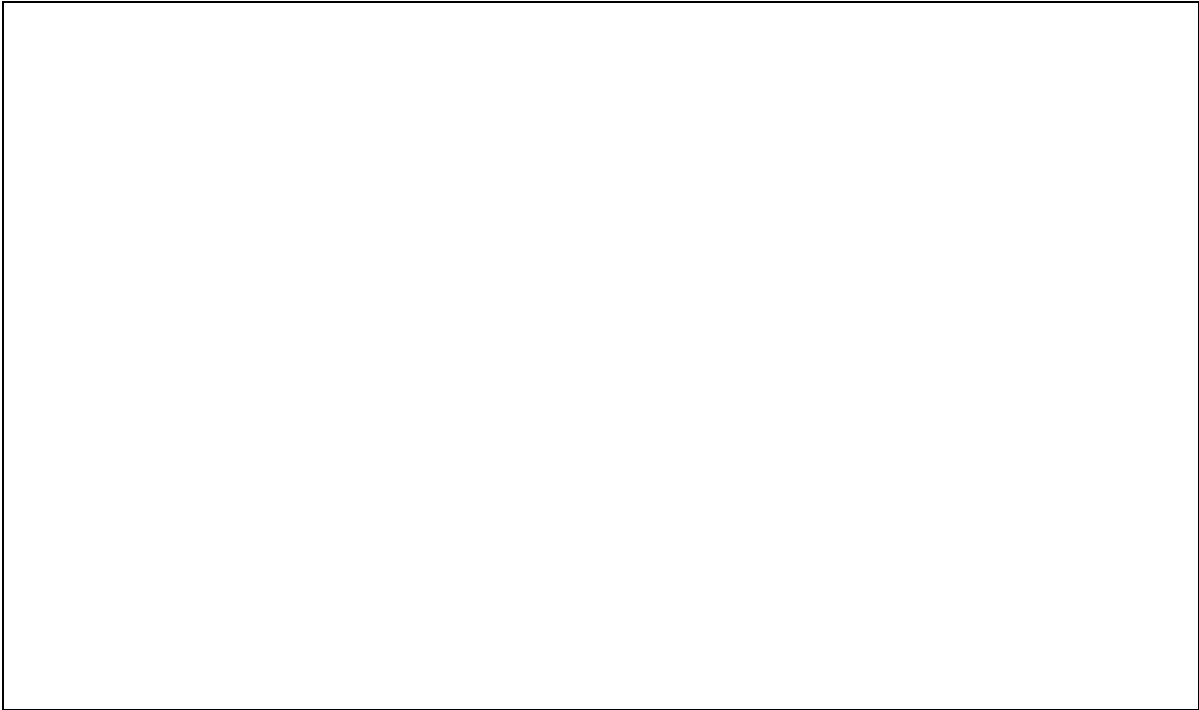


Figure 44. Acceleration away from traffic-control devices: Medium trucks and buses.



Figure 45. Acceleration away from traffic-control devices: Heavy trucks.

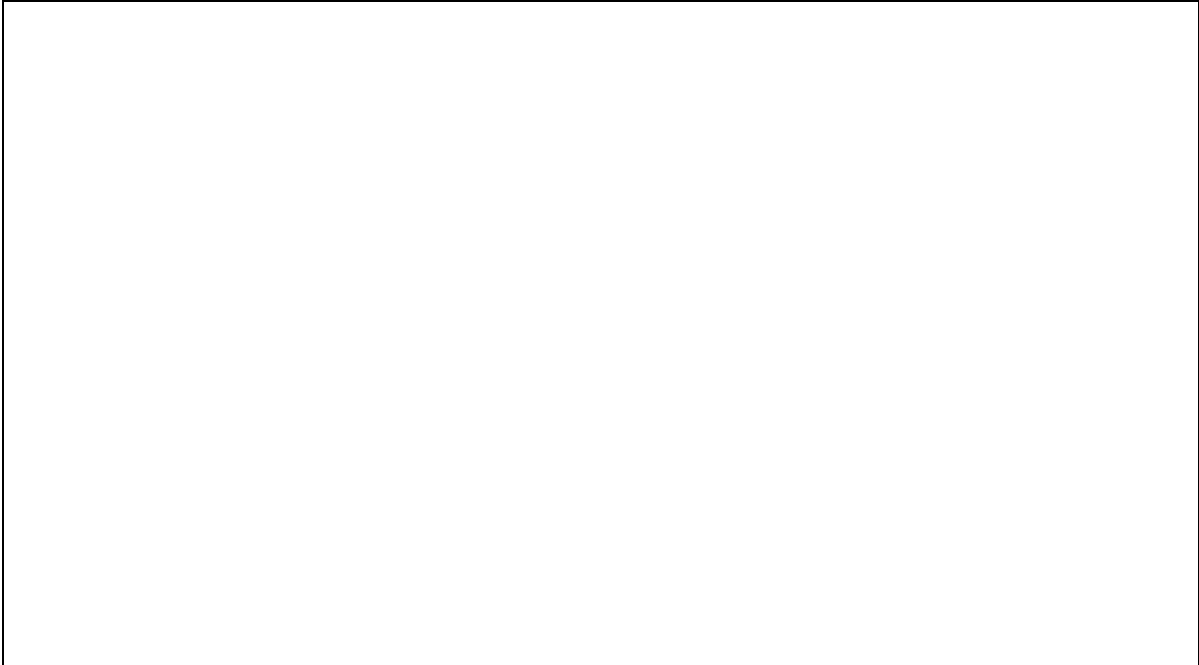


Figure 46. Deceleration caused by upgrades 1.5 percent or more: Heavy trucks.

In summary, vehicle type tells which vehicle's curves to use. Roadway grade determines the crawl speed for that vehicle type. The entrance speed, s_{entrance} , determines whether heavy trucks accelerate or decelerate. Finally, the entrance speed and subsegment length, x , determine the speed, s_x , at distance x along the subsegment — including the subsegment's exit speed, s_{exit} , when x is set to the full subsegment length.

Example: Roadway 16 in Figure 41: Roadway 16 in Figure 41 contains upgrades, which affect only heavy trucks. The sketches in Figure 47 show the resulting heavy-truck speeds as a function of distance along Roadway 16. No other vehicle speeds are affected by upgrades.

In the first segment (1.2 percent up), heavy-truck speeds are not yet affected. They therefore equal the user's heavy-truck input speed for this roadway segment. The second segment (1.7 percent up) causes TNM to start tracking heavy-truck speeds, because its grade equals 1.5 percent or more. Heavy trucks start on this segment at their input speed and then decelerate according to the deceleration curve for heavy trucks on a 1.7- percent upgrade. At the end of the segment, their speed is reduced to approximately one-third of input speed. Equally important, TNM is still tracking heavy-truck speeds because they have not accelerated back to the user's input speed. For this reason, speed is *continuous* from segment to segment (no abrupt changes). Heavy-truck speeds on the third segment (1.3 percent up) therefore start out at the exit speed of the prior segment and then start to increase as heavy trucks accelerate on this less-steep upgrade. Acceleration occurs here because the entrance speed is less than the heavy-truck crawl speed for a 1.3 percent upgrade.

When heavy trucks reach the fourth segment (0.0 percent), they begin to accelerate more rapidly because there is no grade on this segment. In fact, on this segment, heavy trucks happen to accelerate fully back up to input speed. At this point, TNM stops tracking heavy-truck speeds. It also stops enforcing speed continuity from segment to segment. Note that the user's heavy-truck input speed was reached on this segment partly due to the vehicle acceleration and partly because this segment has a lower input speed.

The fifth segment (1.8 percent up) again causes TNM to start tracking heavy-truck speeds, and therefore heavy trucks decelerate as shown. Note that they start out at the heavy-truck *input speed* for this segment, even though this means their speed abruptly increases from its value on the prior segment. TNM allows such abrupt speed changes, whether or not upgrades are involved, whenever the user decides to abruptly change input speeds from segment to segment. Normally TNM does not accelerate/decelerate vehicles from one input speed to the next. Only when TNM is tracking speeds does it provide speed continuity.

Finally, the heavy trucks then accelerate upon entering the sixth segment (1.3 percent down). At the end of this segment, the heavy trucks are still not quite up to input speed. Nevertheless, this is the end of the full roadway and therefore TNM stops tracking speeds.

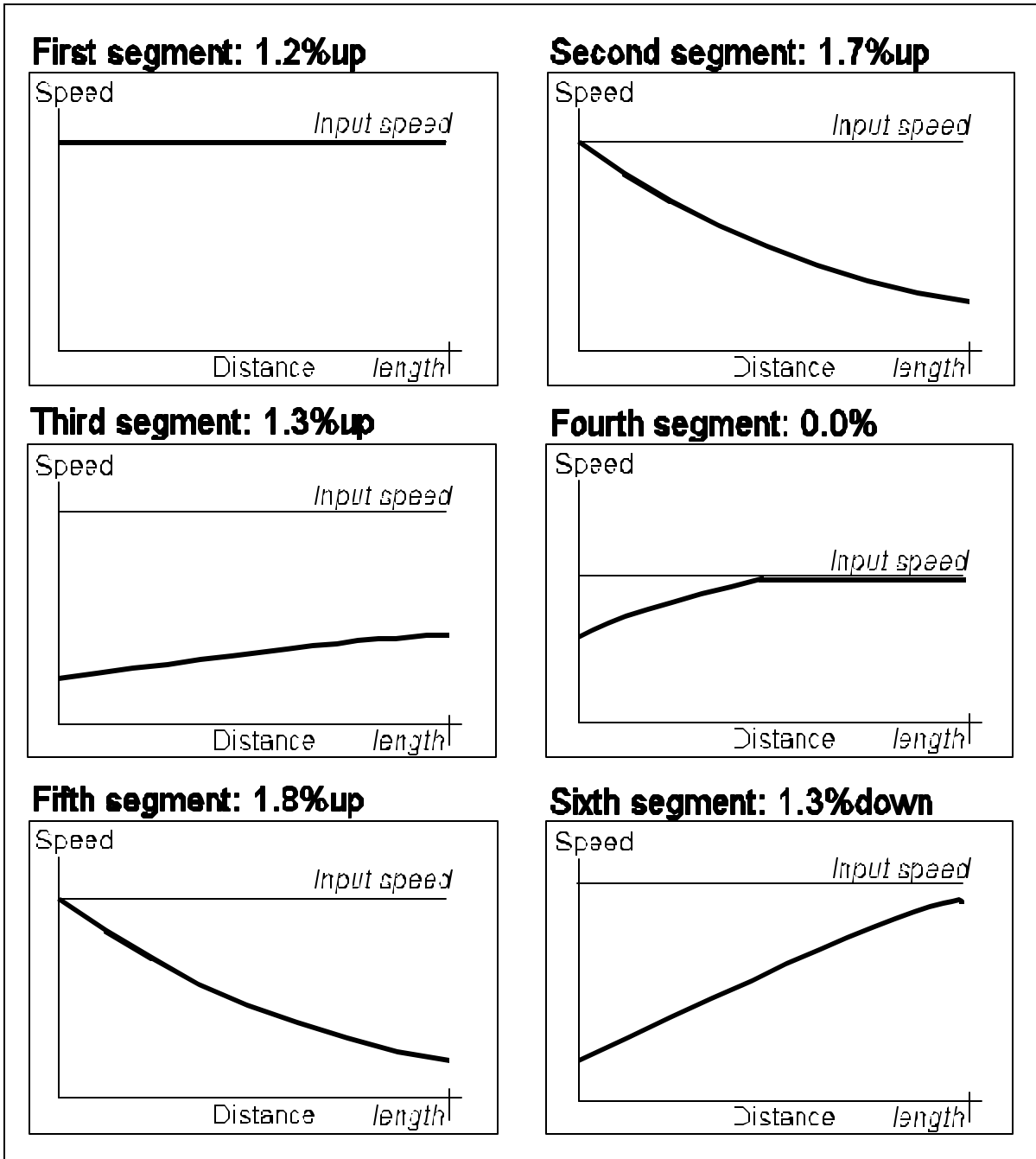


Figure 47. Speeds for Roadway 16: Upgrades.

Example: Roadway 22 in Figure 41: Roadway 22 in Figure 41 contains a traffic-control device (onramp entrance point), which affects the speeds of all vehicle types. The sketches in Figure 48 show only the resulting heavy-truck speeds, as a function of distance along Roadway 22. Speeds for other vehicle types are tracked similarly, though they vary in their details.

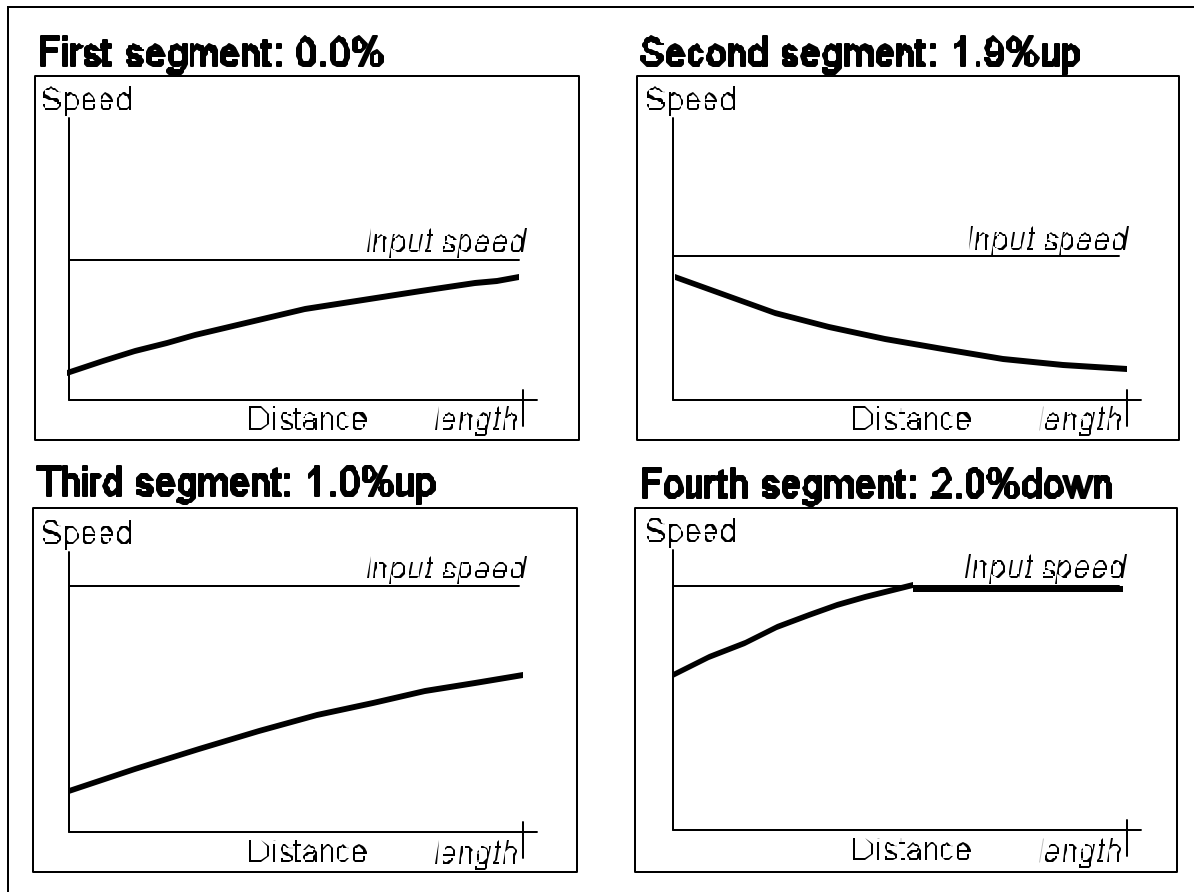


Figure 48. Speeds for Roadway 22: Traffic-control devices and subsequent grades.

The first segment (0.0 percent) starts with a traffic-control device: onramp entrance point. This type of traffic-control device allows a non-zero speed constraint. The one shown in the figure is relatively low, but not quite zero. TNM starts tracking speeds for all vehicles, with this as the initial start speed. Then heavy trucks accelerate according to the heavy-truck acceleration curve for level (zero percent) grade. At the end of the segment, they have not quite reached heavy-truck input speed for this roadway segment.

Speed is continuous from the first to the second segment (1.9 percent up) because TNM is still tracking heavy-truck speeds. (On the other hand, if heavy trucks had managed to accelerate up to input speed in the first segment, then TNM would stop tracking them. In turn, their speed would abruptly change upon entering the second segment, up to heavy-truck input speed for this segment.) On this second segment, heavy trucks then decelerate. Note that the upgrade of this segment, by itself, would have caused TNM to track heavy-truck speeds, even if it had stopped tracking them part way through the first segment.

On the third segment (1.0 percent up), heavy trucks then accelerate upwards towards their crawl speed on this grade. After entering the fourth segment (2.0 percent down), they accelerate more rapidly because of the downgrade. On this segment they happen to reach input speed, and therefore TNM stops tracking heavy-truck speeds.

B.6.1 Some additional points Each vehicle's speed is calculated independently of the others, because the user is free to enter different input speeds for different vehicles. Some commonality exists, however. TNM only contains vehicle dynamics (acceleration/deceleration curves) for three vehicle types: autos, medium trucks and heavy trucks. Other vehicles "mimic" these three. In particular, buses mimic medium trucks and motorcycles mimic autos. In addition, user-defined vehicles mimic whatever TNM vehicle the user designates as most similar.

APPENDIX C

HORIZONTAL GEOMETRY AND ACOUSTICS

Once speeds and emission levels are known, FHWA TNM[®] next computes free-field sound levels, ignoring all attenuating mechanisms except acoustical divergence. This appendix describes the acoustical algorithms associated with these horizontal-geometry, free-field computations:

- # The concept of an elemental triangle
- # The equations for free-field sound energy and sound level.

In addition, this appendix outlines TNM's free-field "sorting" calculations, which it uses to sort roadway segments from most to least important before vertical geometry and attenuation calculations.

C.1 Elemental Triangles

Initially, TNM defines source-to-receiver elemental triangles by the closest angular spacing, at the receiver, of all object endpoints in the XY plane, as shown in Figure 49.

To ensure sufficient precision where object endpoints are not closely spaced (as in the figure), TNM divides elemental triangles so that the maximum subtended angle is no larger than a fixed size (10 degrees in TNM, Version 1.0). For example, Figure 50 shows Figure 49 after TNM imposes upon it a maximum angle of 10 degrees. Note that the last angle subdivision might well be less than 10 degrees. It is the "left-over" angle.

TNM does not further subdivide elemental triangles. Attenuation for the elemental triangles equals the (energy) average of the attenuation along the two sides (legs) of the triangle.

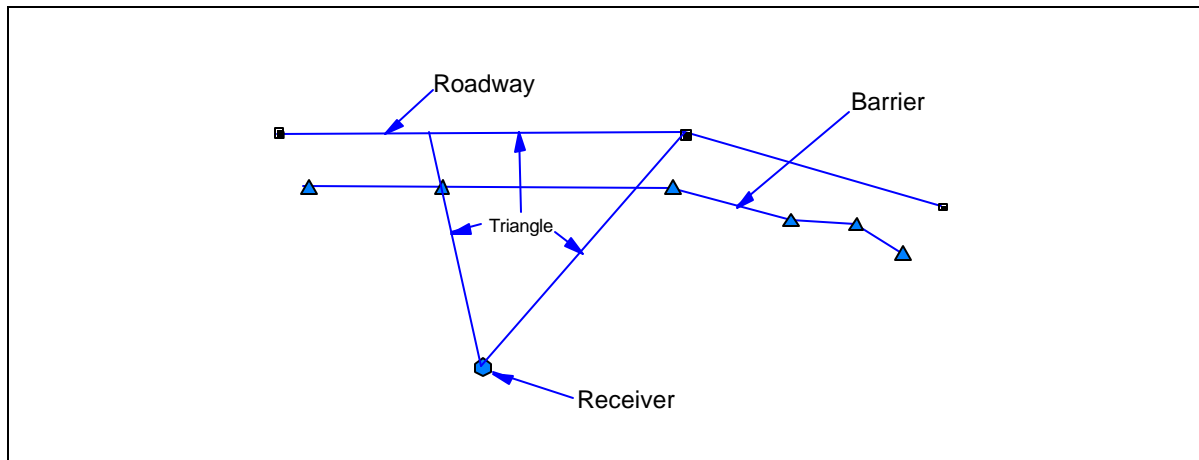


Figure 49. Initial elemental triangle.

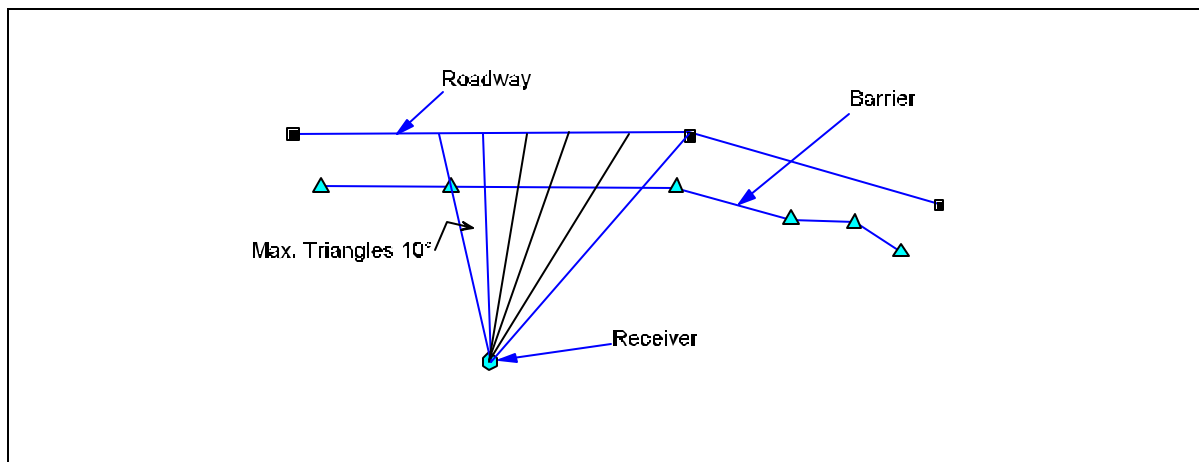


Figure 50. Maximum elemental triangle set to 10 degrees.

C.2 Equations for Traffic Sound Energy and Sound Level

C.2.1 Definitions

TNM's acoustical calculations involve the following indices and variables:

- i index over vehicle types: built-in types and user-defined types.
- h index over subsource heights: 0 and 3.66 meters (12 feet) for heavy trucks and user-defined vehicles that mimic heavy trucks; 0 and 1.5 meters (5 feet) for all other vehicles.
- s "effective" vehicle speed, in kilometers per hour. Speed depends upon roadway segment. It may also differ by vehicle type — either because the user enters a different input speed or because TNM calculates a different speed due to upgrades and traffic-control devices.
- v vehicle volume, in vehicles per hour.

- v_{equiv} equivalent hourly vehicle volume, in vehicles per hour.
- a_h average hourly traffic, in vehicles per hour, which only applies to computation of L_{Aeq1h} , and only when user inputs traffic percentages instead of volumes.
- a_d average daily traffic, in vehicles per 24 hour, which only applies to computation of L_{dn} and L_{den} .
- D_i percentage of total hourly traffic: vehicle type i , which only applies to computation of L_{Aeq1h} , and only when user inputs traffic percentages instead of volumes.
- $D_{i, day}$ percentage of average daily traffic: vehicle type i , daytime, which only applies to computation of L_{dn} (daytime equals 7 am to 10 pm) and L_{den} (daytime equals 7 am to 7 pm).
- $D_{i, even}$ percentage of average daily traffic: vehicle type i , evening, which only applies to computation of L_{den} (evening equals 7 pm to 10 pm).
- $D_{i, night}$ percentage of average daily traffic: vehicle type i , nighttime, which only applies to computation of L_{dn} and L_{den} (nighttime equals 10 pm to 7 am).
- f 1/3rd-octave-band nominal center frequency, in Hz.
- d_1 distance from receiver to first point of roadway subsegment, in meters (see Figure 51).
- d_2 distance from receiver to second point of roadway subsegment, in meters (see Figure 51).
- d perpendicular distance from receiver to roadway subsegment, in meters, where subsegment is extended if needed to meet the perpendicular (see Figure 51).
- " angle subtended at the receiver by the roadway subsegment, in degrees (see Figure 51).
-) L user-entered adjustment factor for a particular receiver/roadway-segment pair, in dB.

TNM computes traffic *sound levels* — L_{Aeq1h} , L_{dn} and L_{den} — only as its very last calculation step for each receiver. Prior to this last step, it calculates traffic *sound energies* instead. As discussed further below, sound levels (L) and sound energies (E) are related by:

$$L = 10 \times \text{Log}_{10}(E), \quad (14)$$

where "Log₁₀" denotes the common logarithm (base 10).

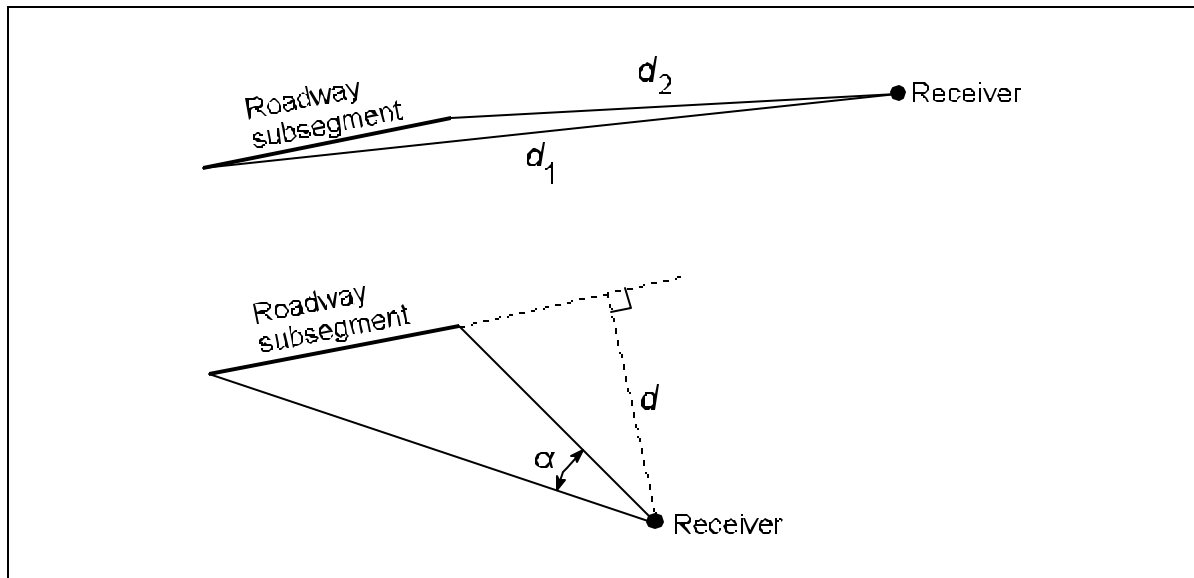


Figure 51. Definition of relevant distances and angles.

C.2.2 Traffic sound energy: "Reference" conditions As its first step in computing free-field sound energy, TNM converts vehicle emission spectra to *traffic* sound energy at specific "reference" conditions. As a result, subsequent computed values refer to full streams of traffic, rather than to individual vehicles.

The word "reference" indicates that the computed traffic sound energies are for a hypothetical reference position at 15 meters (50 feet) from an infinitely long, straight roadway. The 15-meter (50-foot) position substitutes temporarily for actual receiver positions. TNM converts from this reference position to actual receiver positions later. The infinite straight roadway substitutes for the actual roadway length and its curvature. TNM converts to this actual roadway geometry later, as well. Finally, the words "free field" indicates no attenuation from intervening objects (barriers, building rows, terrain lines, ground zones, and tree zones). TNM accounts for such attenuation later, as well.

To compute reference traffic sound energies, TNM first computes an equivalent hourly volume. Separately for each vehicle type, i :

$$\begin{aligned}
 v_{i,\text{equiv}} &= v_i \text{ for } L_{\text{Aeq1h}}, \text{ volume input} \\
 &= \frac{a_h r_i}{100} \text{ for } L_{\text{Aeq1h}}, \text{ percentage input} \\
 &= \frac{a_d (r_{i,\text{day}} + 10r_{i,\text{night}})}{2400} \text{ for } L_{\text{dn}} \\
 &= \frac{a_d (r_{i,\text{day}} + 3r_{i,\text{even}} + 10r_{i,\text{night}})}{2400} \text{ for } L_{\text{den}} .
 \end{aligned} \tag{15}$$

Use of this effective volume allows all subsequent calculations to be identical for the three optional metrics: L_{Aeq1h} , L_{dn} and L_{den} . Such an effective traffic volume is possible for L_{dn} and L_{den} because TNM's input does not allow differing vehicle speeds for the different portions of the day.

In the L_{den} portion of this equation, evening percentages are multiplied by a factor of 3. The accepted international standard for this multiplier is 3.162, which corresponds to an evening sound-level increment of 5.0 decibels. Instead of 3.162, however, TNM uses a factor of 3 to conform to state law of California, the only state that uses L_{den} for traffic-noise assessment. This factor of 3 corresponds to an evening sound-level increment of 4.8 decibels. It is anticipated that this subtle difference will be of no practical consequence in the computations.

TNM then converts from vehicle emissions to "reference" traffic sound energy as follows:

$$E_{\text{traf, ref, upper}}(s_i, v_{i, \text{equiv}}, f) = 0.0476 \left(\frac{v_{i, \text{equiv}}}{s_i} \right) E_{\text{emis, } i, \text{ upper, ff}}$$

$$E_{\text{traf, ref, lower}}(s_i, v_{i, \text{equiv}}, f) = 0.0476 \left(\frac{v_{i, \text{equiv}}}{s_i} \right) E_{\text{emis, } i, \text{ lower, ff}}$$
(16)

for each vehicle type, i , where speed, s , is in kilometers per hour.

In this equation, the factor of 0.0476 results from the complex geometrical relationship between the maximum passby sound energy for a single vehicle, E_{emis} (on the right of the equation), and the time-average sound energy for a full stream of traffic, E_{traf} (on the left of the equation). This factor of 0.0476 corresponds to the term -13.2 dB in Eq. (2) of Section 2 — that is, $10 \times \log_{10}(0.0476) = -13.2$ dB.

Speed enters the equation above, in the denominator, to account for sound-level "duration" during vehicle passbys. Larger vehicle speeds result in shorter durations and therefore lower energy-average sound levels.

Physically, this last equation represents each vehicle type's contribution to sound energy, separately for its two vertical subsources, for a hypothetical "reference" location 15 meters (50 feet) from an infinitely long straight roadway, without influence of intervening ground (that is, free field).

Conceptually, if the upper-height and lower-height sound energies were added, this would yield the total sound energy from that vehicle type. They cannot be added at this point in the calculation, however, because the attenuation from roadway to receiver differs for upper-height and lower-height energies. Also conceptually, one might think of adding together the zero-height sound energies for all vehicle types, so that attenuation could be applied just once to this composite energy. TNM does not do this, however, because it must be able to diagnose sound levels by vehicle type, if desired by the user.

C.2.3 Traffic sound energy at true receiver: Free field Next TNM takes into account the actual receiver and its subdivided source-receiver triangle, still assuming free field propagation. Figure 49, above, shows the two possible geometric situations: (1) receiver nearly on the extended roadway segment; and (2) receiver relatively clear of the extended roadway segment.

TNM first performs a numerical test to distinguish between these two geometric situations and then computes, as follows:

- # If: (1) the perpendicular distance, d , is less than 0.3 meters (1 foot); and also (2) the angle subtended, θ , is less than 20 degrees, then TNM computes the free-field traffic sound energy at the receiver as follows:

$$E_{\text{traf, upper, ff}}(s_i, v_i, \text{equiv}, f) = 15.9 \left(\frac{|d_2 - d_1|}{d_2 d_1} \right) E_{\text{traf, ref, upper}}$$

$$E_{\text{traf, lower, ff}}(s_i, v_i, \text{equiv}, f) = 15.9 \left(\frac{|d_2 - d_1|}{d_2 d_1} \right) E_{\text{traf, ref, lower}}$$
(17)

for each vehicle type, i . The absolute-value signs are needed to ensure that the expression in parentheses is positive.

In this equation, the factor of 15.9 results from the complex geometrical relationship between the receiver and the two ends of the traffic segment. This factor corresponds to the term 12 dB in Eq. (4) of Section 2 — that is, $10 \times \text{Log}_{10}(15.9) = 12$ dB.

- # Otherwise, TNM computes the free-field traffic sound energy at the receiver as follows:

$$E_{\text{traf, upper, ff}}(s_i, v_i, \text{equiv}, f) = \left(\frac{\alpha}{180} \right) \left(\frac{15}{d} \right) E_{\text{traf, ref, upper}}$$

$$E_{\text{traf, lower, ff}}(s_i, v_i, \text{equiv}, f) = \left(\frac{\alpha}{180} \right) \left(\frac{15}{d} \right) E_{\text{traf, ref, lower}}$$
(18)

for each vehicle type, i . In this equation, θ is in degrees and d is in meters.

C.2.4 Traffic sound energy at true receiver: Attenuated Next TNM attenuates the free-field traffic sound energy at each receiver to account for all intervening TNM objects, including the ground, plus the user-entered adjustment factor, ΔL , for this receiver/roadway-segment pair.

To determine the effect of intervening TNM objects, the model submits vertical geometries of the two legs of the source-receiver triangle to its vertical-geometry routines, which return attenuation fractions, $N_{h, f, \text{barrs}}$, for each of the three possible subsources heights, h , for each frequency, f , and for each possible barrier-height perturbation. The vertical geometry routines compute attenuations for each leg of the elemental triangle and return (energy) average attenuations for the triangle as a whole. For the details on the vertical geometry algorithms, see Appendix D.

Then TNM combines its previous computations with these values of N and ΔL , to compute the attenuated traffic sound energy at the receiver, as follows:

$$E_{\text{traf}, h, \text{atten}, \text{barrs}}(s_i, v_i, \text{equiv}, f) = (\phi_{h, f, \text{barrs}}) (10^{\Delta L/10}) E_{\text{traf}, h, \text{ff}}, \quad (19)$$

for each vehicle type, i , and each relevant subsorce height, h . In this equation, the subscript "barrs" indicates that the result depends upon the heights of intervening, perturbable barriers.

This equation relates to others in this technical manual as follows. The term A_s of Eq.(1) in Section 1 equals $10 \times \text{Log}_{10} (N_{h, f, \text{barrs}})$. In addition, the term $*P_{\text{Total}} / P_{\text{Freefield}}^*$ in the last equation of Appendix D equals the square root of $N_{h, f, \text{barrs}}$. In energy terms, attenuating mechanisms such as sound barriers multiply energy by a value less than unity, thus decreasing the sound energy. In sound-level terms, attenuating mechanisms reduce sound levels equivalently, through subtraction. Note that when $N_{h, f, \text{barrs}}$ is less than unity, then $10 \times \text{Log}_{10} (N_{h, f, \text{barrs}})$ is negative — that is, A_s is negative.

C.2.5 Traffic sound levels (L_{Aeq1h} , L_{dn} and L_{den}) at the true receiver: Attenuated

TNM must calculate all of the prior values for all barrier perturbations, because they affect the attenuation between source and receiver. For these computations, TNM computes energies instead of levels. Once the user chooses a barrier design, however, TNM is ready to combine energies into the total energy at the receiver, and then to convert sound energies to sound levels.

For any given barrier design (combination of specific barriers heights, one per barrier segment), TNM finally computes the total traffic sound level at a receiver as follows:

$$L_{\text{traf}} = 10 \times \text{Log}_{10} \left(\sum_{\substack{\text{all freqs,} \\ f}} \left\{ \sum_{\substack{\text{all subdivided} \\ \text{triangles}}} \left[\sum_{\substack{\text{all vehicle} \\ \text{types, } i}} \left(\sum_{\substack{\text{threesubsource} \\ \text{heights, } h}} \left[E_{\text{traf}, h, \text{atten}, \text{specific} \\ \text{barr heights}} \right] \right) \right] \right\} \right). \quad (20)$$

The sound level computed by this equation depends upon the input traffic, as follows:

$$\begin{aligned} L_{\text{traf}} &= L_{\text{Aeq1h}} && \text{if the user has entered } L_{\text{Aeq1h}} \text{ traffic, either as volumes or} \\ & && \text{percentages} \\ &= L_{\text{dn}} && \text{if the user has entered } L_{\text{dn}} \text{ traffic} \\ &= L_{\text{den}} && \text{if the user has entered } L_{\text{den}} \text{ traffic} \end{aligned}$$

C.3 Outline of Free-field Sorting Computations

The calculations above are needed within TNM's main calculation loop, in which it computes attenuated sound levels at all receivers, for all combinations of barrier heights. Prior to this main calculation loop, TNM computes free-field sound levels (no attenuation, no subdivision of roadway segments) to sort roadway segments from *most* to *least* important. This section outlines these free-field, sorting calculations.

To perform the sorting calculations:

- # TNM first determines the entrance and exit speeds of each vehicle type on the roadway segment under computation, using Appendix B. From these two speeds, TNM then computes the roadway segment's average speed, s_i , where i is an index over vehicle types.
- # Then TNM computes $E_{\text{emis}, i}(s_i, 500 \text{ Hz})$, using Appendix A, for each vehicle type, i . Note that the model computes only at 500 Hz for these sorting calculations.
- # Then TNM computes an equivalent hourly volume, $v_{i, \text{equiv}}$, from Eq. (15) above, for each vehicle type, i .
- # Then TNM computes $E_{\text{traf, ref}}(s_i, v_{i, \text{equiv}}, 500 \text{ Hz})$ from the following modification of Eq. (16):

$$E_{\text{traf, ref}}(s_i, v_{i, \text{equiv}}, 500 \text{ Hz}) = 0.0476 \left(\frac{v_{i, \text{equiv}}}{s_i} \right) E_{\text{emis}, i}, \quad (21)$$

for each vehicle type, i , where speed, s , is in kilometers per hour.

- # Then TNM makes the relevant geometric test. Based upon the outcome of that test, the model then computes $E_{\text{traf, ff}}(s_i, v_{i, \text{equiv}}, 500 \text{ Hz})$ from either a modified Eq. (17) or a modified Eq. (18).

Modified Eq (17):

$$E_{\text{traf, ff}}(s_i, v_{i, \text{equiv}}, 500 \text{ Hz}) = 15.9 \left(\frac{|d_2 - d_1|}{d_2 d_1} \right) E_{\text{traf, ref}}, \quad (22)$$

for each vehicle type, i .

Modified Eq. (18):

$$E_{\text{traf, ff}}(s_i, v_{i, \text{equiv}}, 500 \text{ Hz}) = \left(\frac{\alpha}{180} \right) \left(\frac{15}{d} \right) E_{\text{traf, ref}}, \quad (23)$$

for each vehicle type, i , where perpendicular distance, d , is in meters.

- # Then TNM computes $E_{\text{traf, atten}}(s_i, v_{i, \text{equiv}}, 500 \text{ Hz})$ from the following modification of Eq. (19) above:

$$E_{\text{traf, atten}}(s_i, v_{i, \text{equiv}}, 500 \text{ Hz}) = \left(10^{\Delta L/10} \right) E_{\text{traf, ff}}, \quad (24)$$

for each vehicle type, i . This modification accounts for only the user-entered adjustment factor between the receiver and roadway segment under consideration. It ignores all other attenuations and is therefore computed very quickly.

Then TNM sums traffic energies over all vehicle types, using the following modification of Eq. (20) above:

$$E_{\text{traf}} = \sum_{\substack{\text{all vehicle} \\ \text{types, } i}} [E_{\text{traf, atten}}]. \quad (25)$$

Finally, for this receiver TNM sorts all roadway segments according to the energies computed by Eq. (25), from high to low. This is the order in which these roadway segments are then computed, for this receiver, in TNM's main calculation loop.

Note that this sorting process proceeds quickly, because: (1) its computations are free field rather than attenuated; and (2) roadway segments are not subdivided during computation.

Once roadway segments are sorted in this manner, then TNM does its full set of attenuated/subdivided computations *in the sorted roadway order*. As a result, for these very time-consuming computations, TNM considers the most important roadway segments first and the least important last.

During these time-consuming computations, as TNM finishes with each individual roadway segment it computes a running total of the attenuated sound level up to that point in the computation. It then adds to this running total the *free-field* sound level from all *remaining* roadway segments. If this remaining free-field sound level contributes less than 1 decibel to the running total, then TNM stops its computations. Certainly the remaining *attenuated* sound level cannot be significant if the remaining *unattenuated* sound level is not.

Because of this sorting process, TNM avoids computing attenuated sound levels for roadway segments that are completely insignificant and thereby reduces computation time.

APPENDIX D

VERTICAL GEOMETRY AND ACOUSTICS

This appendix describes the details of the acoustical propagation algorithms and mathematics of the “vertical geometry.” It also presents much of the logic that is used in creating and evaluating propagation paths. Much of the material in this appendix was prepared during the TNM's design, as a concept and design document; therefore, the style of writing is somewhat different from that of the other appendices.

D.1 Overview

The vertical geometry computations are performed for a single line or cross-section between a source and receiver. This portion of the model evaluates all of the elements or objects that are present between the source and receiver. It is called the “vertical geometry” because the geometry at this level is two dimensional - in the vertical plane of the source and receiver. It is at this level that all of the terrain and shielding computations are made.

The vertical geometry algorithms receive vertical geometry information between source and receiver pairs from the “horizontal geometry” routines. The vertical geometry section computes attenuation for each leg of the elemental triangle in α -octave bands, then (energy) averages the attenuations. The average attenuation values are then applied to the entire elemental triangle.

Below, Section D.2 discusses the various elements that can be found in the vertical geometry and the approximations that are made to reduce computation time. Section D.3 discusses how the elements are combined to create propagation paths from the source to the receiver. Finally, Section D.4 presents the mathematics used to calculate the ground effect and shielding attenuation between the source and the receiver.

D.2 Vertical Geometry Elements and Approximation

The vertical geometry is defined by an X-Z cross section of the horizontal geometry. Z is the Z-axis, and X is a projection of the X-Y plane in the horizontal geometry onto the line from the source to the receiver. The geometry is defined such that it always starts with the source and ends with the receiver. For purposes of definition in this document, it is assumed that sound propagates from the source on the left to the receiver on the right. Surfaces in the geometry have a left face, a right face, or both depending on whether the surface(s) face the source or the receiver. A surface is said to face left if it faces toward the source. A surface is said to face right if it faces toward the receiver. If it faces neither left nor right, the surface is said to be flat. Figure 52 shows the definitions of various surfaces in the vertical geometry.

An element of vertical geometry is defined as any object that can affect propagation between the source and the receiver. The set of elements includes sources, receivers, ground points, barriers, berms, ground zones, tree zones and buildings. Propagation is affected by the presence of a reflecting surface or a diffraction point. The following section lists and describes the elements affecting sound propagation that are modeled in TNM.

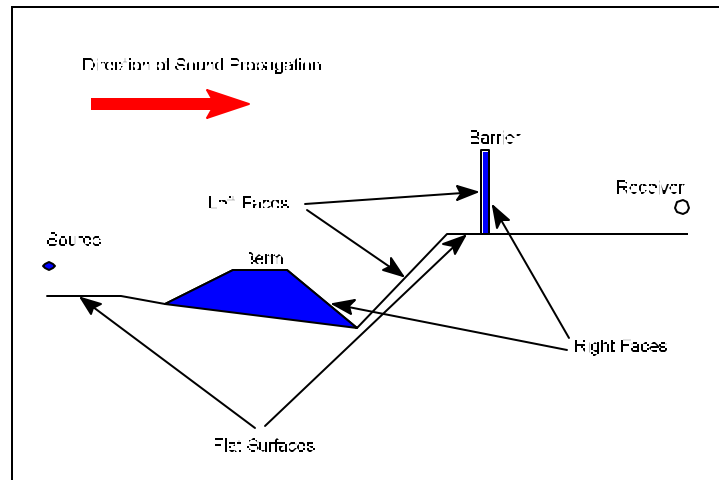


Figure 52. Vertical geometry definitions.

D.2.1 Elements of Vertical

Geometry. This section provides definitions of the elements of the vertical geometry and how they are used. Details on the implementation and governing equations are given in Section D.4.

Ground points: Other than the source and the receiver, ground points are the most commonly encountered component of the vertical geometry. Ground points are created at the source and receiver locations and from other objects such as terrain lines. Ground points are passed from the horizontal geometry routines and are stored as points of known elevation and distance from the source. The model assumes that the ground between any two points changes linearly. The line segment between ground points is called a ground segment. Each ground segment has a ground impedance assigned to it. (The user specifies ground type or a value of Effective Flow Resistivity to define the “acoustic hardness” of the ground. These values are converted to impedance.) The ground impedance is passed from the horizontal geometry routines. The ground location is critical in that it defines where reflections and diffractions may need to be modeled.

Diffraction (“diffraction points”) can occur at ground points when two ground segments meet to form an angle other than 180 degrees. Diffraction points are also formed when any two ground segments with different impedances meet at any angle. In addition to diffraction, ground segments can also serve to reflect sources, receivers, diffraction points and other objects in the geometry that are positioned to the left of the segment. Reflections in the ground are calculated as normal propagation paths but with the reflected geometry and a (complex) multiplicative factor based on the ground impedance of the reflecting segment. For reflections in the segment, the direction of sound propagation for the image is toward the reflecting segment, until the path reaches the reflecting segment. At this point, sound propagation continues toward the receiver (see Section D.3.3 for more detail). A single ground impedance value is assigned to each segment.

Impedance discontinuities: Impedance discontinuities are points where two ground segments of different impedances meet, such as at the edge of a roadway, where acoustically hard ground meets soft ground. These points always form a diffraction point, but may or may not be modeled depending on the expected contribution to the total sound level at the receiver (see Fresnel Zones in Section D.4.4). The diffraction is calculated based on the impedances and angles of the segments on either side of the common point.

Barriers: Barriers are structures that stand vertically in the Z-axis direction, and have a height and a base. They also have surface impedances associated with them on each side. Reflections in barrier surfaces are modeled like reflections in ground segments, and impedances are computed from user-entered Noise Reduction Coefficients. The default surface is acoustically hard, with a reflection coefficient of unity.

Barriers have diffracting points at the bottom of the left face, the top, and the bottom of the right face (see Figure 53). Barriers also have reflecting surfaces on both the left and the right face. The left face can reflect the geometry to the left of the barrier in the same way a ground segment does. As described above, α -octave absorption coefficients are given for each face, therefore the associated attenuation is attributed to reflections in the barrier surface. The right face can reflect the receiver only. The barrier top and bottom are assumed to have zero width.

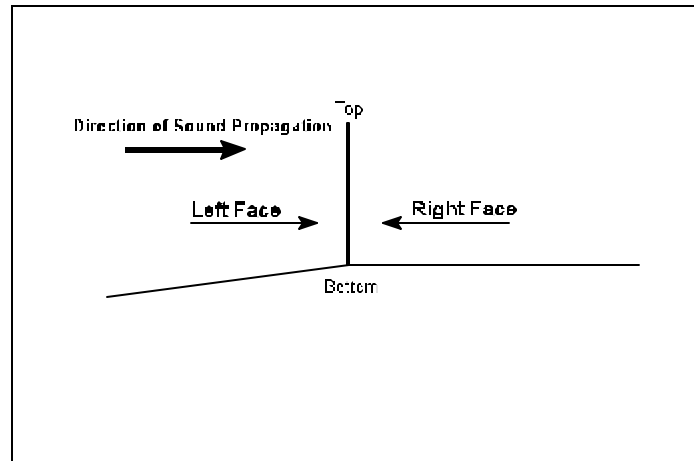


Figure 53. Barrier face definitions.

As with impedance discontinuities, barrier diffraction is only modeled when the contribution of the diffracted components are significant, as determined by the Fresnel zone test (see Section D.4.4).

Berms: A berm is a special type of ground line formation that acts like a barrier. To the user, it is a shorthand method for entering a specific combination of ground lines. Berms are implicitly modeled with a ground point algorithm. A berm is modeled as two wedges that share a flat top surface. (Ground effects are calculated for the berm's flat top.) Although TNM maintains a default value of 0 for berm top width, the width can be changed. However, TNM has shown some apparent anomalies in the diffraction algorithms for berms with a top width.

A berm consists of (normally) soft ground segments with user-specified sloped sides and top width. The vertical geometry receives the center point (x,z) coordinate of the berm (this point is used as a ground point) the height, the angle made with the leg and the berm line, and a pointer to the berm element that contains the widths of the top and bottom of the berm. From this information, the model calculates the ground points that form the berm by finding its intersections with the ground present around the berm center using geometric routines. Like wall-type barriers, diffraction from the intersection of the side of the berm and the ground (base corners, D_{cor}) will be computed, along with the reflection (image) of the source in the sides of the berm and reflection along the top of the berm.

Like wall-type barriers, berms can be specified with multiple heights (perturbations), as shown in Figure 54. The multiple height indexing will be handled inside this algorithm and results for the perturbations will be returned. If the berm is perturbed, all possible base corners and top locations are computed. (Note that the Z_0 base height of the berm is a true ground point, or a point of known ground elevation.) The user is allowed to put barriers on berms. In this case the berm is not perturbable.

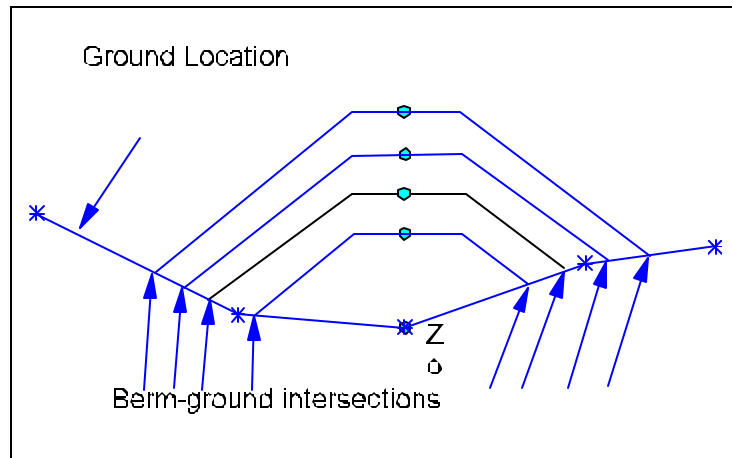


Figure 54. Example berm, shown at four perturbation heights.

Tree zones: Tree zones are areas of the vertical geometry through which propagation paths may pass. Tree zones begin at a vertical segment that is anchored to a specific ground point and extends from the ground upward in the Z direction to a user-defined height. Zones end at a segment anchored to another ground point and extending from the ground up to the same user-defined height. The model determines the distance the propagation path passes through this zone (see Figure 55). The ground type under the tree zone is determined by the ground type for the ground segments beneath the Tree Zone and is independent of the Tree Zone. Ground propagation through the Tree Zone is calculated ignoring the Tree Zone (i.e., in the normal way). The Tree Zone simply adds additional attenuation to the propagation paths. Details of tree attenuation are given in section D.4.6.

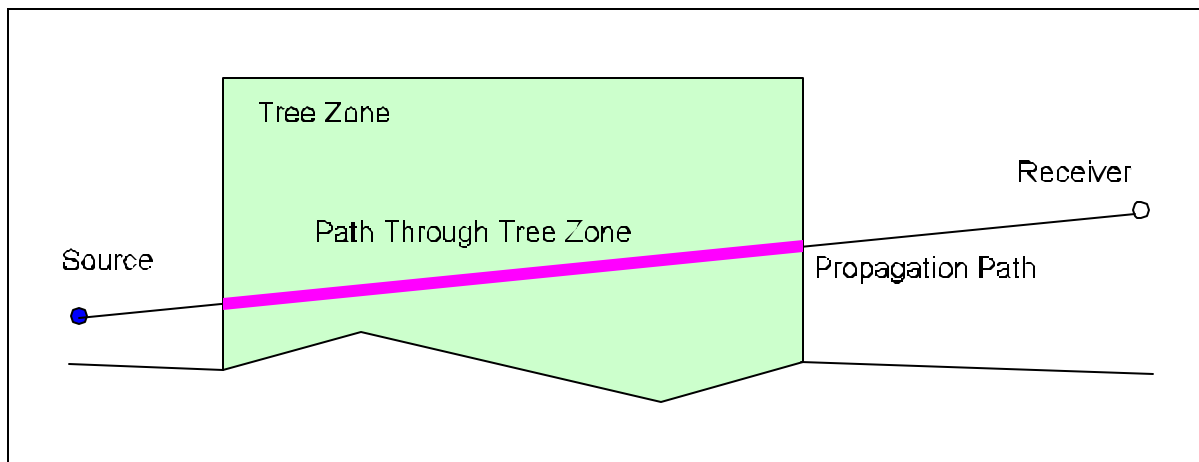


Figure 55. Propagation path through tree zone.

Rows of buildings: Rows of buildings are similar to tree zones in that they only affect propagation paths that pass through them. A building percentage is assigned to each row. The building percentage represents the amount of linear space, for each building row, that contains building structures. This percentage is used to determine the total shielding provided by the building row.

D.2.2 Approximations. This section describes several approaches taken within the TNM's vertical geometry routines to reduce computation time.

Perturbable barrier reduction: The TNM is designed to handle up to two perturbable barriers in the source-receiver path. If three or more perturbable barriers are encountered, TNM chooses the most effective pair of barriers based on their *input* heights. This test is performed at the beginning of the evaluation of a given vertical geometry, and TNM then discards all other perturbable barriers for the remainder of the analysis. The choice of the most effective pair of barriers is made with the “Foss selection algorithm” [Foss 1976]. This is a relatively simple and quick procedure that computes attenuation for two barriers in series from path length differences. The procedure follows directly from Foss' scale model measurements, which show good agreement with the algorithm. The equations and an illustration are given in Section D.4.10.

Ground smoothing: The purpose of ground smoothing is to “smooth” away multiple ground points that have small effects on the overall shape of the ground. Smoothing is performed to reduce computation time by minimizing the number of diffraction points and the number of reflecting segments in the vertical geometry to be modeled where the effect on the sound level would be small. The smoothing algorithm has been designed to make only small changes to the vertical geometry. Only inflection points in terrain of the same ground type are considered for smoothing (including small berms); ground-impedance discontinuities are never smoothed away.

The ground-smoothing algorithm looks at three or more points in series. It fixes a line between the outer two points and then checks the perpendicular distance from this line to all the points between. This distance is checked against “max_point_offset,” a variable that fixes the maximum allowable deviation from a line. If the distance for a point is less than *max_point_offset*, the point is thought to lie close enough to the line formed by the two outer points to be ignored in the propagation calculations. Therefore, the inner point can be removed from the geometry. Points that fail this test are flagged as necessary inflection points in the geometry. The TNM is structured to allow *max_point_offset* values to be set separately for upward and downward deviations.

Geometry simplification: The TNM works with up to two highest path points (HPPs) between the source and receiver. If more than two HPPs exist in the source-receiver path, the Foss selection algorithm is used to reduce the number of HPPs to the two most effective. The simplification is very similar to that used for the selection of the perturbable barriers, however it is applied to both barrier tops and ground points that are HPPs.

Regression ground and ground-impedance averaging: The TNM next evaluates the complexity of the geometry and if necessary, approximates it as discussed below. To enable TNM to handle complex geometry and to improve run time for those cases, straight-line approximations to the ground has been combined with a method of ground-impedance averaging [Boulanger 1997]. This (combined) approach is used where more diffraction points are encountered than the De Jong model can properly handle, such as would be encountered with one or more intervening roadways or hilly terrain. Potential diffraction points occur at each impedance discontinuity and at each ground inflection point that has not been smoothed away by the initial smoothing algorithm.

The ground regression is performed differently for two different frequency regions. For the potentially most significant diffraction point in the geometry, a test is performed to determine if the point is in the source-to-receiver Fresnel zone for $N > -0.3$. If the point is inside that zone, a transition frequency, f_T ,

at which the point moves outside of the Fresnel zone is computed. Then, for frequencies above f_T , the ground regression algorithm approximates the ground between “source” and “receiver” (either of which can be a highest path point), and the sound propagation paths are generated (see below) based on that representation of the ground. For frequencies below f_T , the point is designated a “near-highest path point” (NHPP) and the ground regression algorithm is used separately to approximate the ground between the source and the NHPP and again between the NHPP and the receiver. A separate set of propagation paths are then generated for the revised geometry, including the NHPP as a diffraction point.

Any impedance discontinuities present in the original geometry are projected onto the regression ground line(s), and the ground-impedance averaging is performed.

The Boulanger approach to ground-impedance averaging is used for cases where more than one impedance discontinuity is present in the local geometry between source and receiver or highest path points. Instead of computing the multiple diffraction paths explicitly, this approach computes a Fresnel ellipse about the reflection point on the ground and computes the *area* inside the ellipse represented by each type of ground. Then, an average reflection coefficient is computed from the reflection coefficient for each ground type weighted by the ratio of its area to the total area. The average reflection coefficient is used, and no diffraction terms are computed at all. However, the size of the ellipse is a function of frequency, so the average impedance and therefore the reflection coefficient will often change for each $\frac{1}{2}$ octave band. Section D.4.6 explains this approach further and includes an illustrative figure.

Path significance test: A Fresnel zone test is used for each propagation path generated, to determine if the path is significant enough to be included for computation. A path is considered significant and is computed if the receiving point falls into the region where the Fresnel number is greater than -0.3. This quick test was incorporated into the TNM to avoid the time-consuming computation of the many possible diffraction paths in the more complex geometries with barriers. This test is performed for bright-zone diffractions only; all diffraction paths where the receiving point is in the shadow zone are assumed to be significant.

D.3 Propagation Paths

A propagation path is defined as any path that starts at the source and ends at the receiver. The path can be reflected in surfaces, be diffracted around specific obstructions, or pass through tree zones or rows of buildings. For any given vertical geometry there will usually be multiple propagation paths. All of the propagation paths associated with a single vertical geometry are summed at the receiver to yield a net sound pressure and resulting attenuation relative to free field.

A single propagation path is made up of propagation segments. Propagation segments start and end with path points. A path point can be a source, a diffracting point or a receiver. (see Section D.3.2 for more on diffractions). Only sources can start a propagation path, and are found only at the beginning of the first segment. Only receivers can end a propagation path, and are found only at the end of the last segment. The complete set of propagation paths for a vertical geometry contains paths with all possible combinations of sources (real and image), diffraction points, and receivers (real and image) connected in the direction of sound propagation (ignore back propagation). For a diffraction point to be used in a path one of the following two conditions must exist: (1) the next point in the path must fall

in the Fresnel Zone of the geometry formed by it, the diffraction point in question, and the path point just before the diffraction (see Section D.4.4); or (2) the next point must be in the shadow of the diffraction point in question and the path point just before the diffraction.

Propagation paths always start at the source or an image source. From there, all possible propagation segments are formed, by connecting the source to either a diffraction point or the receiver in the direction of sound propagation (this is to the right for all real sources and diffraction points, but may change when dealing with images). To make this connection, the source must have an unobstructed view of the point. If the connection is made to the receiver, the path ends. If the connection is made to a diffraction path a test must be made to see if the diffraction point is either in the Fresnel zone or in the shadow. If it passes this test, the diffraction point becomes the new effective source or "emitter," and the process continues with an attempt to connect to another diffraction point or a receiver. This process continues until all propagation paths end at a receiver.

The Fresnel zone calculation (see Section D.4.4) is frequency dependent. The test to determine if the path that includes the diffraction will significantly contribute to the total sound pressure at the receiver is done using a low frequency (250 Hz) as the cutoff. Any paths with diffractions that don't meet this criteria are ignored. For a path to be modeled, all the diffractions in the path must pass the Fresnel zone test. As a time saving measure, the transition frequency, based on the Fresnel zone, is saved for each path. This is the lowest frequency above which at least one of the diffractions in the path is insignificant (fails the Fresnel zone test).

Reflections in ground segments and barriers can add extra propagation paths. Reflected propagation paths start at the source image in the surface and propagate toward the image reflecting surface. The propagation progresses normally using the reflected geometry. The entire geometry to the left of a reflecting segment, including reflections in those segments being reflected, is reflected into the segment. At the reflecting surface, the path continues normal propagation to the receiver using the real geometry. This way the complete reflected field and all reflected paths are modeled.

The following sections discuss various elements that can describe propagation paths.

D.3.1 Free field. This is the simplest propagation path to be calculated. It is simply the straight line (line of sight) path from the true source to the true receiver. The free field path ignores all obstructions and images in the vertical geometry.

D.3.2 Diffractions. "Diffractions" are used to model areas of propagation paths that pass around edges in the vertical geometry. An edge can be a point where two ground segments meet, the top of a barrier or the bottom of a barrier. Where the sound wave diffracts over an edge, energy from the original wave is redirected. An "altered" wave now propagates from the diffraction point. The energy from the original wave decreases in magnitude based on the Chi (P) function, which is dependent on the angles and distances to the source and the receiver from the diffraction point. The diffraction field has a maximum of half the sound pressure of the free field on the "grazing line." The grazing line is the line formed by the source and the diffraction point. The Fresnel integral function is used to calculate the reduction in energy, and is based on the P function. Since sound appears to emanate from the diffraction point, the diffraction point is, for the purposes of the model, mechanically treated as a

"sound emitter" with similar properties to a real source (except that a propagation path cannot start with a diffraction point) when constructing propagation paths.

See Fresnel Zones in Section D.4.4, for details on when diffraction points are included in a propagation path.

Single diffractions: Single diffractions involve a source, a diffraction point, and a receiver. For example, diffraction points can be points where two ground segments meet, the top of a barrier, or the bottom of a barrier. An example of the diffraction geometry with a barrier top as the diffraction point is shown in Figure 56. To calculate the diffraction coefficients, the following effective distances must be known: the source to the diffraction point, the diffraction point to the receiver, and the source to the receiver. In addition, the angles that the source-diffraction point and diffraction point-receiver segments make with the left side of the diffracting surface must be determined. These values are used to calculate P in the diffraction coefficient. This is explained in more detail in Section D.4.3.

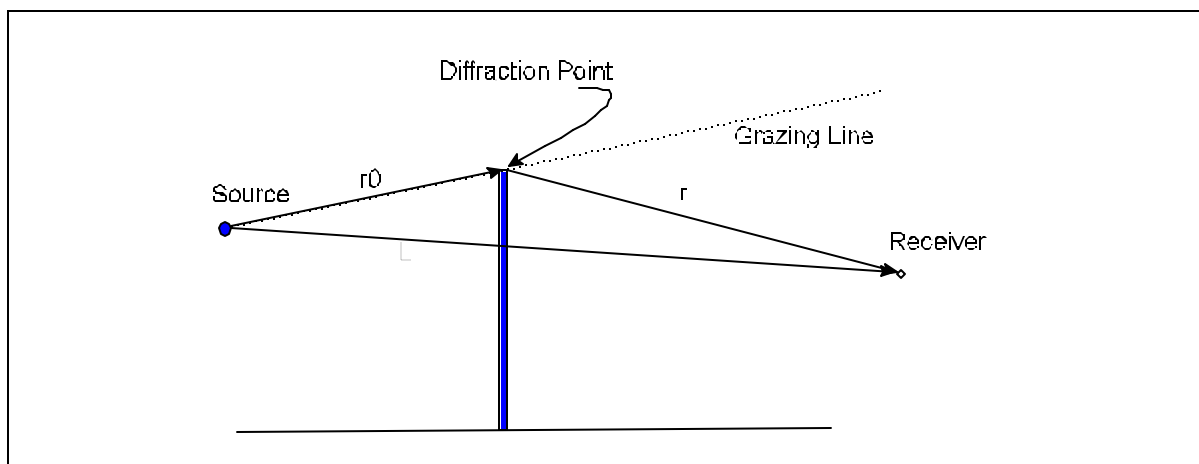


Figure 56. Single diffraction geometry.

Multiple diffractions: Multiple diffractions are very similar to single diffractions. The paths consist of more than one diffraction point, a source, and a receiver, as shown in Figure 57. They are modeled with multiple single diffractions, multiplied together. Each diffraction point in the path is modeled with one single diffraction calculation. For each single diffraction in a multiple diffraction case, the angle about a diffraction point and the total path length are kept constant while the source and the receiver are moved to their effective locations, so that proper angles and path lengths are preserved. To determine the effective location of the source, the first propagation path segment on the source side of the diffraction is fixed. Segments following this one back, moving back toward the source, are rotated about any intermediate points so that they extend the left segment along the same line. The same is then done on the receiver side of the diffraction to position it in its effective location (see Figure 58). The new rotated geometry is used to calculate the diffraction resulting from this diffraction point using the single diffraction algorithm. This is repeated for each diffraction point in the path. The diffraction coefficients are then multiplied together to calculate the total diffraction for the path.

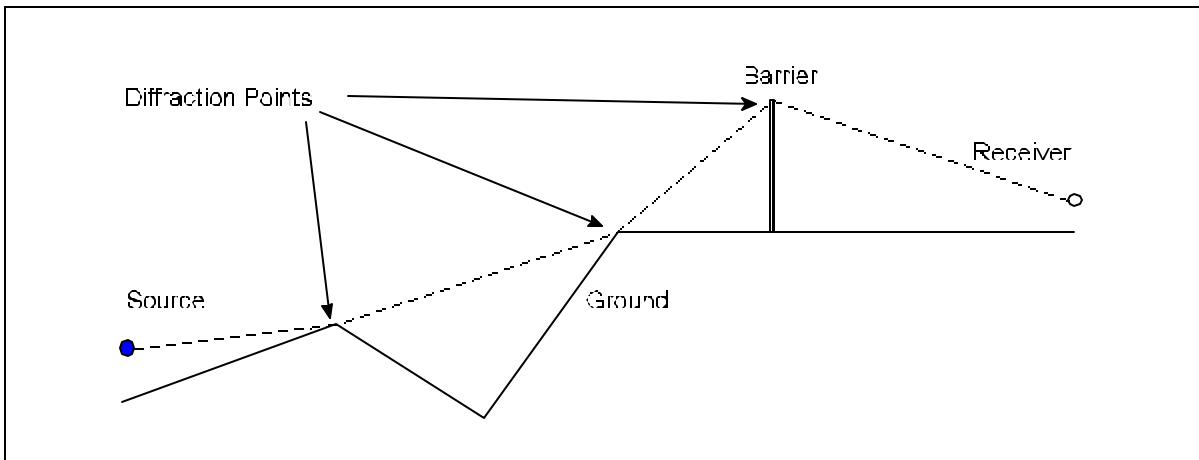


Figure 57. Example of multiple diffraction.

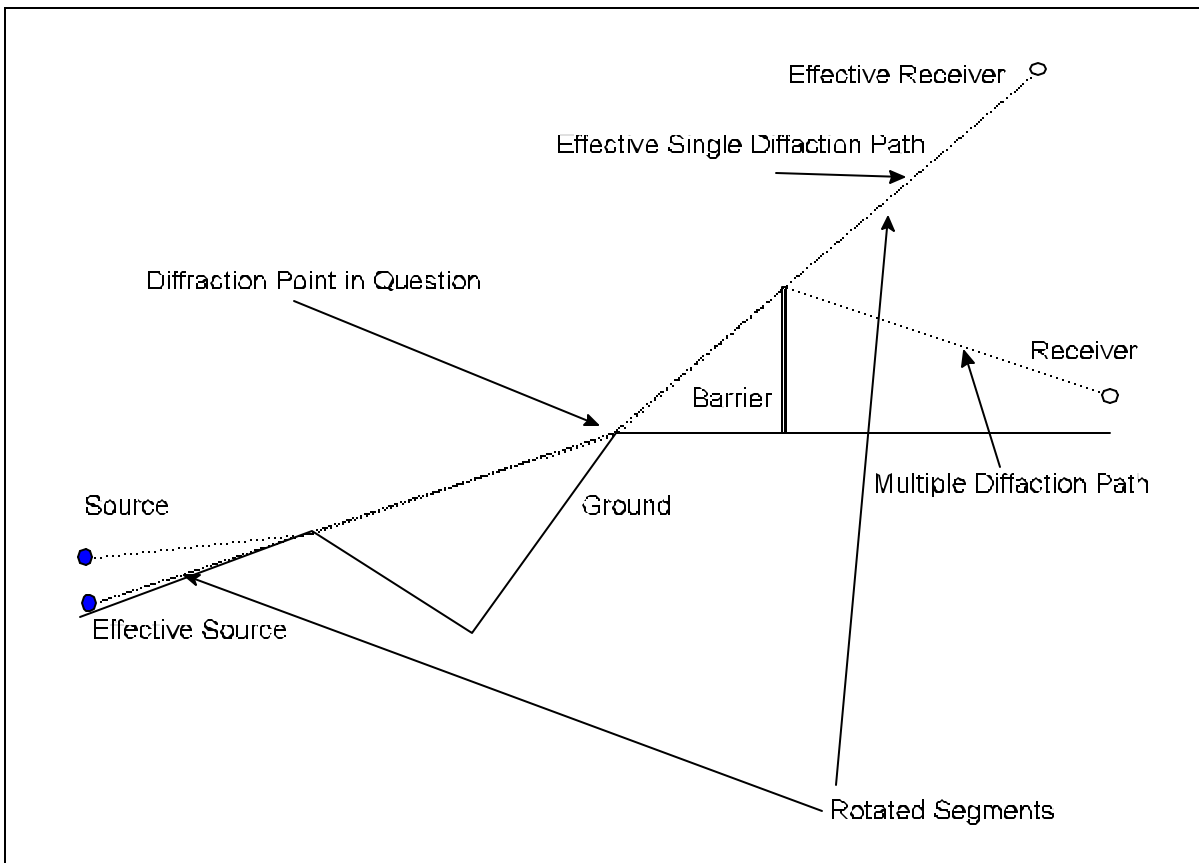


Figure 58. Example of an effective single diffraction from a multiple diffraction path.

D.3.3 Reflections. Reflections create extra propagation paths that can result in increased sound

pressure at the receiver. This section discusses how and where reflections are accounted for in the vertical geometry.

Reflections in ground segments: Every segment in the vertical geometry may reflect the geometry above or to the left of it. To check if a segment reflects, first extend the line defined by the segment endpoints in both directions. Take the right most point from the vertical geometry that lies to the left of the left end of the real segment, if one exists. Objects directly over the right most end point are excluded. Reflect this point and the entire vertical geometry to the left of that point, including all reflections that take place in the geometry being reflected, about the reflecting segment. The geometry of Figure 59 shows some examples of reflections. (Note that left is defined as the side closest to the source and right is defined as the side closest to the receiver.)

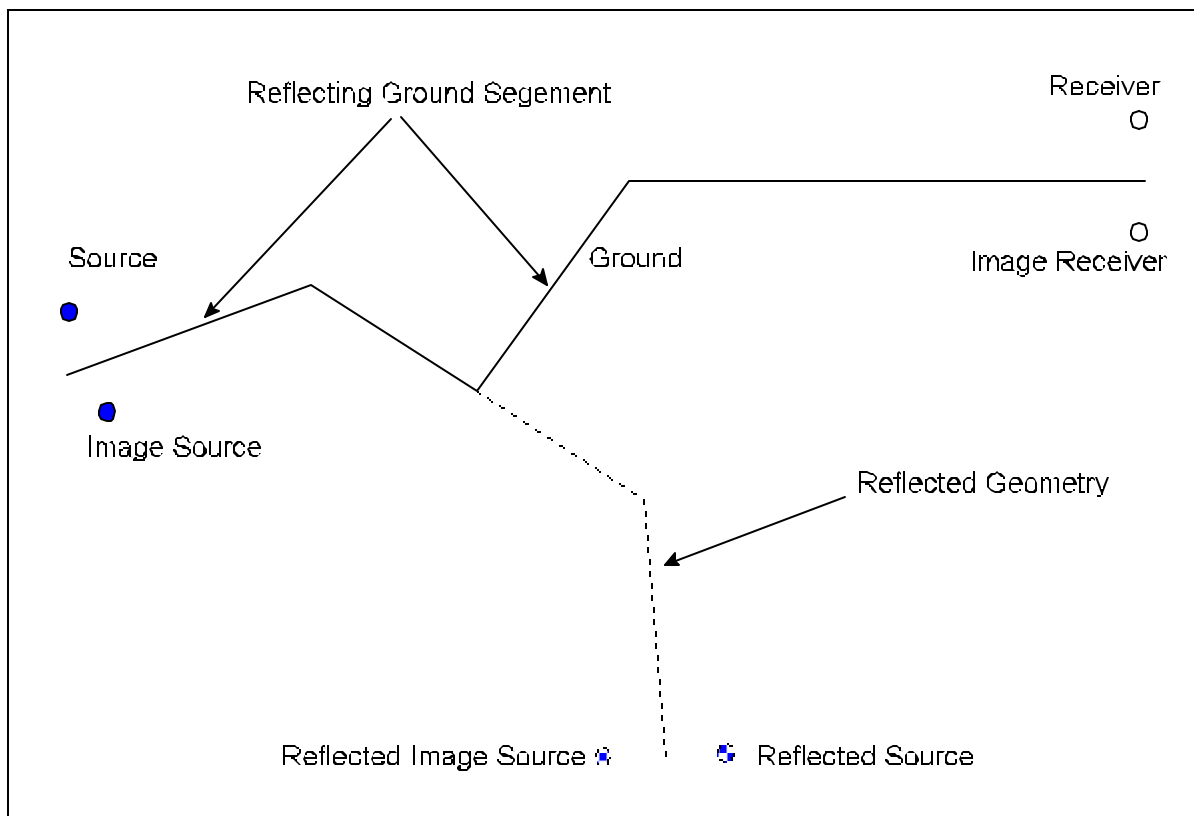


Figure 59. Example of a geometry with reflections.

The direction of sound propagation is, for the real source and diffractions points, always to the right, toward the receiver. The direction of propagation from reflected (image) sources and diffractions point may not always be to the right, but it is in the direction of the receiver. For image propagation path points, the direction of propagation is always toward the segment that reflected the points. For compound reflections, this starts with the segment that last reflected the point to the segment that first reflected it. Figure 60 shows a few examples of the direction of propagation. Propagation paths are also drawn to image receivers.

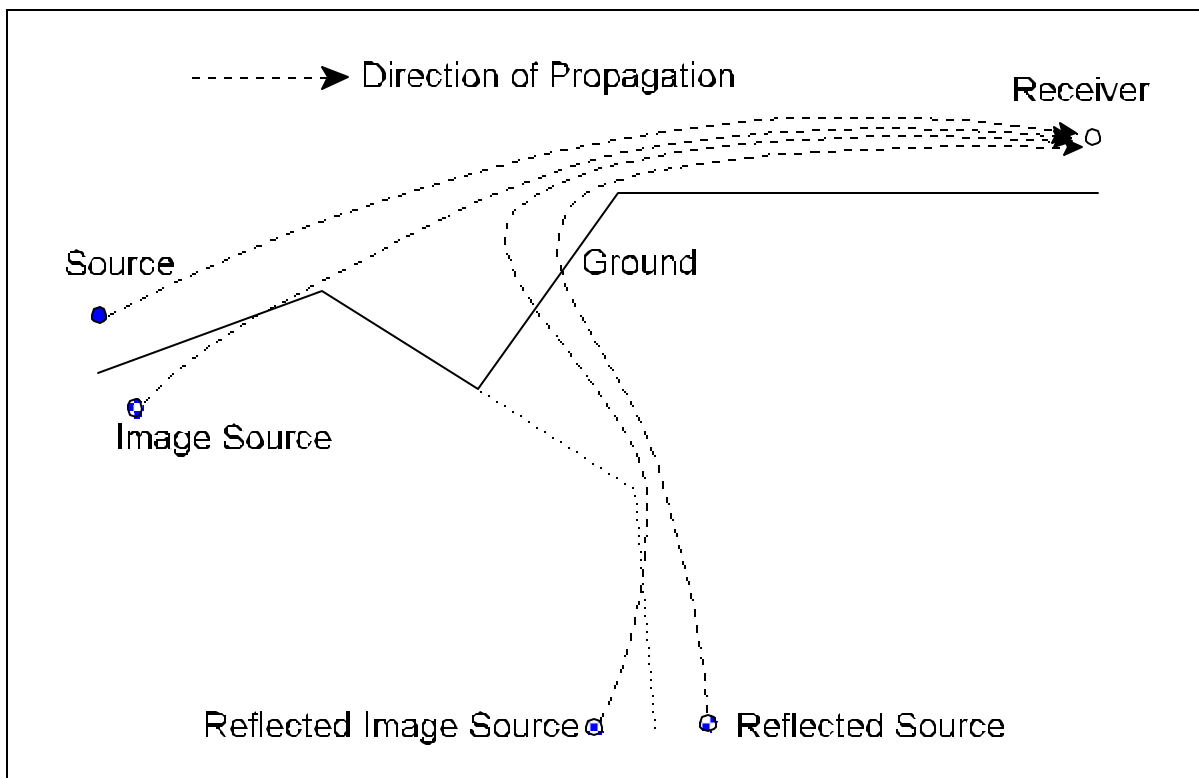


Figure 60. Example directions of propagation paths.

When starting at one point, only diffraction points closer to the receiver, along the direction of propagation, can be used when creating the propagation path from the source to the receiver. Points not in the direction of propagation are ignored. This prevents the propagation path from using any point in the geometry.

Each reflected path must be multiplied by the proper reflection coefficient for every segment that reflects the path. This requires the knowledge of each segment's ground or surface impedance. When an image ground segment reflects an image point, the real ground segment's impedance is used.

Reflections in berms: Since berms are special cases of ground segments, they are treated just like ground segments.

Reflections in barriers: Reflected images in barriers are handled in the same way as images in ground segments. Barriers have different impedances associated with them, however. One value of impedance is assigned to each side of the barrier, depending on the NRC entered by the user.

D.3.4 Propagation path generation algorithm. This section describes the path generation algorithm in a logical form called pseudocode. The Path Generation Algorithm is called by the calculation function in the TNM Acoustical Module. The calculate function calls the path generation algorithm with a sorted, smoothed and simplified version of the Vertical Geometry Object List (VGOL). The types of objects in the list are Source Points, Ground Points, Barrier Points, Building

Points and Receiver Points. Each point in the list is sorted based on its location on the source-to-receiver axis. This list does not contain Tree Zone points. The algorithm generates propagation paths and applies the acoustical functions in TNM to them to calculate \mathbf{a} -octave band sound pressure levels at the receiver.

Path generation algorithm:

Start with the Vertical Geometry Object List.

Set all \mathbf{a} -octave band sound pressure totals to zero.

Set Highest Path Tree Zone Penetration Distance to zero.

Create a Propagation Point List (PPL) from the VGOL:

Starting at the source's ground point, and ending with the receiver's ground point. Include all points from the VGOL object list in the order in which they appear in the list.

Barriers have the following diffraction points:

First point: Base on the source side

2nd point: Top

3rd point: Base on the receiver side.

Source ground point is placed before the source.

Receiver ground point is placed after the receiver.

Rows of Buildings have no diffraction points, but their ground points are in the list (with a reference to the top).

Ground Points are a single point.

The PPL has the following structure: [source ground point] [source] [1st point] [2nd point] [] ... [] [receiver] [receiver ground point].

Create surface-vectors (normal to the segment) for each point in the PPL.

Assign each point in the PPL a reflection level of zero.

If there is a reflecting barrier in the PPL, then each point to the Left of it has a reflection level of one.

Create propagation paths with the PPL and VGOL and sum partial sound pressures.

Return \mathbf{a} -octave band sound pressures for the receiver.

Propagation path creation algorithm:

With a PPL:

Create a Path List Structure.

Create Path Nodes with each source, receiver and diffraction point in the PPL.

Label the Path Nodes in increasing order, starting at the source and ending at the receiver, where the source is Node 1, and the receiver is Node N.

(Note: Rows of buildings, the ground under the source, and the ground under the receiver cannot be targets because they are not diffraction points.)

Loop (i) over all Path Nodes from 1 to N-1 :

Set point i to be the emitter.

Loop (j) over all Path Nodes from i to N-1:

Set point j+1 to be the target.

Check to see if a Line-of-sight (LOS) exists between the emitter and the target.

If LOS exists:

Create a link with emitter and target and Assign to Path Node as exiting and entering respectively.

Add a Path to the Path List for each unique Path Node combination starting with the source and ending with the receiver.

Loop (i) over all Path Nodes from 1 to N-1:
 Set M to the number of outward going Path Links.
 If M = 0 then go to top of Loop.
 Copy all Paths Ending in Node i M-1 times.
 Loop (j) from 1 to M.
 Add Path Node at the end of Path Link j to the end of jth Path ending in Path Node i.
 Call Fresnel Zone Filter Algorithm with the Path j.
 Delete any Path not ending with the receiver.
 For each Path in the Path List:
 If the Path has too many diffraction points (reference to the Highest Path), then delete it.
 If the Path wasn't deleted, calculate the path's partial sound pressure.
 Sum α -octave band partial pressure results to VGOL α -octave band pressure totals.
 Delete all Paths in the Path List, Nodes, and Node Links.

D.4 Propagation Path Calculations and Mathematical Description

The mathematical model used to calculate the attenuations due to the vertical geometry between the source and the receiver was in large part developed from work by De Jong, Chessell, Delany, Boulanger and Foss [De Jong 1983] [Chessell 1977] [Delany 1970][Boulanger 1997] [Foss 1976]. De Jong's methodology was used as the basis for the diffraction field model. Work by Chessell, Delany and Boulanger was used to calculate reflections in surfaces, and Foss' double-barrier method was used to simplify the vertical geometry.

The following sections describe the mathematical and logical functionality used for calculating propagation path sound pressures.

D.4.1 Definitions TNM's acoustical calculations in the vertical plane involve the following variables:

"	barrier-reflection parameter: single-frequency absorption coefficient, dimensionless
*	path-length difference caused by diffraction, in meters
λ	wavelength of propagating acoustic wave, in meters
<	diffraction parameter: normalized exterior wedge angle, dimensionless
F	reflection parameter: effective flow resistivity of the reflecting surface, in mks Rayls
N	reflection parameter: grazing angle of incidence, in radians
N	diffraction parameter: angle clockwise from the left wedge face to the edge-receiver line, in radians

N_0	diffraction parameter: angle clockwise from the left wedge face to the edge-source line, in radians
P	parameter within the Fresnel integral, dimensionless
$Atten_{row}$	building-row parameter: attenuation due to a row of intervening buildings, in dB
c	speed of sound, in meters per second
D	multiplicative diffraction factor, dimensionless
f	frequency of a propagating acoustic wave, in Hertz
F	Foss parameter: higher of the two barrier attenuations, in dB
$F(P)$	Fresnel integral
$F(w)$	reflection parameter: ground-wave function, dimensionless
$F_{linear-Gap}$	building-row parameter: linear gap fraction of the intervening row of buildings, dimensionless
f_{rN}	Atmospheric parameter: nitrogen relaxation frequency, in Hertz
f_{rO}	Atmospheric parameter: oxygen relaxation frequency, in Hertz
h	Atmospheric parameter: molar concentration of water vapor, in percent
h_r	Atmospheric parameter: relative humidity, in percent
$IL_{Barrier}$	building-row parameter: insertion loss of the row of buildings, in dB, computed as if the row of buildings had no gaps
IL_{eff}	Foss parameter: effective insertion loss for two barriers in sequence, in dB
J	Foss parameter: attenuation for the modified geometry, in dB
k	wave number of a propagating acoustic wave, in inverse meters
L	diffraction parameter: propagation path length over the top of the intervening barrier or wedge, in meters
N	Fresnel number, dimensionless
N'	building-row parameter: Fresnel number (at 630 Hz) for the row of buildings, dimensionless
NRC	barrier-reflection parameter: Noise Reduction Coefficient, dimensionless

p_0	Atmospheric parameter: standard reference pressure, 101.325 kiloPascal
$p_{\text{free-field}}$	free-field pressure of a propagating acoustic wave, in kiloPascal
P_{path}	pressure at the receiver, in kiloPascal, after the propagating sound undergoes one or more diffractions or reflections
p_{sat}	Atmospheric parameter: saturation vapor pressure, in kiloPascal
P_{total}	Total pressure at the receiver due to all N propagation paths combined, in kiloPascal
Q	reflection parameter: reflection coefficient of a spherical acoustic wave from a surface, dimensionless
Q_1	reflection parameter: reflection coefficient from the left (first) surface of a diffracting corner
Q_2	reflection parameter: reflection coefficient from the right (second) surface of a diffracting corner
r	diffraction parameter: distance from the diffraction edge to the receiver, in meters
r	reflection parameter: total distance between source and receiver, in meters
R	barrier-reflection parameter: reflection factor, dimensionless
R	free-field, direct-line (passing through intervening obstructions) distance from source to receiver, in meters
r_0	diffraction parameter: distance from the diffraction edge to the source, in meters
R_p	reflection parameter: reflection coefficient of a plane acoustic wave from a surface, dimensionless
t	“dummy” variable within the Fresnel integral
T	Foss parameter: total distance between source and receiver, in meters
T	Atmospheric parameter: ambient air temperature, in K
T	diffraction parameter: interior (below-the-ground) wedge angle, in radians
T_0	Atmospheric parameter: reference air temperature, 293.15 K
T_{01}	Atmospheric parameter: triple-point isotherm temperature, 273.16 K
T_{Celsius}	Atmospheric parameter: temperature, in C
$T_{\text{Fahrenheit}}$	Atmospheric parameter: temperature, in F

T_{Kelvin}	Atmospheric parameter: temperature, in K
w	reflection parameter: numerical distance for a reflecting spherical wave, dimensionless
W	Foss parameter: distance between the two barriers, in meters
Z	reflection parameter: acoustic impedance of the reflecting surface, dimensionless
Z_0	reflection parameter: acoustic impedance of air, dimensionless

D.4.2 Free field. The free-field sound pressure calculation is used as one of the factors for each propagation path; it is given by:

$$P_{free-field} = \frac{e^{ikR}}{kR} \quad (26)$$

where the wave number, k , is defined as

$$k = \frac{2\pi f}{c} \quad (27)$$

and where f is the frequency in Hertz; c is the speed of sound, 345 m/sec (772 miles per hour); and R is the free-field, direct-line distance from the source to the receiver.

D.4.3 Fresnel integral. The Fresnel integral is one of the functions used in computing the diffraction coefficient (see next section). It is used to calculate the magnitude and phase shift incurred by a propagation path that diffracts from an inflection in the ground or an impedance discontinuity. The Fresnel integral is defined by the following equation:

$$F(\chi) = \int_{\chi}^{\infty} e^{it^2} dt \quad (28)$$

The complex exponential can be substituted with cosine and sine terms using Euler's equation:

$$F(\chi) = \int_{\chi}^{\infty} (\cos(t^2) + i \sin(t^2)) dt \quad (29)$$

TNM computes this function with a "C" programming language algorithm from Baker [Baker 1992]

D.4.4 Diffraction function. The complete diffraction term is defined by the following function:

$$D = \frac{R e^{-i\frac{\pi}{4}}}{L \sqrt{\pi}} e^{ik(L-R)} e^{-ik^2 F(\chi)} \tag{30}$$

where L is defined as the propagation path length. (In Figure 61, which shows the diffraction geometry, $L = r_0 + r$.)

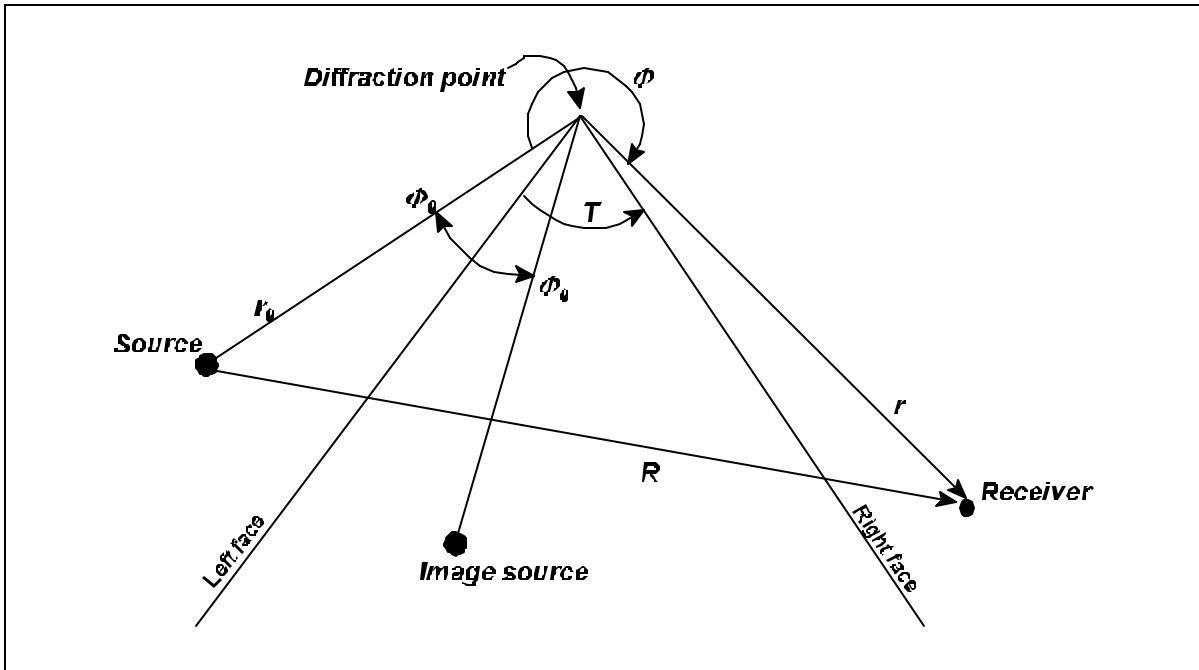


Figure 61. Diffraction geometry.

D is multiplied by a sign function that is positive when the receiver is in the dark zone and negative when the receiver is in the bright zone. To adjust the diffraction field to make it consistent with empirical results, D is also multiplied by an adjustment factor, A . A is currently set to 1.0. The factor Q is included to account for the surface impedances at the diffracting edge (see Section D.4.5). This results in the following equation:

$$D = (\text{sgn})ADQ \tag{31}$$

Chi function: The chi (χ) function is used to pass information about the diffracting geometry to the Fresnel function. It takes into account the distances from the diffraction point for the effective source

and the receiver, the angle formed about the diffraction point, and the top angle of the obstruction causing the diffraction. The P function has the following forma

$$\chi = \left(\frac{krr_0}{2L} \right)^{1/2} \left| \frac{\cos(\pi/v) - \cos((\phi - \phi_0)/v)}{(1/v)\sin(\pi/v)} \right| \tag{32}$$

where

$$v = \frac{(2\pi - T)}{\pi} \tag{33}$$

and T is the positive “top angle” of the wedge ($T = 0$ for a barrier, and $T = \mathbf{B}$ for a flat surface). (The absolute value missing from De Jong’s publication is shown here; the sign of N_0 is accounted for as defined below.)

The angles N (ϕ) and N_0 (ϕ_0) are measured in radians, referenced to the left side of the diffracting obstruction. Clockwise measured angles are positive. Angles for images of the source in the obstruction are measured in a counterclockwise direction and have negative angles. The geometry is defined in Figure 61.

For diffracting edges like barriers, where the interior wedge angle, T , is 0, P can be simplified to the following equation:

$$\chi = \sqrt{\frac{k(L - R)(L + R)}{2L}} \tag{34}$$

(De Jong’s simplification allowed $L + R = 2L$, but the above formulation retains the distinction, since it is more precise.)

Single diffraction: A propagation path with a single diffraction is calculated by substituting the correct values in the diffraction function to calculate D . The total sound pressure for the path is then found by multiplying the free-field path sound pressure by the diffraction coefficient. The following equation is used to calculate the sound pressure for a propagation path with a single diffraction, assuming that material at the diffraction point is acoustically hard:

$$P_{path} = P_{free-field} D \tag{35}$$

If the material at the diffraction point is other than acoustically hard, D is multiplied by the reflection coefficient, Q , which is described below in Section D.4.5.

Multiple diffraction: Multiple diffractions are modeled by multiplying single diffractions. First, for each diffraction point, the effective geometry must be calculated for the source and the receiver. This information is then used to calculate the effective single diffraction for that point. This is repeated for

each diffraction point in the propagation point. Once all diffractions have been calculated for the propagation path, they are all multiplied together. The product is used as the effective diffraction for the propagation path. The effective diffraction is then multiplied by the free-field sound pressure to calculate the pressure for the propagation path. The following equation represents the calculation for a propagation path with N diffractions, for the case where each diffraction point is acoustically hard:

$$P_{path} = P_{free-field} \prod_{i=1}^N D_{effective,i} \tag{36}$$

If the material at the diffraction points is not acoustically hard, D_i is multiplied by the reflection coefficient, Q_i , for each material type. The reflection coefficient is defined below in Section D.4.5.

Corner discontinuities: Corner diffractions are those that occur when two segments in the vertical geometry meet in an acute angle, to form a corner. Diffractions at corner discontinuities are calculated with the same diffraction coefficient function as follows:

$$D_{cor} = \frac{R}{L} \frac{e^{-i\frac{\pi}{4}}}{\sqrt{\pi}} e^{ik(L-R)} e^{-ik^2 F(\chi)} \tag{37}$$

Fresnel zone/path significance test: The Fresnel zone test is a quick test for significance of diffraction paths. It was incorporated into the TNM to avoid the time-consuming computation of all diffraction paths, whether they are important or not. The Fresnel zone test is performed only for points in the “bright” zone, where line of sight exists between source and receiver. Under this definition, the source can be a reflected source, a secondary emitting point such as a barrier top, or a reflected emitting point, and the receiver can be a secondary receiving point, real or reflected. All diffraction paths where the receiving point is in the shadow zone are assumed to be significant. If a path is not found to be significant, then the combination of points that created the diffraction are not included in the detailed calculation described above. The test is simply a check to see if the receiver lies within a hyperbola defined by the source and the diffraction point. The hyperbola is defined by the following equation:

$$N = \frac{2\delta}{\lambda} \tag{38}$$

N is the Fresnel Number. δ is called the path length difference and equals $(r_o+r) - R$. (Note that the hyperbola is defined using $R - (r_o+r)$. Conventions in acoustics multiply the expression $(r_o+r) - R$ by -1, so that N is positive in the dark zone.) λ is the wavelength and equals c/f , where c is the speed of sound in m/sec and f is the frequency in Hz. A receiver is said to be inside the Fresnel zone (and the diffraction is significant) if $N > -0.3$, in the bright zone only.

D.4.5 Reflection coefficients. Coefficients of reflection Q are calculated using the model defined in Chessell [Chessell 1977]. This model uses the user-specified effective flow resistivity of the reflecting segment and calculates the magnitude and phase change to the propagation path that reflected it. This model is dependent on frequency, effective flow resistivity of the reflecting segment, and the

geometry defined by the propagation path. The value, Q is computed from the absorption coefficients according to the following equation:

$$Q = R_p + F(w) (1 - R_p) \tag{39}$$

where R_p is the term for the incident wave and is calculated with the following equation:

$$R_p = \frac{\sin\phi - \frac{Z_0}{Z}}{\sin\phi + \frac{Z_0}{Z}} \tag{40}$$

Here, Z_0 is defined as the impedance of air ($D_0c_0 = 1.18 \text{ kg/m}^3 * 345 \text{ m/sec}$). N is the angle of incidence of the propagation path on the reflecting segment. Z is the acoustic impedance of the reflecting surface. For ground segments, Z is defined by the following equation, which was derived from empirical measurements of many fibrous porous materials [Delany 1970]. This equation has been shown to be a good model for various ground surfaces ranging in impedance from snow to grass to asphalt [Embleton 1983].

$$Z = \left[1 + .051 \left(\frac{f}{\sigma} \right)^{-0.75} + .077 \left(\frac{f}{\sigma} \right)^{-0.73} i \right] Z_0 \tag{41}$$

Here, F is the effective flow resistivity (EFR) for the reflecting segment in MKS Rayls. Values for F are entered for ground segments based on the type of material selected for the ground.

$F(w)$ is the ground wave function. It is defined by the following equation:

$$F(w) = \begin{cases} 1 + ie^{-w} \sqrt{\pi w} - 2e^{-w} \sum_{n=1}^{\infty} \frac{w^n}{(n-1)! (2n-1)} & |w| < 10 \\ -\sum_{n=1}^{\infty} \frac{(2n)!}{2^n n! (2w)^n} & |w| \geq 10 \end{cases} \tag{42}$$

where w , known as the “numerical distance,” is defined as follows:

$$w = \frac{1}{2} ikr \frac{(\sin\phi + Z_0/Z)^2}{1 + \sin\phi Z_0/Z} \tag{43}$$

where k is the wave number and r is the total distance between the source and the receiver, through the medium.

Reflections in barrier surfaces: For computing the effects of reflections in the barrier surfaces, a similar approach is taken as for ground segments, except that values of EFR (F) had to be derived to correspond to the user-specified Noise Reduction Coefficient (NRC) on the barrier surfaces.

The single-frequency absorption coefficient is given in terms of the “reflection factor”, R :

$$\alpha = 1 - |R|^2 \tag{44}$$

where

$$R = \frac{Z - Z_0}{Z + Z_0} \tag{45}$$

and Z_0 is the impedance of air. The barrier surface impedance, Z , is derived from the EFR from Delany's empirical fit for fibrous materials, given in Eq. (41), above. NRC is defined as the arithmetic average of the absorption coefficients, α , at 250 Hz, 500 Hz, 1000 Hz, and 2000 Hz. In an iterative process, individual values of EFR were found that corresponded to values of NRC in steps of 0.05 between 0.0 and 1.0.

Table 10 lists the EFR values used for all user-selectable NRC values.

Table 10. Effective Flow Resistivity used for values of Noise Reduction Coefficient (NRC).

NRC	EFR(cgs rayls)
0.00	20000.0
0.05	4250.0
0.10	1570.0
0.15	865.0
0.20	555.0
0.25	385.0
0.30	282.0
0.35	214.0
0.40	165.0
0.45	129.0
0.50	102.0
0.55	81.0
0.60	64.0
0.65	50.0
0.70	39.0
0.75	30.0
0.80	22.0
0.85	16.0
0.90	10.4

Table 10. Effective Flow Resistivity used for values of Noise Reduction Coefficient (NRC).

NRC	EFR(cgs rayls)
0.95	5.5
1.00	0.1

Table 11 shows the effective α -octave band absorption coefficients used within TNM when calculating reflections in barrier surfaces for selected values of NRC.

Table 11. Absorption coefficients as a function of frequency, for selected values of Noise Reduction Coefficient (NRC).

α -O.B. Freq.	α -Octave Band Absorption Coefficients for Selected Values of NRC					
	0.05	0.30	0.50	0.70	0.80	0.90
50	0.01	0.05	0.09	0.18	0.26	0.41
63	0.01	0.05	0.11	0.21	0.30	0.46
80	0.01	0.06	0.13	0.24	0.35	0.52
100	0.01	0.07	0.15	0.28	0.39	0.57
125	0.01	0.09	0.17	0.32	0.44	0.63
160	0.01	0.10	0.21	0.37	0.50	0.68
200	0.02	0.12	0.24	0.42	0.56	0.73
250	0.02	0.14	0.27	0.47	0.61	0.78
315	0.02	0.16	0.31	0.53	0.67	0.82
400	0.03	0.19	0.36	0.59	0.72	0.86
500	0.03	0.22	0.41	0.64	0.77	0.89
630	0.04	0.26	0.46	0.70	0.81	0.91
800	0.05	0.30	0.52	0.75	0.85	0.94
1000	0.06	0.34	0.58	0.79	0.88	0.95
1250	0.06	0.39	0.63	0.83	0.91	0.96
1600	0.08	0.44	0.69	0.87	0.93	0.97
2000	0.09	0.50	0.74	0.90	0.95	0.98
2500	0.11	0.55	0.78	0.92	0.96	0.99
3150	0.12	0.61	0.83	0.94	0.97	0.99
4000	0.15	0.67	0.86	0.95	0.98	0.99
5000	0.17	0.72	0.89	0.97	0.98	0.99
6300	0.20	0.77	0.92	0.97	0.99	1.00
8000	0.23	0.81	0.94	0.98	0.99	1.00

a -O.B. Freq.	a -Octave Band Absorption Coefficients for Selected Values of NRC					
	0.05	0.30	0.50	0.70	0.80	0.90
10000	0.27	0.85	0.95	0.99	0.99	1.00

Reflected paths: Paths reflected by segments in the vertical geometry are multiplied by the reflection coefficient Q , defined in the previous section. The angle of incidence at the intersection of the propagation path, the effective flow resistivity of the reflecting segments material, and the frequency are used to determine Q for the reflection. This factor is multiplied with the propagation path to account for energy loss and phase shift due to the reflection. A propagation path is multiplied by one coefficient for each segment that reflects the path. Figure 62 shows a simple propagation path that contains one reflection and one diffraction. The equation for that propagation path has the following form:

$$P_{path} = P_{free-field} Q D \tag{46}$$

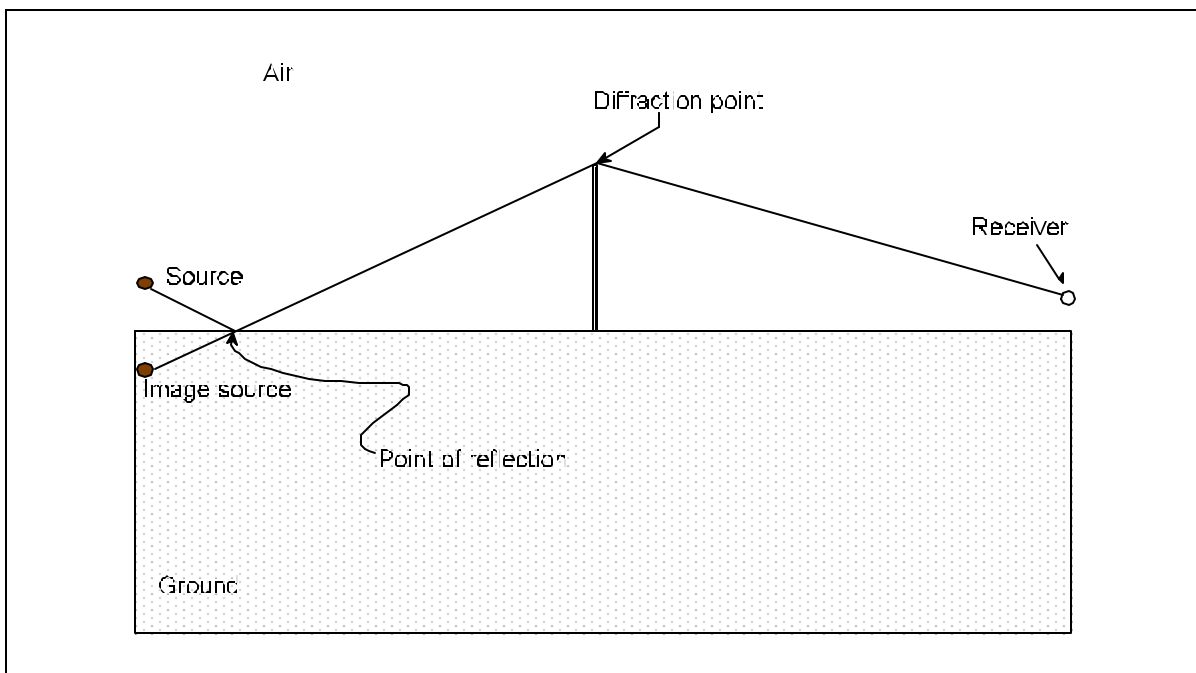


Figure 62. Example geometry showing reflection.

Impedance discontinuities: Propagation paths with diffractions at impedance discontinuities are multiplied by the difference between the segment impedance on the source's side and the receiver's side. Figure 63 shows a sample geometry with a propagation path containing a diffraction at an impedance discontinuity. The following expression shows the form of the equation for the propagation path in Figure 63:

$$P_{path} = P_{free-field} (Q_1 - Q_2) D \tag{47}$$

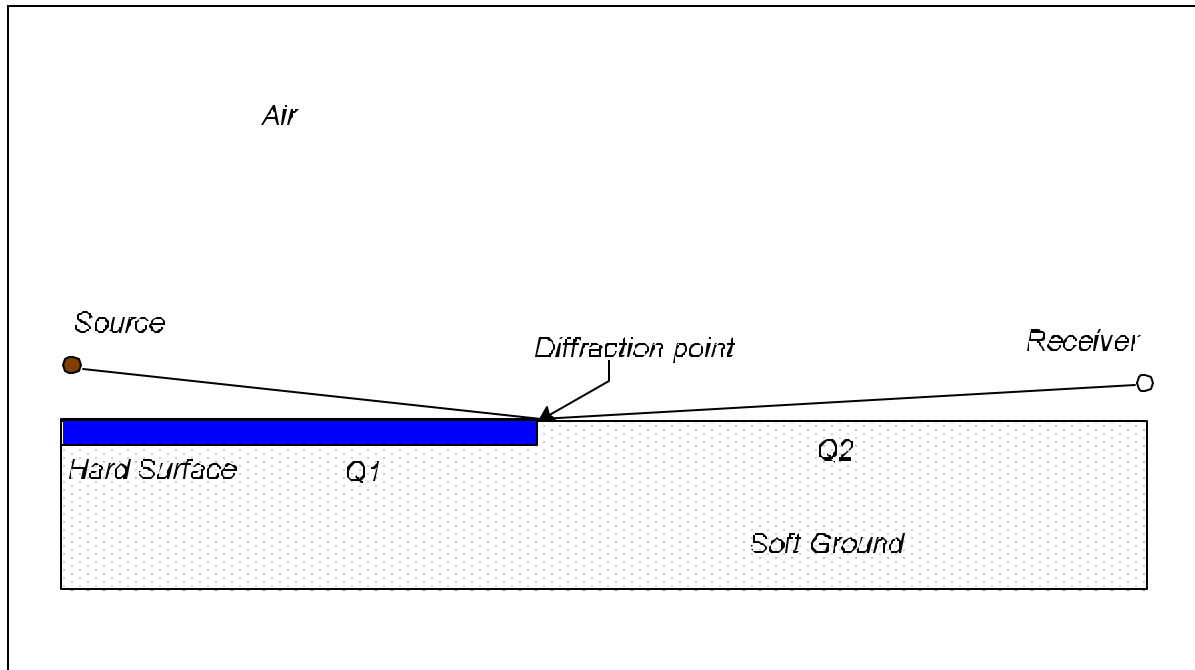


Figure 63. Example geometry showing an impedance discontinuity.

Corner diffractions: A propagation path containing a diffraction formed by two ground segments meeting or a ground segment and a barrier meeting point is multiplied by the reflection coefficient to the left and to the right of the point in the following form:

$$P_{path} = P_{free-field} (Q_1 - Q_2) D_{cor} \tag{48}$$

Figure 64 shows a sample geometry for a corner diffraction. The incidence angle for Q1 is measured from the Q1 surface and the incidence angle for Q2 is measure from the Q2 surface.

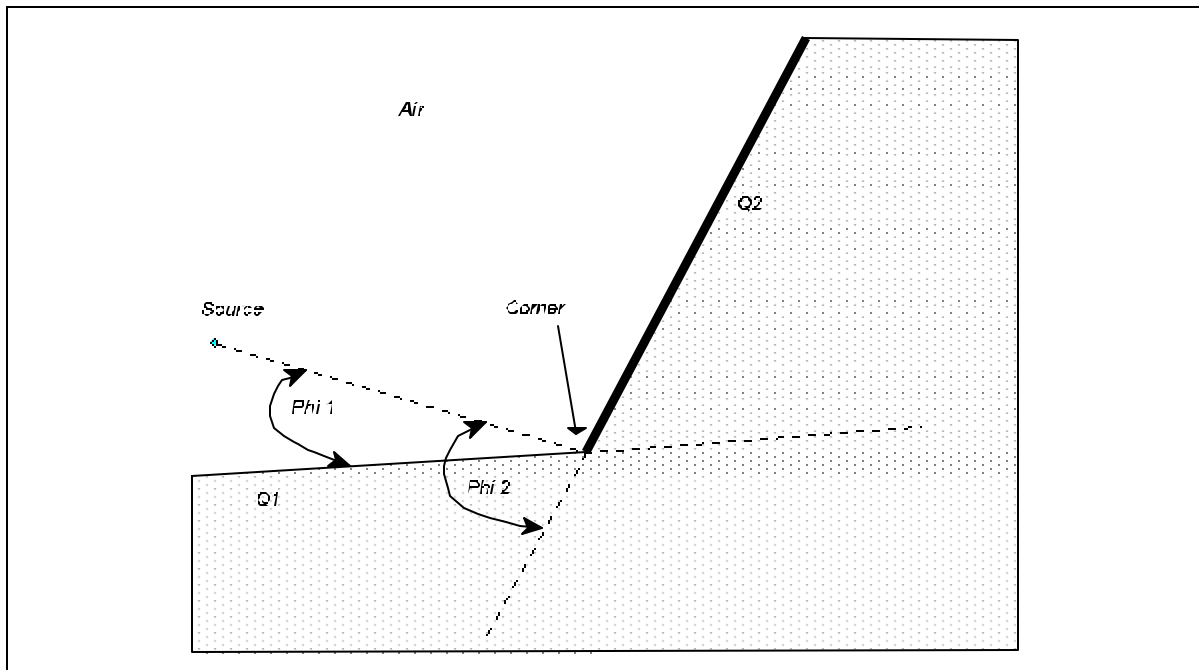


Figure 64. Example geometry for corner diffraction.

D.4.6 Ground-impedance averaging. The Boulanger approach to ground-impedance averaging is then used for cases where: (1) more than one impedance discontinuity is present in the local geometry between source and receiver or highest path points; or (2) a single discontinuity has not been chosen to be computed explicitly (as it would if designated a *near* highest path point). Instead of computing the multiple diffraction paths explicitly, this approach computes a Fresnel ellipse about the reflection point on the ground and computes the *area* inside the ellipse represented by each type of ground. Then, an average reflection coefficient is computed from the reflection coefficient for each ground type weighted by the ratio of its area to the total area. The average reflection coefficient is used, and no diffraction terms are computed at all. However, the size of the ellipse is a function of frequency, so the average impedance and therefore the reflection coefficient will often change for each $\frac{1}{2}$ octave band. Figure 65 shows how the averaging applies at two different frequencies. At low frequencies, where the Fresnel ellipse is large, two discontinuities are encountered, and three different sections of ground are incorporated in the average; their areas are represented by A_1 and A_3 , which are soft ground, and A_2 in the center, which is hard ground. At such low frequencies, the reflection coefficient is based on an average of soft and hard ground. However, at high frequencies, where the ellipse is small, only hard ground is encompassed and the reflection coefficient is based on hard ground only.

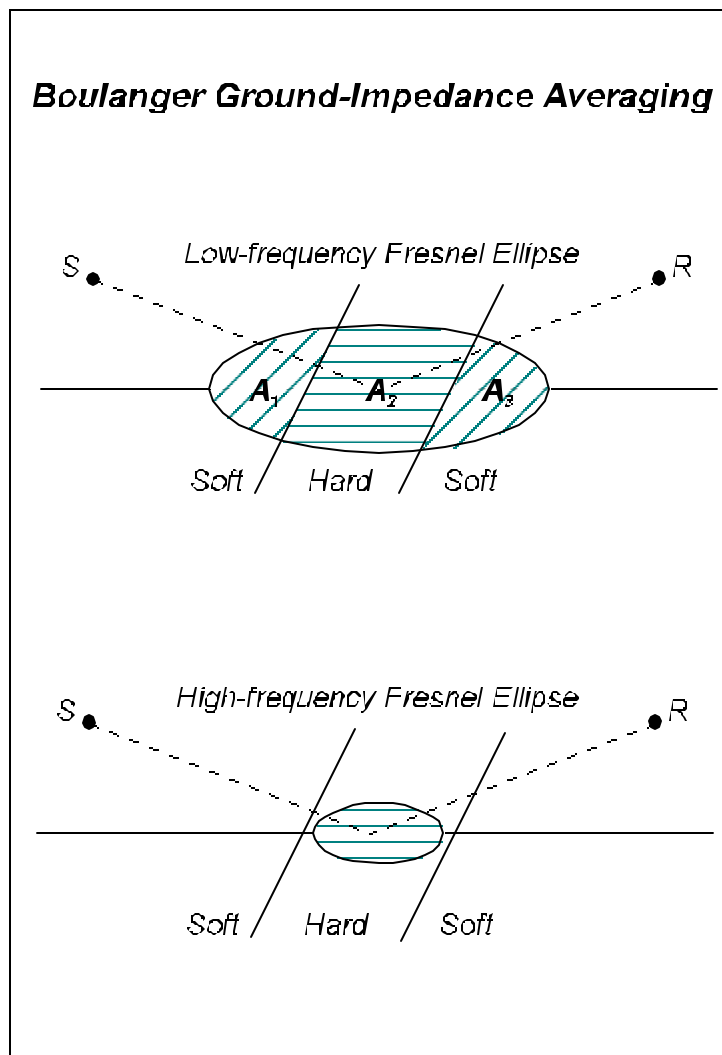


Figure 65. Ground impedance evaluation at two frequencies.

D.4.7 Tree zones. The TNM incorporates tree zones as an optional element in the propagation path. Tree zones have both ground height and top height, and, therefore, define ground points at their edges. The vertical geometry algorithms compute the distance the propagation paths travel through tree zones. For simplicity, the model calculates attenuation for the highest path only. This attenuation is then applied to all of the other paths, except a scale factor is applied based on the ratio of the lengths of the highest path to the other paths. TNM uses the 1996 ISO standard attenuation for dense foliage [ISO 9613-2], which is defined as “sufficiently dense to completely block the view along the propagation path; i.e., it is impossible to see a short distance through the foliage.” The octave-band attenuation as a function of distance through foliage is given in Table 12. In TNM, the octave-band values shown in Table 12 are applied to each of the a -octave bands within the associated octave band.

Table 12. Attenuation through dense foliage.

Octave-band center frequency (Hz)	63	125	250	500	1K	2K	4K	8K
Attenuation (dB, total) for d_f less than 10 meters	0	0	0	0	0	0	0	0
Attenuation (dB, total) for d_f between 10m and 20m	0	0	1	1	1	1	2	3
Attenuation (dB per meter) for d_f between 20m and 200m	0.02	0.03	0.04	0.05	0.06	0.08	0.09	0.12
Maximum attenuation (dB) for $d_f \leq 200m$	4	6	8	10	12	16	18	24

D.4.8 Rows of buildings. In the initial identification of rows of buildings, the two highest-path points on either side of the group of building rows are identified. Often, these two points are source and receiver, but a barrier or ground line may interrupt the source-receiver path and will be substituted as “effective” source or receiver points. Next, all building rows that interrupt the effective source-receiver path are identified. Rows that do not interrupt the propagation path are ignored. For each row (independently) that interrupts the path, the row attenuation is computed based on the German rail industry equation:

$$Atten_{row} = \text{MAX} \left(0, -10 \times \text{Log}_{10} \left(F_{Linear-Gap} + 10^{-\frac{IL_{Barrier}}{10}} \right) \right) \quad (49)$$

where $F_{linear\ gap}$ is the gap fraction associated with the building row and $IL_{Barrier}$ is the insertion loss of the building row, as if it were a solid barrier. Users define “building percentage,” which is $100(1 - F_{linear\ gap})$. The building-as-barrier attenuation, $IL_{Barrier}$, is computed with the geometry of the effective source and receiver and the building under evaluation alone. The attenuation is computed from the path length difference and Fresnel number at 630 Hz (so that $N = *$), the ISO attenuation equation for $N > 0$, and a smooth-fitting form for $N < 0$ that goes to 0 where N is approximately -0.25:

$$IL_{Barrier} = \begin{cases} 10 \times \text{Log}_{10}(3 + 20N') & N' > 0 \\ 4.77 - 9.54\sqrt{|N'|} & N' \leq 0 \end{cases} \quad (dB) \quad (50)$$

The rows of buildings with the highest $Atten_{row}$ is selected as the “best row,” and $Atten_{row}$ is computed as the appropriate attenuation for that row in each a -octave band. Attenuation attributed to each remaining row of buildings that interrupts the propagation path is 1.5 dB in each a -octave band. Maximum attenuation for any number of rows of buildings is a function of frequency, and matches the frequency dependence of barrier attenuation. The maximum has been set to 10 dB(A) based on a

typical traffic noise spectrum. The maximum building-row attenuation by frequency is given in Table 13.

Table 13. Maximum attenuation for rows of buildings by frequency.

a -Octave Band Center Freq., Hz	Max. Atten. (dB)	a -Octave Band Center Freq., Hz	Max. Atten. (dB)
50	5.30	800	9.65
63	5.43	1000	10.33
80	5.59	1250	11.05
100	5.77	1600	11.89
125	5.99	2000	12.69
160	6.28	2500	13.52
200	6.59	3150	14.40
250	6.94	4000	15.33
315	7.37	5000	16.23
400	7.86	6300	17.17
500	8.38	8000	18.15
630	8.98	10000	19.08

Interactions with the ground are not affected by the presence of rows of buildings.

D.4.9 Atmospheric absorption. The 1993 ISO standard [ISO 9613-1] is used to compute atmospheric absorption for TNM. The user is allowed to specify temperature and relative humidity, but not atmospheric pressure. Standard atmospheric pressure of one atmosphere at sea level is used as the reference pressure (101.325 kPa, 760 mm or 29.92 in. of Hg). The following equations are taken from the ISO standard, with the atmospheric pressure variable set to the above constant value.

The atmospheric absorption coefficient, A_{atm} in decibels per meter, is given by:

$$A_{atm} = 8.686 f^2 \left[\left(1.84 \times 10^{-11} \sqrt{\frac{T}{T_0}} \right) + \left(\frac{T_0}{T} \right)^{5/2} \left(\frac{0.01275 e^{-2239.1/T}}{\left(f_{rO} + \frac{f^2}{f_{rO}} \right)} + \frac{0.1068 e^{-3352.0/T}}{\left(f_{rN} + \frac{f^2}{f_{rN}} \right)} \right) \right] \quad (51)$$

where T_0 is defined as 293.15 Kelvin (20° C), the reference air temperature, T is the ambient air temperature in Kelvin, h is the molar concentration of water vapor, in percent, and f is the frequency of sound, in this case the nominal 1/3 octave-band center frequency, in Hz.

The oxygen relaxation frequency, f_{rO} , in Hz, is defined as:

$$f_{rO} = 24 + 4.04 \times 10^4 h \left(\frac{0.02 + h}{0.391 + h} \right) \quad (52)$$

and the nitrogen relaxation frequency, f_{rN} , in Hz, is defined as:

$$f_{rN} = \sqrt{\frac{T_0}{T}} \left(9 + 280 h e^{-4.170 \left(\left(\frac{T_0}{T} \right)^{1/3} - 1 \right)} \right) \quad (53)$$

The following equations are used to convert the units of the input temperature and humidity values to those required for the above equations.

For temperature:

$$T_{\text{Celsius}} = \frac{5}{9} T_{\text{Fahrenheit}} - 32 \quad (54)$$

$$T_{\text{Kelvin}} = T_{\text{Celsius}} + 273.15 \quad (55)$$

For humidity:

$$h = h_r \frac{p_{\text{sat}}}{p_{\text{so}}} \quad (56)$$

where h_r is the relative humidity in percent (user input), p_{sat} is the saturation vapor pressure, and p_{so} is the standard reference pressure of 101.325 kPa.

Also,

$$\frac{p_{\text{sat}}}{p_{\text{so}}} = 10^C \quad (57)$$

where

$$C = -6.8346 \left(\frac{T_{01}}{T} \right)^{1.261} + 4.6151 \quad (58)$$

In this last equation, T_{01} equals 273.16 K, the triple-point isotherm temperature.

While these equations are relatively complex, the attenuation per meter is only computed once for each $\frac{1}{3}$ -octave band, since the user can specify the temperature and humidity only once per study problem. The default temperature is 20° Celsius (68° Fahrenheit, 293.15 Kelvin) and the default humidity is 50-percent relative humidity (RH).

Atmospheric attenuation per meter at 20° Celsius (68° F), 50- percent RH and one atmosphere (the default conditions), as a function of 1/3-octave band center frequency, are given in Table 14.

Table 14. Atmospheric absorption by frequency for default atmospheric conditions.

1/3-Octave Band Center Freq., Hz	Atten. (dB/m)	1/3-Octave Band Center Freq., Hz	Atten. (dB/m)
50	7.8081e-05	800	3.9070e-03
63	1.2245e-04	1000	4.6647e-03
80	1.9355e-04	1250	5.7114e-03
100	2.9387e-04	1600	7.4506e-03
125	4.3979e-04	2000	9.8870e-03
160	6.7073e-04	2500	1.3640e-02
200	9.5388e-04	3150	1.9711e-02
250	1.3097e-03	4000	2.9666e-02
315	1.7436e-03	5000	4.4239e-02
400	2.2389e-03	6300	6.7625e-02
500	2.7281e-03	8000	1.0529e-01
630	3.2678e-03	10000	1.5884e-01

D.4.10 Foss selection algorithm. As described above in various sections, the vertical geometry algorithms simplify geometries to contain at most two obstructions to reduce the amount of time required to calculate the attenuation. When the number of obstructions received by the vertical geometry is greater than two, all pairs of obstructions are evaluated for their approximate effective attenuation using the Foss double-barrier algorithm [Foss 1976]. The pair of obstructions with the highest computed attenuation are selected for use. These two obstructions are then used to calculate the

attenuation for the vertical geometry based on using the full De Jong model. In the case of two or more pairs having the same attenuation, the first pair in the list is used. This algorithm assumes that any barriers beyond the first two would provide negligible additional attenuation.

Potentially, this algorithm is used twice in the calculation process. The first is to reduce the number of perturbable obstructions (barriers or berms) to two if more than two are present. The TNM can only handle attenuations from up to two perturbable obstructions in its tables for a given vertical geometry. In this pass, only the perturbable obstructions are considered, and the test is performed using the user's "input" heights. Perturbable obstructions not selected are completely removed from the calculation process for this vertical geometry only (subsequent vertical geometries may select a different obstruction pair given the same set of barriers to choose from). The second possible occasion the Foss algorithm is used, is to reduce the number of obstructions from the current vertical geometry before calculating the attenuation. This evaluation is performed for every perturbation combination for the perturbable obstructions that are retained. In this pass all obstructions are considered (except perturbable obstructions removed in the first pass described above). The Foss algorithm is used to select the best pair of obstructions, and all others are completely removed from the geometry. The De Jong model is then applied to this geometry. The results are stored in the results matrix in the location designated for this perturbation of the selected perturbable objects.

A brief description of the Foss double-barrier attenuation model follows. Figure 66 shows the parameters of the double-barrier calculations.

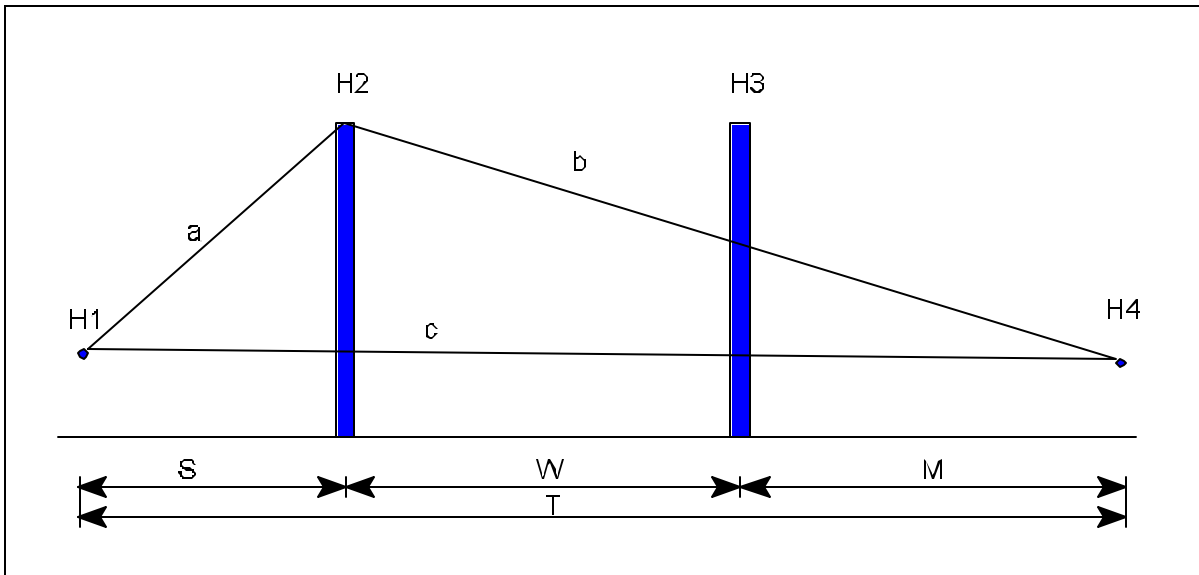


Figure 66. Foss double-barrier geometry.

The effective attenuation is calculated using the following equation:

$$IL_{eff} = F + J - \left[6e^{-\frac{2W}{T}} + 1.3 \left(e^{-\frac{35W}{T}} - 1 \right) \right] \left(1 - e^{-\frac{J}{2}} \right) \quad (59)$$

A detailed explanation of this equation can be found in [Foss 1976]; it is outlined here. W , the width between the barriers, and T , the total distance, are shown in Figure 66. The attenuation is calculated for each barrier alone, ignoring the other, using an approach similar to that used in STAMINA [Barry 1978]. The higher of the two attenuations equals F , and its associated barrier is designated as the “best” barrier. Then, depending on which is closer, either the source or the receiver is moved to the top of the best barrier. A modified barrier geometry is then drawn from the top of the best barrier over the other barrier to actual source or receiver. The attenuation for this modified geometry is J .

D.4.11 Total sound pressure. The total sound pressure for a given vertical geometry is calculated by summing over all the propagation paths for that geometry. The following equation shows the sound pressure calculation for a vertical geometry with N propagation paths:

$$P_{Total} = \sum_{i=1}^N P_{path_i} \tag{60}$$

D.4.12 Attenuation. The final attenuation for a vertical geometry, A_s is calculated in reference to the free-field sound pressure as:

$$A_s = 20 \times \text{Log}_{10} \left| \frac{P_{Total}}{P_{free-field}} \right| \tag{61}$$

for each leg of the elemental triangle. The attenuation fraction, needed by the horizontal geometry, is defined as $N_s = 10^{(A_s/10)}$ — computed for both legs of the triangle: N_{SL} , N_{SR} . Then the average over the triangle is computed as $N_{SAvg} = \frac{1}{2} (N_{SL} + N_{SR})$. This is equivalent to $N_{n.f.barrs}$ in Eq. 19 in Appendix C, Section C.2.4.

APPENDIX E

PARALLEL BARRIER ANALYSIS

When a roadway is flanked by parallel reflective barriers, retaining walls, or a combination of the two, sound reflects back and forth across the roadway many times before ultimately progressing outwards towards nearby receivers. These multiple reflections increase the sound level at nearby receivers, so that a receiver's intervening barrier or retaining wall provides less attenuation than otherwise. The increase in sound level due to multiple reflections from parallel barriers or retaining walls is called parallel-barrier degradation.

TNM computes parallel-barrier degradation for explicitly entered cross-sectional (two-dimensional) geometries. Once computed, the user must generalize these degradations for the full set of TNM receivers and then must enter appropriate adjustment factors for these receivers, to account for multiple reflections.

This appendix:

- # Overviews the computation of parallel-barrier degradation
- # Describes all required input for the computations
- # Describes the parallel-barrier ray tracing procedure
- # Provides equations for ray acoustic energies, both at the source and as the rays propagate
- # Describes the computation of parallel-barrier degradation
- # Mentions that the user must generalize these parallel-barrier degradations to TNM's regular sound-level receivers.

E.1 Overview

Sometimes highway projects contain cross sections where the highway is depressed below grade and thereby flanked by vertical retaining walls. Figure 67 shows a typical depressed section in a highly urbanized area. In addition to the cross-sectional geometry, the figure also shows: (1) the center lines of each roadway, including a ramp that is descending into the depressed section; and (2) adjacent residential buildings.

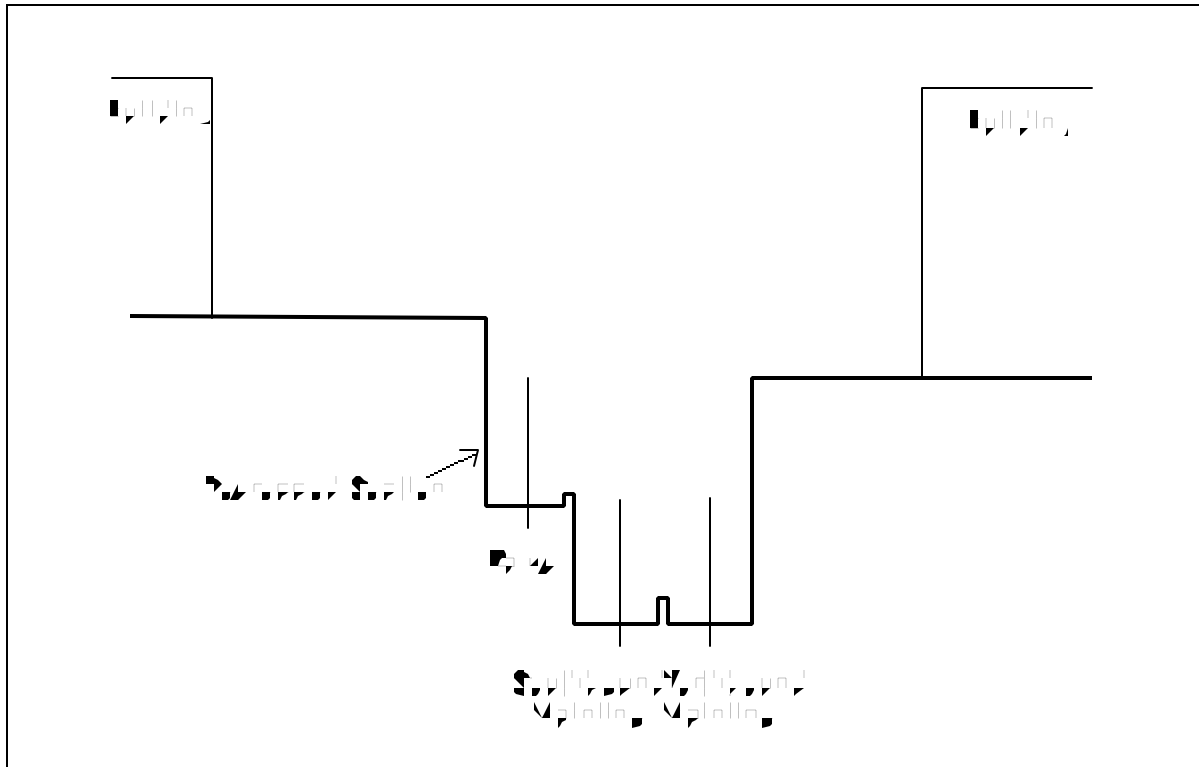


Figure 67. Typical depressed section in a highly urbanized area.

At other times, highway projects contain cross sections where the highway is flanked by vertical reflective noise barriers, one on each side. Other cross sections sometimes contain a combination of vertical reflective barriers and vertical reflective retaining walls.

Two things change acoustically when a roadway is flanked in these ways by parallel reflective barriers or retaining walls. First, direct lines-of-sight between receivers and traffic are interrupted by the intervening barrier or retaining wall — the one on the receiver's side of the roadway. When this happens, some receivers no longer have direct view of some traffic-noise sources. The intervening barrier or retaining wall reduces noise levels at receivers with reduced views of the traffic.

Second, the parallel barriers or retaining walls cause multiple reflections of the noise, from side to side across the roadway. The resulting reverberation tends to increase noise levels at nearby receivers. This noise increase due to reverberation may partially offset the noise reduction due to interruption in the lines-of-sight. As a result, the intervening barrier or retaining wall does not provide as much noise reduction as it would without the reverberation — that is, without the presence of the barrier or retaining wall on the opposite side of the roadway.

TNM's regular sound-level computations can predict the sound-level reduction due to an intervening barrier or retaining wall. However, TNM's regular sound-level computations cannot take multiple reflections into account. For this reason, they cannot predict the "reverberation" effect — that is, the parallel-barrier degradation — due to parallel barriers or retaining walls.

Separately from its regular sound-level computations, TNM does predict parallel-barrier degradation in two dimensions, as described in the remainder of this appendix [Menge 1991]. Once computed, the user must then generalize these parallel-barrier degradations for all actual TNM receivers and then must enter appropriate adjustment factors for these receivers, to account for multiple reflections.

E.2 Overview of Parallel-barrier Computations

TNM begins its computation of parallel-barrier degradation by tracing individual acoustic rays outward from each traffic noise subsource. Some rays come close enough to receivers or diffraction edges to contribute their portion of sound energy. Others do not come close enough and are lost to the sky. In TNM Version 1.0, “close enough” means within 0.3 meters (1 foot).

To compute parallel-barrier degradation, TNM first computes ray energies twice:

Multiple reflections: Each ray is reflected according to NRCs input by the user.

No multiple reflections: The same as for multiple reflections, except for the following.

When a ray reflects from one of the flanking barriers or retaining walls, its energy is completely absorbed, as if the barrier or wall was not there. In this manner, rays that reach the diffracting edge after barrier reflections are reduced in strength to zero, and thereby eliminated. As a result, all reverberantly reflected rays are eliminated. Only those rays remain that reach the diffracting edge either directly from the source or after reflection from the pavement or other non-barrier surfaces.

TNM's parallel-barrier computations allow complete flexibility in: (1) cross-sectional geometry; (2) the location of roadways between the parallel barriers or retaining walls; and (3) the location of adjacent receivers. The resulting parallel-barrier degradation is a function of: (1) traffic on each roadway; (2) the location of the roadways; (3) the detailed location, orientation, and NRC of each reflecting surface; (4) the location of the diffracting edges at each side of the cross section; and (5) the location of each receiver.

E.3 Required Input

Figure 68 shows the required input for TNM parallel-barrier computations, embedded in an HZ coordinate system, where H means “horizontal.” (The rays in this figure are discussed later.) Parallel-barrier input consists of three types: roadway input, cross-section input, and analysis-location (or receiver) input.

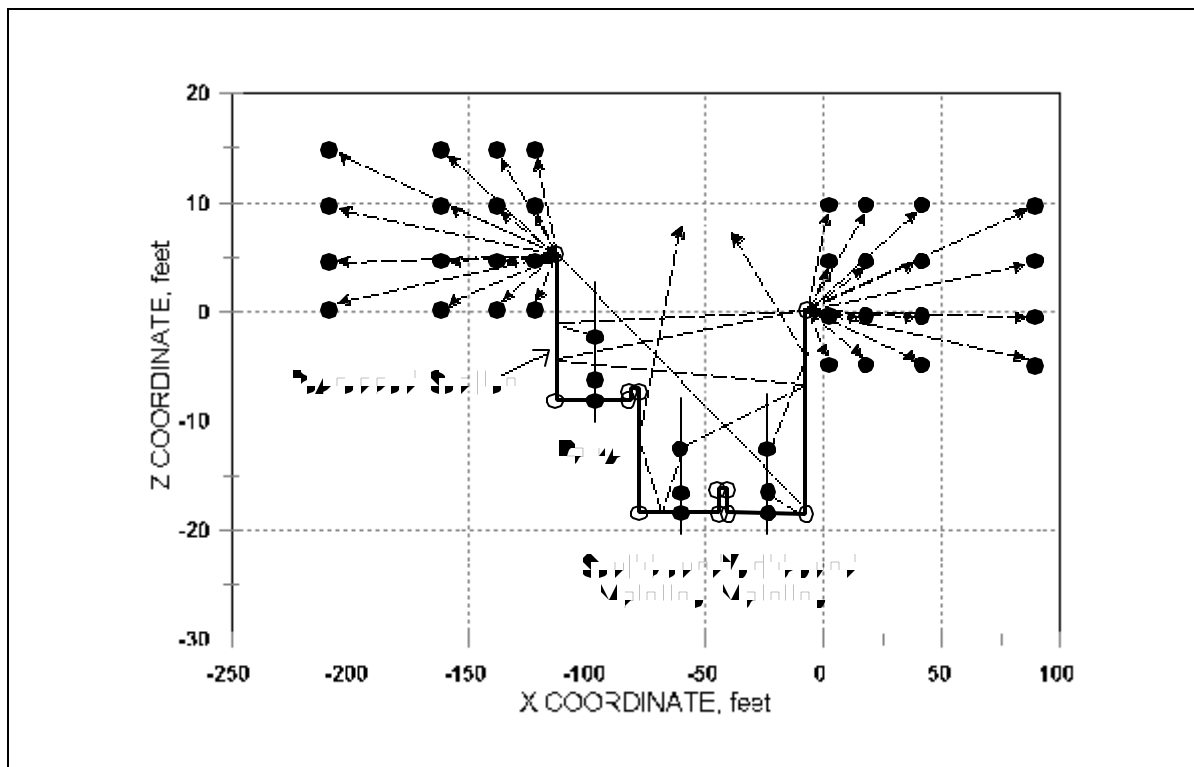


Figure 68. Detailed input and representative rays.

E.3.1 Roadway input. Each traffic stream appears in the figure as a separate roadway, represented by three subsource dots and a vertical line connecting them. These subsource dots correspond to TNM’s built-in subsource heights: zero; 1.5 meters (5 feet); and 3.66 meters (12 feet). The user needs to enter only the H position of each roadway. TNM computes all the Z coordinates, including the intersection with the roadway.

In addition to location, roadway input includes traffic speed and hourly traffic volume for each vehicle type. TNM needs this traffic input to predict the effect of reverberation, because reverberation depends upon the relative sound energy from each roadway and each roadway’s three subsources.

For example, if heavy trucks dominate the noise level at a certain receiver, reverberation may not affect that receiver’s noise level significantly, because it may still have direct line-of-sight to the truck exhaust stacks. The same might be true if ramp traffic dominates the noise level at some receivers. On the other hand, if the dominant source of traffic noise for a receiver is significantly shielded by the intervening barrier or retaining wall, then the effect due to reverberation might be larger.

E.3.2 Cross-section input. Cross-section input appears in Figure 68 as a single, thick connected line, from one diffracting edge to the opposite one. The user enters the HZ coordinates for each point along this cross-section line. The user also enters a NRC for each surface element. Unfortunately, when performing a parallel barrier analysis, NRCs are not inherited from the main TNM run. Typical NRCs might be 0.0 (or perhaps 0.05, which will have essentially the same result) for pavement, vertical retaining walls, and reflective noise barriers; 0.6 for sloped, grassed areas within the cross section; and 0.60 to 0.95 for absorptive noise barriers or for special absorptive material applied to retaining walls.

The computations assume that this cross-sectional geometry continues unchanged up and down the roadway, in both directions. For this reason, if the cross-section changes rapidly along the roadway, the user must: (1) use TNM's parallel-barrier analysis several times, with varying cross-sectional geometry; and then (2) combine the separate results for each receiver, weighting most heavily the results for the roadway geometry directly adjacent to the receiver location.

E.3.3 Receiver input. Receiver input consists of each receiver's HZ coordinates. Note that parallel-barrier receivers are called "analysis locations" within TNM, to distinguish them from TNM's receivers for sound-level computations. Within this appendix, however, they are called "receivers," for simplicity.

E.4 Ray Tracing

TNM generates 10,000 rays outward from each roadway subsource (three per roadway). TNM spaces these 10,000 rays equally in direction around the subsource, with a randomized initial direction. TNM then traces each ray outward from the source and reflects if from the surface segments it hits. Several rays appear in Figure 68, above.

Reflection is purely "specular" as from a mirror, without scattering. TNM remembers the surface segment for each reflection, so it can later reduce that ray's acoustic energy according to the surface's NRC. In addition, TNM remembers the total length of each ray as it progresses outward.

If a ray approaches within 0.3 meters (1 foot) of a receiver, the ray contributes to the receiver's sound level. In addition, if a ray approaches within 0.3 meters (1 foot) of a diffracting edge, the ray is diffracted to receivers on that side of the roadway. Rays that come within 0.3 meters (1 foot) of receivers or diffracting edges are called "successful" rays. Rays that "miss" receivers and diffracting edges escape to the sky and are forgotten by TNM.

E.5 Ray Acoustic Energies

Each ray starts out with acoustic energy proportional to the strength of its source. It then is reduced in energy as it either reflects from a surface or diffracts over a barrier top towards receivers.

E.5.1 Initial ray energy. Computations of initial ray energy first proceed separately for each vehicle type on the parallel-barrier roadway, and then are combined into the three required sources: bottom, middle and top. These computations use several of the same equations that are used for TNM's regular sound-level calculations.

From the user's parallel-barrier input, TNM determines the vehicle type, i , and the pavement type, p . Then from these values of i and p , TNM combines its emission-level regression coefficients (A, B, C, L, M, N, P and Q) with the vehicle speed, s_i , for that vehicle type, to compute

$$E_{Aemis, i}(s_i) = (0.6214 s_i)^{A/10} 10^{B/10} + 10^{C/10} \quad (62)$$

and

$$\begin{aligned} r_i(500 \text{ Hz}) &= L + (1 - L - M) \left[1 + e^{(N \log_{10} 500 + P)} \right]^Q \\ &= L + (1 - L - M) \left[1 + e^{(2.7N + P)} \right]^Q, \end{aligned} \quad (63)$$

where speed, s , is in kilometers per hour. Note that TNM assumes cruise throttle for all vehicles, because the difference in effective source height between cruise and full-throttle vehicles is not sufficiently large to effect these computations. Also note that parallel-barrier degradation is computed at a frequency of 500 Hz, as an approximation to the degradation for the full A-weighted sound level.

Next TNM computes

$$\begin{aligned} E_{Aemis, i, \text{upper, ff}}(s_i) &= \left(\frac{r_i}{r_i + 1} \right) E_{Aemis, i} \\ E_{Aemis, i, \text{lower, ff}}(s_i) &= \left(\frac{1}{r_i + 1} \right) E_{Aemis, i}. \end{aligned} \quad (64)$$

Then it computes

$$\begin{aligned}
 E_{\text{eq, upper}} &= 0.0476 \left(\frac{v_i}{s_i} \right) E_{\text{Aemis, } i, \text{ upper, ff}} \\
 E_{\text{eq, lower}} &= 0.0476 \left(\frac{v_i}{s_i} \right) E_{\text{Aemis, } i, \text{ lower, ff}} ,
 \end{aligned}
 \tag{65}$$

where v_i is the parallel-barrier traffic volume and s_i is the traffic speed, in kilometers per hour, for this vehicle type, i . Finally, TNM combines results for all vehicle types into the three required source reference noise levels (abbreviated here as $E_{\text{eq, ref}}$), as follows:

$$\begin{aligned}
 E_{\text{eq, ref, 0 meters (0 feet)}} &= \sum_{\substack{i = \text{all vehicle} \\ \text{types}}} (E_{\text{eq, lower, } i}) \\
 E_{\text{eq, ref, 1.5 meters (1.5 feet)}} &= \sum_{\substack{i = \text{all vehicle} \\ \text{types except} \\ \text{heavy trucks}}} (E_{\text{eq, upper, } i}) \\
 E_{\text{eq, ref, 3.6 meters (12 feet)}} &= E_{\text{eq, upper, } i = \text{heavy trucks}} .
 \end{aligned}
 \tag{66}$$

In this manner, each TNM parallel-barrier roadway becomes three subsources: the first at a Z coordinate of TNM's parallel-barrier roadway Z coordinate, the second 1.5 meters (5 feet) above this Z coordinate, and the third 3.66 meters (12 feet) above it. All three of these subsources have the same H coordinate.

Note that each ray carries this initial energy with it, rather than only 1/10,000th of the energy. The resulting parallel-barrier degradation is not affected, because it is a relative measure of sound level (with and without the reverberation).

E.5.2 Reduction in ray energy as the ray propagates outward. As each ray progresses outward, its relative energy is affected by the following acoustical mechanisms:

- # Divergence
- # Ground attenuation
- # Reflection
- # Barrier attenuation.

This section describes each of these effects upon ray energy. Note that TNM's parallel-barrier computations ignore any affects due to wind or temperature gradients, consistent with TNM's full sound-level computations.

Divergence: Sound level drops off from a line source by 3 decibels per distance doubling. Correspondingly, sound energy is reduced by half for each distance doubling. Because TNM's ray tracing is two dimensional, this divergence is completely accounted for by the diverging rays themselves. For example, if the source-receiver distance is doubled, then only half as many rays will "hit" the receiver. As a result, no additional computations are needed to account for divergence. Line-source divergence is automatic with two-dimensional ray tracing.

Ground attenuation: TNM accounts for ground by explicitly incorporating an additional divergence of 1.5 decibels per distance doubling into the parallel-barrier computations. To incorporate this additional divergence, TNM divides each ray's energy by 1.414 for every doubling of distance, starting at 8.84 meters (29 feet) from the roadway.

Reflection, NRC: Two parameters influence ray reflection: the surface's NRC and the proximity of the reflection point to a diffraction edge.

To account for the surface's NRC upon reflection, TNM multiplies the ray's energy by the NRC, which is always less than 1.0. In this manner, energy is absorbed out of the ray by the material of the reflecting surface. This occurs for all reflecting surfaces: roadway, grassed slopes, retaining walls, barriers, and so forth. Even though TNM's parallel barrier degradation is computed at 500 Hz, sound energy, as a result of surface reflections, is reduced according to the composite NRC of the surface, not the absorption coefficient at 500 Hz.

Reflection near a barrier top: When a sound wave reflects near the top of a barrier, the lower portion of the wave front strikes the barrier and is reflected, while the upper portion misses it and is therefore not reflected. Instead, this upper portion diffracts over the barrier top to its other side. TNM combines this partial reflection of wave fronts with ray tracing, as shown in Figure 69.

The top portion of the figure shows a traced ray that reflects near the barrier top. Shown to the left is the actual reflection. Shown to the right is TNM's method of computing the reduction in energy due to the barrier top's proximity. First the source is replaced by its image behind the barrier. Then the barrier is flipped on its head, thereby coming down from the sky to the same barrier-top position. The resulting geometry yields an image source in direct view of the receiver, plus a diffraction from the flipped barrier top. This diffraction combines with the direct path, to reduce its intensity according to TNM's regular sound-level algorithm for barriers. When the ray just grazes the barrier top, then the combined effect of the direct and diffracted rays is 6 decibels less than the direct ray alone. Half the (coherent) energy is lost upon reflection, because only half the wave front reflects.

The bottom portion of Figure 69 shows the comparable situation, but where the reflection just misses the barrier top. To the left is the actual reflection. Even though the ray does not look as if it reflects, TNM must reflect it from a "phantom" upward extension of the barrier, for sound-level continuity. Shown to the right are the image source and the flipped barrier. In this case, the direct line-of-sight between image source and receiver is interrupted by the flipped barrier. As a result, only the diffracted ray reaches the receiver, reduced by the flipped barrier's attenuation. When the ray just barely misses the barrier top, then the diffracted rays contributes 6 decibels less than the direct ray alone would have contributed, had it reached the receiver. Relative to the direct ray, half the (coherent) energy is lost upon this phantom reflection, because only half the wave front reflects.

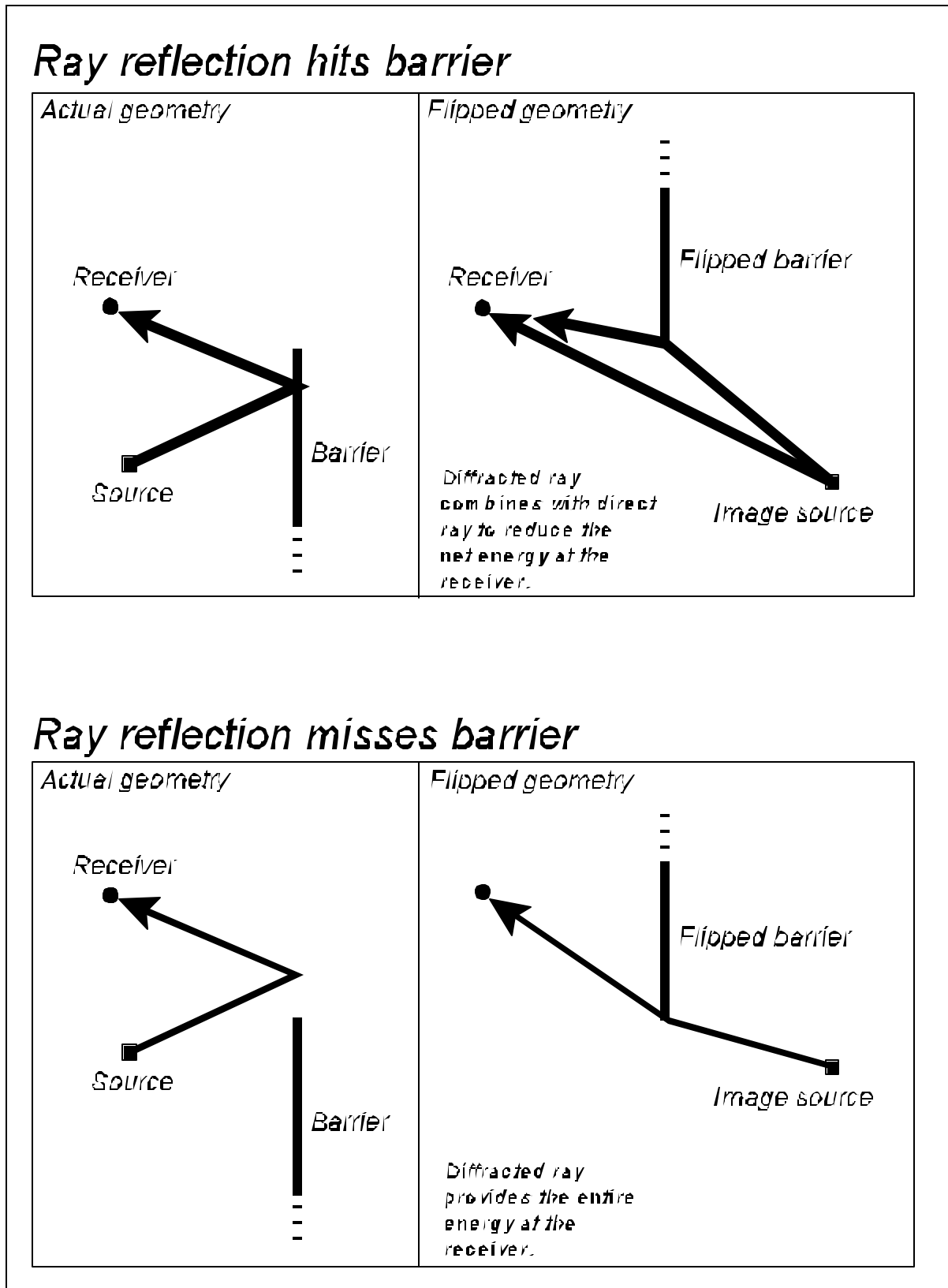


Figure 69. Partial reflection near tops of parallel barriers.

Barrier attenuation: Upon diffraction over the top edge of a barrier or retaining wall, TNM multiplies the ray's energy by $10^{(-A/10)}$, where the barrier attenuation, A, is computed with TNM's line-source barrier equation. In addition, TNM adds additional divergence to account for the increased distance between the ray target (diffraction edge) and the receiver.

Combination of barrier and ground attenuation: TNM retains the larger of these two attenuations and ignores the other.

E.6 Computation of Parallel-barrier Degradation

To compute parallel-barrier degradation, TNM first computes ray energies twice:

Multiple reflections: Each ray is reflected according to NRCs input by the user.

No multiple reflections: The same as for multiple reflections, except for the following.

When a ray reflects from one of the flanking barriers or retaining walls, its energy is completely absorbed, as if the barrier or wall was not there. In this manner, rays that reach the diffracting edge after barrier reflections are reduced in strength to zero, and thereby eliminated. As a result, all reverberantly reflected rays are eliminated. Only those rays remain that reach the diffracting edge either directly from the source or after reflection from the pavement or other non-barrier surfaces.

To compute for no multiple reflections, TNM must determine which of the user's surfaces are flanking barriers and retaining walls. Most obviously, the left-most and the right-most surface segments must be these flanking ones. In addition, TNM assumes that additional surface segments contiguous with these two are also part of the flanking barriers/walls, as long as the contiguous ones are collinear with the left-most and right-most segments.

After these two computations, TNM converts the resulting energies to sound levels. For each receiver, the difference in noise level between these two computation (multiple reflections and no multiple reflections) is the direct effect of multiple reflections — that is, of reverberation between the parallel retaining walls and/or barriers. This effect is called parallel-barrier degradation. For example, if this parallel-barrier degradation is 4 decibels, then the reverberation from the opposite wall/barrier has increased the noise level by 4 decibels, relative to the situation without multiple reflections.

E.7 Generalization to TNM Sound-level Receivers

TNM computes parallel-barrier degradation for explicitly entered two-dimensional cross-sectional geometries. Once computed, the user must generalize these degradations for the actual TNM receivers and then enter appropriate adjustment factors for these receivers, to account for multiple reflections.

E.8 Calibration of Results with Field Measurements

The algorithm described above overestimates parallel-barrier degradation in some instances, compared to field measurements. For this reason, TNM results are calibrated to field measurements before reported to the user.

E.8.1 Initial comparisons of measured and predicted degradations Three sets of measured field data were used to calibrate TNM’s parallel-barrier degradation:

- # Route 99 in California [Hendriks 1991]: w/h ratio = 15:1
- # I-495 in Montgomery County, Maryland [Fleming 1992]: w/h ratio = 9:1
- # Dulles Airport experimental barrier [Fleming 1990]: w/h ratio = 6:1

These measurement sets are summarized in [Fleming 1994]. In this list of measurement sets, w/h is the width-to-height ratio of the measurement site’s cross section; width, w, is the total distance between the parallel barriers; and height, h, is the average of the two barrier heights *relative to the roadway elevation*. Table 15 summarizes the initial comparison of field measurements and TNM computations, before calibration.

**Table 15. Parallel-barrier degradations:
Initial comparison of measured and computed values.**

Data set	Width/Height ratio (w/h)	Parallel-barrier degradations					
		Measured, dB		Computed, dB		Overprediction (computed minus measured), dB	
		Range	Avg	Range	Avg	Range	Avg
Route 99, California	15:1	0.1 to 1.4	0.9	0.8 to 3.9	2.6	+0.1 to +3.0	+1.7
I-495, Montgomery County MD	9:1	0.6 to 2.8	2.0	1.0 to 4.7	3.0	+0.2 to +1.9	+1.0
Dulles Airport	6:1	-0.6 to 5.8	1.7	0.1 to 4.9	2.0	-4.8 to +2.7	+0.3

All comparisons in this table involve nine microphone positions: three distances, three heights each. Measurements on Route 99 and I-495 involve many hundreds of vehicles, as they passed by. Dulles measurements involve controlled passbys of four heavy trucks.

As the table shows, overprediction is significant for w/h ratios around 15:1, but not significant for smaller w/h ratios around 6:1. Although the table does not show it, overprediction also varied systematically with microphone height and distance from the roadway.

E.8.2 Sensitivity to assumed source height Parallel-barrier degradation computed by TNM is very sensitive to TNM’s built-in vertical subsources heights and built-in vertical energy splits (see

Appendix A). For example, degradation was initially computed for five different source heights, as shown in Table 16, using Route-99 traffic and roadway geometry.

Table 16. Sensitivity of computed degradations to assumed source height.

Assumed source height	Computed parallel-barrier degradation, dB	
	Range	Average
0.03 meters (0.1 feet)	1.0 to 5.7	3.4
0.7 meters (2.3 feet)	0.7 to 4.7	2.7
2.44 meters (8 feet)	0.6 to 2.6	1.6
3.05 meters (10 feet)	0.6 to 2.4	1.1
3.66 meters (12 feet)	0.2 to 0.6	0.4
<i>For comparison, vehicle emissions split per Stamina- 2.0 heights:</i> 0 meters (0 feet) for automobiles 0.7 meters (2.3 feet) for medium trucks 2.44 meters (8 feet) for heavy trucks	0.8 to 4.0	2.6

These sensitivity results show clearly that computed TNM degradation depends critically upon the specific subsource heights used for computation, and in turn upon the subsource-height energy split for any pair of subsource heights.

E.8.3 Calibration method For adequate accuracy, TNM parallel-barrier computations obviously need to be calibrated against measurements. Overprediction of degradation is too large without such calibration. The following method was used to determine a calibration method for TNM’s parallel-barrier computations:

- # **Parallel-barrier computations:** First, the three parallel-barrier measurement sites were entered as TNM parallel-barrier input. For this input, cross-sectional shape within the roadway section was carefully matched and field-measurement traffic volumes and speeds were used. Then for each of these three sites, parallel-barrier degradation was computed at each site’s nine microphone locations.
- # **Comparison and regressions:** For all three sites combined, each microphone’s measured and computed degradation ($g_{meas,mic}$ and $g_{comp,mic}$, respectively) were tabulated along with their ratio, $R_{mic} = g_{meas,mic} / g_{comp,mic}$. Note that R times g_{comp} yields g_{meas} . For this reason, R_{mic} is a first cut at the required calibration multiplier.

Then R_{mic} was plotted and regressed against the following independent variables:

The microphone cross-section's w/h ratio, $r_{w/h,mic}$, where

$$r_{w/h,mic} = \frac{(H_{diff,right} - H_{diff,left})}{(\overline{Z_{diff}} - \overline{Z_{road}})} \quad (67)$$

In this equation,

$$\begin{aligned} H_{diff,right} &= \text{the H coordinate of the right - end diffraction point} \\ H_{diff,left} &= \text{the H coordinate of the left - end diffraction point} \\ \overline{Z_{diff}} &= \text{the average Z coordinate of the two diffraction points} \\ \overline{Z_{road}} &= \text{the average Z coordinate of all the roadways (at the pavement).} \end{aligned} \quad (68)$$

The microphone's horizontal distance from the near barrier, $d_{horiz,mic}$, where

$$d_{horiz,mic} = |H_{mic} - H_{diff,near}| \quad (69)$$

In this equation,

$$\begin{aligned} H_{mic} &= \text{the H coordinate of the microphone (analysis location)} \\ H_{diff,near} &= \text{the H coordinate of the near diffracting edge.} \end{aligned} \quad (70)$$

The microphone's height above the top barrier edges, $d_{vert,mic}$, where

$$d_{vert,mic} = Z_{mic} - \overline{Z_{barr\ tops}} \quad (71)$$

In this equation,

$$\begin{aligned} Z_{mic} &= \text{the Z coordinate of the microphone (analysis location)} \\ \overline{Z_{barr\ tops}} &= \text{the average Z coordinate of the tops of the two barriers.} \end{aligned} \quad (72)$$

E.8.4 Calibration results. The regression produced the following adjustments to the computed output of TNM's parallel-barrier code:

$$g_{\text{calibrated, mic}} = \left(g_{\text{computed, mic}} \right) \left[1 + e^{\left(4r_{w/h, \text{mic}} - 21.42 \right)} \right]^{-0.019} + 0.072 + 0.04d_{\text{vert, mic}} - 0.003d_{\text{horiz, mic}} , \quad (73)$$

subject to the constraint that

$$g_{\text{calibrated, mic}} \leq g_{\text{computed, mic}} . \quad (74)$$

In these two equations, $g_{\text{calibrated, mic}}$ is the calibrated degradation at a given microphone and $g_{\text{computed, mic}}$ is the degradation computed directly by the parallel-barrier code. The three independent variables ($r_{w/h, \text{mic}}$, $d_{\text{horiz, mic}}$, and $d_{\text{vert, mic}}$) are defined in Eqs. (65), (67) and (69), respectively.

APPENDIX F

CONTOURS

FHWA TNM[®] computes sound levels and analyzes barrier designs primarily at receivers individually entered by the user. In addition to this primary intent, TNM also allows the user to compute contours within specified contour zones. Three types of contours are available:

- # Sound-level contours for a specified barrier design, in the user's chosen set of sound-level units:
 L_{Aeq1h} , L_{dn} , or L_{den}
- # Insertion-loss contours for a specified barrier design
- # Level-difference contours between two specified barrier designs.

This appendix discusses TNM's computation of these three types of sound-level contours.

F.1 Contour computations

To compute contours, TNM:

- # Generates an initial, regular grid within the user's contour zone
- # Interpolates the ground elevation at all grid points
- # Computes the sound level at each grid point, at 1.5 meters (5 feet) above the interpolated ground
- # Subdivides each grid cell, as needed, to obtain the user's requested contour precision.

Contour computations are linked to "remembered" barrier designs. Through this linkage, TNM sets the height of each barrier segment in the design to one particular value, from among all the possible height perturbations.

Barrier designs are linked in the following ways:

- # For sound-level contours, the user first chooses a "remembered" barrier design, with its particular barrier heights. Then TNM uses these heights to compute sound levels at all grid points.
- # For insertion-loss contours, the user first chooses a "remembered" barrier design, with its particular barrier heights. TNM uses these heights to compute sound levels, with barriers. Then TNM reduces the height of all perturbable barriers to zero, to compute sound levels without barriers. TNM then subtracts the two sets of grid values, to obtain the barrier insertion loss at all grid points.
- # For level-difference contours, the user chooses *two* "remembered" barrier designs. TNM computes sound levels at the grid points from both, then subtracts them. Note that any two barrier designs in the same TNM run will automatically have the same coordinate system.

Sometimes barriers that are not in the chosen barrier design may affect sound levels within the contour zone. Generally this is not the case, however. Generally the user includes all influential barriers in the

chosen barrier design. To compute, however, TNM must know *all* barrier heights, even those not in the chosen barrier design.

To be conservative, TNM assigns zero height to all barriers not in the chosen barrier design. For a perturbable barrier to have a non-zero height for contour computations, the user *must* include it in the barrier design and thereby set its height as desired.

Once TNM obtains computed values at all grid and necessary subgrid points, it generates a so-called “grid” file with these computed values, the XY coordinates of the grid points, and other miscellaneous data. It then submits this grid file to the computer program NMPLOT, which computes the corresponding contours and returns them to TNM.

This exchange between TNM and NMPLOT is essentially transparent to the user. The user may, however, name the grid file and thereby recall it for later use — or even run it independently under NMPLOT Version 3.05.

F.2 Details about Barrier Perturbations

Barrier input contains three values associated with perturbations:

- # Perturbation increment
- # Number of perturbations up
- # Number of perturbations down.

Fixed, barrier-like features: If a user wishes to model an existing wall, or a Jersey barrier along the highway, or even a large building, then the user sets all three of the above parameters to zero. TNM then knows that such barriers are never perturbed down to their zero height. They are fixed features within the input, always there and always full height.

Perturbable barriers: If a user wishes to model a perturbable noise barrier along the highway, the user enters values for the above three parameters to indicate the height perturbations desired. TNM then computes the acoustics for all height perturbations, including zero height. In addition, TNM perturbs this barrier down to zero height as the baseline condition for insertion loss calculations.

Non-perturbable barriers: A third possibility exists, as well: the user wishes to model a non-perturbable noise barrier along the highway and to later learn its insertion loss. To do this, the user must enter *at least one non-zero perturbation value*: either: (1) non-zero number of perturbations up; or (2) non-zero number down; or (3) non-zero perturbation increment. This non-zero value tells TNM to perturb the barrier down to zero height for insertion loss calculations, even though the barrier top does not perturb.

F.3 Details about Grid Spacing

TNM determines initial grid spacing automatically, using the dimensions of the user's contour zone. First, TNM determines the smaller contour-zone width, either the X-width or the Y-width:

$$\begin{aligned} X\text{-width} &= x_{\max} - x_{\min} \\ Y\text{-width} &= y_{\max} - y_{\min} \end{aligned} \tag{75}$$

Then TNM divides the *smaller of these two* by 10, to obtain the initial grid spacing. This spacing is used in both directions, X and Y, even though it is derived from only one of them.

After computing sound levels at each grid point, TNM then loops back through the grid to decide upon subdivision. The left frame in Figure 70 shows a grid "cell" composed of four grid points: 1, 2, 3 and 4. TNM has already computed sound levels at these four points. To decide whether or not to subdivide this cell into four smaller cells:

- # TNM computes sound levels at three additional points, marked A, B and C in the figure.
- # TNM subtracts the computed level at point A from the algebraic average at points 1 and 2.
- # TNM subtracts the computed level at point B from the algebraic average at points 1 and 3.
- # TNM subtracts the computed level at point C from the algebraic average at points 1 and 4.
- # If *all* of these differences are within the user's requested precision, then TNM does not subdivide this cell. On the other hand, if *any one of them* is greater than the user's requested precision, then:
 - # TNM subdivides cell 1234, as shown to the right in the figure, to obtain four cells.
 - # TNM individually tests and possibly subdivides each of the resulting four cells.

Subdivision stops when the differences are within the user's requested precision. In addition, subdivision automatically stops when the size of a subgrid falls below the user's "minimum subgrid size." For example, if the user is interested in geographic resolution down to only 10 meters (33 feet), then a minimum subgrid size of 10 meters (33 feet) would prevent TNM from subdividing any finer.

Note that TNM has to contain some limit on the depth of subdivision. Without such a limit, TNM would never stop subdividing in regions with sound-level discontinuities. Such discontinuities occur from front to back of a barrier or a building row. In addition, they occur across roadways, although most users will not include roadways within contour zones.

Also, although contour zones can intersect any other type of TNM input, users are cautioned against the intersection of barriers and roadways (this includes a roadway's width) with contour zones. The reason

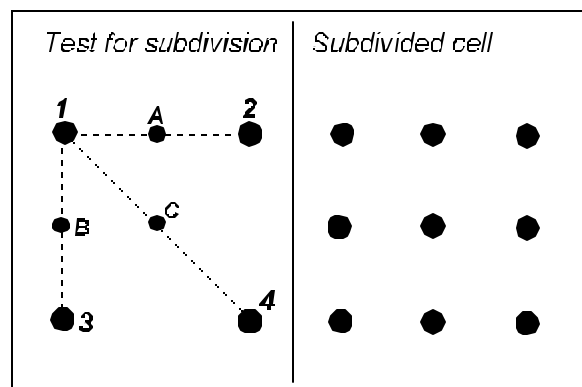


Figure 70. Subdivision of grid cells during contouring.

is that contouring logic can break down in areas of steep noise gradients, such as exist around the ends of barriers and on roadways.

F.4 Details about Computation Heights

To compute sound levels, TNM must know the Z coordinate of the ground at each grid/subgrid point. TNM computes at ear-height above this ground Z coordinate, using the user-entered receiver height above the ground. To determine the ground's Z coordinate at each grid/subgrid point:

- # TNM augments the user's input by replacing every line segment (roadway, barrier, building row, terrain line, edge of tree zone) with a series of closely spaced points. These points define the Z coordinate of the ground continually along the line segment, from the input Z coordinates of its endpoints. Without such augmentation of Z coordinates, a line segment would define the ground only at its two endpoints.
- # TNM drops a regularly spaced "net" down over the augmented input, with a net spacing equal to the initial grid spacing. Then TNM interpolates the ground Z coordinates at each grid point from all the Z coordinates for the augmented input.
- # Then TNM adds 1.5 meters (5 feet) to all ground Z coordinates, to approximate ear height. Note that receiver heights above the ground may differ from receiver to receiver and so TNM cannot make this contour-receiver height specific to any single input-receiver's height.
- # During subdivision, TNM determines the Z coordinate of each new subgrid point by interpolating between previously determined Z coordinates.

APPENDIX G

MODEL VERIFICATION

This appendix provides a comparison of TNM results to measurements and to the model results of others. Comparisons are made to five different data sets, three of which involved point-source geometry, and the remaining two involved in-situ measurements of barrier performance along actual highways. The first comparison is with Embleton's model for reflection from ground of finite impedance [Embleton 1983]. The second is to measurements by Parkin and Scholes over grassland [Parkin 1965], the third is to measurements of a noise barrier by Scholes, also over grassland [Scholes 1971]. The fourth and fifth are to measurements of noise barrier performance at two different highway locations by Hendriks and Fleming, respectively [Hendriks 1991][Fleming 1992]. Overall, the agreement with measurements is found to be very satisfactory.

G.1 Ground Reflection Model

The TNM's model for reflection coefficients is based on the approach of Chessell [Chessell 1977], which incorporates the single-parameter ground-impedance model first proposed by Delany and Bazley [Delany 1970]. Embleton, Piercy and Daigle further developed the model and conducted measurements to determine empirically the relationship between ground type and effective flow resistivity (EFR) [Embleton 1983]. Figures 71 through 74 present a comparison of the TNM model with Embleton's model for Embleton's published geometry and four values of EFR. The geometry was: source height = 0.31 meters (1.0 feet); receiver height = 1.22 meters (4.0 feet); source-to-receiver distance = 15.2 meters (50 feet). The values of EFR span the range from very soft ground (powder snow, EFR = 10 cgs Rayls) to hard ground (10,000 cgs Rayls).

Plotted in the figures are values of the "ground effect" in dB, which represents the difference between the free-field (no-ground) condition and the condition with the ground. At low frequencies, the ground adds up to 6 dB, due to pressure doubling. In the middle frequencies and over soft ground (EFR = 100 to 500) the fairly broadband "ground-effect dip" exhibits significant reductions in sound level due to destructive interference.

G.2 Measurements Over Grassland

The TNM's reflection model is compared with very carefully-conducted measurements of sound propagation over grassland by Parkin and Scholes [Parkin 1965]. The atmospheric conditions for the measurements were a normal temperature gradient (no strong lapse or inversion) and zero vector wind (no components in the source-to-receiver direction). The ground surface at the site, called "Hatfield," was grass up to 5 centimeters (2 inches) high covering silty soil. The ground was especially flat, within ± 0.3 meters (1 foot) for more than 500 meters (1500 feet). The source was a jet engine at a height of 1.8 meters (6.0 feet) and the microphone heights were all 1.5 meters (5.0 feet) above the ground. One-third octave band sound level measurements were made at the following distances: 35 m (114 ft), 62 m (202 ft), 110 m (360 ft), 195 m (640 ft) and 348 m (1140 ft).

The TNM was exercised at the same geometric locations, and an EFR of 325 cgs Rayls was chosen as most likely to represent the characteristics of the ground at Hatfield. Figures 75 through 79 present the comparison of measured and modeled ground effect in α -octave bands.

G.3 Measurements of Barrier Insertion Loss

The complete TNM reflection and diffraction model was compared with the careful barrier insertion loss measurements of Scholes [Scholes 1971]. Like the Parkin propagation measurements, the barrier measurements were also conducted at the Hatfield site. Numerous measurements were conducted at different distances, with different barrier and receiver heights, and under different atmospheric conditions. The comparisons with the TNM were made with a limited set of the measured data. The atmospheric conditions were neutral with zero vector wind. Comparisons are made for the following geometry: source height of 0.7 m (2.3 ft); barrier heights of 1.8 m (6 ft) and 4.9 m (16 ft); microphone heights of 1.5 m (5 ft), 3 m (10 ft), 6 m (20 ft), and 12 m (40 ft); source-to-barrier distance of 10 m (33 ft); and barrier-to-receiver distance of 30 m (100 ft). Measurements were made with and without the barrier and the resulting insertion loss reported in octave bands. For a direct comparison, the TNM's α -octave band values were combined (energy sum prior to subtraction) to obtain octave-band values. As with the Parkin comparisons, an EFR of 325 cgs Rayls was assumed for the grass-covered Hatfield site. Figures 80 through 87 present the barrier insertion loss comparisons.

G.4 Measurements of In-Situ Barrier Performance

Comparisons between STAMINA and TNM for two recent studies show unprecedented predictive accuracy in the case of TNM. It should be pointed out that these two studies exercise the majority of the most-commonly used components within TNM, including barriers, propagation over acoustically soft ground, and moderately-changing terrain elevation. The comparisons are summarized below:

G.4.1 Rt. 99 in Sacramento, California. The study [Hendriks 1991] included sound-level measurements performed BEFORE and AFTER barrier construction, and the resultant INSERTION LOSS associated with the barrier. It consisted of 4 roadways, 1 barrier of interest in the AFTER case, 3 terrain lines, and 10 receivers. The receivers were located as follows: 1 reference microphone at 5 ft directly above the position of the barrier, 3 receivers placed at a 15-ft offset position behind the position of the barrier at 5-ft, 15-ft, 23-ft elevations, 3 receivers placed at a 75-ft offset position at the same elevations, and 3 receivers placed at a 200-ft offset position, also at the same elevations. The three microphone elevations will be referred to as low, middle, and high hereafter. The results shown in Tables 17 through 19 reflect sound levels adjusted for the reference microphone in accordance with ANSI S12.8-1987 [ANSI 1987].

Table 17. Rt. 99 CA: BEFORE (no barrier) levels.

Receiver	Measured Levels	Predicted Levels			
		STAMINA	Delta (Measured-STAMINA)	TNM	Delta (Measured-TNM)
200'-high	70.9	74.5	-3.6	70.2	0.7
200'-middle	71.0	74.5	-3.5	69.3	1.7
200'-low	64.7	74.5	-9.8	67.7	-3.0
75'-high	75.2	77.7	-2.5	75.5	-0.3
75'-middle	75.4	77.8	-2.4	74.2	1.2
75'-low	71.9	74.7	-2.8	72.4	-0.5
15'-high	79.5	80.5	-1.0	79.2	0.3
15'-middle	79.3	80.6	-1.3	78.6	0.7
15'-low	75.8	79.0	-3.2	76.8	-1.0
Average Delta			-3.34		-0.02

Table 18. Rt. 99 CA: AFTER (barrier) levels.

Receiver	Measured Levels	Predicted Levels			
		STAMINA	Delta (Measured-STAMINA)	TNM	Delta (Measured-TNM)
200'-high	65.0	70.2	-5.2	66.3	-1.3
200'-middle	63.4	69.4	-6.0	64.7	-1.3
200'-low	60.6	68.5	-7.9	62.5	-1.9
75'-high	72.0	75.8	-3.8	73.3	-1.3
75'-middle	66.9	72.6	-5.7	68.1	-1.2
75'-low	63.4	69.8	-6.4	63.9	-0.5
15'-high	80.4	80.9	-0.5	79.3	0.7
15'-middle	71.8	75.9	-4.1	71.6	0.2
15'-low	63.0	67.6	-4.6	63.2	-0.2
Average Delta			-4.91		-0.76

Table 19. Rt. 99 CA: Barrier insertion loss.

Receiver	Measured Levels	Predicted Levels			
		STAMINA	Delta (Measured-STAMINA)	TNM	Delta (Measured-TNM)
200'-high	6.4	4.8	1.6	4.4	2.0
200'-middle	8.1	5.6	2.5	5.1	3.0
200'-low	4.6	6.5	-1.9	5.7	-1.1
75'-high	3.7	2.4	1.3	2.7	1.0
75'-middle	9.0	5.7	3.3	6.6	2.4
75'-low	9.0	5.4	3.6	9.0	0.0
15'-high	-0.4	0.1	-0.5	0.0	-0.4
15'-middle	8.0	5.2	2.4	7.5	0.5
15'-low	13.3	11.9	1.4	14.1	-0.8
Average Delta			1.57		0.73

G.4.2 I-495 in Montgomery County, Maryland The study [Fleming 1992] only included sound-level measurements performed AFTER barrier construction. It consisted of 2 roadways, 1 barrier, and 10 receivers. The receivers were located as follows: 1 reference microphone at 5 ft directly above the position of the barrier, 3 receivers placed at a 16-ft offset position behind the position of the barrier at 7.9-ft, 18.3-ft, 28.9-ft elevations, 3 receivers placed at a 65.5-ft offset position at the same elevations, and 3 receivers placed at a 131-ft offset position, also at the same elevations. The three elevations will be referred to as low, middle, and high hereafter. The results shown in Table 20 reflect sound levels adjusted for the reference microphone in accordance with ANSI S12.8-1987.

Table 20. I-495 MD: AFTER (barrier) levels.

Receiver	Measured Levels	Predicted Levels			
		STAMINA	Delta (Measured-STAMINA)	TNM	Delta (Measured-TNM)
131'-high	67.9	71.2	-3.3	67.3	0.6
131'-middle	65.25	70.1	-4.85	65.2	0.05
131'-low	62.8	69.3	-6.5	63.9	-1.1
65.5'-high	72.15	73.95	-0.2	72.75	-0.6
65.5'-middle	67.9	71.25	-1.85	66.45	1.45
65.5'-low	64.75	68.75	-4.3	63.45	1.3
16'-high	80.3	80.4	-0.1	80.6	-0.3
16'-middle	73.15	75.6	-2.45	72.8	0.35
16'-low	66.45	67.7	-1.25	62.8	3.65
Average Delta			-3.07		0.60

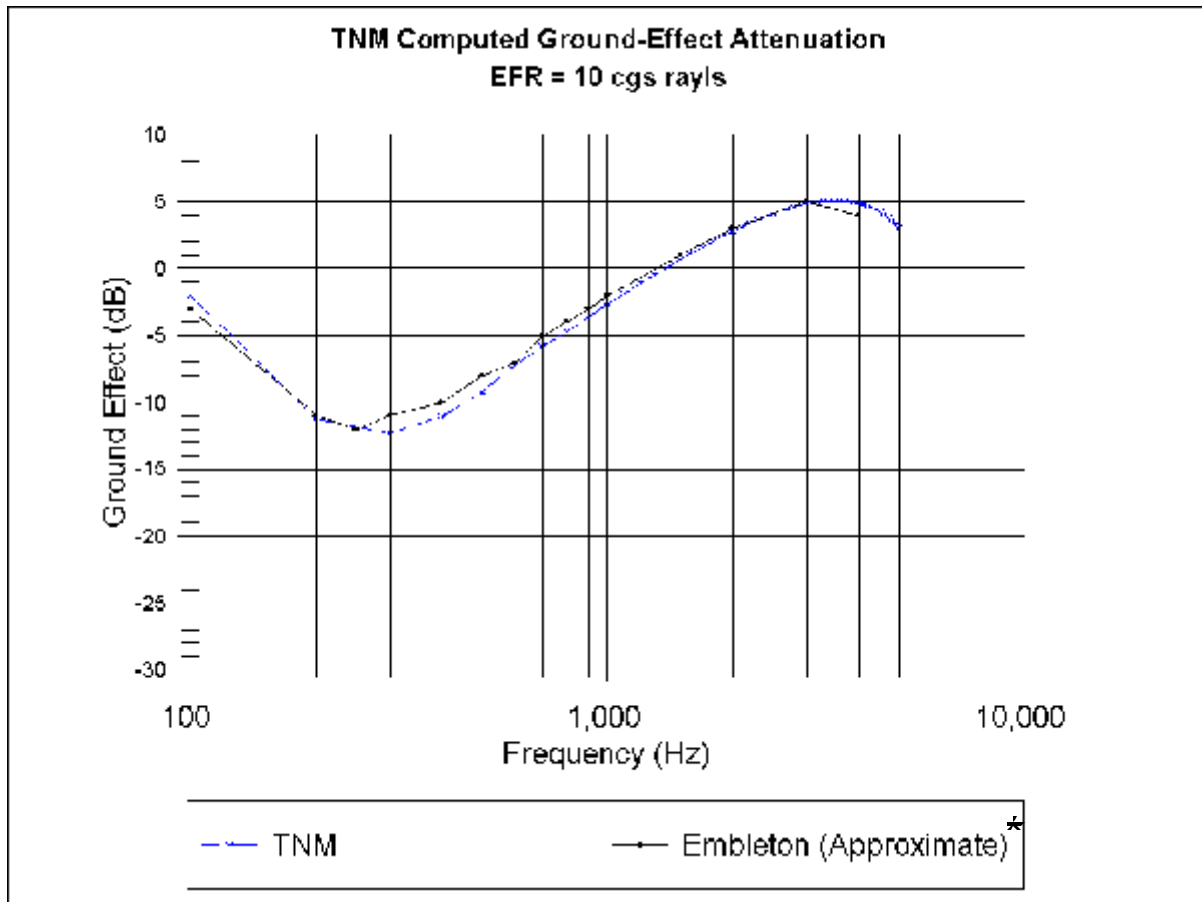


Figure 71. Ground-effect model comparison, EFR = 10 cgs Rays.

* This comparison was based on published graphs of the Embleton model.

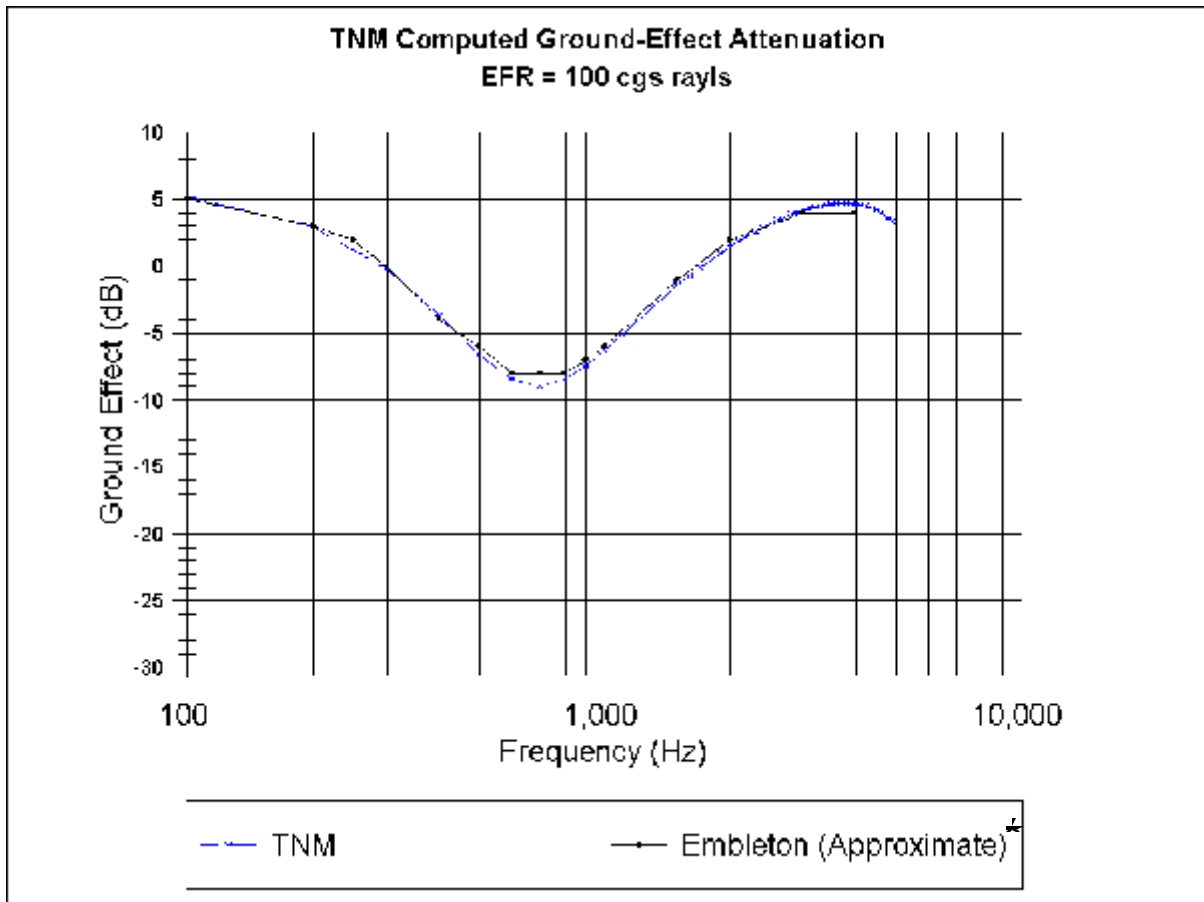


Figure 72. Ground-effect model comparison, EFR = 100 cgs Rayls.

* This comparison was based on published graphs of the Embleton model.

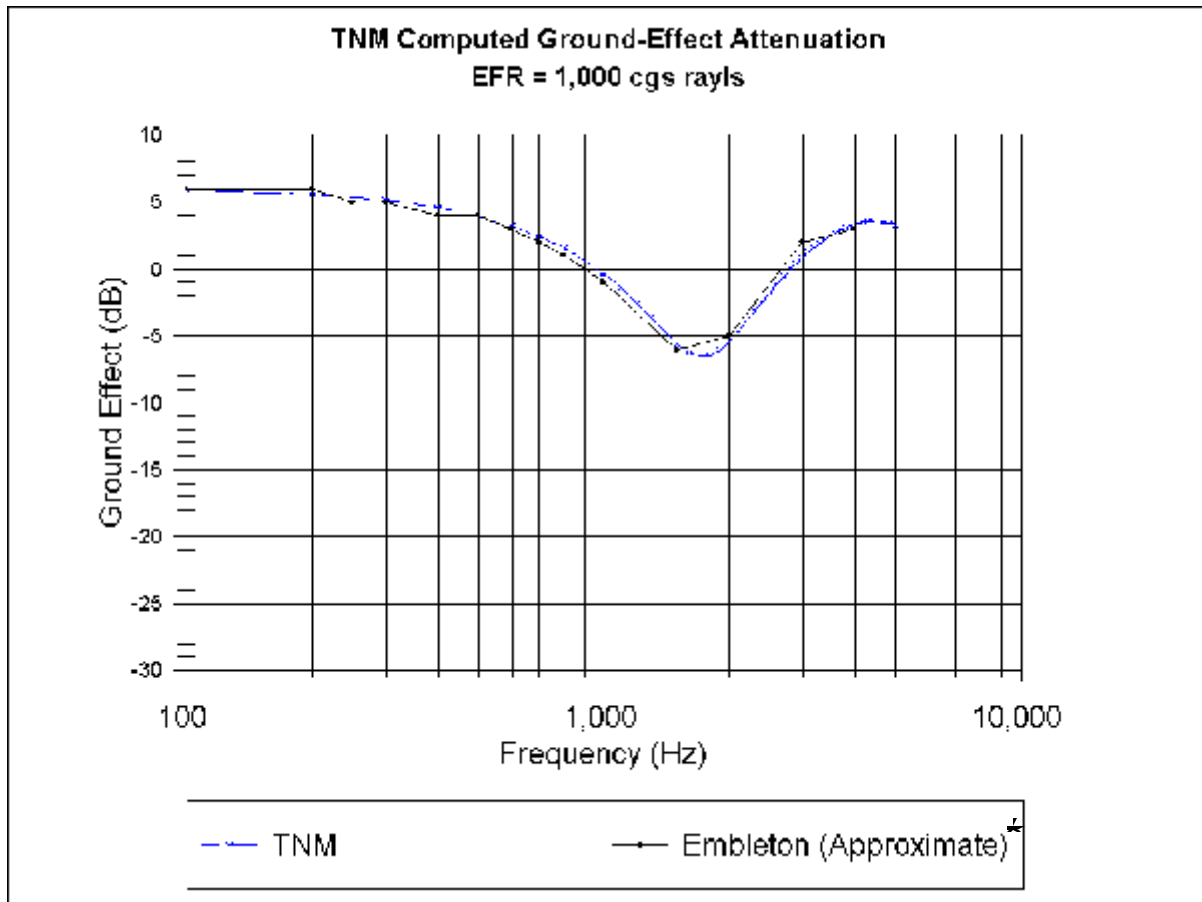


Figure 73. Ground-effect model comparison, EFR = 1000 cgs Rayls.

* This comparison was based on published graphs of the Embleton model.

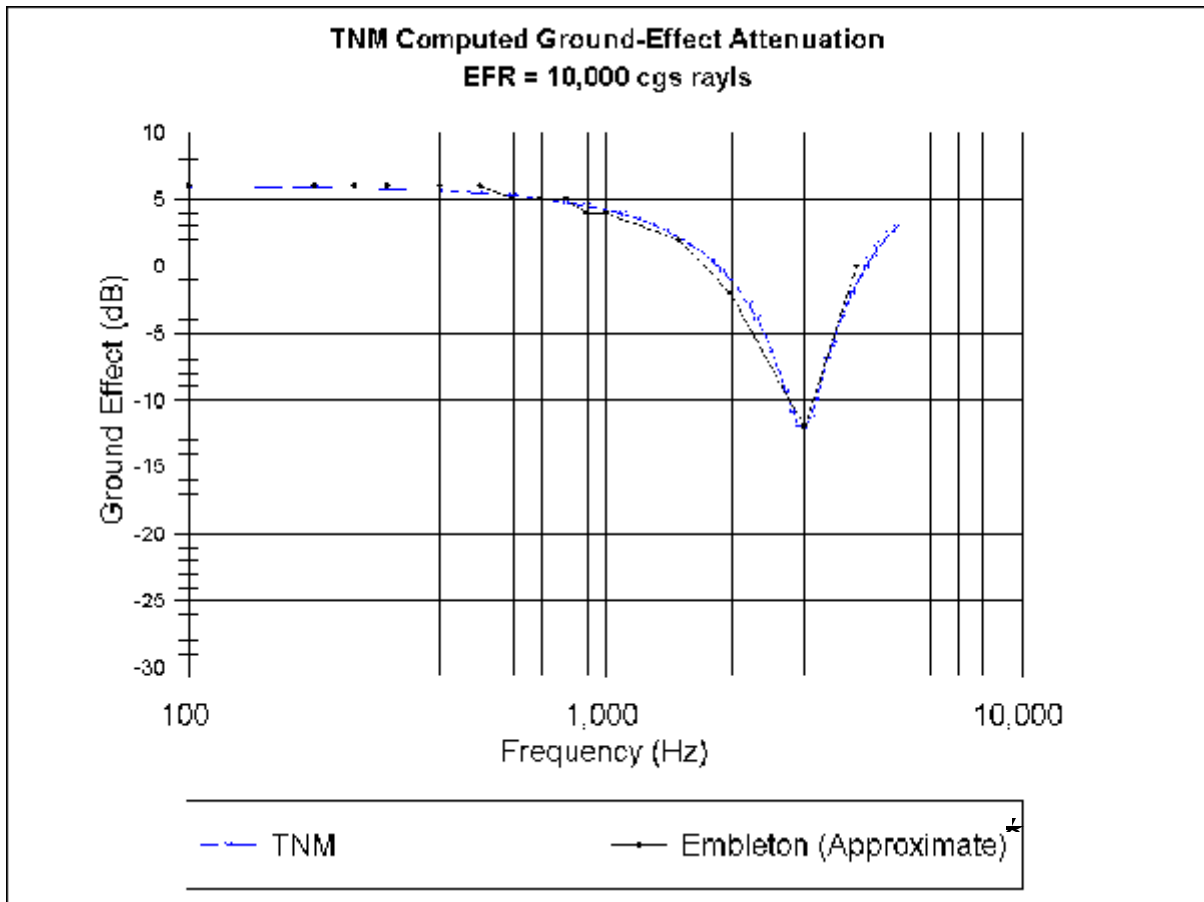


Figure 74. Ground-effect model comparison, EFR = 10,000 cgs Rayls.

* This comparison was based on published graphs of the Embleton model.

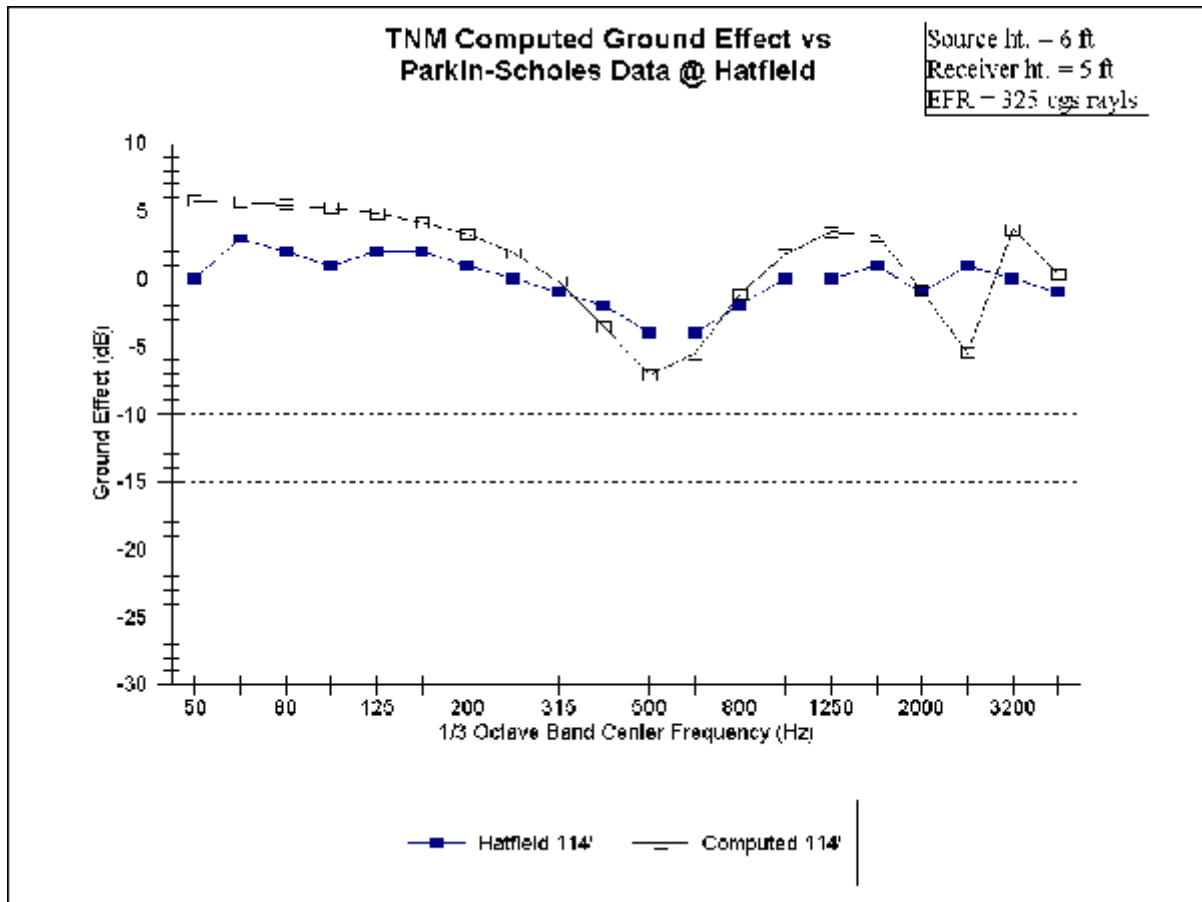


Figure 75. Comparison with measurements over grassland, distance = 35 meters (114 feet).

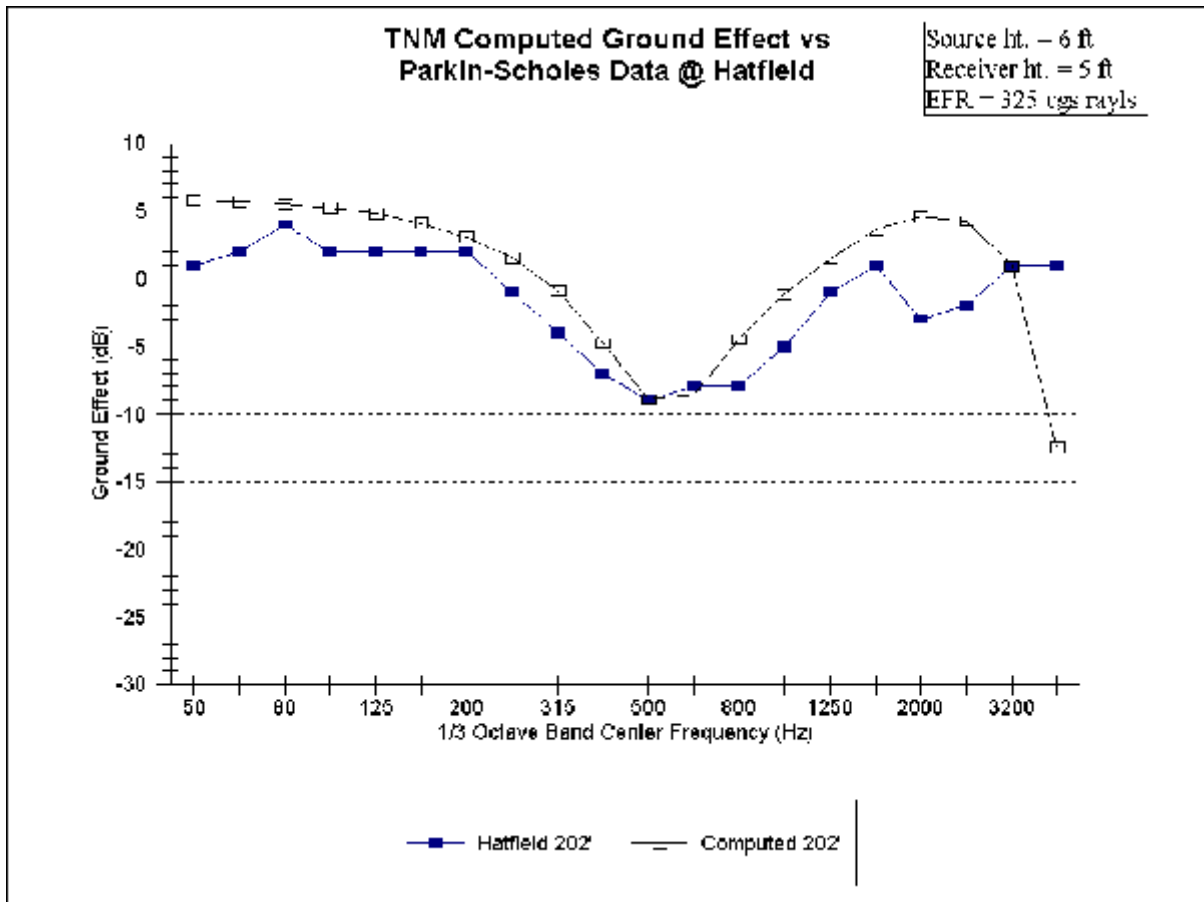


Figure 76. Comparison with measurements over grassland, distance = 62 meters (202 feet).

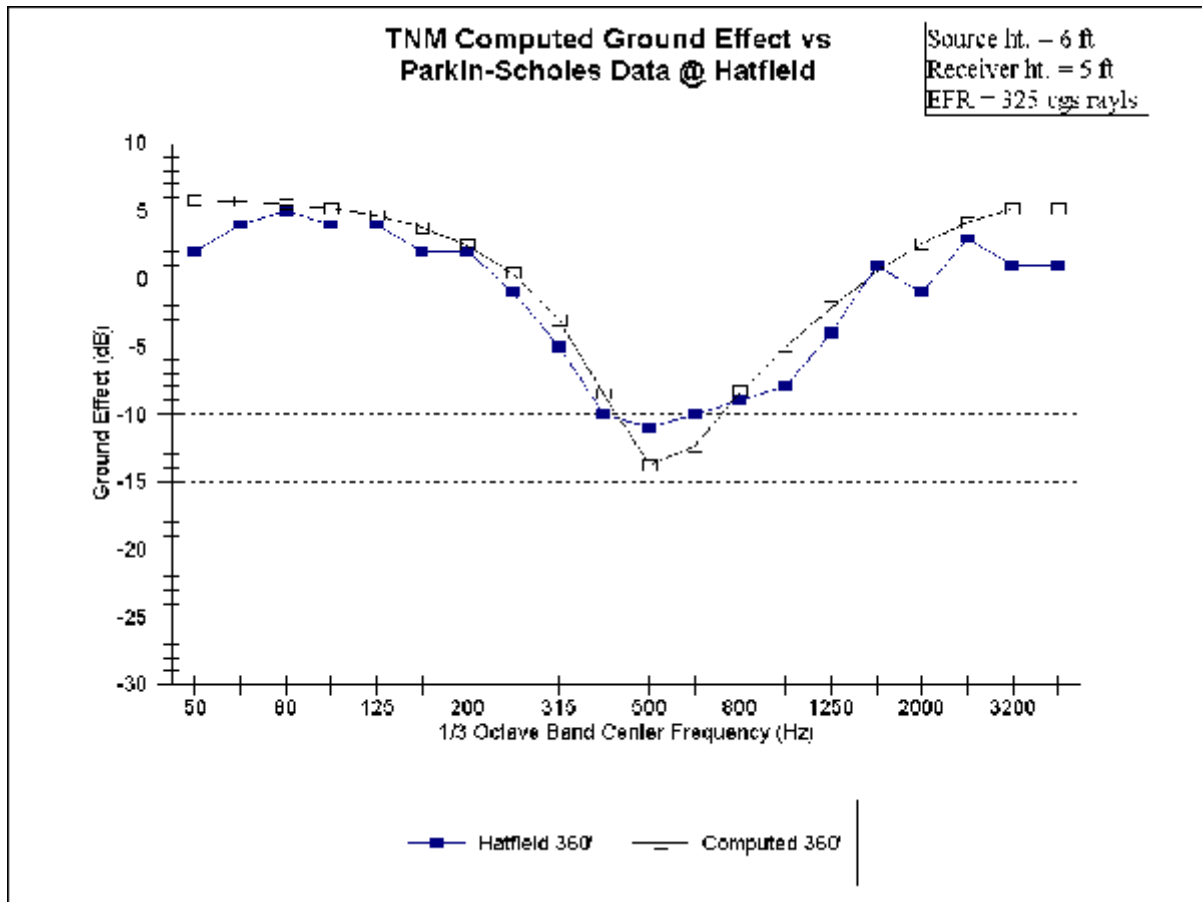


Figure 77. Comparison with measurements over grassland, distance = 110 meters (360 feet).

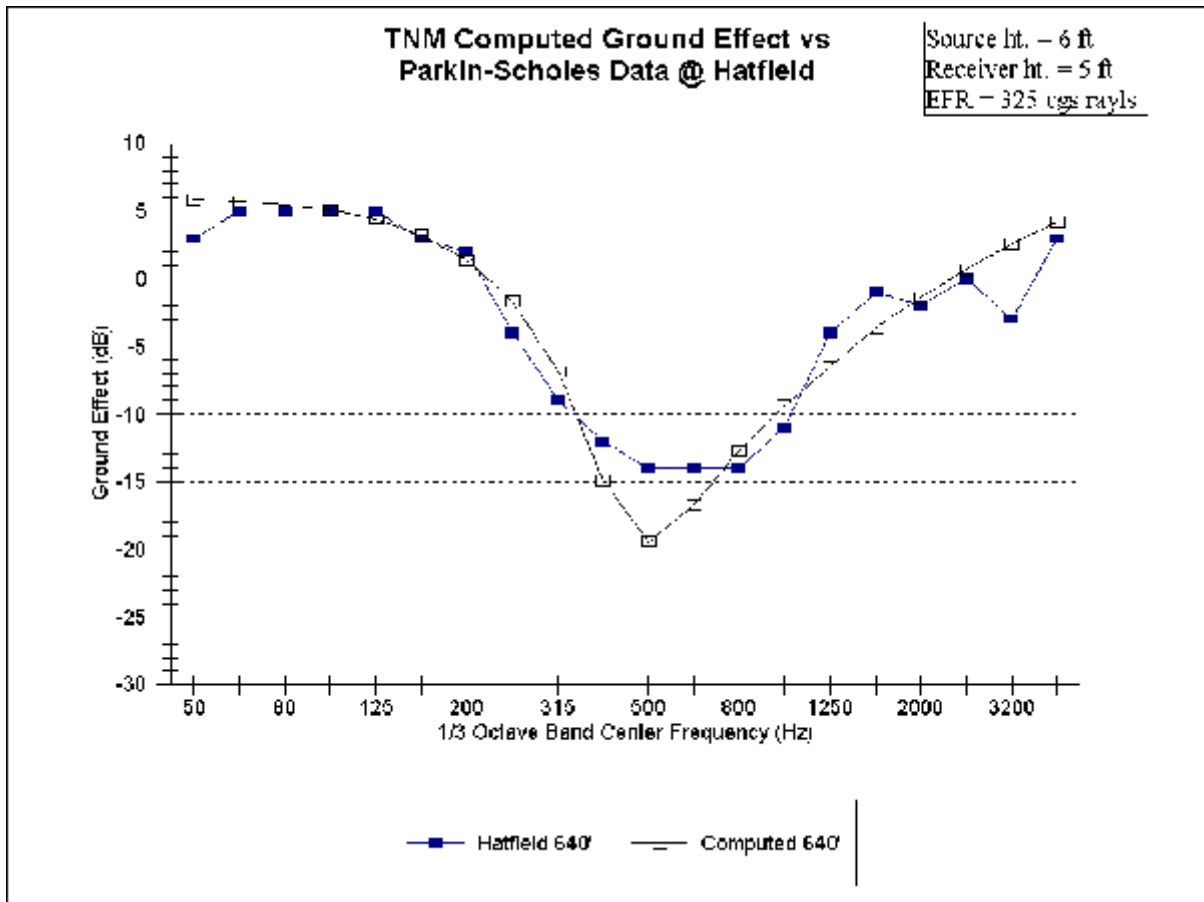


Figure 78. Comparison with measurements over grassland, distance = 195 meters (640 feet).

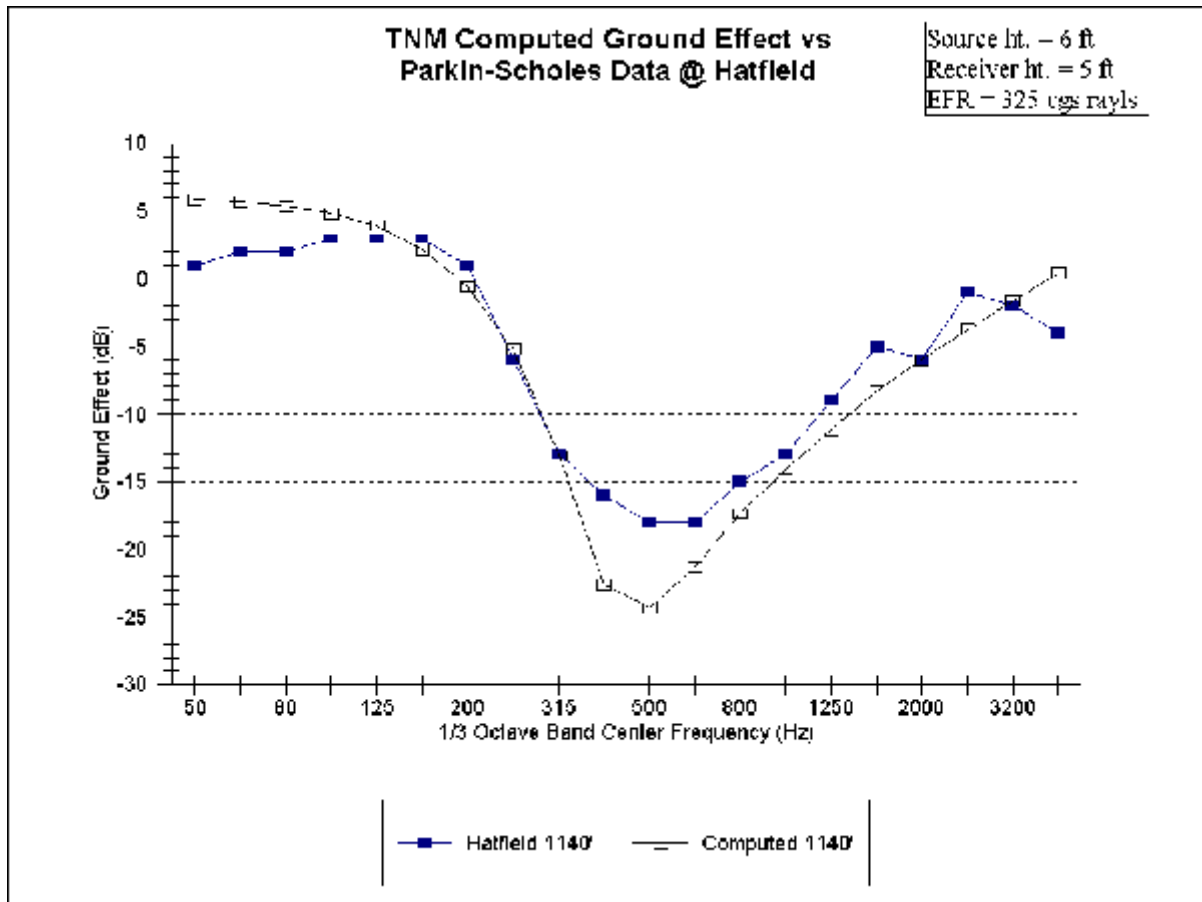


Figure 79. Comparison with measurements over grassland, distance = 348 meters (1140 feet).

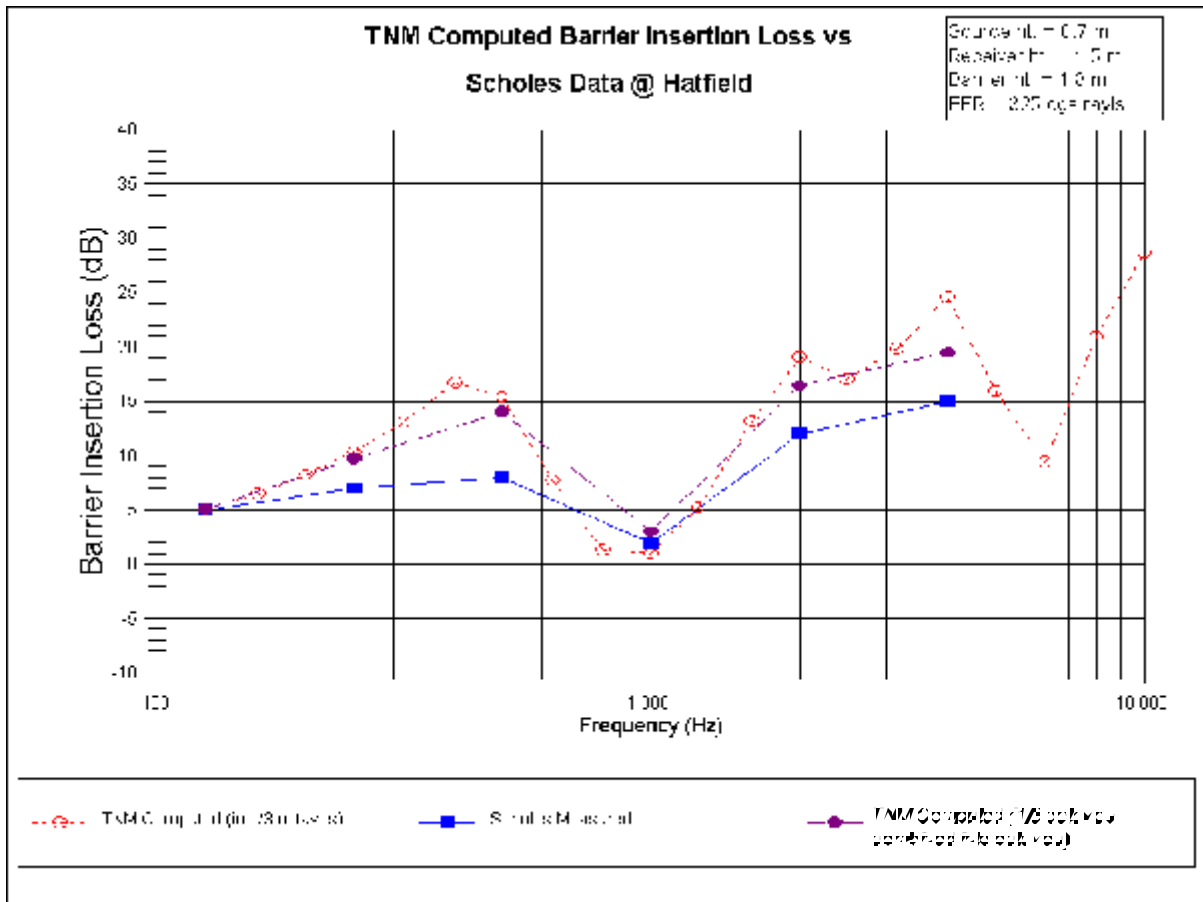


Figure 80. Comparison of barrier insertion loss in octave bands, receiver ht. = 1.5 m (5 ft), barrier ht. = 1.8 m (6 ft).

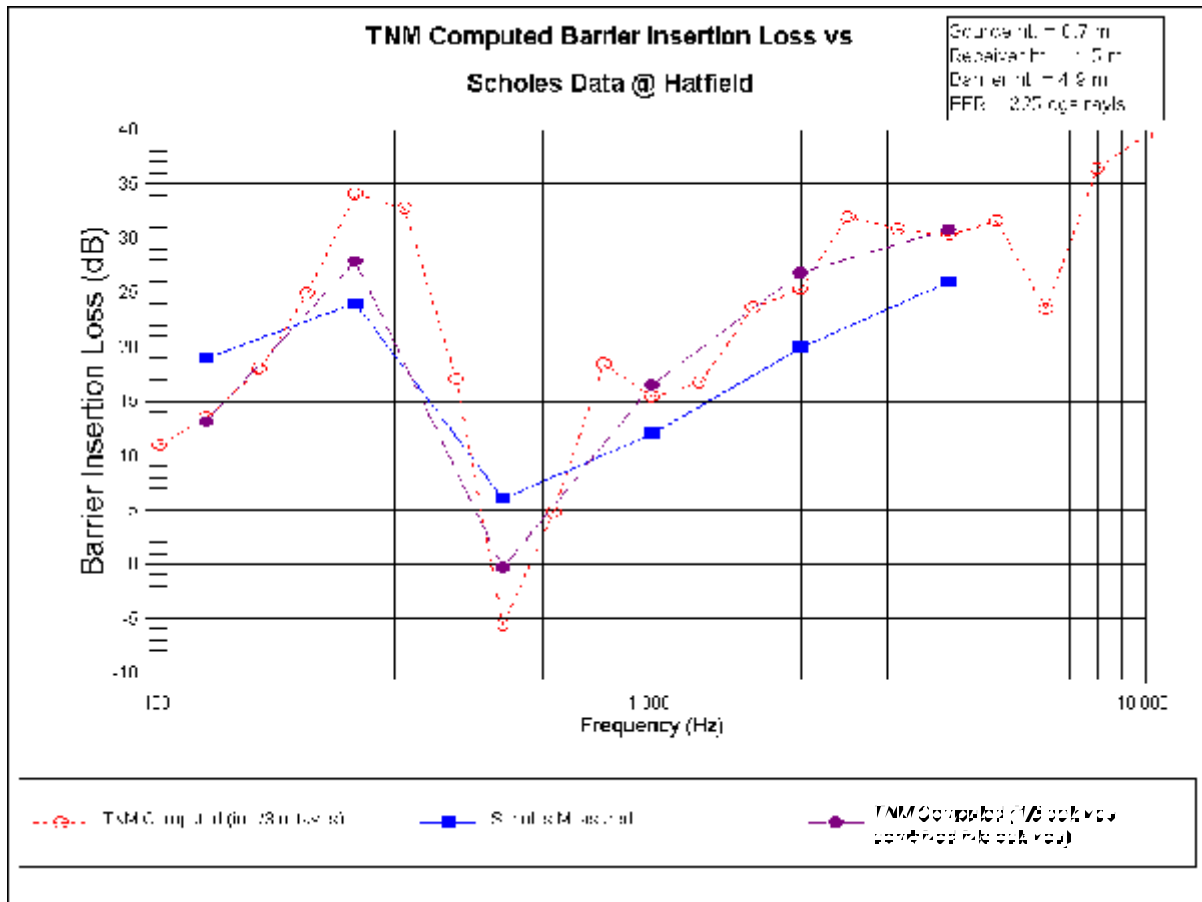


Figure 81. Comparison of barrier insertion loss in octave bands, receiver ht. = 1.5 m (5 ft), barrier ht. = 4.9 m (16 ft).

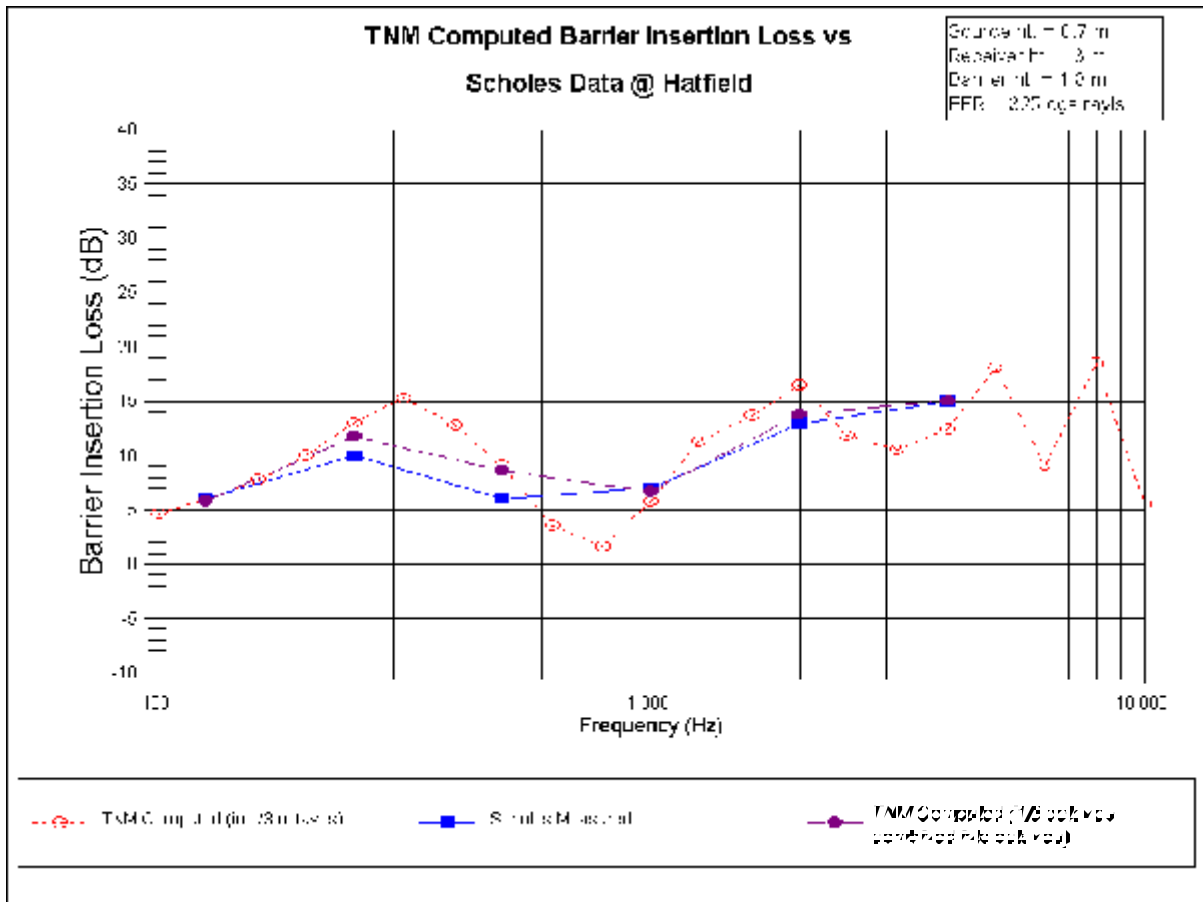


Figure 82. Comparison of barrier insertion loss in octave bands, receiver ht. = 3 m (10 ft), barrier ht. = 1.8 m (6 ft).

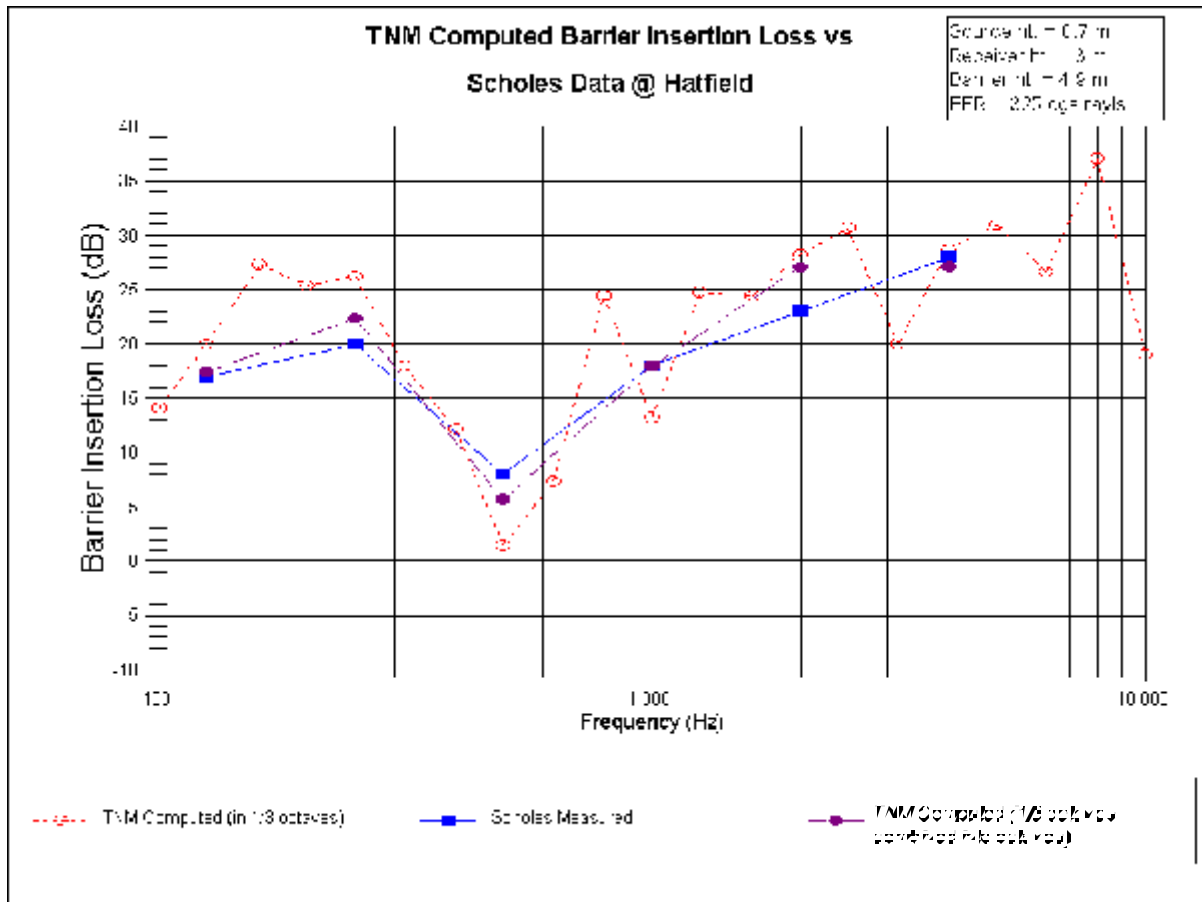


Figure 83. Comparison of barrier insertion loss in octave bands, receiver ht. = 3 m (10 ft), barrier ht. = 4.9 m (16 ft).

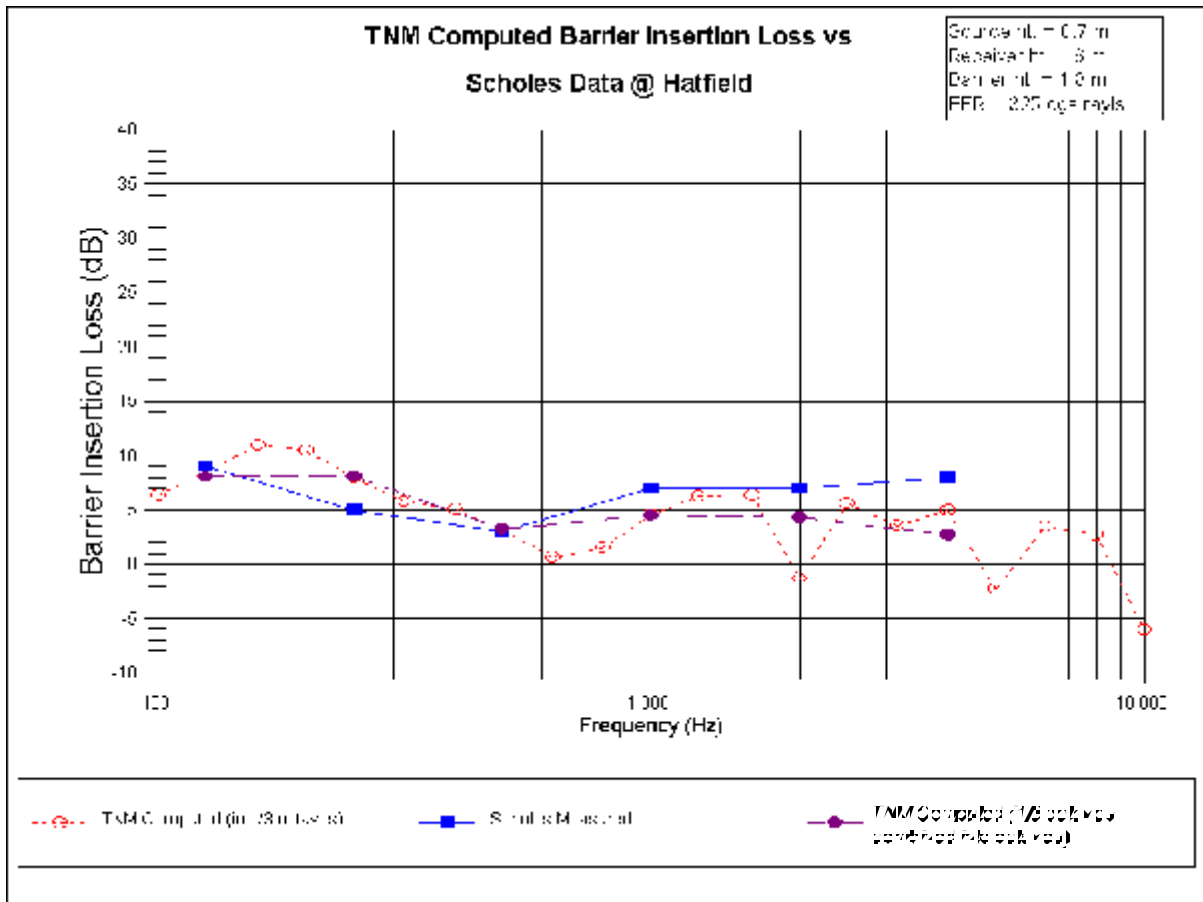


Figure 84. Comparison of barrier insertion loss in octave bands, receiver ht. = 6 m (20 ft), barrier ht. = 1.8 m (6 ft).

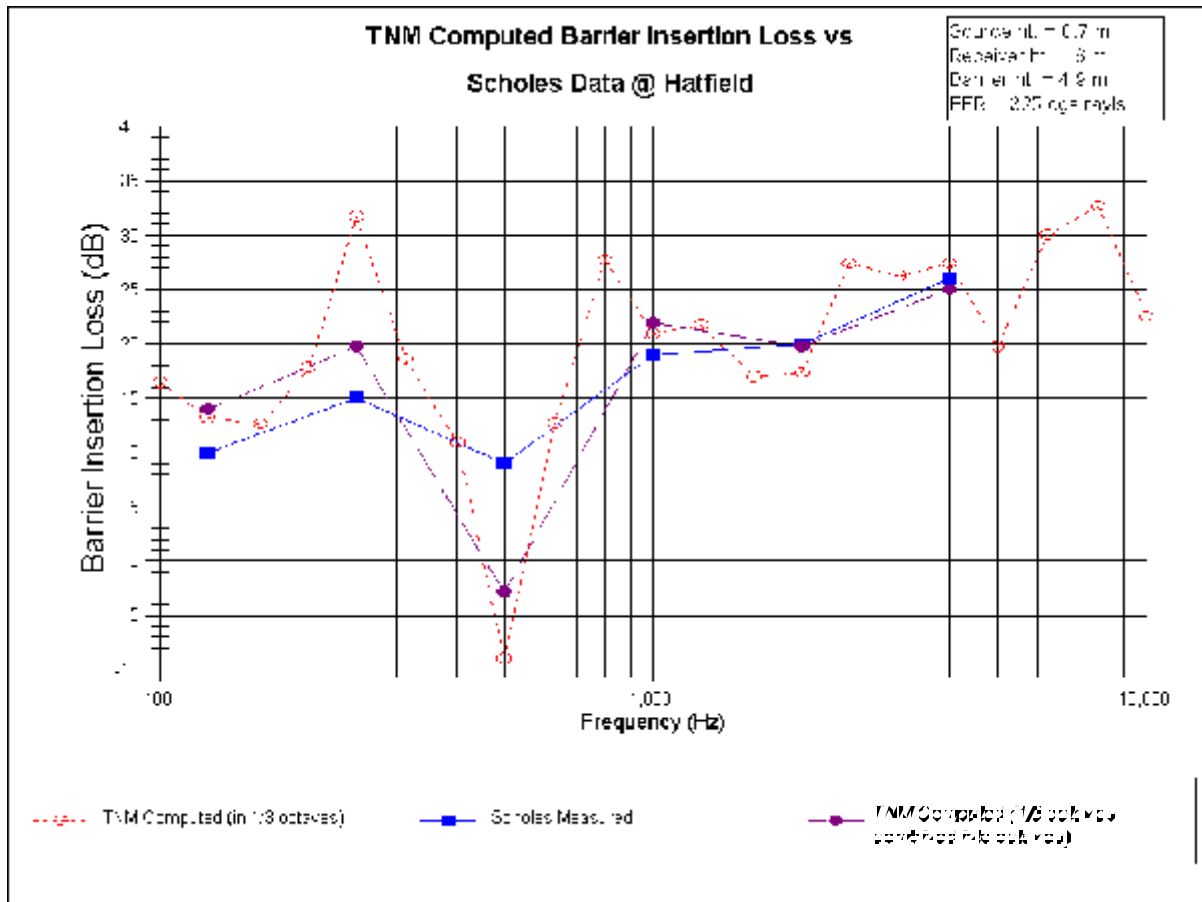


Figure 85. Comparison of barrier insertion loss in octave bands, receiver ht. = 6 m (20 ft), barrier ht. = 4.9 m (16 ft).

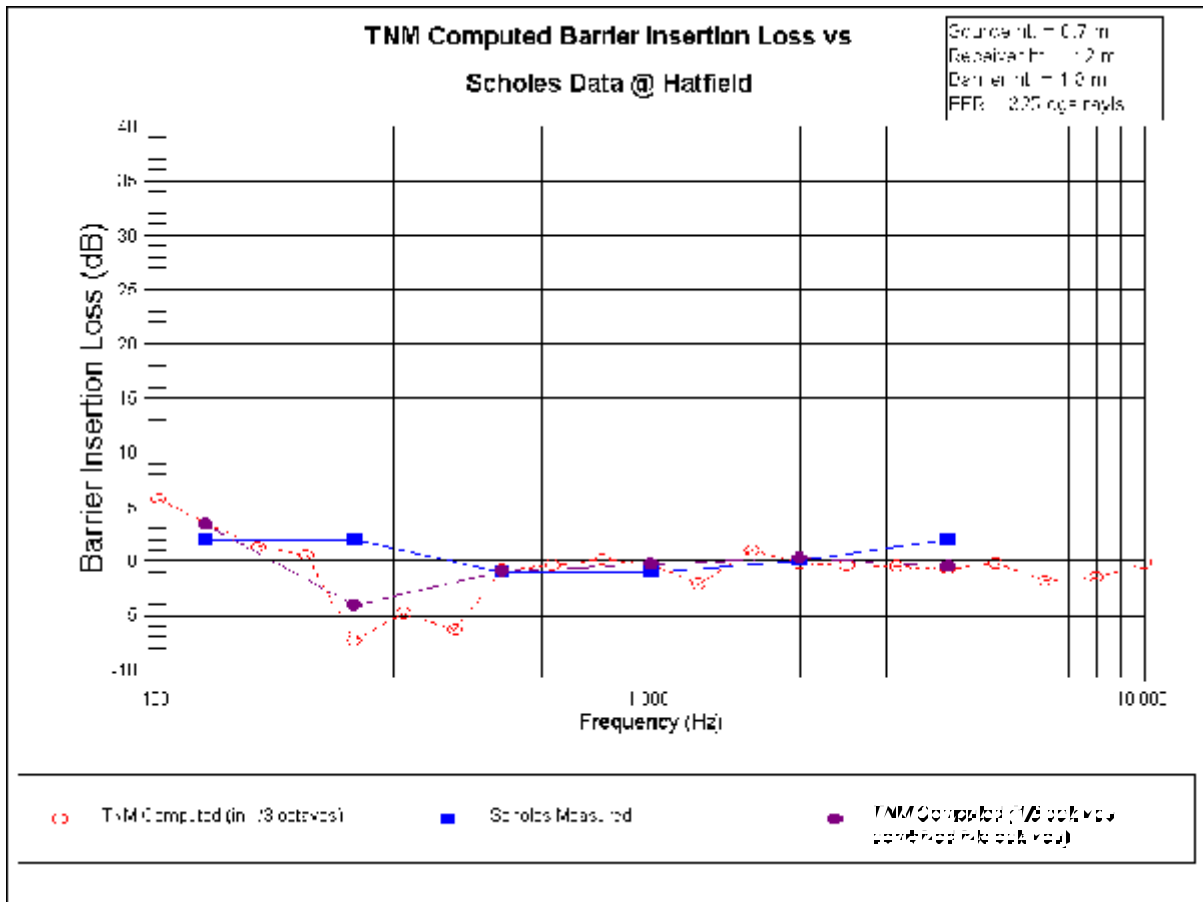


Figure 86. Comparison of barrier insertion loss in octave bands, receiver ht. = 12 m (40 ft), barrier ht. = 1.8 m (6 ft).

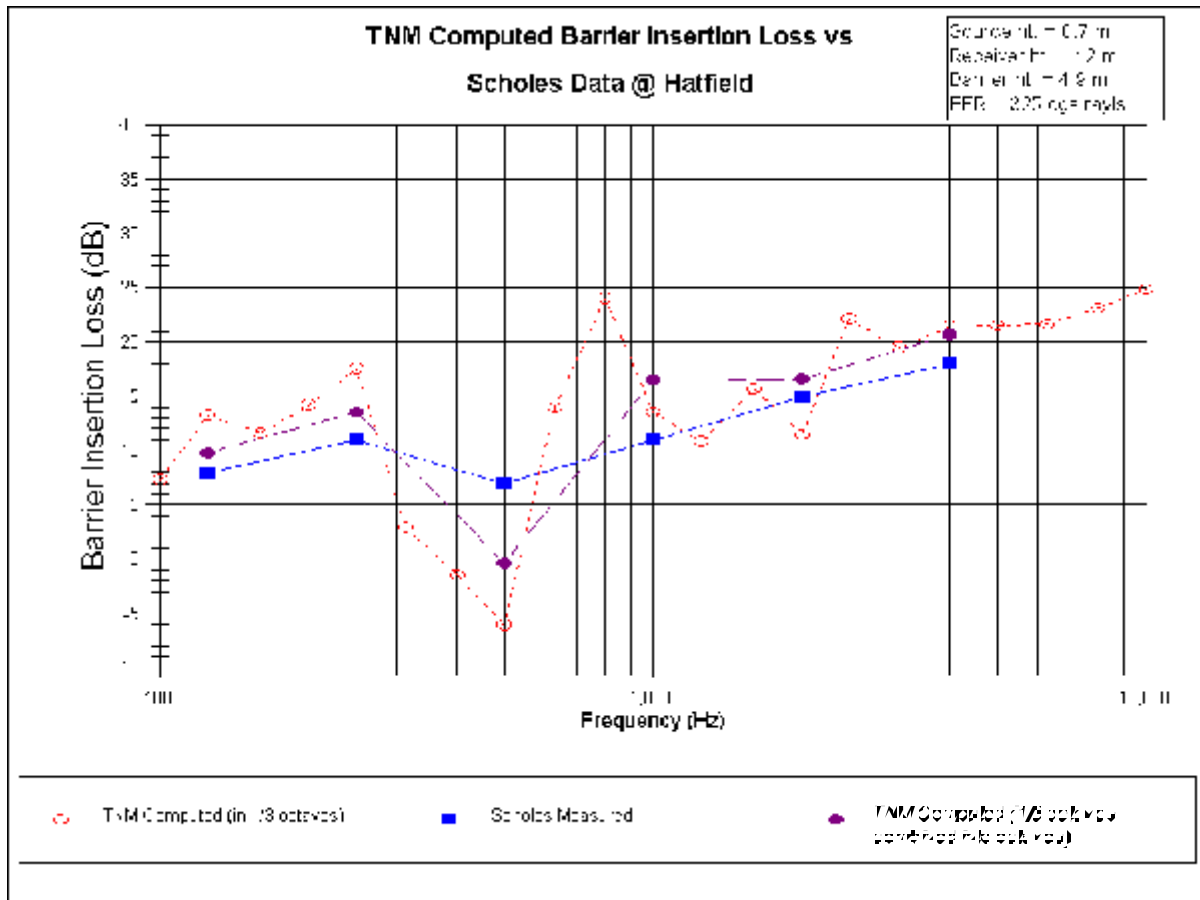


Figure 87. Comparison of barrier insertion loss in octave bands, receiver ht. = 12 m (40 ft), barrier ht. = 4.9 m (16 ft).

REFERENCES

- AASHTO 1990 American Association of State Highway and Transportation Officials. *A Policy on Geometric Design of Highway and Streets: 1990*. Washington DC: 1990.
- Anderson 1998 Anderson, Grant A., C. Lee, G. Fleming, C. Menge. *FHWA Traffic Noise Model (FHWA TNM[®]), Version 1.0: User's Guide*. Report No. FHWA-PD-96-009 and DOT-VNTSC-FHWA-98-1. Cambridge, MA: U.S. Department of Transportation, John A. Volpe Transportation Systems Center, Acoustics Facility, January 1998.
- ANSI 1994 "Acoustical Terminology." *American National Standard*, ANSI S1.1-1994. New York: American National Standards Institute, 1994.
- ANSI 1987 "Methods for Determination of Insertion Loss of Outdoor Noise Barriers." *American National Standard*, ANSI S12.8-1987. New York: American National Standards Institute, 1987 (Updated version to be published).
- Barry 1978 Barry, T.M., and J. Regan. *FHWA Traffic Noise Prediction Model*. Report No. FHWA-RD-77-108. Washington, DC: Federal Highway Administration, December 1978.
- Baker 1992 Baker, Louis. *C Mathematical Function Handbook*. McGraw-Hill, pp. 129-132, 1992.
- Boulanger 1997 Boulanger, Patrice, T. Waters-Fuller, K. Attenborough, and K. M. Li. "Models and measurements of sound propagation from a point source over mixed impedance ground." *J. Acoust. Soc. Am.*, vol. 102, no. 3, pp. 1432-1442, 1997.
- Bowlby 1997 Bowlby, William, R. Wayson, S. Chiguluri, M. Martin, L. Herman. *Interrupted Flow Reference Energy Mean Emission Levels for the FHWA Traffic Noise Model*. Report No. FHWA-PD-97-019 and DOT-VNTSC-FHWA-97-1. Cambridge, MA: U.S. Department of Transportation, John A. Volpe Transportation Systems Center, Acoustics Facility, January 1997.
- Chessell 1977 Chessell, C. I. "Propagation of Noise Along a Finite Impedance Boundary." *J. Acoust. Soc. Am.*, vol. 62, no. 4, pp. 825-834, 1977.
- Coulson 1996 Coulson, Robert K. *Vehicle Noise Source Heights & Sub-Source Spectra*. Boca Raton, FL: Florida Atlantic University, November 1996.
- De Jong 1983 De Jong, B. A., A. Moerkerken, and J. D. van der Toorn. "Propagation of Sound over Grassland and over an Earth Barrier." *Journal of Sound and Vibration*, vol. 86, no. 1, pp. 23-46, 1983.
- Delany 1970 Delany, M. E., and E. N. Bazley. "Acoustical Properties of Fibrous Absorbent Materials." *Applied Acoustics*, vol. 3, pp. 105-116, 1970.
- Embleton 1983 Embleton, T. F. W., J. E. Piercy, and G. A. Daigle. "Effective Flow Resistivity of Ground Surfaces Determined by Acoustical Measurements." *J. Acoust. Soc. Am.*, vol. 74, pp. 1239-1244, 1983.

- Fleming 1995 Fleming, Gregg G., A. Rapoza, C. Lee. *Development of National Reference Energy Mean Emission Levels for the FHWA Traffic Noise Model*. Report No. FHWA-PD-96-008 and DOT-VNTSC-96-2. Cambridge MA: John A. Volpe National Transportation Systems Center, Acoustics Facility, November 1995.
- Fleming 1994 Fleming, Gregg G., E. Rickley. *Performance Evaluation of Experimental Highway Noise Barriers*. Report No. DOT-VNTSC-FHWA-94-16 and FHWA-RD-94-093. Cambridge MA: John A. Volpe National Transportation Systems Center, 1994.
- Fleming 1992 Fleming, Gregg G. and E. Rickley. *Parallel Barrier Effectiveness Under Free-flowing Traffic Conditions*. Report No. FHWA-RD-92-068 and DOT-VNTSC-FHWA-92-1. Mclean VA: Federal Highway Administration, Office of Engineering and Highway Operations Research and Development, April 1992.
- Fleming 1990 Fleming, Gregg G. and E. Rickley. *Parallel Barrier Effectiveness: Dulles Noise Barrier Project*. Report No. FHWA-RD-90-105 and DOT-TSC-FHWA-90-1. Cambridge MA: U.S. Department of Transportation, John A. Volpe National Transportation Systems Center, Acoustics Facility, May 1990.
- Foss 1976 Foss, Rene N. *Noise Barrier Screen Measurements: Double Barriers*. Research Program Report 24.3. Olympia, WA: Washington State Highway Commission, August 1976.
- Hendriks 1991 Hendriks, Rudolf W. *Field Evaluation of Acoustical Performance of Parallel Highway Noise Barriers Along Route 99 in Sacramento, California*. Report No. FHWA/CA/TL-91/01. Sacramento CA: California Department of Transportation, January 1991.
- ISO 1996 "Acoustics - Attenuation of Sound During Propagation Outdoors - Part 2." *International Organization for Standardization, ISO/DIS 9613-2:1996*. Geneva, Switzerland: International Organization for Standardization, 1996.
- ISO 1993 "Acoustics - Attenuation of Sound During Propagation Outdoors - Part 1: Calculation of the Absorption of Sound by the Atmosphere." *International Organization for Standardization, ISO 9613-1:1993*. Geneva, Switzerland: International Organization for Standardization, 1993.
- Kurze 1988 Kurze, U. J. *Prediction Methods for Road Traffic Noise*. Lecture notes: International Seminar on Road Traffic Noise Evaluation by Model Studies. Grenoble. September 5, 1988.
- Lee 1997 Lee, Cynthia S.Y. and Gregg G. Fleming. *Measurement of Highway-Related Noise*. Report No. FHWA-PD-96-046 and DOT-VNTSC-FHWA-96-5. Cambridge, MA: U.S. Department of Transportation, John A. Volpe National Transportation Systems Center, Acoustics Facility, May 1996.
- Menge 1991 Menge, C. W., G. Anderson, T. Breen, C. Bajdek, A. Hass. *Noise Analysis Technical Report: Brooklyn-Queens Expressway, Queens Boulevard to Grand Central Parkway*. Report No. 290800. Lexington, MA: Harris Miller Miller & Hanson Inc., April 1991.

- Moulton 1990 Moulton, C.L. *Air Force Procedure for Predicting Aircraft Noise Around Airbases: Noise Exposure Model (NOISEMAP), User's Manual*. Report No. AAMRL-TR-90-011. Wright-Patterson Air Force Base, OH: U.S. Air Force, February 1990.
- Olmstead 1996 Olmstead, Jeffrey R., et. Al. *Integrated Noise Model (INM) Version 5.1 User's Guide*. Report No. FAA-AEE-96-02. Washington, DC: Federal Aviation Administration, December 1996.
- Parkin 1965 Parkin, P. H. and W. E. Scholes, "The Horizontal Propagation of Sound from a Jet Engine Close to the Ground, at Hatfield," *J. Sound Vib.*, vol. 2, no. 4, pp. 353-374, 1965.
- Scholes 1971 Scholes, W. E., A. C. Salvidge, and J. W. Sargent, "Field Performance of a Noise Barrier," *J. Sound Vib.*, vol. 16, pp. 627-642, 1971.
- TRB 1985 Transportation Research Board. *Highway Capacity Manual*. Special Report 209. Washington DC: National Research Council, 1985.

INDEX

-A-

Absorption coefficients	15, 75, 92-94
Acoustic energy	105, 109, 110
Acoustic pressure	20
Acoustic rays	20, 107
Acoustic wave	85-87
Acoustical characteristics	vi
Acoustical energy	51
Acoustics Facility	ix, 7, 145-147, 161
Air Force	147
American National Standards Institute	145
Atmospheric absorption	v, 2, 17, 100, 102
Atmospheric conditions	2, 102, 123, 124
Automobiles	v, 7, 23, 32, 37, 38, 45, 54, 56, 116, 155
A-weighted emission levels	7, 25
A-weighted sound level	7, 23, 25, 110
A-weighted sound levels	v

-B-

Barrier perturbations	69, 120
Barrier points	84
Boulangier	13, 19, 78, 85, 97, 145
Bright-zone diffractions	19, 78
Building points	84
Bus	v, 1, 7, 9, 23, 29, 35, 44, 47, 48, 54, 56, 61, 155

-C-

CAD programs	vi
Calibration	115, 116, 118
CD-ROM	ix, 156
Chessell	13, 85, 92, 123, 145
CNEL (see L_{den})	
Coefficients of reflection	92
Community Noise Equivalent Level (see L_{den})	
Computer hardware	155
Contours	vi, vii, 2, 7, 21, 119, 120, 155
Contour-receiver height	122
Contour-zone	121
Corner	87, 91, 96, 97
Cross-sectional geometry	20, 105, 107, 109, 114

-D-

Day-night average sound level (see L_{dn})	
dB	12, 14, 17, 65, 67, 68, 86, 99, 100, 102, 115, 116, 123
De Jong	13, 14, 18, 77, 85, 102, 103, 145

Dense foliage	2, 17, 98, 99
Dense-graded asphaltic concrete	v, 1, 7, 24, 37, 40, 42
DGAC (see Dense-graded asphaltic concrete)	
Diffractions	13, 19, 74, 78-80, 82, 87, 90, 91, 95, 96
Digitizer	vi, 155, 156
Divergence	v, 20, 63, 111, 112, 114
DNL (see L_{dn})	
DXF files	vi
DXF format	155

-E-

Ear height	122
Earth Barrier	145
Effective Flow Resistivity (see EFR)	
EFR	2, 13-15, 74, 85, 92-94, 123, 124, 128-131, 146
Elemental roadway segment	12
Elemental triangle	10-12, 18, 50, 63, 64, 69, 73, 104
Elements of vertical geometry	74
Embleton	13, 14, 123, 128-131, 146
Emission constants	25
Emission data	ix, 1, 7
Emission equations	23
Emission level	1, 7, 9, 23
Emissions data base	v, 7
Energy split	9, 31, 45-48, 116
Energy-average emission levels	24
Entrance speeds	51, 52
Equivalent sound level (see L_{Aeq1h})	
Euler's equation	88
Exit speed	51, 52, 58

-F-

FAA (see Federal Highway Administration)	
Federal Aviation Administration's Integrated Noise Model (see INM)	
Federal Highway Administration	v, vii-ix, xiii, 1, 7, 8, 23, 25, 49, 63, 119, 145-147, 155-157
Federal Highway Administration's Traffic Noise Model (see TNM)	
FHWA (see Federal Highway Administration)	
FHWA policy	1, 25
FHWA TNM (see TNM)	
FHWA Traffic Noise Model (see TNM)	
Field grass	14
Field measurements	vi, 25, 115
Foss	18, 77, 85-88, 102, 103, 146
Free field	1, 2, 10, 20, 29, 66-68, 71, 78-80, 88
Free-field path sound pressure	90
Free-field pressure	87
Free-field sound energy	63, 66
Free-field sound level	vii, 10, 63, 71

Free-field sound pressure 88, 91, 104
 Free-field traffic sound energy 68
 Frequencies 9, 12, 14, 19, 78, 97, 98, 123
 Fresnel 13, 19, 75, 78-80, 85-89, 91, 97, 99
 Fresnel diffraction theory 13
 Fresnel ellipse 19, 78, 97
 Fresnel integral 80, 86-88
 Fresnel number 19, 78, 86, 91, 99
 Fresnel zone 19, 75, 78, 79, 85, 91
 Full throttle 8, 9, 24, 29, 32-36, 39, 41, 46-48

-G-

Geometry vii, ix, 7, 10, 12, 13, 16-21, 63, 66, 68, 69, 73-86, 89-92, 94-99, 102-105, 107, 109, 112, 116, 123, 124
 Geometry algorithms 12, 17, 18, 69, 73, 98, 102
 Grazing line 80
 Ground effects vii, 1-3, 12, 13, 20, 29, 75
 Ground points 3, 13, 16-18, 74, 75, 77, 84, 98
 Ground reflection model 123
 Ground type 2, 14, 16, 18, 19, 74, 76-78, 97, 123

-H-

Heavy truck v, 1, 7-9, 23, 24, 34, 41-43, 46, 47, 49, 51-55, 57, 58, 60, 61, 64, 108, 115, 116, 155
 Heavy-truck acceleration curve 60
 Heavy-truck speeds 49, 51, 52, 58-60
 Highest path point 18, 19, 77, 78, 97
 Highway cross-section 13
 Highway noise barriers v, 146, 155
 Highway traffic noise 1, v-vii
 High-level flow chart 3, 5
 Horizontal geometry vii, ix, 10, 63, 73, 74, 104
 Horizontal propagation of sound 147
 HPPS (see Highest Path Point)
 Humidity 17, 86, 100-102

-I-

Impedance 13-15, 18, 19, 74, 75, 77, 78, 83, 88, 92, 93, 95-98, 123, 145
 Impedance discontinuity 14, 18, 19, 74, 75, 77, 78, 88, 95-97
 Impedances 74, 75, 83, 89
 INM 2, 147
 Insertion loss vii, 14, 16, 20, 86, 99, 119, 120, 124, 126, 137-145, 155
 Insertion-loss contours 21, 119
 Integrated Noise Model (see INM)
 International Organization for Standardization 146
 ISO 9613-1 17, 100, 146
 ISO 9613-2 98

-J-

Jet engine 123, 147

-L-

L_{Aeq1h} vi, 2, 10, 12, 21, 65, 67, 69, 119
 Lawn 14
 L_{den} vi, 2, 12, 21, 65, 67, 69, 119
 L_{dn} vi, 2, 12, 21, 65, 67, 69, 119
 Level-difference contours vi, 21, 119
 Line-of-sight 3, 20, 84, 106, 108, 112

-M-

McTrans 156, 157
 Microphone 23, 24, 115-118, 123, 124, 126
 Microphone array 24
 Microphone height 24, 115, 123, 124
 Microphone locations 116
 Microphone positions 115
 Model Verification vii, 21, 123
 Motorcycle v, 1, 7, 9, 23, 36, 44, 48, 54, 56, 61, 155

-N-

Near-highest path point 19, 78
 NHPP (see Near-highest path point)
 NMPLLOT 2, 21, 120
 Noise barrier v, vi, 106, 109, 120, 123, 145-147, 155
 Noise Reduction Coefficient 14-16, 20, 83, 86, 93, 94, 107, 109, 112
 Noise-emission equations 23
 Non-zero speed constraint 60
 NRC (see Noise Reduction Coefficient)

-O-

Octave band 7, 17, 19, 78, 84, 85, 94, 97-100, 102, 123, 124
 OGAC (see Open-graded asphaltic concrete)
 1HEQ (see L_{Aeq1h})
 One-third octave-band spectra v
 On-ramp start points v, 2, 9
 Open-graded asphaltic concrete v, 1, 7, 24, 38, 40, 43
 OPTIMA vi, vii, 155

-P-

Parallel barrier analysis 3, 20, 105, 109, 155
 Parallel Barriers vi, vii, 3, 20, 105-107, 113, 115
 Parallel-barrier computations 20, 107, 108, 111, 112, 116
 Parallel-barrier degradation 20, 105-107, 110, 111, 114-116
 Parallel-barrier ray tracing procedure 105

Parallel-barrier receivers	109
Parkin	123, 124, 147
Path generation algorithm	83, 84
Path link	85
Path list	84, 85
Path node	84, 85
Pavement	v, 1, 7, 8, 13, 14, 20, 24-26, 29-31, 37-43, 107, 109, 110, 114, 155
PCC (see Portland cement concrete)	
Perturbable barriers	18, 69, 77, 119, 120
Point-receiver segments	80
Point-source geometry	21, 123
Point-source mathematics	12, 13
Portland cement concrete	v, 1, 7, 24, 29, 38, 41, 43
Propagation paths	17, 19, 20, 73, 74, 76, 78-80, 82-84, 87, 95, 98, 104
Pseudocode	83

-R-

Ramp traffic	108
Ray tracing	20, 105, 109, 112
Receiver points	84, 99
Reflective barriers	105, 106, 109
Reflective retaining walls	106
Regression	13, 18, 19, 25, 26, 52-55, 77, 78, 110, 118
Relative humidity	17, 86, 100-102
RH (see relative humidity)	
Rows of buildings	vi, 13, 17, 76, 78, 84, 99, 100, 155

-S-

Scholes	123, 124, 147
Single-barrier diffraction	14
Soil	14, 123
Sound level	vi, 1-3, 7, 10, 18, 19, 21, 23, 25, 63, 64, 69, 71, 74, 77, 105, 109-112, 119, 123, 124, 155
Sound-level contours	vi, vii, 21, 119
Sound-level descriptors	2
Source points	84
Source-receiver path	18, 77, 99
Source-receiver triangle	68
Source-to-receiver elemental triangles	63
Source-to-receiver Fresnel zone	19, 78
Source-to-receiver line of sight	16
Speed-computation process	50
STAMINA	vi, vii, 104, 116, 124-127, 155
Statistical analysis	24
Subgrid point	120, 122
Subsource	v, ix, 23, 24, 26, 29, 30, 64, 68, 69, 107-109, 116
Subsource height	ix, 24, 26, 30, 69

Subsource measurements 24

-T-

Throttle condition 8, 25, 26, 30
 TNM v-ix, xiii, 1-3, 5, 7-10, 12-21, 23-26, 29, 30, 49-53, 55, 58, 60, 61, 63, 65-71, 74, 75,
 77, 78, 83, 84, 88, 91, 94, 98, 100, 103, 105, 107-112, 114-116, 119-127, 155-157
 Toll booths v, 2, 9
 Topography vi
 Traffic v-vii, 1, 2, 8-12, 14, 17, 20, 24-26, 49-52, 55-57, 59, 60, 64-69, 71, 99, 106-108,
 111, 116, 145, 146, 155
 Traffic noise v-vii, 1, 8, 20, 99, 107, 108, 145, 146, 155
 Traffic Noise Model (see TNM)
 Traffic percentages 65
 Traffic signals v, 2, 9, 10, 49
 Traffic speed 49, 108, 111
 Traffic volume 12, 67, 108, 111
 Traffic-control device v, vii, 9, 24, 49, 50, 52, 55-57, 60, 65
 Tree zone 10, 76, 84, 122
 Tree zone points 84

-U-

User-defined height 76
 User-defined vehicle 23, 25, 26, 29, 49, 51, 61, 64, 155
 User-entered adjustment factor 65, 68, 71
 User-entered receiver height 122
 User-entered traffic control devices 8

-V-

Vehicle acceleration 55, 58
 Vehicle emissions 26, 29, 67, 116
 Vehicle Noise Emission 1, 2, 7, 8, 10
 Vehicle spectra 7
 Vehicle speed 2, 7, 9, 11, 24-26, 49, 51-55, 58, 64, 67, 110
 Vehicle speed computation 7, 9
 Vehicle type v, 1, 8, 9, 11, 12, 23-26, 29, 30, 51, 52, 54, 58, 59, 61, 64-71, 108, 110, 111, 155
 Vehicles v, 1, 7-11, 20, 23-26, 29, 49, 51-55, 58, 60, 61, 64-66, 110, 115, 155
 Vertical Geometry vii, ix, 12, 13, 16-18, 63, 68, 69, 73-79, 82, 84, 85, 91, 94, 98, 102-104
 Vertical subsources 24, 26, 29, 67
 Vertical-plane cross-section geometry 20

-W-

Water 14, 86, 100
 Wave front 112
 Wave number 86, 88, 92
 Width-to-height ratio 115

-Z-

Zone 10, 13, 16, 19, 21, 75, 76, 78, 79, 84, 85, 89, 91, 119-122



FEDERAL HIGHWAY ADMINISTRATION TRAFFIC NOISE MODEL (FHWA TNM®)

VERSION 1.0
January 1998

The Federal Highway Administration (FHWA) is pleased to announce the release of the Traffic Noise Model, Version 1.0 (FHWA TNM). The FHWA TNM is an entirely new, state-of-the-art computer program used for predicting noise impacts in the vicinity of highways. It uses advances in personal computer hardware and software to improve upon the accuracy and ease of modeling highway noise, including the design of effective, cost-efficient highway noise barriers.

The FHWA TNM contains the following components:

- # Modeling of five standard vehicle types, including automobiles, medium trucks, heavy trucks, buses, and motorcycles, as well as user-defined vehicles.
- # Modeling of both constant-flow and interrupted-flow traffic using a 1994/1995 field-measured data base.
- # Modeling of the effects of different pavement types, as well as the effects of graded roadways.
- # Sound level computations based on a one-third octave-band data base and algorithms.
- # Graphically-interactive noise barrier design and optimization.
- # Attenuation over/through rows of buildings and dense vegetation.
- # Multiple diffraction analysis.
- # Parallel barrier analysis.
- # Contour analysis, including sound level contours, barrier insertion loss contours, and sound-level difference contours.

These components are supported by a scientifically-founded and experimentally-calibrated acoustic computation methodology, as well as an entirely new, and more flexible data base, as compared with that of its predecessor, STAMINA 2.0/OPTIMA. The Data Base is made up of over 6000 individual pass-by events measured at forty sites across the country. It is the primary building block around which the acoustic algorithms are structured.

The most visible difference between the FHWA TNM and STAMINA 2.0/OPTIMA, is TNM's Microsoft® Windows interface. Data input is menu-driven using a digitizer, mouse, and/or keyboard. Users also have the ability to import STAMINA 2.0/OPTIMA files, as well as roadway design files saved in CAD, DXF format. Color graphics will play a central role in both case construction and visual analysis of results.

Computer Requirements

The recommended computer system requirements for TNM Version 1.0 are:

- # Computer: IBM-compatible PC;
- # Processor: 120 MHz Pentium (or faster);
- # Memory: 32 MB (or more);
- # Disk Drive: 3.5 inch, 1.44 MB;
- # Mouse input device;
- # Monitor: Accelerated Super VGA (1024 x 768), 16 colors, configured with "small" fonts;
- # Software: Microsoft® Windows 3.1 (or later): Note: TNM will run under Microsoft® Windows 95 or Windows NT, however, TNM is a 16-bit program and will not take full advantage of the 32-bit architecture associated with Windows 95 or NT.
- # 10 MB of hard-disk space for the TNM system (including sample runs); and
- # Up to 1 MB of hard-disk space for each TNM run.

To digitize coordinates from plan sheets and roadway profiles, the following is required:

- # Digitizer: Any manufacturer/model that meets the LCS/Telegraphics Wintab Interface Specification, preferably with a 16-button puck. The digitizer manufacturer should provide the file WINTAB.DLL, which must be resident on the hard disk for digitizer use.

The FHWA TNM Package: The FHWA TNM package includes the following:

- # Two TNM manuals: This User's Guide and the TNM Technical Manual (Note: The User's Guide and Technical Manual may be photocopied. See below for information on how to order additional copies of either document.);
- # The FHWA TNM software on three 3½" diskettes;
- # One CD-ROM with the "TNM Trainer" tutorial; and
- # The TNM registration card located on the last page of this User's Guide. Please fill out and return this card. Registered owners are entitled to receive technical support (see Section 1.8) and information on upgrades and supplementary guides.

Copyright: FHWA TNM is a registered copyright.

Trademark: FHWA TNM is a registered trademark.

Availability: The FHWA will distribute TNM Version 1.0 free of cost to every State Department of Transportation (DOT). All State DOTs may make sufficient copies of the TNM package for internal use only. For all other users, TNM will be distributed by the McTrans Center at the University of Florida. Non-State DOT users have three McTrans licensing options for the FHWA TNM: (1) they may purchase a single license, which is valid for a distinct address (or site); (2) they may purchase an unlimited agency license, which is valid for multiple addresses (or sites) within the same organization; or (3) they may purchase a license for training or educational purposes. A McTrans order form is attached. Purchase the FHWA TNM by selecting from the following McTrans product ordering numbers:

<u>Product No.</u>	<u>Description</u>	<u>Cost</u>
TNM.WIN	FHWA TNM (for single site license):	\$695.00
TNM.AL	FHWA TNM (for unlimited agency license):	\$2750.00
TNM.TC	FHWA TNM (for training/educational license):	\$2750.00
TNM.D	FHWA TNM User's Guide:	\$20.00
TNM.DS	FHWA TNM Technical Manual:	\$20.00

Further information on TNM can be found on the McTrans website (<http://www-mctrans.ce.ufl.edu>). Purchase orders, checks, or money orders payable to "**McTrans**", with this Order Form, may be sent to:

McTrans Center	PHONE:	(352) 392-0378
University of Florida	FAX:	(352) 392-3224
512 Weil Hall		
P.O. Box 116585		
Gainesville, FL 32611-6585		

McTrans Order Form*

FALL97

For McTrans use only:

McTrans Center
University of Florida
512 Weil Hall
PO Box 116585
Gainesville, FL 32611-6585
FEID # 59-6002052

(352) 392-0378
Messages 1-800-226-1013
McFAX (352) 392-3224
McLink (352) 392-3225
E-mail: mctrans@ce.ufl.edu
http://mctrans.ce.ufl.edu

ORDER NO. _____
DATE RECEIVED _____
MEMBER NO. _____

SHIP TO:



BILL PURCHASE ORDER TO:

MEMBER NUMBER (IMPORTANT)

NAME _____ TITLE _____
ORGANIZATION _____ DEPARTMENT _____
ADDRESS (DO NOT USE P.O. BOX NUMBER) _____
CITY, STATE, ZIP _____
() ()
PHONE _____ FAX _____
E-MAIL ADDRESS _____

FIRM NAME _____
ATTENTION _____
ADDRESS _____
CITY, STATE, ZIP _____
FEID NO. OR SOCIAL SECURITY NO. _____

CHECK IF NEW ADDRESS OR NEW MEMBER

NEW MEMBERS:

Please specify area(s) of interest:

- Highway Design, Pavements, Bridge Design & Hydraulics
- Safety and Accident Records
- Traffic Engineering
- Urban Transportation Planning
- Environmental (air, water and noise analysis)
- Construction Management
- Maintenance
- Transit
- Surveying & Photogrammetry

No.	Product No.	Description (INCLUDE REGISTRATION NO. FOR UPGRADES OR ADD-ONS.)	Quantity	Unit Cost	Total Cost
1					
2					
3					
4					
5					
6					
7					
8					
9					

Use additional copies if needed.

Please indicate method of payment below (U.S. Dollars only):

- Check enclosed, No. _____ payable to University of Florida-McTrans Center
U.S. dollar checks drawn on U.S. banks, or money orders, please.
- VISA/MC No. _____ Expires ____ - ____
Name as it appears on card _____
- Purchase Order Enclosed, No. _____
(Terms: Net 30 days, copy of Purchase Order must accompany order.)
- If you wish us to ship by FedEx (only) include your FedEx No. _____

Subtotal _____
 OUTSIDE U.S. & CANADA Estimated Shipping: 25% (Maximum \$25 per item) _____
 FLORIDA CUSTOMERS ONLY, add 6% sales tax plus county surtax, or your
 FL Tax Exempt No. _____
 Processing \$10.00
 Total amount enclosed* _____
 Check if you require 5.25-inch disk


*Orders will not be accepted without this form (copy is OK), and an approved method of payment for the proper amount, including processing.

THANK YOU FOR YOUR SUPPORT.

Please fill out and return the registration card below to:

Volpe Center
Acoustics Facility, DTS-34
55 Broadway
Cambridge, MA 02142

Registered owners are entitled to receive technical support and information on upgrades and supplementary guides.



**FHWA TNM[®] Version 1.0
Registration Card**

Last name _____ *First name* _____

Company name (if applicable)

Mailing address

City _____ *State/Province* _____ *Country* _____ *Zip/Postal code* _____

Telephone number _____ *Fax number* _____

Email address

PC serial number _____ *PC processor/speed* _____ *PC memory* _____